

**Synthesis of Multifunctional Reactive Dyes and Their Application
onto Wool Fabric by Inkjet Printing**

Saira Faisal

Submitted in accordance with the requirements for the degree of
Degree of Philosophy

The University of Leeds
Department of Colour Science
School of Chemistry

December 2013

The candidate confirms that the work submitted is her own, except where work which has formed part of jointly-authored publications has been included. The contribution of the candidate and the other authors to this work has been explicitly indicated below. The candidate confirms that appropriate credit has been given within the thesis where reference has been made to the work of others.

The syntheses and applications of, triazine based dyes in magenta, yellow and blue hue (Chapter 3,4,5) along with comparative study with commercial reactive inks (Chapter 10) were presented in a conference as follows.

1. Saira FAISAL, Long LIN and Matthew CLARK. "Novel reactive colorants and their application onto textile substrates by Inkjet printing". In "*12th Congress of the International Colour Association*". 8th – 12th July 2013, Newcastle-upon Tyne, United Kingdom.

The syntheses and applications of, triazine based dyes in magenta, yellow and blue hue (Chapter 3,4,5) were presented in a conference as follows.

2. Saira FAISAL, Long LIN and Matthew CLARK. "Novel reactive dyes and their application onto textile substrates by Inkjet printing". In "*29th International Conference on Digital Printing Technology*". September 29th – October 3rd 2013, Seattle, United States of America.

I was responsible for 95% of the total contribution in above. The contributions of the other Authors were 5% of the work, this being limited to the correction of the draft paper and provision of relevant advice.

This copy has been supplied on the understanding that it is copyright material and that no quotation from the thesis may be published without proper acknowledgement.

The right of Saira Faisal to be identified as Author of this work has been asserted by her in accordance with the Copyright, Designs and Patents Act 1988.

Dedicated to
My Grandmother (Late)

Acknowledgements

I would like to express my sincere gratitude to **Professor Long Lin** for his guidance, understanding, patience, and most importantly, excellent supervision during my studies. I can only cherish with gratitude the invaluable suggestions and timely discussions offered by him which made this piece of work possible. I would also like to extend my gratitude to **Dr. Matthew Clark** who supervised the early years of this project for his valuable guidance. His mentorship was paramount in providing a well-rounded experience consistent my long-term career goals.

I would also like to thank **Dr. Julie Fisher** who has offered me unfailing advice and support.

I am also grateful to *Mr Algy Kazlauciunas, Mr Mohammad Asaf, Mr Martin Huscroft* and *Mr. Ian Blakeley* for providing excellent technical services for my work.

I would like to thank *NED University of Engineering and Technology, Karachi Pakistan* for financial support for this study.

I wish to express my deep sense of gratitude to my parents, in-laws, family and friends who always stood firmly behind me in moments of despair and revived my spirit and determination.

Finally, special thanks to my husband **Faisal**, who inspired me and provided constant encouragement during the entire process. To my little girl, **Warishah**, who missed out lots of Mummy time while I pursued my studies.

Abstract

Inkjet printing provides a favourable method for wool printing because of the ability to produce economical short print runs and providing flexibility in print design.

This work focused on the synthesis and characterisation of series of novel multifunctional reactive dyes in magenta, blue and yellow hue based on chlorotriazines and chloropyrimidine reactive groups and their modification by: (1) replacing labile chlorine(s) by other labile sulfophenoxy group(s) and (2) replacing the imino bridging group by an aliphatic amino group.

This study also focused on the formulation of a set of inks based on parent and modified dyes in magenta, yellow and blue hue, their application onto wool via inkjet printing, and evaluation of percent fixation along with their stability in ink formulations and colour fastness properties. Moreover, the results were also compared with commercially successful Jettex R Inks (DyStar).

The research has shown that reactive dyes based on chlorotriazines and chloropyrimidine can be modified by the incorporation of sulfophenoxy group(s) onto the reactive group of the dye.

The modified dyes, when inkjet printed onto the wool, were able to react with the wool fibre and show excellent fixation results. The incorporation of more than one reactive group on the dye chromophore has shown an increase in percent fixation compared to dyes with only one reactive group. Moreover, modified inks showed excellent colour fastness to light and wash.

Additionally, comparative analysis of modified dye-based inks and commercially successful 'Jettex R' inks illustrates that the novel inks are superior in terms of percent fixation and colour fastness properties.

List of Abbreviations

CE	Capillary Electrophoresis
CZE	Capillary Zone Electrophoresis
MEKC	Micellar Electrokinetic Capillary Chromatography
EOF	Electroosmotic Flow
SDS	Sodium dodecyl sulfate
TLC	Thin layer chromatography
IR	Infrared
FT-IR	Fourier Transform-Infrared Spectroscopy
ATR	Attenuated Total Reflectance
CMC	Carboxymethyl cellulose
DMF	N,N-dimethylformamide
NMMO	N-methylmorpholine N-oxide
dpi	dots per inch
cP	Centipoise

Table of Contents

Acknowledgements	iv
Abstract	v
List of Abbreviations	vi
Table of Contents	vii
List of Figures	xix
List of Schemes.....	xxvi
List of Tables.....	xxviii
Preface	xxx
1 Introduction.....	1
1.1 Reactive Dyes	1
1.1.1 History of Reactive Dye Development.....	2
1.1.1.1 First Commercial Ranges of Reactive Dyes for Cellulosic Fibres.....	3
1.1.1.2 First Commercial Ranges of Reactive Dyes for Polyamide Fibres	3
1.1.2 Structure of Reactive Dyes.....	3
1.1.2.1 Chromophore.....	4
1.1.2.2 Solubilising Groups	4
1.1.2.3 Bridging Group.....	4
1.1.2.4 Reactive Group.....	4
1.1.2.4.1 Nucleophilic Aromatic Substitution.....	5
1.1.2.4.2 Michael Addition.....	5
1.1.3 Reactive Groups for Wool	5
1.1.3.1 Triazine	6
1.1.3.2 Diazine	8
1.1.4 Multifunctional Reactive Dyes.....	8
1.2 Wool.....	9
1.2.1 Fibre Morphology.....	9
1.2.2 Composition of Wool.....	12
1.2.3 Chemical Structure	12
1.2.4 Mechanism of Wool Coloration	14

1.2.5	Dyes for Wool Coloration	15
1.3	Textile Printing.....	16
1.3.1	Development of Textile Printing	16
1.3.2	Inkjet Printing	17
1.3.3	Classification of Inkjet Printing Technology	18
1.3.3.1	Continuous Inkjet	18
1.3.3.2	Drop-on-Demand Inkjet.....	18
1.3.4	Applications of Inkjet for Textile Printing	19
1.3.4.1	Early Developments.....	19
1.3.5	Changes in the Textile Printing Market	20
1.3.6	Mass Customisation.....	20
1.3.6.1	Change in the Business Model	21
1.3.6.2	Quick Response and Just in Time Delivery	21
1.3.6.3	Economic Factors in Textile Printing	21
1.3.6.4	Ecology	22
1.3.7	Improving Textile Printing Industry Through the Use of Inkjet Technology	22
1.3.7.1	Limitation of Inkjet Printing	25
1.3.8	Inks for Textile Inkjet Printing	26
1.3.8.1	Dye Based Inks.....	26
1.4	Inkjet Printing of Wool with Reactive Inks	27
1.4.1	Reactive Inks for Wool	27
1.4.2	Pre-Treatment for Inkjet Printing of Wool.....	29
1.5	Aims of Research	30
1.6	References.....	32
2	General Procedure and Instrumentation	39
2.1	Capillary Electrophoresis.....	39
2.1.1	Principles of Capillary Electrophoresis (CE)	39
2.1.1.1	Capillary Zone Electrophoresis (CZE)	40
2.1.1.2	Micellar Electrokinetic Chromatography (MEKC)	41
2.1.2	Analysis Parameters.....	42
2.2	Thin Layer Chromatography (TLC).....	43
2.2.1	Analysis Parameters.....	45
2.3	Infrared (IR) Spectroscopy	45

2.3.1	Fourier Transform-Infrared Spectroscopy (FT-IR)	46
2.3.2	Attenuated Total Reflection (ATR)	47
2.3.3	Analysis Parameters.....	48
2.4	Elemental Analysis.....	48
2.5	Inkjet Printing Procedure.....	48
2.5.1	Fabric Pre-Treatment	49
2.5.2	Ink Preparation	49
2.5.2.1	Purification of Synthesised Dyes.....	49
2.5.2.2	Ink Formulation	50
2.5.2.2.1	Measurement of Surface Tension.....	51
2.5.2.2.2	Measurement of Viscosity	51
2.5.3	Application onto Wool Fabric	52
2.5.4	Fixation of Prints	52
2.5.5	Washing-off.....	53
2.6	Stability of Dye based Inks	53
2.7	Determination of Percent Fixation (Fibre-Dye Bond)	53
2.7.1	Analysis Parameters.....	54
2.8	Colour Fastness Testing.....	54
2.8.1	Light Fastness Testing	54
2.8.2	Wash Fastness Testing	55
2.9	Microwave-Irradiated Synthesis	55
2.9.1	Principle of Microwave-Irradiated Synthesis.....	57
2.9.1.1	Dipolar Polarisation	57
2.9.1.2	Conduction Mechanism	58
2.9.2	Advantages of Microwave-Irradiated Synthesis	58
2.9.3	Analysis Parameters.....	59
2.10	Miscellaneous Procedures.....	59
2.10.1	Completion of Diazotization	59
2.10.2	Completion of Diazo-Coupling	59
2.10.3	Freeze Drying	59
2.11	References.....	59

3	Synthesis, Modification, Characterisation of Magenta Dichlorotriazine Dyes and Their Application onto Wool Fabric by Inkjet Printing.....	65
3.1	Introduction.....	65
3.2	Experimental.....	67
3.2.1	Materials.....	67
3.2.2	Synthesis and Characterisation of Magenta 5-Amino-4-Hydroxy-3-[(2-sulfohenyl)azo]-2,7-Naphthalenedisulfonic Acid Dye ($d1_m$).....	67
3.2.2.1	Synthesis of $d1_m$	67
3.2.2.1.1	Diazotization.....	67
3.2.2.1.2	Coupling.....	68
3.2.2.2	Characterisation of $d1_m$	68
3.2.3	Synthesis and Characterisation of Magenta 5-[(4,6-Dichloro-1,3,5-triazin-2-yl)amino]-4-Hydroxy-3-[(2-Sulfohenyl)azo]-2,7-Naphthalenedisulfonic Acid Dye ($d2_{mt}$).....	70
3.2.3.1	Synthesis of $d2_{mt}$	70
3.2.3.2	Characterisation of $d2_{mt}$	71
3.2.4	Synthesis and Characterisation of Modified Magenta 5-[[4-Chloro-6-(4-sulfohenoxy)-1,3,5-triazin-2-yl]amino]-4-Hydroxy-3-[(2-sulfohenyl)azo]-2,7-Naphthalenedisulfonic Acid Dye ($d3_{mtm}$).....	74
3.2.4.1	Synthesis of $d3_{mtm}$	74
3.2.4.2	Characterisation of $d3_{mtm}$	75
3.2.5	Synthesis and Characterisation of Modified Magenta 5-[[4,6-(4-Sulfohenoxy)-1,3,5-triazin-2-yl]amino]-4-Hydroxy-3-[(2-sulfohenyl)azo]-2,7-Naphthalenedisulfonic Acid Dye ($d4_{mtd}$).....	77
3.2.5.1	Synthesis of $d4_{mtd}$	77
3.2.5.2	Characterisation of $d4_{mtd}$	79
3.2.6	Application of Magenta Dyes ($d2_{mt}$, $d3_{mtm}$ and $d4_{mtd}$) onto Wool Fabric by Inkjet Printing.....	82
3.2.7	Characteristics of Inks ($d2_{mt}$, $d3_{mtm}$ and $d4_{mtd}$).....	82
3.2.7.1	Surface Tension and Viscosity of Inks.....	82
3.2.7.2	Stability of Dye ($d2_{mt}$, $d3_{mtm}$ and $d4_{mtd}$) Based Inks.....	82

3.2.8	Evaluation of Percent Fixation of Magenta Dyes (d_{2mt} , d_{3mm} and d_{4mtd}) by Different Fixation Methods	85
3.2.8.1	Method 1: Batching at Room Temperature.....	85
3.2.8.2	Method 2: Batching at 65 °C.....	86
3.2.8.3	Method 3: Steaming.....	87
3.2.9	Light Fastness.....	88
3.2.10	Wash Fastness	88
3.3	Conclusions.....	89
3.4	References.....	90
4	Synthesis, Modification, Characterisation of Yellow Dichlorotriazine Dyes and Their Application onto Wool Fabric by Inkjet Printing.....	93
4.1	Experimental	93
4.1.1	Materials.....	93
4.1.2	Synthesis and Characterisation of Yellow 7-[(4-Amino-2-methylphenyl)azo]-1,3-Naphthalenedisulfonic Acid Dye (d_{5y}).....	94
4.1.2.1	Synthesis of d_{5y}	94
4.1.2.1.1	Diazotization	94
4.1.2.1.2	Coupling.....	94
4.1.2.2	Characterisation of d_{5y}	95
4.1.3	Synthesis and Characterisation of Yellow 7-[(4,6-Dichloro-1,3,5-triazin-2-yl)amino -2-methylphenyl]azo]-1,3-Naphthalenedisulfonic Acid Dye (d_{6yt})	97
4.1.3.1	Synthesis of d_{6yt}	97
4.1.3.2	Characterisation of d_{6yt}	98
4.1.4	Synthesis and Characterisation of Modified Yellow 7-[(4-Chloro-6-(4-sulfophenoxy)-1,3,5-triazin-2-yl)amino-2-methylphenyl]azo]-1,3-Naphthalenedisulfonic Acid, Dye (d_{7ym})	101
4.1.4.1	Synthesis of d_{7ym}	101
4.1.4.2	Characterisation of d_{7ym}	101
4.1.5	Synthesis and Characterisation of Modified Yellow 7-[(4,6-(4-Sulfophenoxy)-1,3,5-triazin-2-yl)amino-2-methylphenyl]azo]-1,3-Naphthalenedisulfonic Acid Dye (d_{8ytd}).....	104
4.1.5.1	Synthesis of d_{8ytd}	104
4.1.5.2	Characterisation of d_{8ytd}	105

4.1.6	Application of Yellow Dyes ($d_{6_{yt}}$, $d_{7_{ym}}$ and $d_{8_{ytd}}$) onto Wool Fabric by Inkjet Printing	107
4.1.7	Characteristics of Formulated Inks ($d_{6_{yt}}$, $d_{7_{ym}}$ and $d_{8_{ytd}}$)	108
4.1.7.1	Surface Tension and Viscosity of Inks	108
4.1.7.2	Stability of Dye ($d_{6_{yt}}$, $d_{7_{ym}}$ and $d_{8_{ytd}}$) Based Inks	108
4.1.8	Evaluation of Percent Fixation of Yellow Dyes ($d_{6_{yt}}$, $d_{7_{ym}}$ and $d_{8_{ytd}}$) by Different Fixation Methods	111
4.1.8.1	Method 1: Batching at Room Temperature.....	111
4.1.8.2	Method 2: Batching at 65 °C.....	112
4.1.8.3	Method 3: Steaming.....	113
4.1.9	Light Fastness	114
4.1.10	Wash Fastness	114
4.2	Conclusions.....	115
4.3	References.....	116
5	Synthesis, Modification, Characterisation of Blue Dichlorotriazine Dyes and Their Application onto Wool Fabric by Inkjet Fabric	118
5.1	Experimental	118
5.1.1	Materials.....	118
5.1.2	Synthesis and Characterisation of Blue 1-Amino-4-[(3-amino-4-sulfohenyl)amino)]-Anthraquinone-2-Sulfonic Acid Dye (d_{9_b}).....	118
5.1.2.1	Synthesis of d_{9_b}	118
5.1.2.2	Characterisation of d_{9_b}	119
5.1.3	Synthesis and Characterisation of Blue 1-Amino-4-[[3-(4,6-dichloro)-1,3,5-triazin-2-yl]amino]-4-(sulfohenyl)amino)]-Anthraquinone-2-Sulfonic Acid Dye ($d_{10_{bt}}$)	121
5.1.3.1	Synthesis of $d_{10_{bt}}$	121
5.1.3.2	Characterisation of $d_{10_{bt}}$	122
5.1.4	Synthesis and Characterisation of Modified Blue 1-Amino-4-[3-(4-chloro-6-(4-sulfohenoxy)-1,3,5-triazin-2-yl)amino]-4-(sulfohenyl)amino)]-Anthraquinone-2-Sulfonic Acid Dye ($d_{11_{bm}}$)	124
5.1.4.1	Synthesis of $d_{11_{bm}}$	124
5.1.4.2	Characterisation of $d_{11_{bm}}$	125

5.1.5	Synthesis and Characterisation of Modified Blue 1-Amino-4-[3-(4,6-(4-sulfophenoxy)-1,3,5-triazin-2-yl)amino]-4-(sulfophenylamino)]-Anthraquinone-2-Sulfonic Acid Dye (d12 _{btd}).....	127
5.1.5.1	Synthesis of d12 _{btd}	127
5.1.5.2	Characterisation of d12 _{btd}	128
5.1.6	Application of Blue Dyes (d10 _{bt} , d11 _{btm} and d12 _{btd}) onto Wool Fabric by Inkjet Printing	131
5.1.7	Characteristics of Formulated Inks (d10 _{bt} , d11 _{btm} and d12 _{btd}).....	131
5.1.7.1	Surface Tension and Viscosity of Inks	131
5.1.7.2	Stability of Dye (d10 _{bt} , d11 _{btm} and d12 _{btd}) Based Inks ...	131
5.1.8	Evaluation of Percent Fixation of Blue Dyes (d10 _{bt} , d11 _{btm} and d12 _{btd}) by Different Fixation Methods	134
5.1.8.1	Method 1: Batching at Room Temperature.....	134
5.1.8.2	Method 2: Batching at 65 °C.....	134
5.1.8.3	Method 3: Steaming.....	135
5.1.9	Light Fastness	136
5.1.10	Wash Fastness	137
5.2	Conclusions.....	137
5.3	References.....	138
6	Synthesis, Modification, Characterisation of Magenta Trichloropyrimidine Dyes and Their Application onto Wool Fabric by Inkjet Printing.....	140
6.1	Introduction.....	140
6.1.1	Synthesis Route 1	141
6.1.2	Synthesis Route 2	142
6.2	Experimental	143
6.2.1	Materials.....	143
6.2.2	Conventional Heating Methods for the Synthesis of Magenta 5-[(2,5,6-trichloro-4-pyrimidinyl)amino]-4-Hydroxy-3-[(2-sulfophenyl)azo]-2,7-Naphthalenedisulfonic Acid Dye (d13 _{mp})	144
6.2.2.1	Conventional Heating Method (Route 1).....	144
6.2.2.2	Conventional Heating Method (Route 2).....	144

6.2.3	Investigation of Conventional Heating Method (Route 1) for the Synthesis of Magenta Trichloropyrimidine Dye (d13 _{mp}).....	144
6.2.3.1	Percent Conversion to d13 _{mp} Under Various Temperature	144
6.2.3.2	Percent Conversion to d13 _{mp} Under Different Molar Ratio.....	147
6.2.4	Optimisation of Microwave-Irradiated Synthesis of Dye d13 _{mp}	149
6.2.5	Comparative Study of Conventional and Microwave-Irradiated Synthesis of Dye d13 _{mp}	153
6.2.6	Synthesis of Magenta 5-[(2,5,6-Trichloro-4-pyrimidinyl)amino]-4-Hydroxy-3-[(2-sulfophenyl)azo]-2,7-Naphthalenedisulfonic Acid Dye (d13 _{mp})	155
6.2.6.1	Optimised Conventional Heating Method (Route 1).....	155
6.2.6.2	Optimised Microwave-Irradiated Method	156
6.2.6.3	Characterisation of Magenta 5-[(2,5,6-Trichloro-4-pyrimidinyl)amino]-4-Hydroxy-3-[(2-Sulfophenyl)azo]-2,7-Naphthalenedisulfonic Acid Dye (d13 _{mp})	157
6.2.7	Synthesis of Modified Magenta 5-[(2-(4-Sulfophenoxy)-5,6-dichloro-4-pyrimidinyl)amino]-4-Hydroxy-3-[(2-sulfophenyl)azo]-2,7-Naphthalenedisulfonic Acid Dye (d14 _{mpm}).....	159
6.2.7.1	Conventional Heating Method	159
6.2.7.2	Optimising Microwave-Irradiated Method	161
6.2.8	Comparative Study of Conventional and Microwave-Irradiated Synthesis of Dye d14 _{mpm}	163
6.2.9	Synthesis of Modified Magenta 5-[(2-(4-Sulfophenoxy)-5,6-dichloro-4-pyrimidinyl)amino]-4-Hydroxy-3-[(2-sulfophenyl)azo]-2,7-Naphthalenedisulfonic Acid Dye (d14 _{mpm}).....	163
6.2.9.1	Characterisation of Modified Magenta 5-[(2-(4-Sulfophenoxy)-5,6-dichloro-4-pyrimidinyl)amino]-4-Hydroxy-3-[(2-sulfophenyl)azo]-2,7-Naphthalenedisulfonic Acid Dye (d14 _{mpm})	164
6.2.10	Application of Magenta Dyes (d13 _{mp} and d14 _{mpm}) onto Wool Fabric by Inkjet Printing.....	167
6.2.11	Characteristics of Formulated Inks (d13 _{mp} and d14 _{mpm})	167
6.2.11.1	Surface Tension and Viscosity of Inks	167

6.2.11.2	Stability of Dye (d13 _{mp} and d14 _{mpm}) Based Inks	167
6.2.12	Evaluation of Percent Fixation of Magenta Pyrimidine based Dyes (d13 _{mp} and d14 _{mpm}) by Various Fixation Methods.....	169
6.2.13	Light Fastness	170
6.2.14	Wash Fastness	170
6.3	Conclusions.....	171
6.4	References.....	171
7	Synthesis, Modification, Characterisation of Blue Trichloropyrimidine Dyes and Their Application onto Wool Fabric by Inkjet Printing.....	174
7.1	Experimental	174
7.1.1	Materials.....	174
7.1.2	Conventional Heating Method for the Synthesis of Blue 1-Amino-4-[3-[(2,5,6-trichloro-4-pyrimidinyl)amino]-4-(Sulfophenyl)amino]-Anthraquinone-2-Sulfonic Acid Dye (d15 _{bp})	174
7.1.2.1	Conventional Heating Method	174
7.1.3	Investigation of Conventional Heating Method for the Synthesis of Blue Trichloropyrimidine Dye (d15 _{bp})	175
7.1.3.1	Percent Conversion to d15 _{bp} Under Various Temperature	175
7.1.3.2	Percent Conversion to d15 _{bp} Under Different Co-Solvents.....	177
7.1.4	Optimisation of Microwave-Irradiation Method for the Synthesis of Blue Trichloropyrimidine Dye d15 _{bp}	179
7.1.5	Comparative Study of Conventional and Microwave-Irradiated Synthesis of Dye d15 _{bp}	180
7.1.6	Synthesis of Blue 1-Amino-4-[3-[(2,5,6-Trichloro-4-pyrimidinyl)amino]-4-(sulfophenyl)amino]-Anthraquinone-2-Sulfonic Acid Dye (d15 _{bp}).....	181
7.1.6.1	Optimised Conventional Heating Method	181
7.1.6.2	Optimised Microwave Irradiation Method	182
7.1.6.3	Characterisation of Blue 1-Amino-4-[3-[(2,5,6-Trichloro-4-pyrimidinyl)amino]-4-(sulfophenyl)amino]-Anthraquinone-2-Sulfonic Acid Dye (d15 _{bp}).....	183

7.1.7	Synthesis of Modified Blue 1-Amino-4-[3-[[2-(4-Sulfophenoxy)-5,6-trichloro-4-pyrimidinyl]amino]-4-(sulfophenyl)amino]-Anthraquinone-2-Sulfonic Acid Dye (d16 _{bpm})	185
7.1.7.1	Conventional Heating Method	185
7.1.7.2	Optimisation of Microwave-Irradiation Method	187
7.1.8	Comparative Results of Conventional and Microwave-Assisted Synthesis of d16 _{bpm}	188
7.1.9	Synthesis of Modified Blue 1-Amino-4-[3-[[2-(4-sulfophenoxy)-5,6-trichloro-4-pyrimidinyl]amino]-4-(sulfophenyl)amino]-Anthraquinone-2-Sulfonic Acid Dye (d15 _{bp}) using Optimised Microwave-irradiation Method	189
7.1.9.1	Characterisation of Modified Blue 1-Amino-4-[3-[[2-(4-sulfophenoxy)-5,6-trichloro-4-pyrimidinyl]amino]-4-(sulfophenyl)amino]-Anthraquinone-2-Sulfonic Acid Dye (d16 _{bpm})	190
7.1.10	Application of Blue Dyes (d15 _{bp} and d16 _{bpm}) onto Wool Fabric by Inkjet Printing	192
7.1.11	Characteristics of Formulated Inks (d15 _{mp} and d16 _{bpm})	192
7.1.11.1	Surface Tension and Viscosity of Inks	192
7.1.11.2	Stability of Dye (d15 _{bp} and d16 _{bpm}) Based Inks	192
7.1.12	Evaluation of Percent Fixation of Blue Dyes (d15 _{bp} and d16 _{bpm}) by Different Fixation Methods	194
7.1.13	Light Fastness	195
7.1.14	Wash Fastness	195
7.2	Conclusions	196
7.3	References	196
8	Synthesis, Modification and Characterisation of Yellow Trichloropyrimidine Dyes for Inkjet Inks	198
8.1	Experimental	198
8.1.1	Materials	198
8.1.2	Synthesis of Yellow 7-[(2,5,6-Trichloro-4-pyrimidinyl)amino]-2-[(methylphenyl)azo]-1,3-Naphthalenedisulfonic Acid Dye (d17 _{yp})	198
8.1.2.1	Conventional Heating Method	198
8.1.2.2	Optimised Microwave-Irradiation Method	199
8.1.2.2.1	Optimised Conditions for Synthesis of d17 _{yp}	199

8.1.3	Comparative Study of Conventional and Microwave-Irradiated Synthesis of Dye d17 _{yp}	200
8.1.4	Characterisation of Yellow 7-[(2,5,6-Trichloro-4-pyrimidinyl) amino]-2-[(methylphenyl)azo]-1,3-Naphthalenedisulfonic Acid Dye (d17 _{yp}).....	201
8.1.5	Synthesis of Modified Yellow 7-[[2-(4-Sulfophenoxy)-5,6-dichloro-4-pyrimidinyl]amino]-2-[(methylphenyl)azo]-1,3-Naphthalenedisulfonic Acid Dye (d18 _{ypm}).....	203
8.1.5.1	Conventional Heating Method	203
8.1.5.2	Optimisation of Microwave-Irradiation Method	204
8.1.6	Comparative Results of Conventional and Microwave-Irradiated Synthesis of d18 _{ypm}	205
8.1.7	Characterisation of Modified Yellow 7-[[2-(4-Sulfophenoxy)-5,6-dichloro-4-pyrimidinyl]amino]-2-[(methylphenyl)azo]-1,3-Naphthalenedisulfonic Acid Dye (d18 _{ypm}).....	206
8.2	Conclusions	208
8.3	References.....	209
9	Synthesis, Modification and Characterisation of Magenta Bis-Dichlorotriazine Dye for Inkjet Inks	210
9.1	Experimental	211
9.1.1	Materials.....	211
9.1.2	Synthesis of Bis-Ethylenediamine Intermediate (d19 _{di})	211
9.1.2.1	Characterisation of Bis-Ethylenediamine Intermediate (d19 _{di})	212
9.1.3	Synthesis of Bis-Dichlorotriazine Dye (d20 _{mbt})	214
9.1.3.1	Characterisation of Bis-Dichlorotriazine Dye (d20 _{mbt}).....	215
9.1.4	Synthesis of Bis-(Monochlorotriazine/Sulfophenoxy) Dye (d21 _{bis}).....	217
9.1.4.1	Characterisation of Bis-(Monochlorotriazine/Sulfophenoxy) Dye (d21 _{bis}).....	218
9.2	Conclusions.....	220
9.3	References.....	221

10	Comparative Analysis of Synthesised Dyes-Based Inks and Commercial Jettex R Reactive Inks for Wool Fabric	222
10.1	Introduction.....	222
10.2	Materials	222
10.3	Results and Discussion	223
10.3.1	Characteristics of DyStar Inks.....	223
10.3.1.1	Surface Tension and Viscosity of Inks	223
10.3.2	Comparative Study of Percent Fixation of Inks	224
10.3.3	Light Fastness	225
10.3.4	Wash Fastness	226
10.4	Conclusions.....	227
10.5	References.....	228
11	Conclusion and Future Work	229
11.1	Conclusion	229
11.2	Future Work.....	234
	Appendix – A (List of Synthesised Dyes)	235
	Appendix – B (Printed Samples)	237
	Appendix – C (Elemental Analysis).....	244
	Appendix – D (¹H NMR).....	245

List of Figures

Figure 1.1: Chemical structure of Supramino Orange R.....	2
Figure 1.2: General structure of a reactive dye	4
Figure 1.3: Nucleophilic aromatic substitution reaction	5
Figure 1.4: Michael addition reaction	5
Figure 1.5: Chemical structure of cyanuric chloride	7
Figure 1.6: Chemical structure of 2,4,5,6-tetrachloropyrimidine	8
Figure 1.7: Schematic of the structure of a fine merino wool fibre	10
Figure 1.8: Scanning electron micrograph of wool fibre showing overlapping cuticle cells	10
Figure 1.9: Ortho-cortex and para-cortex region in wool	11
Figure 1.10: Schematic diagram showing cuticle and cortical cells surrounded by cell membrane complex	11
Figure 1.11: Typical amino acid structure	12
Figure 1.12: General structure of wool keratin polypeptide	13
Figure 1.13: Covalent bonds and non-covalent interactions in wool	13
Figure 1.14: Amphoteric behaviour of wool	14
Figure 1.15: Diffusion of dye molecules into the cortex of a wool fibre	15
Figure 1.16: Schematic representation of inkjet technologies A) continuous inkjet B) drop-on-demand inkjet.....	19
Figure 1.17: Comparison of production routes of traditional and inkjet textile printing	25
Figure 1.18: General structure of new triazine based dyes for inkjet printing	31
Figure 1.19: General structure of new pyrimidine based dyes for inkjet printing	31
Figure 1.20: General formula for modified bis-dichlorotriazine dye for Inkjet Printing	32
Figure 2.1: Schematic diagram of a capillary electrophoresis (CE) system	40
Figure 2.2: Diagrammatic representation of the CZE separation process	41
Figure 2.3: Schematic illustration of the separation principle of MEKC	42
Figure 2.4: A multiple reflection ATR system	47
Figure 2.5: Sequence of substrate preparation and inkjet printing	49

Figure 2.6: Inverted temperature gradients in microwave versus conventional heating	57
Figure 2.7: Dipolar interaction – dipolar molecules in reaction mixture will try to align with an oscillating electric field	57
Figure 2.8: Ionic conduction – charged particles in reaction mixture will follow the applied electric field	58
Figure 3.1: Electropherogram of magenta dye chromophore $d1_m$. CZE conditions: running buffer, 6mM potassium dihydrogen phosphate and acetonitrile (10% v/v) pH 9.0; pressure injection 0.5 psi for 10 s; voltage 25 kV; detection at 542 nm.....	69
Figure 3.2: FT-IR spectrum of magenta dye chromophore $d1_m$	70
Figure 3.3: Electropherograms showing reaction progress of synthesis of $d2_{mt}$. (a) Starting dye chromophore $d1_m$; (b) $d1_m - d2_{mt}$ after 0.5 hour reaction time; (c) Final product $d2_{mt}$. CZE conditions: same as Figure 3.1.	72
Figure 3.4: FT-IR spectrum of magenta dichlorotriazine dye $d2_{mt}$	73
Figure 3.5: Electropherograms showing reaction progress of synthesis of $d3_{mtm}$. (a) Starting dye $d2_{mt}$; (b) $d2_{mt} - d3_{mtm}$ after 1 hour reaction time; (c) Final product $d3_{mtm}$. CZE conditions: same as Figure 3.1.	76
Figure 3.6: FT-IR spectrum of magenta mono-substituted modified dye $d3_{mtm}$	77
Figure 3.7: Electropherograms showing reaction progress of synthesis of $d4_{mtd}$. (a) Starting dye $d2_{mt}$; (b) $d2_{mt} - d3_{mtm} - d4_{mtd}$ after 0.5 hour reaction time; (c) $d3_{mtm} - d4_{mtd}$ after 4.5 hours reaction time; (d) Final product $d4_{mtd}$. CZE conditions: same as Figure 3.1.....	80
Figure 3.8: FT-IR spectrum of magenta di-substituted dye $d4_{mtd}$	81
Figure 3.9: Electropherograms showing $d2_{mt}$ based ink stability. (a) Fresh ink; (b) Ink after one month storage at room temperature.	83
Figure 3.10: Electropherograms showing $d3_{mtm}$ based ink stability. (a) Fresh ink; (b) Ink after twelve months storage at room temperature.	84
Figure 3.11: Electropherograms showing $d4_{mtd}$ based ink stability. (a) Fresh ink; (b) Ink after twelve months storage at room temperature.	84
Figure 3.12: Percent fixation of $d2_{mt}$, $d3_{mtm}$ and $d4_{mtd}$. Fixation conditions: Batch at 65 °C for 30 to 180 minutes under moist conditions.....	86
Figure 3.13: Percent fixation of $d2_{mt}$, $d3_{mtm}$ and $d4_{mtd}$. Fixation conditions: Steaming for 5, 10, 15, 20 and 25 minutes	87
Figure 4.1: Electropherogram of yellow dye chromophore $d5_y$. MEKC conditions: running buffer, 20 mM sodium tetraborate, 50 mM sodium dodecyl sulphate (SDS), pH 9.3; pressure injection 0.5 psi for 10 s; voltage 25 kV; detection at 420 nm	96

Figure 4.2: FT-IR spectrum of yellow dye chromophore d5 _y	96
Figure 4.3: Electropherograms showing reaction progress of synthesis of d6 _{yt} . (a) Starting yellow dye chromophore d5 _y ; (b) d5 _y –d6 _{yt} after 1.5 hours reaction; (c) Final product d6 _{yt} . MEKC conditions: same as Figure 4.1.....	99
Figure 4.4: FT-IR spectrum of yellow dichlorotriazine dye d6 _{yt}	100
Figure 4.5: Electropherograms showing reaction progress of synthesis of d7 _{ym} . (a) yellow dichlorotriazine dye d6 _{yt} ; (b) d6 _{yt} – d7 _{ym} after 0.5 hour reaction; (c) Final product d7 _{ym} . MEKC conditions: same as Figure 4.1	102
Figure 4.6: FT-IR spectrum of mono-substituted yellow dye d7 _{ym}	103
Figure 4.7: Electropherograms showing reaction progress of synthesis of d8 _{ytd} . (a) yellow dichlorotriazine dye d6 _{yt} ; (b) d7 _{ym} –d8 _{ytd} after 3.5 hours reaction; (c) Final product d8 _{ytd} . MEKC conditions: same as Figure 4.1	106
Figure 4.8: FT-IR spectrum of di-substituted yellow dye d8 _{ytd}	107
Figure 4.9: Electropherograms showing d6 _{yt} based ink stability. (a) Fresh ink; (b) Ink after fifteen days storage at room temperature.....	109
Figure 4.10: Electropherograms showing d7 _{ym} based ink stability. (a) Fresh ink; (b) Ink after six months storage at room temperature	110
Figure 4.11: Electropherograms showing d8 _{ytd} based ink stability. (a) Fresh ink; (b) Ink after six months storage at room temperature	110
Figure 4.12: Percent fixation of d6 _{yt} , d7 _{ym} and d8 _{ytd} . Fixation conditions: Batch at 65 °C for 30 to 180 minutes under moist conditions	112
Figure 4.13: Percent fixation of d6 _{yt} , d7 _{ym} and d8 _{ytd} . Fixation conditions: Steaming for 5, 10, 15, 20 and 25 minutes	113
Figure 5.1: Electropherogram of blue dye chromophore d9 _b . CZE conditions: running buffer, 15mM ammonium acetate and acetonitrile (40% v/v) pH 9.3; pressure injection 0.5 psi for 10 s; voltage 25 kV; detection at 596 nm.....	120
Figure 5.2: FT-IR spectrum of blue dye chromophore d9 _b	120
Figure 5.3: Electropherograms showing reaction progress of synthesis of d10 _{bt} . (a) blue dye chromophore d9 _b ; (b) d9 _b – d10 _{bt} after 1.5 hours reaction time; (c) Final product d10 _{bt} . CZE conditions: same as Figure 5.1	123
Figure 5.4: FT-IR spectrum of blue dichlorotriazine dye d10 _{bt}	124
Figure 5.5: Electropherograms showing reaction progress of synthesis of d11 _{btm} . (a) blue dichlorotriazine dye d10 _{bt} ; (b) d10 _{bt} – d11 _{btm} after 1.5 hours reaction; (c) Final product d11 _{btm} . CZE conditions: same as Figure 5.1	126
Figure 5.6: FT-IR spectrum of blue mono-substituted dye d11 _{btm}	127

Figure 5.7: Electropherograms showing reaction progress of synthesis of d12 _{btd} . (a) blue dichlorotriazine dye d10 _{bt} ; (b) d11 _{btm} – d12 _{btd} after 4 hours reaction; (c) Final product d12 _{btd} . CZE conditions: same as Figure 5.1	129
Figure 5.8: FT-IR spectrum of blue di-substituted dye d12 _{btd}	130
Figure 5.9: Electropherograms showing d10 _{bt} based ink stability. (a) Fresh ink; (b) Ink after one month storage at room temperature.	132
Figure 5.10: Electropherograms showing d11 _{btm} based ink stability. (a) Fresh ink; (b) Ink after one month storage at room temperature	133
Figure 5.11: Electropherograms showing d12 _{btd} based ink stability. (a) Fresh ink; (b) Ink after one month storage at room temperature	133
Figure 5.12: Percent fixation of (d10 _{bt} , d11 _{btm} and d12 _{btd}). Fixation conditions: Batch at 65 °C for 30 to 180 minutes under moist conditions.....	135
Figure 5.13: Percent fixation of (d10 _{bt} , d11 _{btm} and d12 _{btd}). Fixation conditions: Steaming for 5, 10, 15, 20 and 25 minutes	136
Figure 6.1: Electropherograms showing conversion of reactants to d13 _{mp} using conventional heating method (route 1) at; (a) 50 °C; (b) 60 °C; (c) 70 °C; (d) 85 °C; (e) 100 °C. CZE conditions: running buffer, 6mM potassium dihydrogen phosphate and acetonitrile (10% v/v) pH 9.0; pressure injection 0.5 psi for 10 s; voltage 25 kV; detection at 542 nm.	146
Figure 6.2: Electropherograms showing conversion of reactants to d13 _{mp} using conventional heating method (route 1); (a) 1:1 molar ratio; (b) 1:2 molar ratio. CZE conditions: same as Figure 6.1.....	148
Figure 6.3: Electropherograms showing conversion of reactants to d13 _{mp} using microwave irradiation at; (a) 50 °C; (b) 80 °C; (c) 110 °C; (d) 130 °C. CZE conditions: same as Figure 6.1.	150
Figure 6.4: Electropherograms showing conversion of reactants to d13 _{mp} using microwave-irradiated method (sodium phosphate buffer, pH 7.0); (a) 130 °C; (b) 100 °C. CZE conditions: same as Figure 6.1	152
Figure 6.5: Comparison of reaction times, conversions and yields obtained by conventional heating and microwave irradiation (d13 _{mp})	154
Figure 6.6: Electropherograms showing reaction progress of synthesis of d13 _{mp} . (a) magenta dye chromophore d1 _m ; (b) d1 _m – d13 _{mp} after 4 hours reaction; (c) Final product d13 _{mp} . CZE conditions: same as Figure 6.1	158
Figure 6.7: FT-IR spectrum of magenta trichloropyrimidine dye d13 _{mp}	159
Figure 6.8: Electropherograms showing reaction progress of synthesis of d14 _{mpm} by conventional heating (a) magenta dye d13 _{mp} ; (b) d13 _{mp} – d14 _{mpm} after 56 hours reaction time. CZE conditions: same as Figure 6.1	161

Figure 6.9: Effect of reactant concentration on rate of reaction (d14 _{mpm}).....	162
Figure 6.10: Comparison of reaction times, conversions and yields obtained by conventional heating and microwave irradiation (d14 _{mpm}).....	163
Figure 6.11: Electropherograms showing reaction progress of synthesis of d14 _{mpm} . (a) magenta dye d13 _{mp} ; (b) d13 _{mp} – d14 _{mpm} after 2.5 hours reaction time; (c) Final product d14 _{mpm} . CZE conditions: same as Figure 6.1.....	165
Figure 6.12: FT-IR spectrum of magenta mono-substituted dye d14 _{mpm}	166
Figure 6.13: Electropherograms showing d13 _{mp} based ink stability. (a) Fresh ink; (b) Ink after eight months storage at room temperature.....	168
Figure 6.14: Electropherograms showing d14 _{mpm} based ink stability. (a) Fresh ink; (b) Ink after eight months storage at room temperature.....	168
Figure 6.15: Percent fixation of d13 _{mp} and d14 _{mpm} under various fixation methods.....	169
Figure 7.1: Electropherograms showing conversion to d15 _{bp} using conventional heating method at: (a) 50 °C; (b) 70 °C; (c) 80 °C; (d) 90 °C. CZE conditions: running buffer, 15 mM ammonium acetate and acetonitrile (40% v/v) pH 9.3; pressure injection 0.5 psi for 10 s; voltage 25 kV; detection at 596 nm.....	176
Figure 7.2: Electropherograms showing percent conversion to d15 _{bp} using conventional heating method: (a) Water-acetone; (b) Water-ethanol. CZE conditions: same as Figure 7.1.	178
Figure 7.3: Electropherograms showing percent conversion to d15 _{bp} using microwave-irradiation method: (a) Water-acetone (Na ₂ CO ₃) at 80 °C; (b) Sodium phosphate buffer pH 7.0 at 85 °C; (c) Sodium phosphate buffer pH 7.0 at 100 °C. CZE conditions: same as Figure 7.1.....	179
Figure 7.4: Comparison of reaction times, conversions and yields obtained by conventional heating and microwave heating.....	181
Figure 7.5: Electropherograms showing reaction progress of synthesis of d15 _{bp} . (a) blue dye chromophore d9 _b ; (b) d9 _b – d15 _{bp} after 1.5 hours reaction time; (c) final product d15 _{bp} . CZE conditions: same as Figure 7.1.....	184
Figure 7.6: FT-IR spectrum of blue trichloropyrimidine dye d15 _{bp}	185
Figure 7.7: Electropherograms showing reaction progress of synthesis of d16 _{bpm} . (a) blue dye d15 _{bp} ; (b) d15 _{bp} – d16 _{bpm} after 72 hours reaction time. CZE conditions: same as Figure 7.1.....	186
Figure 7.8: Comparison of reaction times, conversions and yields obtained by conventional heating and microwave irradiation (d16 _{bpm}).....	188

Figure 7.9: Electropherograms showing reaction progress of synthesis of d16 _{mpm} . (a) blue dye d16 _{mpm} ; (b) d15 _{mp} – d16 _{mpm} after 3.5 hours reaction time; (c) Final product d16 _{mpm} . CZE conditions: same as Figure 7.1	190
Figure 7.10: FT-IR spectrum of blue mono-substituted dye d16 _{bpm}	191
Figure 7.11: Electropherograms showing d15 _{bp} based ink stability. (a) Fresh ink; (b) Ink after three months storage at room temperature	193
Figure 7.12: Electropherograms showing d16 _{bpm} based ink stability. (a) Fresh ink; (b) Ink after three months storage at room temperature	193
Figure 7.13: Percent fixation of d15 _{bp} and d16 _{bpm} under various fixation methods.....	194
Figure 8.1: Comparison of reaction times and yields obtained by conventional heating and microwave heating	201
Figure 8.2: Electropherograms showing reaction progress of synthesis of d17 _{yp} . (a) yellow dye chromophore d5 _y ; (b) d5 _y – d17 _{yp} after 30 min reaction time; (c) final product d17 _{yp} . MEKC conditions: running buffer, 20 mM sodium tetraborate, 50 mM sodium dodecyl sulphate (SDS), pH 9.3; pressure injection 0.5 psi for 10 s; voltage 25 kV; detection at 420 nm.....	202
Figure 8.3: FT-IR spectrum of yellow trichloropyrimidine dye d17 _{yp}	203
Figure 8.4: Comparison of reaction times and yields obtained by conventional heating and microwave irradiation (d18 _{ypm})	205
Figure 8.5: Electropherograms showing reaction progress of synthesis of d18 _{ypm} . (a) yellow dye d17 _{yp} ; (b) d17 _{yp} – d18 _{ypm} after 30 min reaction time; (c) Final product d18 _{ypm} . MEKC conditions: same as Figure 8.2	207
Figure 8.6: FT-IR spectrum of yellow mono-substituted dye d18 _{ypm}	208
Figure 9.1: Electropherograms showing reaction progress of synthesis of d19 _{di} . (a) Starting dye d2 _{mi} ; (b) d2 _{mi} – d19 _i after 0.5 hours reaction time; (c) d19 _i – d19 _{di} after 3 hours reaction time; (d) Final product d19 _{di} . CZE conditions: running buffer, 6mM potassium dihydrogen phosphate and acetonitrile (10% v/v) pH 9.0; pressure injection 0.5 psi for 10 s; voltage 25 kV; detection at 542 nm.....	213
Figure 9.2: FT-IR spectrum of bis-ethylenediamine intermediate d19 _{di}	214
Figure 9.3: Electropherograms showing reaction progress of synthesis of d20 _{mbt} . (a) Starting intermediate d19 _{di} ; (b) d19 _{di} – d20 _{mbt} after 1.5 hours reaction time; (c) Final product d20 _{mbt} . CZE conditions: same as Figure 9.1	216
Figure 9.4: FT-IR spectrum of bis-dichlorotriazine dye d20 _{mbt}	217

Figure 9.5: Electropherograms showing reaction progress of synthesis of $d21_{bis}$. (a) Starting intermediate $d20_{mbt}$; (b) $d20_{mbt} - d21_{bis}$ after 3 hours reaction time; (c) Final product $d21_{bis}$. CZE conditions: same as Figure 9.1	219
Figure 9.6: FT-IR spectrum of bis-sulfophenoxy dye ($d21_{bis}$)	220
Figure 10.1: Comparison of percent fixation of magenta inks	224
Figure 10.2: Comparison of percent fixation of blue inks	224
Figure 10.3: Comparison of percent fixation of yellow inks	224
Figure 11.1: Optimal conditions for Microwave-irradiated synthesis of trichloropyrimidine dyes	232
Figure 11.2: Optimal conditions for Microwave-irradiated synthesis of modified mono-substituted dyes	233

List of Schemes

Scheme 1.1: Reduction of wool by sodium bisulfite	29
Scheme 3.1: Hydrolysis of dichlorotriazine dye	65
Scheme 3.2: Diazotisation of 2-aminobenzenesulfonic acid with nitrous acid leads to diazonium salt	67
Scheme 3.3: Azo coupling of diazonium salt with H-acid to form magenta dye chromophore $d1_m$	68
Scheme 3.4: Preparation of condensation product $d2_{mt}$ from magenta azo chromophore and cyanuric chloride	71
Scheme 3.5: Mono substitution of dye $d2_{mt}$ with 4HBSA to yield dye $d3_{mtm}$	75
Scheme 3.6: Preparation of di-substituted dye $d4_{mtd}$ from magenta dichlorotriazine dye $d2_{mt}$ and 4HBSA	78
Scheme 4.1: Diazotization of 7-amino-1,3-naphthalenedisulfonic acid with nitrous acid to form diazonium salt	94
Scheme 4.2: Coupling of diazonium salt with m-toluidine to yield $d5_y$	95
Scheme 4.3: Preparation of condensation product $d6_{yt}$ from yellow azo chromophore and cyanuric chloride	98
Scheme 4.4: Mono substitution of dye $d6_{yt}$ with 4HBSA to yield dye $d7_{ytm}$	101
Scheme 4.5: Preparation of di-substituted $d8_{ytd}$ from yellow dichlorotriazine dye $d6_{yt}$ and 4HBSA	105
Scheme 5.1: Synthesis of $d9_y$ by Ullmann coupling reaction	119
Scheme 5.2: Preparation of condensation product $d10_{bt}$ from blue anthraquinone chromophore and cyanuric chloride	122
Scheme 5.3: Condensation of dye $d10_{bt}$ with 4HBSA to yield dye $d11_{btm}$	125
Scheme 5.4: Preparation of di substituted dye $d12_{btd}$ from blue dichlorotriazine dye $d10_{bt}$ and 4HBSA	128
Scheme 6.1: Condensation of 2,4,5,6-tetrachloropyrimidine with dye chromophore ^[6]	141
Scheme 6.2: Substitution of 2,5,6-trichloropyrimidine dye	141
Scheme 6.3: Route 2 for the synthesis of trichloropyrimidine dyes [7]	142
Scheme 6.4: Condensation of tetrachloropyrimidine with magenta dye chromophore $d1_m$ to yield $d13_{mp}$ by conventional heating method	155

Scheme 6.5: Condensation of tetrachloropyrimidine with magenta dye chromophore $d1_m$ to yield $d13_{mp}$ by microwave-irradiated method.....	156
Scheme 6.6: Mono substitution of dye $d13_{mp}$ with 4HBSA to yield dye $d14_{mpm}$ by conventional heating.....	160
Scheme 6.7: Mono substitution of dye $d13_{mp}$ with 4HBSA to yield dye $d14_{mpm}$ with microwave irradiation.....	164
Scheme 7.1: Condensation of 2,4,5,6-tetrachloropyrimidine with blue dye chromophore $d9_b$ to yield $d15_{bp}$ by conventional heating method.....	182
Scheme 7.2: Condensation of 2,4,5,6-tetrachloropyrimidine with blue dye chromophore $d9_b$ to yield $d15_{bp}$ by microwave irradiation method.....	183
Scheme 7.3: Mono substitution of dye $d15_{bp}$ with 4HBSA to yield dye $d16_{bpm}$ by conventional heating.....	186
Scheme 7.4: Mono substitution of dye $d15_{bp}$ with 4HBSA to yield dye $d16_{bpm}$ by microwave irradiation.....	189
Scheme 8.1: Condensation of 2,4,5,6-tetrachloropyrimidine with yellow dye chromophore $d5_y$ to yield $d17_{yp}$ by conventional and microwave irradiation method	200
Scheme 8.2: Mono substitution of dye $d17_{yp}$ with 4HBSA to yield dye $d18_{ypm}$ by conventional and microwave irradiation	205
Scheme 9.1: Condensation reaction of $d2_{mt}$ with ethylenediamine	212
Scheme 9.2: Condensation of cyanuric chloride with $d19_{di}$ (intermediate) to yield $d20_{mbt}$	215
Scheme 9.3: Synthesis of bis-sulfophenoxy dye $d21_{bis}$	218

List of Tables

Table 1.1: Reactive groups in Reactive dyes for wool	6
Table 1.2: Comparison between rotary screen printing and inkjet printing	24
Table 1.3: Selection of dyes for inkjet printing of textiles	27
Table 2.1: CE buffer systems for reactive dyes	43
Table 2.2: TLC eluents for reactive dyes	45
Table 2.3: Pre-treatment padding recipe	49
Table 2.4: Solvent–non-solvent mixtures used for the purification of dyes	50
Table 2.5: Ink Recipe	51
Table 2.6: Batching temperatures for fixation	52
Table 2.7: Test conditions for wash fastness	55
Table 3.1: Surface tension and viscosity of magenta inks	82
Table 3.2: Percent Fixation of $d2_{mt}$, $d3_{mtm}$ and $d4_{mtd}$. Fixation conditions: Batching at RT for 2 and 4 hours under moist conditions	85
Table 3.3: Light fastness of magenta dyes ($d2_{mt}$, $d3_{mtm}$ and $d4_{mtd}$) compared to target blue wool reference 6	88
Table 3.4: Wash fastness of magenta dyes ($d2_{mt}$, $d3_{mtm}$ and $d4_{mtd}$)	89
Table 4.1: Surface tension and viscosity of yellow inks	108
Table 4.2: Percent fixation of $d6_{yt}$, $d7_{ytm}$ and $d8_{ytd}$. Fixation conditions: Batching at 25 °C for 2 and 4 hours under moist conditions	111
Table 4.3: Light fastness of yellow dyes ($d6_{yt}$, $d7_{ytm}$ and $d8_{ytd}$) compared to target blue wool reference 6	114
Table 4.4: Wash fastness of yellow dyes ($d6_{yt}$, $d7_{ytm}$ and $d8_{ytd}$)	115
Table 5.1: Surface tension and viscosity of blue Inks	131
Table 5.2: Percent fixation of $d10_{bt}$, $d11_{btm}$ and $d12_{btd}$. Fixation conditions: Batching at RT for 2 and 4 hours under moist conditions	134
Table 5.3: Light fastness of blue dyes ($d10_{bt}$, $d11_{btm}$ and $d12_{btd}$) compared to target blue wool reference 6	137
Table 5.4: Wash fastness of blue dyes ($d10_{bt}$, $d11_{btm}$ and $d12_{btd}$)	137
Table 6.1: Summary of results with conventional heating (route 1) at various temperatures	147

Table 6.2: Summary of results from conventional heating (route 1) at different molar ratios	148
Table 6.3: Optimisation of reaction temperature for microwave-irradiated condensation reaction	151
Table 6.4: Modification of reaction conditions for microwave irradiated condensation reaction	153
Table 6.5: Optimisation of reaction conditions for microwave-irradiated synthesis of d14 _{mpm}	162
Table 6.6: Modification of reaction conditions for microwave irradiated synthesis of d14 _{mpm}	162
Table 6.7: Ink properties	167
Table 6.8: Light fastness of magenta dyes (d13 _{mp} and d14 _{mpm}) compared to target blue wool reference 6	170
Table 6.9: Wash fastness of magenta dyes (d13 _{mp} and d14 _{mpm})	170
Table 7.1: Summary of results with conventional heating at various temperatures.....	177
Table 7.2: Summary of results from conventional heating using different co-solvents	178
Table 7.3: Optimisation of reaction conditions for microwave-irradiated condensation reaction	180
Table 7.4: Optimisation of reaction conditions for microwave-irradiated condensation reaction	187
Table 7.5: Ink measured properties.....	192
Table 7.6: Light fastness of blue dyes (d15 _{bp} and d16 _{bpm}) compared to target blue wool reference 6	195
Table 7.7: Wash fastness of blue dyes (d15 _{bp} and d16 _{bpm}).....	195
Table 10.1: Comparative results of surface tension and viscosity of Inks	223
Table 10.2: Comparative results of light fastness of Inks	226
Table 10.3: Comparative results of wash fastness of Inks	227

Preface

The first two chapters of this thesis describe literature review and general procedures and instrumentation used in this study, followed by seven chapters each presenting synthesis, modification, characterisation, application of parent and novel modified dyes on wool via inkjet and evaluation of their properties. Moreover, the last two chapters present the comparative analysis of inks and conclusions and future work.

The first chapter gives a broad overview of reactive dyes, wool fibre and inkjet printing, with the second chapter providing descriptions of analytical techniques used in this study, the new microwave irradiation method adopted successfully for the synthesis of difficultly synthesised pyrimidine based dyes followed by a procedure of inkjet printing, as well as other tools and methodologies used.

Chapter three, four and five presents synthesis, modification, characterisation and application of magenta, yellow and blue (hue) dyes based on chlorotriazine chemistry respectively. It is shown that modification of chlorotriazine based dyes by replacing one or both labile chlorine(s) by sulfophenoxy group(s) is advantageous and significantly enhanced percent fixation along with stability of dyes in ink formulations. Moreover, novel modified dyes exhibit excellent colour fastness properties.

Chapter six, seven and eight presents a synthesis, modification, characterization and application of chloropyrimidine based dyes in magenta, blue and yellow (hue) by conventional and Microwave-irradiation method respectively. Taking advantage of Microwave-irradiated method new, quick, efficient and high yielding procedure for the synthesis of dyes is developed, which is superior to previously published methods in all aspects, including conversion to products, yields and reaction times.

It is shown that modification of chloropyrimidine based dyes by replacing the one labile chlorine by sulfophenoxy group is advantageous and marginally enhanced percent fixation along with the stability of dyes in ink formulations. Moreover, modified dyes exhibit excellent colour fastness properties. Due to time limitation yellow inks were not evaluated to the full extent.

Chapter nine presents a synthesis, modification and characterization of magenta bis-(monochlorotriazine/sulfophenoxy) dye. However, due to time limitation these inks were also not evaluated to the full extent.

Chapter ten presents the comparative analysis of commercially available and successful Jettex R Inks with properties of synthesised dyes based inks.

Chapter eleven concludes the experimental results of this study, summaries the finding of the current research and provides a suggestion of the future works.

1 Introduction

1.1 Reactive Dyes

Fibre-reactive dyes are coloured compounds that are capable of forming a covalent bond between the reactive groups of the dye molecule and the fibre ^[1-4]. Consequently, in reacting, they become part of the fibre. Usually bonding occurs between a carbon atom of the dye molecule and an oxygen, nitrogen or sulfur atom of a hydroxy, amino or mercapto group respectively of the textile substrate ^[1]. Due to the strength of covalent bond, reactive dyes once applied to the textile substrate resist removal and as a consequence show outstanding wash fastness properties ^[4, 5], which ensure their wide application in textile colouration. In general, reactive dyes are the only textile colorants designed to bond covalently with the substrate on application. They are used for the dyeing and printing of cellulose and to a lesser extent wool fibres. They are valued for their brilliance, variety of hue, their flexibility in application and the all-round good fastness properties ^[6].

Most of the reactive dyes are water soluble, easily applied and because the reactive group may be attached to almost any coloured molecular system, can be used to produce both very bright and very dull shades of all colours. Because of their distinctive advantages, the reactive dyes generally, have made a greater impact on dyeing technology in the few years since their introduction than any other class of dyes in so short time.

Reactive dyes are becoming progressively popular for dyeing and printing wool fibres because of their wide shade range, ease of application and excellent wash fastness properties. Improvement in the structure of reactive dyes such as type and number of reactive groups led to an increased use of reactive dyes ^[7].

Commercial fibre-reactive dyes have been developed for both wool and polyamide but, undoubtedly, the major success has been in the application to cotton and cotton blends.

1.1.1 History of Reactive Dye Development

In 1931 IG Farben Industries patented ^[8, 9] and marketed an acid dye ^[10, 11] containing a chloroacetylamino side chain under the name Supramino Orange R (Figure 1.1). At that time the very good wash-fastness properties of Supramino Orange R were not put down to dye-fibre covalent bonding rather it was believed that increased molecular mass through incorporating a chlorine atom in the side chain was the reason for the enhanced fastness properties.

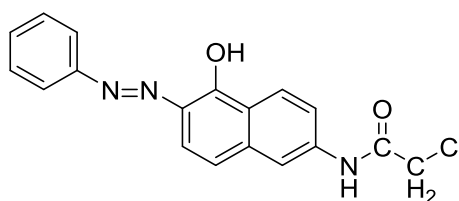


Figure 1.1: Chemical structure of Supramino Orange R

In 1937, a German patent published indicated that dyes could be firmly attached to wool by covalent interactions ^[12].

Ciba ^[13] described reactive dyes for wool containing β -chloro propionylamino groups and recognised the suitabilities of β -chloro propionylamino dyes, which are in most cases freely water-soluble and possess less affinity for the continuous dyeing and printing of cellulosic fibres ^[14].

In a BASF patent containing β -sulfonylpropionamide dyes, sulfonyl group is described and claimed in anthraquinone, azo and phthalocyanine dyes.

From 1948 onwards, Heyna and Schuhmacher and Hoechst concentrated on dyes containing either a vinylsulfone group or a vinylsulfone precursor that led to the marketing of the Remalan dyes for wool in 1952. Patentees did not realise that these were in fact reactive dyes ^[11]. These dyes gave dyeings of high wash fastness on wool, although the improved fastness was not publicly attributed to the formation of a covalent bond between dye and fibre ^[12].

In 1954, Ciba introduced a range of bright reactive dyes for wool under the name Cibalan with improved wash fastness properties which contained the chloroacetamido group originally employed in Supramine Orange R. Once again, there was no public statement of their ability to form covalent bonds with the substrate during dyeing ^[12].

1.1.1.1 First Commercial Ranges of Reactive Dyes for Cellulosic Fibres

The first recognised range of reactive dyes was developed by Rattee and Stephen and marketed by ICI in 1956 under the trade name *Procion*, for use on cellulosic fibres ^[15].

Patenting new reactive dye systems then became intensive as other major dye manufacturing companies rushed to get into this promising area. Hoechst revisited their Remalan Fast wool dyes as mentioned earlier, and quickly devised application conditions making the vinylsulfone dyes suitable for cellulose fibre coloration, thus launching the very successful Remazol range of dyes in 1957 ^[11].

Geigy ^[16] and Sandoz ^[17] developed the less activated pyrimidine ring system and launched 2,5,6-trichloropyrimidine dyes in 1959. Bayer devised the 2,3-dichloroquinoxaline Levafix E dyes and marketed them in 1961.

In all the above, the major drive was to develop molecules to dye cellulose to the widest possible shade gamut giving dyeings of good wash fastness; thus wool where much of the reactive dye innovation started was temporarily side-lined.

1.1.1.2 First Commercial Ranges of Reactive Dyes for Polyamide Fibres

As discussed previously, wool featured highly in the early developments of reactive dyes; in particular Supramino Orange R (IG Ferben), Cibalan Brilliant (Ciba) and Remalan and Remalan Fast (Hoechst). However, probably as wool had only a small share of the textile fibre market; it seemed that the marketing push for selling these dyes as fibre reactive systems was somehow lacking ^[11]. Generally it can be said that only with the advent of truly machine-washable wool in the late 1960s was there sufficient stimulation of the market to encourage widespread use of these dyes on wool ^[18].

1.1.2 Structure of Reactive Dyes

The characteristic structural features of reactive dyes are shown schematically in Figure 1.2, and consist of;

1. Chromophore
2. One or more water-solubilising group
3. Bridging group
4. Reactive group

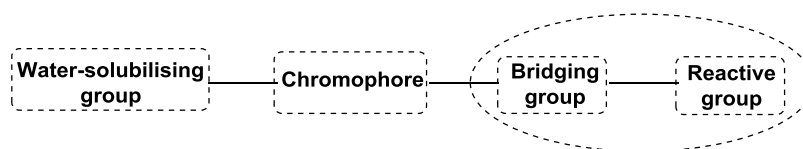


Figure 1.2: General structure of a reactive dye

1.1.2.1 Chromophore

The chromophore is a conjugated double bond system. It is the colour producing part of any dye molecule. Reactive dyes may be prepared in principle from any of the chemical classes of colorant by attaching a fibre reactive group to an appropriate molecule ^[19]. The only structural features necessary are a sufficiency of sulfonic acid groups to ensure adequate water solubility and an amino group to which the reactive group can be attached ^[20].

In practice, most of the reactive dyes belong to the azo chemical class, especially in the yellow, orange and red shade area. Moreover, anthraquinones are used for the preparation of blue reactive dyes ^[2, 20].

1.1.2.2 Solubilising Groups

Solubilising groups provide water solubility, substantivity, migration and ease wash off after dyeing. All reactive dyes contain sodium sulfonate groups for solubility, and dissolve in water to give coloured sulfonate anions and sodium cations both of them are extremely attracted to water and become heavily hydrated. Most reactive dyes have from one to four of these sulfonate groups ^[1].

1.1.2.3 Bridging Group

A bridging group is the group that links the reactive group to the chromophore. The bridging group is necessary for ease of synthesis in order to attach reactive groups to the chromophore. The connecting function of the bridging group can influence the reactivity of the reactive group, degree of fixation, and stability of reactive dyeing ^[2]. The -NH- group is a typical bridging group especially for heterocyclic reactive dyes.

1.1.2.4 Reactive Group

In theory, any group that is capable of reacting with sites in the fibre, *e.g.* hydroxyl groups in cellulosic fibres, and amino and thiol groups in wool, is a

potential reactive group to be incorporated in a reactive dye [12]. In practice there are many restrictions on the type of reactive group employed, such as level of reactivity, stability to hydrolysis, stability of the dye-fibre bond, and, not least, cost and ease of manufacture.

The majority of reactive dyes can be distinguished into two categories depending upon their mode of reaction with fibres, i.e, nucleophilic aromatic substitution and Michael addition reaction. [12, 21].

1.1.2.4.1 Nucleophilic Aromatic Substitution [12]

Reactive dyes with triazine, pyrimidine, quinoxaline, chloroacetamido, and β -sulfatoethylsulfamoyl groups (shown in Table 1.1) as the reactive groups react with the fabric by nucleophilic aromatic substitution. The overall reaction can be represented as Figure 1.3;

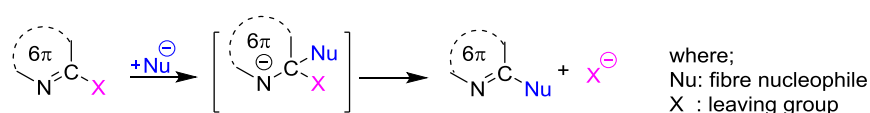


Figure 1.3: Nucleophilic aromatic substitution reaction

1.1.2.4.2 Michael Addition [12]

Reactive dyes with vinylsulfone, acrylamido and α -bromoacrylamido groups as the reactive groups (shown in Table 1.1) function as activated Michael type acceptors. With these types of dyes, covalent bond formation is by the 1,2-*trans* addition of a nucleophile in the fibre across a polarised ethylenic bond. The overall reactions can be represented as Figure 1.4;

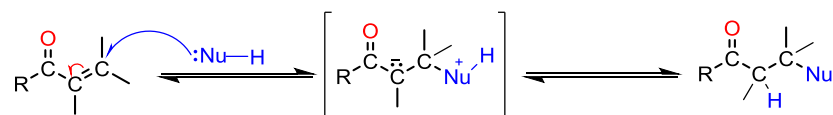
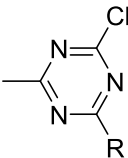
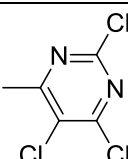
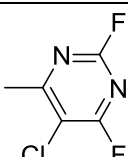
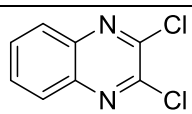


Figure 1.4: Michael addition reaction

1.1.3 Reactive Groups for Wool

The introduction of reactive dyes was an outstanding achievement in the dye chemistry in the later part of the 20th Century. Comprehensive details of developments in the field of reactive dyes are available in the literature [9, 12, 18, 22-26]. However, the main reactive groups suitable for wool are summarised in Table 1.1.

Table 1.1: Reactive groups in Reactive dyes for wool ^[27]

Reactive Groups	Structure	Dye range
Triazinyl (monochloro-, R = NHR')		Procion H (ICI) Cibacron, Cibacrolan (Ciba)
Triazinyl (dichloro-, R = Cl)		Reaction (Geigy) Drimaren (Sandoz)
Pyrimidinyl (2,4-difluoro-5-chloro-)		Drimalan F (Sandoz) Verofix (Bayer) Reactolan (Geigy)
Quinoxaliny (dichloro-)		Levafix E (Bayer)
Chloroacetamido	-NHCOCH ₂ Cl	Cibalanbrilliant (Ciba)
β-Sulphatoethylsulphamoyl	-SO ₂ NRCH ₂ CH ₂ OSO ₃ H	Drimalan (Sandoz)
Vinyl sulphonyl	-SO ₂ CH=CH ₂	Levafix (Bayer)
Acrylamido	-NHCOCH=CH ₂	Remalan, Remazol,
α-Bromoacrylamido	-NHCOC(Br)=CH ₂	Remazolan, Hostalan (Hoechst)

1.1.3.1 Triazine

The work of Rattee and Stephen ^[15] in inventing reactive dyes for cotton represented a major breakthrough in the development of dyes for cellulosic fabrics and was reliant upon the commercial availability and reactivity of an intermediate, 1,3,5-trichlorotriazine, generally known as cyanuric chloride (Figure 1.5).

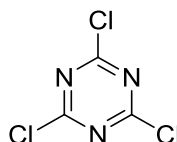


Figure 1.5: Chemical structure of cyanuric chloride

Cyanuric chloride has been known since 1827 ^[25] and has been widely used in pesticides, rubber, explosives and medicinal industries ^[28]. In cyanuric chloride a partial positive charge resides on each alternating carbon atom, adjacent to two electronegative nitrogen atoms and the presence of three highly electronegative chlorine atoms directly attached to the carbon atoms also enhances the positive charge density on the carbon atoms, and hence makes them more susceptible to nucleophilic attack.

With the invention of the first successful reactive dyes for cellulose, Rattee and Stephen ^[15] demonstrated that dyes containing a dichlorotriazine group, under alkaline conditions, could become attached to the cotton through covalent bond formation.

The dichlorotriazine group was introduced into the dye molecule by reaction of an amino containing dyebase with cyanuric chloride to give the reactive dichlorotriazine dye.

The facile reaction of dyebase with cyanuric chloride generally takes place in aqueous medium at around 0 – 5 °C. Replacement of an electronegative chlorine atom by an electron donating amino substituent ensures that the reactivity of the remaining chlorine atoms, towards the further nucleophilic attack, is less than that of cyanuric chloride.

The unique behaviour of cyanuric chloride made possible the efficient manufacture of both dichlorotriazine and monochlorotriazine.

The success of the dichlorotriazine system opened the door for researchers, who immediately began extensive research in this field resulted in the subsequent introduction of Procion H and Cibacron H dyes from ICI and Ciba respectively ^[29]. Inspection of the academic and patent literature indicates that much effort was directed to the evaluation of other nucleophilic groups as potential fibre reactive groups ^[25, 29-31].

1.1.3.2 Diazine

In addition to triazine, 1,3-diazine (pyrimidine) is technically the most important heterocyclic system ^[25]. In pyrimidines the lower reactivity, relative to triazines, is due to the presence of one less ring nitrogen atom ^[2, 25]. Depending on the bridging group, substituents and leaving groups, pyrimidine permits wider range of variations than triazine in regard to the application properties such as reactivity, ease of washing-off and fastness properties ^[32].

The trichloropyrimidine group was introduced into the dye molecule by condensation reaction of an amino based chromophore with 2,4,5,6-tetrachloropyrimidine (shown in Figure 1.6). However, on account of their low reactivity, chloropyrimidines react slowly with amines and are difficult to complete and suffers poor yields ^[25].

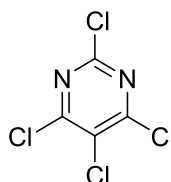


Figure 1.6: Chemical structure of 2,4,5,6-tetrachloropyrimidine

The reactions (nucleophilic aromatic substitution) that cyanuric chloride and 2,4,5,6-tetrachloropyrimidine undergo, are of special importance in two ways:

- 1 Firstly, synthesis of the reactive dyes themselves along with any further modification of ring;
- 2 Secondly, enabling covalent bond formation with fibre.

1.1.4 Multifunctional Reactive Dyes

The functionality of a reactive dye corresponds to the number of reactive groups present in the molecule. The reactive groups may be similar or may differ in chemical constitution. In order to maximise the level of dye fixation, ICI introduced the Procion WE range of dyes, which contain two monochlorotriazine reactive groups. Hydrolysis of one of the reactive groups leaves the other one intact, which is still capable of reacting with fibre. These dyes thus fix to fibre more efficiently resulting in less coloured effluent and greater economy.

Mixed or heterobifunctional reactive dyes *i.e.* dyes having two different reactive groups are claimed to give major advantages (example wide temperature range of application, better dye–fibre bond stability) as compared to monofunctional or homo bifunctional reactive dyes. These types of dyes were designed exclusively in which the two reactive groups are of substantially different reactivities. Only very few dyes with functionalities greater than two have reached marketability and commercialisation and most of these are tri-functional^[25]. Advantages of increasing the number of independent reactive groups on a dye molecule are increased fixation and lower amounts of unreacted and/or hydrolysed dye present in waste water^[33]. Disadvantages include increased washing times of dyed substrates due to higher affinity of the hydrolysed or unfixated dye for the fibre.

1.2 Wool

Wool is the most complex and versatile of all textile fibres. It can be used to make products as diverse as cloth for billiard tables to the finest woven and knitted fabrics. The insulating and moisture absorbing properties of the fibre make fine wool products extremely comfortable to wear. The chemical composition of wool enables it to be easily dyed in shades ranging from pastels to full, rich colours.

1.2.1 Fibre Morphology^[34]

Wool is a staple fibre from the fleece of various breeds of sheep. It is a multicellular, protein hair that tapers from the root to a point. Fibre lengths vary from 4 to 40 cm and diameters from 17 to 40 μm . Wool fibres have complicated structures. The main components are the scaly cuticle, the body of the fibre or cortex, and the cell membrane complex (CMC). The latter surrounds the cells of both the cuticle and cortex in a continuous phase. Coarse fibres may also have a medulla or inner core. The schematic structure of fine wool and complex physical structure of the cuticle cells are shown in Figure 1.7 and Figure 1.8.

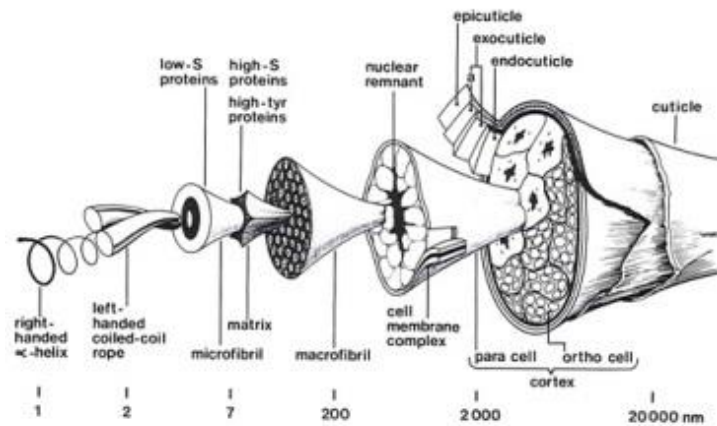


Figure 1.7: Schematic of the structure of a fine merino wool fibre adapted from reference [35]

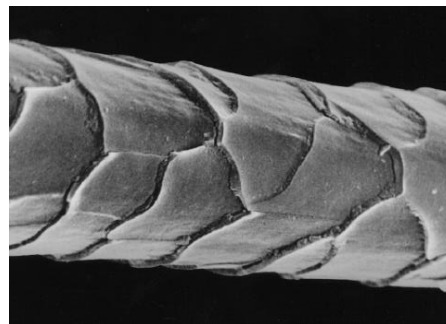


Figure 1.8: Scanning electron micrograph of wool fibre showing overlapping cuticle cells adapted from reference [35]

Microscopic examination shows the scales on the fibre surface that are characteristic of most animal fibres. The overlapping scales point towards the fibre tip. In a fine wool, they constitute about 10% of the fibre. The friction generated by these scales hinders the movement of the wool fibre in the direction of the tip. This is called the directional friction effect and is partly responsible for the felting and shrinkage of wool articles on washing. The scales consist of several layers and are covered with a hydrophobic outer layer called the epicuticle. It is part of the cell membrane complex and covers all the fibre, except the tip where it has been worn away by weathering.

The cortex is composed of spindle-shaped cells made up of fibrils of keratin, in a matrix of high-sulfur proteins, and surrounded by the cell membrane complex. It comprises about 90% of the wool fibre. In fine wools, the cortex appears as two distinct regions rather like two half-cylinders stuck together along their axes.

These two regions, shown in Figure 1.9, are known as orthocortex and paracortex. They spiral around each other along the fibre, following the crimp, the orthocortex always being oriented towards the outside of the crimp wave. This structure is similar to that in a bicomponent synthetic fibre. The crimp arises from the unequal rates of hardening of the keratin that begins in the hair follicle, but occurs at different levels on each side of the wool hair. These two cortical regions differ in structure and reactivity. Basic dyes stain the more accessible orthocortex cells but acid dyes show no preference for either cortex.

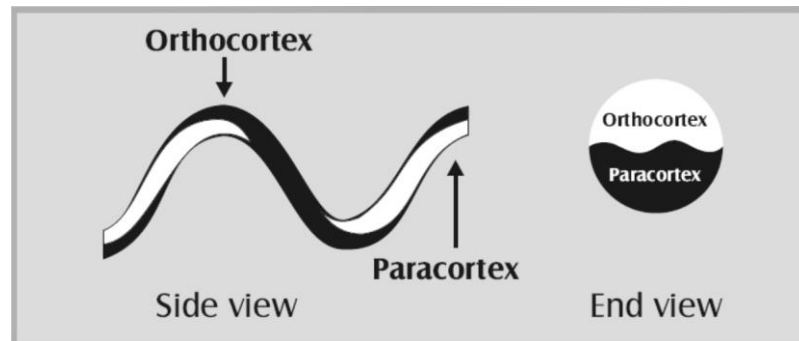


Figure 1.9: Ortho-cortex and para-cortex region in wool adapted from reference ^[36]

The cell membrane complex, shown in Figure 1.10 consists mainly of protein and lipid materials and surrounds all types of cells in a continuous network throughout the fibre. It forms a region of poor mechanical strength compared to the rest of the fibre and fractures first during fibre abrasion, leading to fibrillation into the individual cortical cells or even into protein fibrils within the cells. The membrane complex is weakened by extended dyeing at the boil in acidic solution.

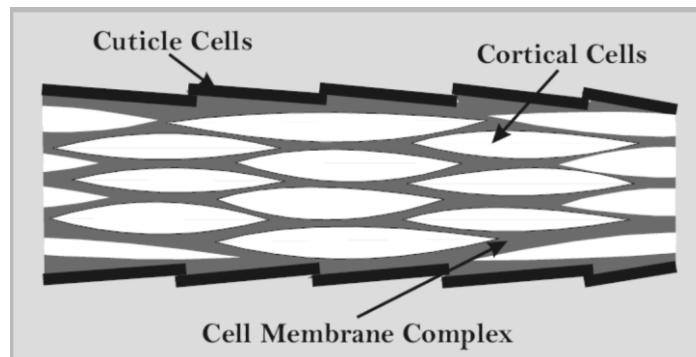


Figure 1.10: Schematic diagram showing cuticle and cortical cells surrounded by cell membrane complex adapted from reference ^[36]

The medulla, if present, is a central core of cells that may contain coloured pigments. It does not run the entire length of the fibre and there may be hollow spaces.

The structure of the proteins in wool differs between the various regions of the fibre. Some of the proteins in the microfibrils are helical, like a spring, which gives the wool its flexibility, elasticity, resilience and good wrinkle recovery properties. Other proteins, particularly in the matrix that surrounds the microfibrils, have a more amorphous structure and are responsible for wool's advantage over other fibres of absorbing a relatively large amount of water without feeling wet (up to around 30% of the mass of the dry fibre). The matrix proteins are also responsible for wool's property of absorbing and retaining large amounts of dyes.

1.2.2 Composition of Wool

Wool is a member of a group of proteins known as keratins. Clean wool contain 82% of the keratinous proteins, 17% of nonkeratinous proteins and approximately 1% nonproteinaceous material such as waxy lipids ^[37].

1.2.3 Chemical Structure

The structure of wool has been studied extensively over many years and is described in far more detail in the literature ^[12, 38-40].

Wool kartin is consist of α -amino acids, which have the general formula shown in Figure 1.11, where the side chain R can be aliphatic, aromatic or other cyclic group.

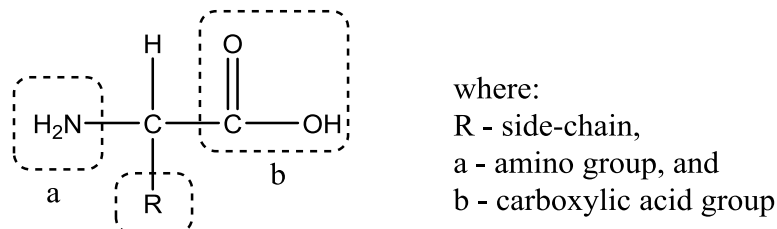


Figure 1.11: Typical amino acid structure

The simplest structure of wool keratin is that of the polypeptide chain formed by the condensation of α -amino acids, with the residues arranged in a manner shown in Figure 1.12, where R₁, R₂, R₃ amino acid side-chains.

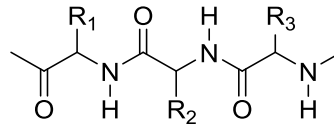


Figure 1.12: General structure of wool keratin polypeptide

The side-chains of various amino acids vary in size and chemical nature. Hence, they are grouped according to their chemical nature such as nonpolar hydrocarbons, polar hydrocarbons, acidic, basic, and amino acids that contain sulfur.

The individual peptide chains in wool are held together by various types of covalent bonds and noncovalent interactions, shown in Figure 1.13.

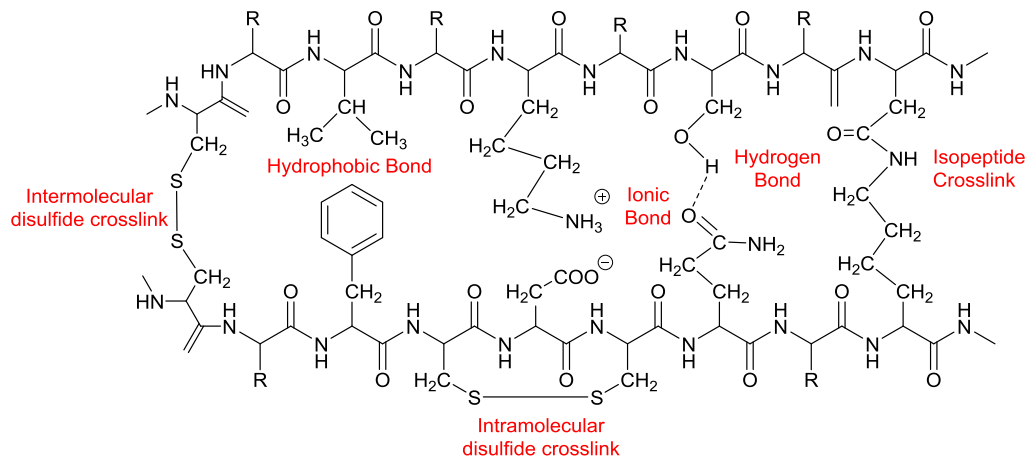


Figure 1.13: Covalent bonds and non-covalent interactions in wool adapted from reference ^[35]

The most important covalent bonds are the sulfur containing disulfide bonds, which are formed during fibre growth by a process called keratinisation. These make keratin fibres insoluble in water and more stable to chemical and physical attack than other types of proteins. Disulfide bonds are involved in the chemical reactions that occur in the setting of fabrics during finishing. In this process, disulfide bonds are rearranged to give wool fabrics smooth-drying properties so that ironing is not required after laundering. Another type of covalent bond is the isopeptide bond, formed between amino acids of lysine and the carboxyl groups of aspartic or glutamic acid.

In addition to the covalent bonds, some other types of interactions also help to stabilise the fibre under both wash and dry conditions. These arise from interactions between the side-chains of the amino acids that constitute wool keratins. Thus,

hydrophobic interactions occur between hydrocarbon side groups; and ionic interactions occur between groups that can exchange protons. These ionic interactions or salt linkages between acidic (carboxyl) and basic (amino) side chains are the most important of the non-covalent interactions.

The carboxyl and amino groups in wool are also important because they give wool its amphoteric or pH buffering properties. This ability to absorb and desorb both acids and alkalis, as shown in Figure 1.14. The ionic groups also control the dyeing behaviour of the fibre, as a result of their interactions with negatively charged dye molecules.

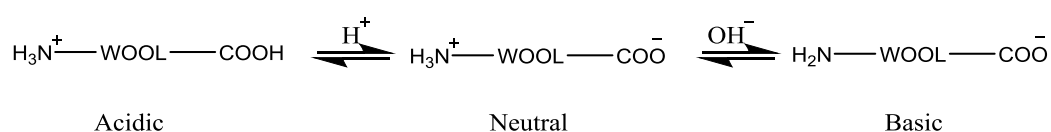


Figure 1.14: Amphoteric behaviour of wool ^[37]

1.2.4 Mechanism of Wool Coloration

A mechanism of wool coloration based on (1) transfer of a dye from the aqueous solution to the fibre surface, (2) adsorption on the surface and (3) diffusion into the fibre. Dyes enter the fibre at the junctions of the cuticle cells, shown in Figure 1.15. Diffusion then occurs through the endocuticle, the CMC and intermacrofibrils. As the dyeing cycle proceeds, dye progressively transfers from the nonkeratinous regions into the sulphur-rich proteins of the matrix surrounding the microfibrils within each cortical cell. Dyes also transfer from the endocuticle into the exocuticle, particularly the A-layer.

At the end of the dyeing cycle if the dyes remains in the nonkeratinous region, rapid diffusion out of the fibre occur, resulting in poor wash fastness properties. Studies concluded that A-layer of the exocuticle is the barrier to the transcellular diffusion across cuticle cells, in untreated wool, dyes find easier route into the fibre interior by an intercellular pathway ^[37].

Reactive dyes may show a different equilibrium distribution between non keratinous and keratinous regions of the fibre, because they can form covalent bonds with proteins in the nonkeratinous regions early in the dyeing cycle. Therefore at equilibrium reactive dyes may be present in the CMC and endocuticle to a greater extent than the non-reactive dyes.

The effect of dye uptake is of even greater importance in printing than in dyeing. The rate of diffusion of dyes in wool is a slow process and in printing this often leads to uneven results, particularly, when the time required to achieve adequate penetration, using steaming is excessive. Thus, wool fabric to be printed is normally treated before printing to enable adequate penetration within a reasonable time under mild steaming conditions.

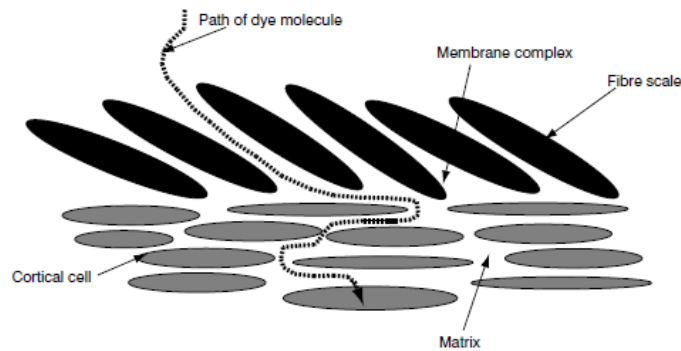


Figure 1.15: Diffusion of dye molecules into the cortex of a wool fibre adapted from reference ^[34]

1.2.5 Dyes for Wool Coloration

The dyes used on wool can be divided into the following groups: acid dyes, chrome dyes, pre-metallised dyes and reactive dyes ^[35, 41]. The conventional method of producing fast dyeing on wool is to employ metallised dyes, which possess large organic weighing groups. In this system, a high wash fastness is achieved by using dyes with a very slow rate of diffusion through the wool fibre.

At present, reactive dyes offer the only viable alternative for products, where very high wash fastness properties are required. Excellent wash fastness with reactive dyes, does not depend upon a slow rate of diffusion of a dye through the fibre, but upon the formation of a stable chemical bond between the dye and fibre.

Environmental requirements are also becoming more regulated and the dyer must take care while selecting dyes for wool dyeings whilst ensuring that production meets the environmental legislation relating to effluent, consumer protection and disposal or recyclability ^[42].

1.3 Textile Printing

1.3.1 Development of Textile Printing

Textile printing involves the production of a predetermined coloured pattern on a fabric, usually with a definite repeat. It can be described as a localised form of dyeing, where colorant is applied to selected areas of the fabric to build up the design ^[43].

Textile printing has a long history although the time and place of origin is not easy to ascertain. The printed garment and carved wooden printing blocks made in Coptic period (400 – 600 AD) have been excavated in Upper Egypt ^[44]. Many block printing goods are found in India and ancient China which can be dated back to the 13th century ^[43].

By the 14th century, wooden block printing was popular in some European countries such as France, Italy and Germany. In block printing, a wooden block with a raised pattern on the surface was dipped into the printing colorant and then pressed face down on to fabric ^[43].

Portuguese traders discovered the potential for coloured cotton markets in Europe. From that time on, the trading between Europe and India increased. This increase in demand for prints initiated the development of printing. In 1752, Francis Nixon adopted copper plate printing in Dublin. Copper plate printing can produce much finer prints than block printing, but it did not replace block printing due to the time and cost required for the preparation of copper plates ^[43].

In 1783, James Bell patented the method of engraved copper roller printing. In 1785, the first machine was invented for continual production with a high speed by using the cylinder. This machine was capable of continuously printing six different colours in sequence with the rollers pressed against the fabric. This invention promoted the textile printing in the United Kingdom especially for high volume production and maintained its position for a long time ^[43].

Screen printing was developed initially for lettering from a stencil printing. It was developed in 1850 by Lyons and used silk gauze as a supporting stencil base. The era of hand screen printing was from 1930 to 1954. Later, further development led to semi-automatic and then fully automatic screen printing machines. These cut production costs significantly.

In the mid-1950s, a screen printing method involving a cylindrical screen was developed. Twenty or more colours can be printed at the same time. The process is much quicker and more efficient than other screen printing methods. Since then rotary screen printing has maintained a dominant share in the market due to high productivity and good print quality.

During the 20th century, Inkjet technologies have greatly affected many industries including the textile printing market. With the launch of several inkjet printers at International Textile Machinery Association (ITMA) in 2003 ^[45-47], this printing method gain momentum and become a promising technique for textile coloration ^[44, 48]. Inkjet printing method has many advantages compared with the traditional screen printing method. It enables mass customisation, which is one of the main driving forces for the development of inkjet printing in the textile market ^[49]. Although inkjet printing only has a small share of textile printing market nowadays ^[50], it is expected that it will replace the dominant position of screen printing in the future when the technical barriers are overcome.

1.3.2 Inkjet Printing

Inkjet printing is a non-contact printing technology in which fine ink droplets are formed and then deposited on the substrate in a defined order to form an image. The simple natural phenomenon of bubble formation when water is heated while making tea led to discovery of this revolutionary technology ^[51]. Though modern inkjet printers were developed in 1979, the first research on the inkjet was carried out by I'Abbe Nollet in France in 1749 ^[52]. In 1878, Rayleigh ^[53] explained the breaking up of liquid stream into droplets and in 1930 this mechanism was used as an inkjet for a recording device. In 1960s, Sweet of Stanford University developed continuous inkjet technology and in 1967, Hertz from Lund Institute in Sweden modified this technology which was licensed to Iris graphics and Stork ^[54]. In 1972, Zoltan, a pioneer of DOD (drop on demand) inkjet printing invented the principle of piezoelectric DOD inkjet printing ^[55]. Researchers at Canon discovered bubble jet technology in 1979 ^[56]. At nearly the same time, researchers at Hewlett Packard (HP) invented the same technology and named it as Thermal Inkjet ^[57].

1.3.3 Classification of Inkjet Printing Technology

Although there are various inkjet printers available in the market, however, industrial inkjet is broadly and most typically classified as either continuous (CIJ) or drop-on-demand (DOD), with variants within each classification. ^[58-60]. Both the inkjet technologies differ in the method of drop generation and in the route to the substrate. They have unique characteristics and place different requirements on the inks that can be used.

1.3.3.1 Continuous Inkjet

The continuous inkjet technology shown in Figure 1.16, generates a constant stream of small ink droplets, which are charged according to the image and controlled electronically. The charged droplets are deflected by a subsequent electric field, while the uncharged ones flow onto the substrate. This means that the imaging signal for charging the droplets corresponds to a negative print image. Continuous inkjet printing usually feeds only a small proportion of the stream of droplets to the substrate. With continuous inkjet generally only a small part of the drop volume covering the sheet in accordance with the print information is applied to the substrate. The large part is fed back into the system.

1.3.3.2 Drop-on-Demand Inkjet

In Drop-on-Demand inkjet technology shown in Figure 1.16, drops are ejected only when needed to form the image. The most important drop-on-demand technologies are thermal inkjet (TIJ) and piezoelectric inkjet printing (PIJ).

Thermal inkjet (also known as “bubble jet”) generates the drops by the heating and localised vaporisation of the liquid in a jet chamber. With piezoelectric inkjet the ink drop is formed and catapulted out of the nozzle by mechanically deforming the jet chamber, an action resulting from an electronic signal and the piezoelectric properties of the chamber wall. Due to the technical conditions, the possible droplet frequencies are lower with thermal droplet generation than with piezoelectric technology.

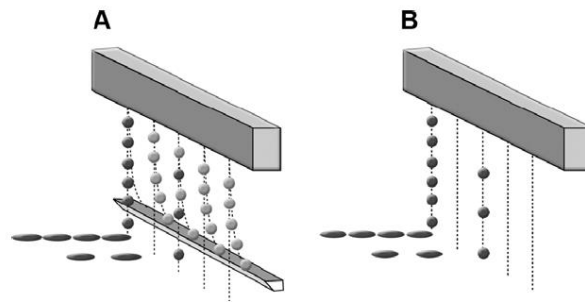


Figure 1.16: Schematic representation of inkjet technologies A) continuous inkjet B) drop-on-demand inkjet adapted from references [60, 61]

1.3.4 Applications of Inkjet for Textile Printing

1.3.4.1 Early Developments

Carpet printing in 1970s was the first textile application of inkjet based on DOD technology [52]. In 1975, Milliken launched a digital carpet printer ‘Milliken Millitron’ the continuous inkjet printers for carpet and upholstery fabrics. In the late 1970s, ‘ChromoJET’ (Zimmer, Austria) followed by ‘Titan MK IV’ (Godfrey Hirst, Australia) were introduced [62]. However, major developments in inkjet printers for textiles began to emerge from 1980s.

In early 1980s, Seiren was the largest fabric printing company in Japan and had used textile inkjet printers based on piezoelectric inkjet printing technology for many years. The approach taken by Seiren was to use number of small inkjet printers (0.1-0.5 yards/min) instead of using high output production machines. Their ‘Viscotecs’ printers have produced 10 million m² of inkjet printed fabrics with a value of approximately 105 million USD [51].

At the 1991 ITMA, Stork launched the earliest commercial inkjet printer ‘TruColor’ based on the continuous inkjet technology [63]. The most interesting development was the incorporation of high purity Procion P (monochlorotriazine, ICI) reactive dyes into the ink formulations. This allowed the subsequent print to be processed in the same manner (steaming and washing) as a conventional print prepared by screen or roller printing [51, 63].

At the ITMA 1995, Stork and Scitex exhibited proofing printers and prototype continuous textile printing machine. Both the proofing and fabric roll printing machines were based on the continuous inkjet principle. The fabric roll printing

machine could print 1.56 metre wide fabric at 4.2 linear metres per hour. The machine used eight-colours made of purified reactive dyes^[60].

At the ITMA 1999, Stork displayed its full line of digital printers, including 'Amethyst' printer, a seven-colour continuous inkjet, used with reactive and acid dyes for printing cellulose and protein fibres. This machine could print at a maximum speed of 17.5 m²/h with a 254 dpi resolution^[52]. Stork has also displayed two machines *viz.*, 'Amber' and 'Zircon', these machine were based on piezoelectric inkjet printing technology^[64]. Also at the ITMA 1999, Encad displayed its four-colour thermal inkjet printer with 300 dpi resolution and speed of 7.5 m²/h. Moreover, Mimaki has showed a printer with an Epson Seiko Piezo head to achieve 720 dpi resolution and seven-colour capability. Perfecta Print AG used Xaar piezo technology and developed a printer with four-colour capability and 200 dpi resolution. This printer can print at a speed of 100 m²/h but was limited to the use of solvent based dye systems.

A number of improvements to existing devices as well as new technologies and new approaches for textile inkjet printing were exhibited at the four yearly ITMA, held in Birmingham in 2003, UK. Comprehensive detail of the developments of inkjet printers is available in the literature^[46]. At this exhibition, many inkjet printers with high resolution; high print speed and stable inks were exhibited; such as 'DReAM' (Reggiani, Italy), 'Monna Lisa' (Robustelli, Italy), 'Artistri-2020' (Dupont, USA), 'Mimaki Tx2-1600' and 'Tx3-600' (Mimaki, Japan)^[46].

Since ITMA 2003, further developments in inkjet printing had been made, the printing speed was improved and also the printing width was increased. For the DReAM, the productivity was improved from 160 m²/h in 2003 to 230 m²/h in 2007 and the width was increased from 1.6 m in 2003 to 3.4 m in 2007^[65].

1.3.5 Changes in the Textile Printing Market

1.3.6 Mass Customisation

The textile printing market is subjected to fluctuations arising from seasonal changes and rapidly altering fashion demands^[66, 67]. Consumers in today's textile market are increasingly obsessed with availability of wide range of choice and flexibility to express their style. The traditional printing techniques are unable to meet these demands due to high volume production requirements, labour costs and

longer lead times for new designs ^[68]. Inkjet printing enables the textile businesses to meet these mass customisation demands economically and efficiently.

1.3.6.1 Change in the Business Model

The traditional business model relies on generating profit through economies of scales but it creates heaps of inventories especially at retailers' end which need to be pushed into the market through seasonal discounting and sales promotions. The end consumer suffers the most because of limited choice ^[69]. Moreover, retailers competing in intensely competitive markets require minimum stocks with frequent replenishments in order to curtail the stock holding costs ^[70]. This calls for provision of fresh and new designs to meet the market changing demands which cannot be matched by the traditional time-inefficient printing processes.

1.3.6.2 Quick Response and Just in Time Delivery

Traditional printing processes are time-inefficient with high lead times (to create a new design or pattern, prepare the screens and print several square metres of sample fabric), setup costs and maintenance. The production sequence also follows lengthy procedures of setting up the machine line for a particular design and changes in design takes a long time resulting in huge machine downtimes. Production of screens itself is a complex, costly and time consuming process. It involves preparation, storage and replacement in case of damage, cleaning and drying of screens after every production run. All this consumes over half the total production time ^[67]. Therefore any changes will lead to inefficiency of the process. Therefore traditional printing is highly inefficient to support the quick response manufacturing strategies and just in time delivery of customised and made to order to products.

1.3.6.3 Economic Factors in Textile Printing

Traditional printing is viable economically for some minimum production runs under which the process is not cost-effective at all. A study in 1997 reported the average run lengths to be 5300 metres in USA, 3200 metres in Asia and 750 metres in Europe ^[66]. With the average run length almost reduced to half in the following eight years ^[71] due to market demands, traditional printing has become highly cost-ineffective and non-competitive.

Productivity is hindered by change-over, setting up and inspection times which further affect the cost in a negative way. Kurt Salmon Associates in 1997 estimated a 45 billion US Dollars loss by the textile industry per year attributed to long manufacturing time cycles leading to high costs of inventory, overruns and stock-outs ^[71].

Sampling is part and parcel of every production floor but it is disadvantageous because it results in downtime of the process because of shorter runs and changeovers. Therefore, there is a need for a process to rapidly produce samples without affecting the main process. This is where inkjet printing can prove to be extremely useful. Hence, textile companies need new quick response, mass customised manufacturing technologies for sampling as well as for short to medium production runs.

1.3.6.4 Ecology

Social pressures and legislative demands to efficiently utilise natural resources of water and energy to minimise waste generation and disposal are becoming stringent day by day. Therefore textile printers are looking for ways to cope up with this challenge and indeed inkjet printing has the potential to provide them a relief through its built-in ecological advantages.

1.3.7 Improving Textile Printing Industry Through the Use of Inkjet Technology

Existing printing technologies are not sufficiently cost-effective and competitive to meet the new requirements of global markets. For traditional printing techniques, sample production time scale is 2 to 8 weeks and the bulk production time scale is 3 to 12 weeks. Moreover, they are labour intensive.

For short runs, traditional printing techniques are uneconomical due to high downtime, high engraving and labour costs, lengthy set-up times for production like colour matching, print paste preparation, sampling, design and registration. Particularly design sampling and screen production are very lengthy and costly processes ^[67].

Inkjet printing has the potential to meet the new market requirements. Furthermore it has the capability to produce printed fabrics with significantly

reduced effluent outputs and with lower water and energy usage. This technology is currently being explored and developed for commercial textile printing and has begun to make the leap into the mainstream.

It has full potential to meet the market demands such as quick response and mass customisation. It also offers unlimited design possibilities with respect to repeat size and colour range. Inkjet printing of textiles offers a number of potential benefits over traditional screen printing methods. It eliminates the set up cost associated with screen preparation and can potentially enable cost effective short run production. It allows visual effects such as tonal gradients and infinite pattern repeat size which cannot be practically achieved by a screen printing technique. It is recognised as the best available technique and is a simple and environmentally clean technology. Other benefits include flexibility, reproducibility, creativity and competitiveness. Comparison of traditional printing and Inkjet printing and their production routes are shown in Table 1.2 and illustrated in Figure 1.17 respectively [67].

Table 1.2: Comparison between rotary screen printing and inkjet printing ^[67]

Features	Rotary Printing	Inkjet Printing
Inks	Aqueous colour pastes in large batches	Pre-formulated inks in small containers supplied by the machine manufacturer
Print speed	Up to 30 – 70 m/min	1 – 4 m/min
Pre-treatment	Nil	Required
Resolution	Usually 100 dpi with maximum of 255 – 300 dpi	Up to 1440 is possible
Screens	Screen cost for engraving, washing and storage	No screens- no washing, no storage
Effluent	More	Much less
Half tones	Difficult	Not a problem
Repeat distance	Restrictions	No restrictions
Registration	Usually designs mis-register at set-up	Instant registration
Strike-offs	Strike-offs on proof may differ from bulk	Strike-offs on bulk machine
Screen contact	There is screen contact with the fabric	No contact with the fabric

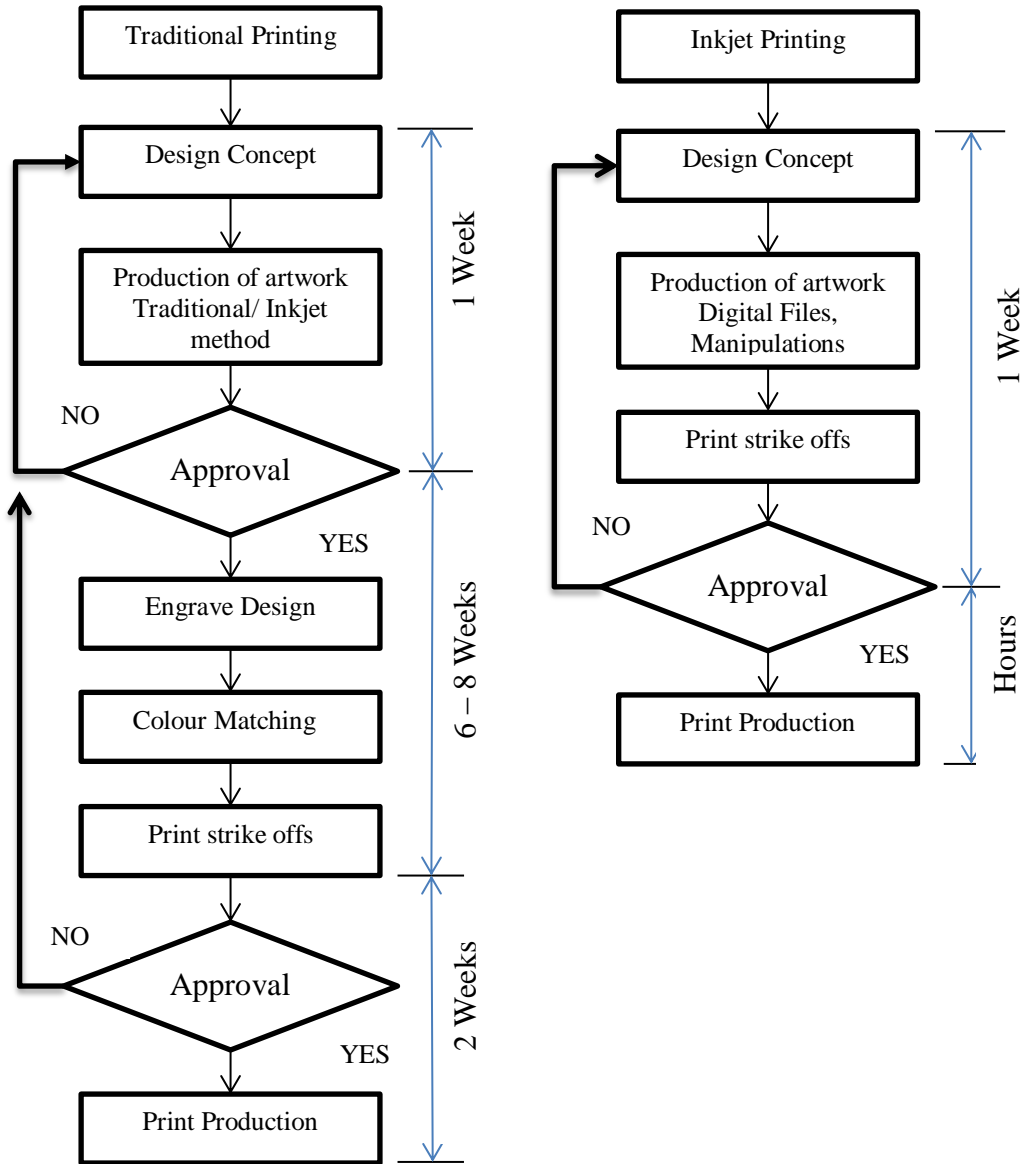


Figure 1.17: Comparison of production routes of traditional and inkjet textile printing ^[67]

1.3.7.1 Limitation of Inkjet Printing

Apart from the above mentioned advantages, there are some disadvantages as well such as slow speed, expensive inks, and extensive substrate pre-treatment and also the limitation of incorporating components required for image definition, achieving good dye fixation, colour yield and fastness properties.

1.3.8 Inks for Textile Inkjet Printing

A traditional textile printer requires 8 to 12 basic colorants and up to 25 supplementary colorants to meet the wider colour space and fastness requirements. Whereas, commercial inks for fabric inkjet printing are now available with up to 8 to 12 colorants including four process colours (C cyan, M magenta, Y yellow and K black) to achieve the required colour gamut. The number of inks available commercially, which can be used for inkjet textile printing is limited. Moreover, each 1% adoption from traditional textile printing to inkjet printing creates a potential for 1.3 million litres of reactive dye ink ^[52].

Therefore, improved ink formulations with required rheology and fixation properties and processes for their fixation are needed to be developed for textile applications.

Significant research activities have been seen over the past decade in the development of inks for textile inkjet printing. The inks must meet following stringent physical and chemical requirements:

1. extremely low salt content
2. high purity
3. non-corrosiveness
4. surface tension in the range of 25 – 60 dynes.cm⁻¹
5. high light and water fastness
6. thermal and chemical stability
7. low viscosity
8. excellent storage stability
9. high solubility (Solubility of > 20% in water; low crystallisation tendency) ^[48]

Depending upon the type of colorants used, inks for inkjet printing of textiles can be broadly classified as dye based inks and pigment based inks.

1.3.8.1 Dye Based Inks

Inks based on reactive, acid and disperse dyes have been developed and are now available commercially ^[52]. Different textile substrates have different dye suitability due to the difference in the mode of dye-fibre interaction. This is shown in Table 1.3.

Table 1.3: Selection of dyes for inkjet printing of textiles ^[72, 73]

Dyes	Fibre
Reactive Dyes	Cotton, silk and wool
Disperse Dyes	Polyester
Acid Dyes	Silk, wool and nylon

1.4 Inkjet Printing of Wool with Reactive Inks

Printing of wool fabrics has always been a small-lot, high fashion activity; this has meant that wool printing did not sit easily in print mills equipped with high productivity rotary screen printing machines capable of printing speeds of 50 m/min. However, even in the cotton fabric printing industry runs of 500 m are now common and likely to become even smaller.

Given the demands for individual designs it could be that the age of mass production printing to a particular colour-way and design is coming to an end; the only way to meet this challenge is to develop inkjet printing processes for textiles. Successful development of these inkjet systems will advantage wool and wool-blend fabric printers with their traditional small run production.

Reactive printing by the *all-in* method is the normal approach for traditional printing, but due to the specific purity requirements for inkjet printing, the traditional printing chemicals are very difficult to directly incorporate into the ink formulations ^[74]. As a result the inkjet printing of wool has generally been carried out by the *two-phase* method, the ink contains only purified dyes, the thickener and auxiliary chemicals been applied to the fabric in a pre-treatment prior to inkjet printing.

1.4.1 Reactive Inks for Wool

Reactive dyes do not form salt-like bonds to protein fibres; instead, covalent bonds are formed in an acidic medium with $-SH$, $=NH$, and $-NH_2$ groups from the polypeptide. This results in products not only with good fastness properties as well as very brilliant shades, thereby significantly enriching the market. The high demand for goods that carry the *Woolmark*, together with the high serviceability associated

with the articles produced from these fibres, justify the additional costs entailed in the use of these dyes.

Vinylsulfone and the monochlorotriazine based dyes being low to medium reactivity cover the majority of the inkjet market ^[75], however, monochlorotriazine is the most popular ^[75-81]. In general, these reactive inks often have a degree of fixation to cotton of only 70% ^[82]. Moreover, in order to achieve the necessary high level of wash fastness, the unfixed or hydrolysed dye must be removed effectively.

For that reason, time-consuming, energy intensive and expensive washing-off procedures are required similar to the conventional washing-off processes used with fibre reactive dyeing. This washing-off process has a major negative environmental impact owing to the large amount of dye and chemicals removed and the large amounts of water required. Furthermore, unfixed reactive dyes in the wastewater may pose an environmental hazard ^[83].

Another common problem with reactive dyes, especially high and medium reactivity dyes, is the susceptibility of reactive group to hydrolysis ^[52, 84]. If the reactive group is hydrolysed, the colorant will not effectively fix to the substrate and will not give optimal colour. In addition, an unfixed dye also adds to the effluent waste and may require further effluent treatment. Furthermore, due to high tendency toward hydrolysis reactive inks do not have sufficient shelf life ^[73].

These problems can be minimised by increasing the fixation rate of reactive inks as high as possible, and by reducing the amount of chemicals used in the pretreatment process. For this purpose, either modification of reactive dyes ^[82, 85-92] or fabric ^[48, 93] were sought.

Fryberg has documented a comprehensive review of dyes for inkjet printing in literature ^[48]. According to Fryberg dyes with sulfo groups are very soluble in water and therefore very well adopted to ink formulation.

Gisler ^[86] prepared trisazo reactive dye based on floropyrimidine reactive group claiming their suitability in inkjet printing of hydroxyl and amino containing fibres.

Eltz and Russ ^[90] prepared series of reactive dyes of increased stability by modification of commercially available dyes with cyanamide and claimed that they are surprisingly stable against hydrolysis and particularly suitable for inkjet printing.

Clark *et al.* ^[91] prepared reactive dyes by modification of commercial Drimarene K dyes with phenolsulfonic acid and claimed that the modified dye-based inks show excellent solubility and stability during storage for up to one year.

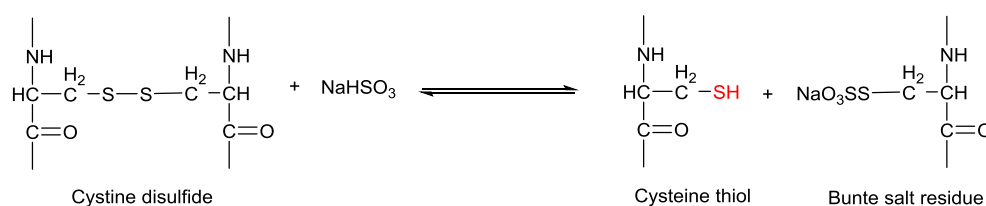
More recently, Maheshwari ^[92] prepared yellow reactive dye of increased water solubility by modification of Reactive Yellow 160 with secondary amines having sulfonate or carboxylate groups. It was claimed that this dye when used in inkjet printing of cotton and wool exhibit good level of fixations and therefore minimal washing-off required.

1.4.2 Pre-Treatment for Inkjet Printing of Wool

Wool fabrics are inkjet printed with reactive dyes by the two-phase method, i.e. the fabric is pre-treated with a pre-treatment liquor and then printed. The pre-treatment liquor is normally applied with the aid of a pad mangle. The fabric is then dried before printing. The main constituents of the aqueous liquor are usually thickener, urea, sodium bisulfite and wetting agent.

Thickeners are employed in printing to preserve the sharpness of edges and outlines by countering the natural wicking effect of the substrate. In addition they hold moisture to enable dyes and chemicals to dissolve and enter the fibres during the steaming stage after printing and drying. They also modify the flow properties (rheology) of the ink or print paste. The thickening agent should not react with either the dye or other chemicals present because, if they do, an insoluble product usually results. This does not wash-off and the fabric becomes stiff ^[58].

Incorporating sodium metabisulfite in the pre-treatment liquor increases the rate of diffusion, improves the colour yield and appearance, and increases the rate of fixation of reactive dyes on wool ^[94, 95]. Bisulfite reacts with the cystine disulfide residues in wool through a reversible reaction, the original disulfide bonds being reformed on rinsing away of excess bisulfite. The cysteine thiol residue generated (shown in Scheme 1.1) is extremely reactive towards reactive dyes ^[96].



Scheme 1.1: Reduction of wool by sodium bisulfite ^[37]

The effect of bisulfite on increasing the rate of reaction is not only due to the formation of highly nucleophilic thiol groups but also due to increased fibre swelling produced by aqueous urea-bisulfite solution ^[95, 97-99]. The effect is more pronounced in low to medium reactivity and high molecular weight reactive dyes. Moreover, bisulfite deactivates the reactive dyes which react by Michael addition reaction ^[94].

Urea is essential in the pre-treatment print paste because during the steaming process, particularly in the saturated steam right after inkjet printing, it is required for swelling the fibres so that the dye can penetrate the fibres rapidly ^[100-102]. Urea also acts as a solvent for the reactive dye in the pre-treatment print paste by absorbing moisture during the steaming process, thereby accelerating the migration of dye from the thickener film into the wool fibre ^[103].

1.5 Aims of Research

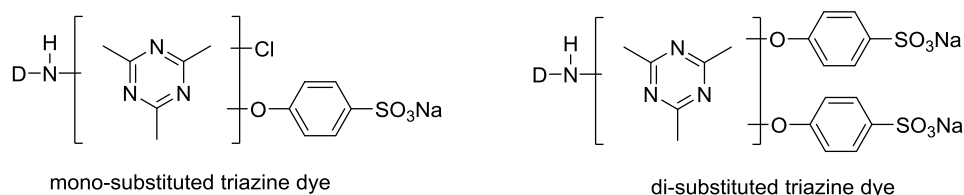
In the latter part of the 20th century, new types of dyes for the traditional applications to textiles continued to be developed and introduced commercially but at a declining rate. At the same time, during this period, research effort in organic colour chemistry has been made in new directions, continued by the opportunities presented by the emergence of a range of novel application techniques, demanding new types of colorants.

In recent years, Inkjet printing applications onto textiles have attracted increasing interest at both academic and industrial levels. As commercial inkjet reactive inks are usually based on dyes with low-to-moderate fixation properties (generally monofunctional reactive dyes), so it is important to maximise dye fixation and ink stability for technical, economic and environmental reasons.

The aim of the research was to design, syntheses and evaluate novel multifunctional reactive dyes in magenta, yellow and blue hues for incorporation in inkjet inks for wool, aimed at superior application properties (fixation), enhanced stability (shelf life) and improved performance properties (colour fastness). The following approaches were adopted:

- Replacing one or both labile chlorine atom(s) of chlorotriazine by the sulfophenoxy reactive group, which is/are displaceable by amino and thiol groups of wool to form a covalent bond between the triazine nucleus and

wool; this approach will be discussed in Chapters 3, 4, and 5. The general formula of these new dyes are shown in Figure 1.18.



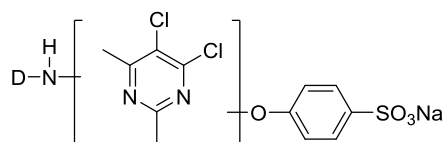
Where,

D means amino based dye chromophore (azo or anthraquinone)
and

the -NH- group in the dye chromophore is directly linked to a carbon atom of the triazine ring.

Figure 1.18: General structure of new triazine based dyes for inkjet printing

- Replacing one labile chlorine atom of chlorodiazine (pyrimidine) by sulfophenoxy reactive group, which is displaceable by amino and thiol groups of wool to form a covalent bond between the diazine nucleus and wool. The study was aimed at highly soluble and stable new reactive dyes, of general formula shown in Figure 1.19, for inkjet printing of wool. This approach will be discussed in Chapters 6, 7, and 8.



Where,

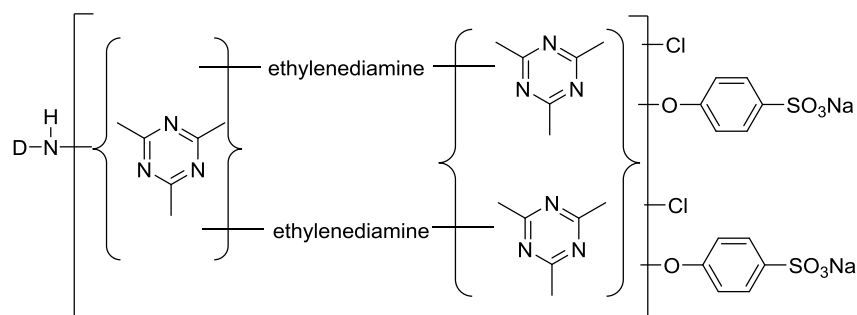
D means amino based dye chromophore (azo or anthraquinone)
and

the -NH- group in the dye chromophore is directly linked to a carbon atom of the pyrimidine ring in 4-position

Figure 1.19: General structure of new pyrimidine based dyes for inkjet printing

- Preparing bis-dichlorotriazine dye in which the chlorotriazine is attached to the triazine ring via a diamine linkage, and then replacing one labile chlorine atom on the chlorotriazine by a sulfophenoxy reactive group, which is displaceable by amino and thiol groups of wool to form a covalent bond between the triazine nucleus and wool. The general formula of this type of

new dye is shown in Figure 1.20; this approach will be discussed in Chapter 9.



Where,

D means amino based dye chromophore
and
ethylenediamine means diamine bridging group

Figure 1.20: General formula for modified bis-dichlorotriazine dye for Inkjet Printing

The new dyes were formulated into a set of inks, applied onto wool fabric through inkjet printing, fixed using different methods and then evaluated in terms of their stability, fixation and colour fastness.

The properties of the new sets of inks were compared to those of the commercially successful 'Jettex R' range from DyStar (see Chapter 10).

1.6 References

1. Zollinger, H. *Color Chemistry: Synthesis Properties, and Applications of Organic Dyes and Pigments*. Weinheim: Wiley-VCH, 2003.
2. Waring, D.R. and Hallas, G. eds. *The Chemistry and Application of Dyes*. New York: Plenum Press, 1994.
3. Taylor, J.A., Pasha, K. and Phillips, D.A.S. The dyeing of cotton with hetero bi-functional reactive dyes containing both a monochlorotriazinyl and a chloroacetyl amino reactive group. *Dyes and Pigments*, 2001, **51**, pp.145-152.
4. Hadfield, H.R. and Lemin, D.R. The use of Reactive Dyes for dyeing Wool and Wool Unions. *Journal of the Textile Institute Transactions*, 1960, **51**, pp.T1351-T1370.

5. Nkeonye, P.O. Reactive Dyes Containing Phosphonic and Carboxylic Acid Reactive Groupings and Their Reactions with Cellulose. *Journal of the Society of Dyers and Colourists*, 1986, **102**, pp.384-391.
6. Lewis, D.M. The Chemistry of Reactive Dyes and Their Application Processes. In: M. Clark, ed. *Handbook of Textile and Industrial Dyeing*. Cambridge: Woodhead Publishing, 2011.
7. Renfrew, A.H.M. and Taylor, J.A. Cellulose reactive dyes: Recent developments and trends. *Review of Progress in Coloration and Related Topics*, 1990, **20**, pp.1-9.
8. Patent GB341461 (1931)
9. Siegel, E. Reactive Groups. In: K. Venkataraman, ed. *The chemistry of synthetic dyes*. New York: Academic Press, 1972.
10. Rattee, I.D. Historical Background. In: I.C.I. Ltd., ed. *Procion Dyestuffs in Textile Printing*. Leeds: Dyestuffs Division, 1960.
11. Morris, K.F., Lewis, D.M. and Broadbent, P.J. Design and application of a multifunctional reactive dye capable of high fixation efficiency on cellulose. *Coloration Technology*, 2008, **124**, pp.186-194.
12. Lewis, D.M. The Dyeing of Wool with Reactive Dyes. *Journal of the Society of Dyers and Colourists*, 1982, **98**, pp.165-175.
13. Patent DE1016230 (1957)
14. Patent BE560032 (1956)
15. Patent GB797946 (1956)
16. Patent BE578933 (1959)
17. Patent BE578742 (1959)
18. Lewis, D.M. Wool Dyeing. *Review of Progress in Coloration and Related Topics*, 1977, **8**, pp.10-23.
19. Christie, R.M. *Colour chemistry*. Cambridge: Royal Society of Chemistry, 2001.
20. Shore, J. ed. *Colorants and auxiliaries : organic chemistry and application properties*. Bradford: Society of Dyers & Colourists, 1990.
21. Stamm, O.A. Mechanisms of Reaction of Reactive Dyes with Cellulosic and other Fibres. *Journal of the Society of Dyers and Colourists*, 1964, **80**, pp.416-422.

22. Zollinger, H. Chemismus der Reaktivfarbstoffe. *Angewandte Chemie*, 1961, **73**, pp.125-136.
23. Rattee, I.D. Reactive Dyes for Cellulose 1953–1983. *Review of Progress in Coloration and Related Topics*, 1984, **14**, pp.50-57.
24. Kleb, K., Siegel, E. and Sasse, K. New reactive dyes. *Angewandte Chemie International*, 1964, **3**, pp.408-416.
25. Beech, W.F. *Fibre-Reactive Dyes* London: Logos Press Ltd., 1970.
26. Taylor, J.A. Recent developments in reactive dyes. *Review of Progress in Coloration and Related Topics*, 2000, **30**, pp.93-108.
27. Medley, J. and Gardner, K. The Production of Fast Dyeings on Wool. *Review of Progress in Coloration and Related Topics*, 1972, **3**, pp.67-72.
28. Rapoport, L. *S-Triazines and Derivatives*. New York: An Interscience Publishers, 1959.
29. Wegmann, J. Some Relations between the Chemical Constitution of Cibacron Dyes and their Dyeing Characteristics. *Journal of the Society of Dyers and Colourists*, 1960, **76**, pp.205-209.
30. Patent GB10169008 (1963)
31. Patent GB937182 (1963)
32. Siegel, E. Reactive Dyes: Reactive Groups. In: K. Venkataraman, ed. *The chemistry of synthetic dyes*. New York ; London: Academic Press, 1978.
33. Rattee, I.D. Reactive Dyes in the Coloration of Cellulosic Materials. *Journal of the Society of Dyers and Colourists*, 1969, **85**, pp.23-31.
34. Broadbent, A.D. Protein fibres. In: *Basic principles of textile coloration*. Bradford: Society of Dyers and Colourists, 2001.
35. Christoe, J.R., Denning, R.J., Evans, D.J., Huson, M.G., Jones, L.N., Lamb, P.R., Millington, K.R., Phillips, D.G., Pierlot, A.P., Rippon, J.A. and Russell, I.M. Wool. In: *Kirk-Othmer Encyclopedia of Chemical Technology*. New York: An Interscience Publication, 2000.
36. *The Chemical & Physical Structure of Merino Wool* [online]. 2006. [Accessed June 12, 2010]. Available from: <http://www.csiro.au/files/files/p9ti.pdf>.
37. Rippon, J.A. The Structure of Wool. In: D.M. Lewis, ed. *Wool Dyeing*. Bradford: Society of Dyers and Colourists, 1992.

38. Leon, N.H. The chemical reactivity and modification of keratin fibres. *Textile Progress*, 1975, **7**, pp.1-70.
39. Hocker, H. Fibre morphology. In: W.S. Simpson and G.H. Crawshaw, eds. *Wool: science and technology*. Cambridge: Woodhead Publishing, 2002.
40. Brady, P. Diffusion of dyes in natural fibres. *Review of Progress in Coloration and Related Topics*, 1992, **22**, pp.58-78.
41. Bird, C.L. *The theory and practice of wool dyeing*. Bradford: Society of Dyers and Colourists, 1963.
42. Parton, K. Practical wool dyeing. In: W.S. Simpson and G.H. Crawshaw, eds. *Wool: science and technology*. Cambridge: CRC Press, 2002.
43. Miles, L.W.C. Traditional methods. In: L.W.C. Miles, ed. *Textile Printing*. Bradford: Society of Dyers and Colourists, 2003.
44. Dawson, T.L. and Hawkyard, C.J. A new millennium of textile printing. *Review of Progress in Coloration and Related Topics*, 2000, **30**, pp.7-20.
45. Moser, L.S. ITMA 2003 review: Textile printing. *Journal of Textile and Apparel Technology and Management*, 2003, **3**, pp.1-15.
46. Glover, B. The latest technology developments in inkjet printing from ITMA 2003. In: T.L. Dawson and B. Glover, eds. *Textile Inkjet printing-A review of ink jet printing of textiles, including ITMA 2003*. Bradford: Society of Dyer and Colourists Technical Monograph, 2004.
47. Tyler, D.J. Textile digital printing technologies. *Textile Progress*, 2005, **37**, pp.1-65.
48. Fryberg, M. Dyes for ink-jet printing. *Review of Progress in Coloration and Related Topics*, 2005, **35**, pp.1-30.
49. Fralix, M.T. From mass production to mass customization. *Journal of Textile and Apparel, Technology and Management*, 2001, **1**, pp.1-7.
50. Ujiie, H. Inkjet Textile Printing Status Report 2010. In: *Digital Inkjet Textile* Hangzhou, China. 2010.
51. Gregory, P. Ink jet printing on textiles. In: T.L. Dawson and B. Glover, eds. *Textile Inkjet printing-A review of ink jet printing of textiles, including ITMA 2003*. Bradford: Society of Dyer and Colourists Technical Monograph, 2004.
52. Ujiie, H. *Digital printing of textiles*. Cambridge: Woodhead Publishing Ltd., 2006.

53. Rayleigh, L. and Strutt, J.W. On the instability of jets. *Proc. London Mathematical Society*, 1879, pp.4-13.
54. Le, H.P. Progress and trends in ink-jet printing technology. *Journal of Imaging Science and Technology*, 1998, **42**, pp.49-62.
55. Patent US3683212 (1972)
56. Patent GB2007162 (1979)
57. Patent US4490728 (1984)
58. Freire, E.M. Ink jet printing technology (CIJ/DOD). In: H. Ujiie, ed. *Digital printing of Textiles*. Cambridge: Woodhead Publishing Ltd, 2006.
59. Ahmed, A. Jet printing for textiles. *Journal of the Society of Dyers and Colourists*, 1992, **108**, pp.422-424.
60. Hudd, A. Inkjet Printing Technologies. In: S. Magdassi, ed. *Chemistry of Inkjet Inks*. New Jersey: World Scientific Publishing Ltd., 2012.
61. Kipphan, H. ed. *Handbook of Print Media Technologies and Production Methods*. New York: Springer, 2001.
62. Dawson, T.L. and Ellis, H. Will ink jets ever replace screens for textile printing? *Journal of the Society of Dyers and Colourists*, 1994, **110**, pp.331-337.
63. Aston, S.O., Provost, J.R. and Masselink, H. Jet printing with reactive dyes. *Journal of the Society of Dyers and Colourists*, 1993, **109**, pp.147-152.
64. Moser, L.S. and Wilson, O.E. Trends in Preparation, Dyeing, and Printing. *Textile Progress*, 2000, **30**, pp.68-83.
65. Yang, K. *Reactive dye ink-jet printing on wool fabrics*. Ph.D. Thesis, University of Leeds, 2008.
66. Gupta, S. Inkjet printing-A revolutionary ecofriendly technique for textile printing. *Indian Journal of Fibre & Textile Research*, 2001, **26**, pp.156-161.
67. Choi, P.S., Yuen, C.W.M., Ku, S.K.A. and Kwan, C.W. Ink-jet printing for textiles. *Textile Asia*, 2003, **34**, pp.21-24.
68. Weiser, J. The future of digital textile printing. *International Textile Bulletin-English Edition*, 2001, **47**, pp.71-73.
69. Ross, T. A primer in digital textile printing. [online], 2001, [Accessed August 12th, 2013]Available from:
<http://www.techexchange.com/thelibrary/DTP101.html>.

70. Holme, I. Technology-Digital Ink Jet Printing of Textiles. *Textiles magazine*, 2004, **31**, pp.11-16.
71. Gherzi, G. New prospects for transfer printing. *Melliand International*, 1997, pp.36-37.
72. Hees, U., Freche, M., Kluge, M., Provost, J. and Weiser, J. Inkjet interactions in inkjet printing- the role of pre-treatments. In: T.L. Dawson and B. Glover, eds. *Textile Inkjet printing-A review of ink jet printing of textiles, including ITMA 2003*. Bradford: Society of Dyer and Colourists Technical Monograph, 2004.
73. Magdassi, S. Ink Requirements and Formulations Guidelines. In: S. Magdassi, ed. *Chemistry of Inkjet Inks*. New Jersey: World Scientific Publishing Ltd., 2012.
74. Yuen, C., Kan, C., Jiang, S., Ku, S., Choi, P. and Wong, K. Optimum condition of ink-jet printing for wool fabric. *Fibers and Polymers*, 2010, **11**, pp.229-233.
75. Noguchi, H. and Shirota, k. Formulation of aqueous inkjet ink. In: H. Ujiie, ed. *Digital printing of textiles*. Cambridge: Woodhead Publishing Ltd., 2006.
76. Provost, J. Ink jet printing on textiles. *Surface Coatings International*, 1994, **77**, pp.36-41.
77. Patent EP709519 (1996)
78. Patent JP09268482 (1997)
79. Patent CN102443314 (2012)
80. Patent WO2003006560 (2003)
81. Patent WO2001072907 (2001)
82. Fei Li, X. and Tincher, W.C. New colorant system for ink jet printing on textiles. *Textile chemist and colorist*, 1999, **11**, pp.37-42.
83. Kanik, M. and Hauser, P.J. Printing of cationised cotton with reactive dyes. *Coloration Technology*, 2002, **118**, pp.300-306.
84. Magdassi, S. ed. *Chemistry of Inkjet Inks*. New Jersey: World Scientific Publication Ltd., 2012.
85. Lewis, D.M. The colouration of wool. In: M. Clark, ed. *Handbook of Textile and Industrial Dyeing*. Cambridge: Woodhead Publishing, 2011.
86. Patent WO2003031520 (2003)

87. Patent CA2448867 (2003)
88. Patent WO2007045830 (2007)
89. Patent US20060107869 (2006)
90. Patent DE4417718 (1995)
91. Clark, M., Yang, K. and Lewis, D.M. Modified 2,4-difluoro-5-chloro-pyrimidine dyes and their application in ink-jet printing on wool fabrics. *Coloration Technology*, 2009, **125**, pp.184-190.
92. Patent IN2009MU00138 (2010)
93. Hauser, P.J. and Kanik, M. Inkjet printing of cationized cotton with reactive inks. In: H. Ujiie, ed. *Digital printing of Textiles*. Cambridge: Woodhead Publishing Ltd, 2006.
94. Lewis, D.M. and Seltzer, I. Print-Batch (Cold)—A New Process for Wool. *Journal of the Society of Dyers and Colourists*, 1972, **88**, pp.327-329.
95. Lewis, D. The dyeing of wool with reactive dyes. *Journal of the Society of Dyers and Colourists*, 1982, **98**, pp.165-175.
96. Baumgarte, U. The reaction of acrylamide dyes with wool and amino acids. *Melliand Textilber*, 1962, **43**, pp.1297-1303.
97. Brady, P.R. The Effect of Urea on Wool Fibres. *Journal of the Society of Dyers and Colourists*, 1976, **92**, pp.56-58.
98. Lewis, D.M. and Seltzer, I. Pad-Batch Dyeing of Wool with Reactive Dyes. *Journal of the Society of Dyers and Colourists*, 1968, **84**, pp.501-507.
99. Lewis, D.M. and Rippon, J.A. eds. *The Coloration of Wool and Other Keratin Fibres*. Bradford: Society of Dyer and Colourists, 2013.
100. Achwal, W.B. Textile chemical principles of digital textile printing (DTP). *Colourage*, 2002, **49**, pp.33-34.
101. Chen, W., Wang, G. and Bai, Y. Best for wool fabric printing—digital inkjet. *Text Asia*, 2002, **33**, pp.37-39.
102. Holme, I. Fibre physics and chemistry in relation to coloration. *Review of Progress in Coloration and Related Topics*, 1976, **7**, pp.1-22.
103. Choi, P., Yuen, C., Ku, S. and Kan, C. Digital ink-jet printing for chitosan-treated cotton fabric. *Fibers and Polymers*, 2005, **6**, pp.229-234.

2 General Procedure and Instrumentation

2.1 Capillary Electrophoresis

Capillary Electrophoresis (CE) is a relatively new technique which has gained popularity over the last two decades due to its high efficiency, short analysis times, wide application and low cost. It is particularly suited for the separation of a wide variety of compounds including DNA, proteins, polynucleotides, amino acids, vitamins, drugs, and dyestuffs^[1, 2]. It has been reported in literature that CE provide superior separation efficiency than HPLC for the analysis of reactive dyes^[2, 3].

In dye manufacturing impurities are often present; these include inorganic salts as well as colourless and coloured organic compounds for instance, hydrolysis products in the production of reactive dyes. Therefore, an effective method of analysis to determine the levels of such impurities and purity of the final product is highly desirable. Henceforth, in this study, capillary electrophoresis (CZE or MEKC) was used to follow the synthesis reactions and to determine the purity of the final product.

2.1.1 Principles of Capillary Electrophoresis (CE)

Capillary electrophoresis involves the separation of chemical compounds based on the differential migration of charged species under the influence of an applied electrical field. Typical small sample volumes are injected into the anodic end of a narrow-bore capillary filled with buffer and are swept towards the cathode by the electroosmotic flow (EOF). The EOF is caused by the application of an electric field on the counter-ions (predominantly cations) accumulated on the negatively charged silanol groups of the capillary wall which form an electrical double layer^[4]. These cations are solvated and carry the bulk of the buffer solution with them as they migrate toward the cathode^[5]. Under these conditions, compounds are separated by their characteristic electrophoretic mobilities which are dependent on the solute's charge and size^[4]. A schematic of a simplified CE system is presented in Figure 2.1.

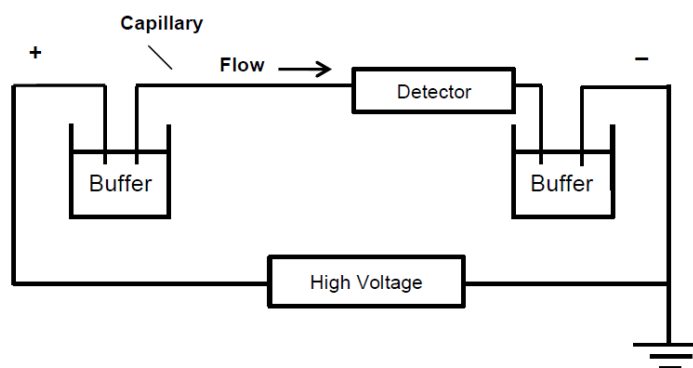


Figure 2.1: Schematic diagram of a capillary electrophoresis (CE) system adapted from reference ^[1]

Success of capillary electrophoresis is also partly due to various possible separation modes which have vastly different operative and separation characteristics which facilitate the analysis of distinctly different classes of chemical compounds using the same instrument. The modes are: Capillary Zone Electrophoresis (CZE), Micellar Electrokinetic Capillary Chromatography (MEKC), Capillary Isoelectric Focusing (CIEF), Capillary Gel Electrophoresis (CGE) and Isotachopheresis (ITP).

By utilising these various modes of capillary electrophoresis, this technique clearly has potential to be a powerful and diverse analytical method for both the dye-consuming and dye-manufacturing industries ^[6].

In this study, CZE (for magenta and blue dyes) and MEKC (for yellow dyes) modes were used.

2.1.1.1 Capillary Zone Electrophoresis (CZE)

Capillary zone electrophoresis (CZE) is also known as free solution capillary electrophoresis. CZE has been the most frequently used mode of CE due to its simplicity and versatility and has a wide application range which includes the analysis of peptides, amino acids, small molecules and dyes. The electrolyte for CZE consists of a relatively simple buffer solution with a suitable known pH value and separation takes place in an uncoated polyimide fused silica column with an internal diameter usually in the range of 25 – 75 μm . The sample is introduced at the anodic end of the capillary and upon the application of an applied potential, charged analytes separate into spatially discrete zones based on their electrophoretic mobilities. Neutral compounds are not capable of migrating in this environment and

co-elute with the EOF [5]. Alteration of the buffer pH is the easiest way to manipulate the mass to charge ratios of ionisable compounds hence influencing their electrophoretic mobilities and subsequent separation. This process is represented in Figure 2.2.

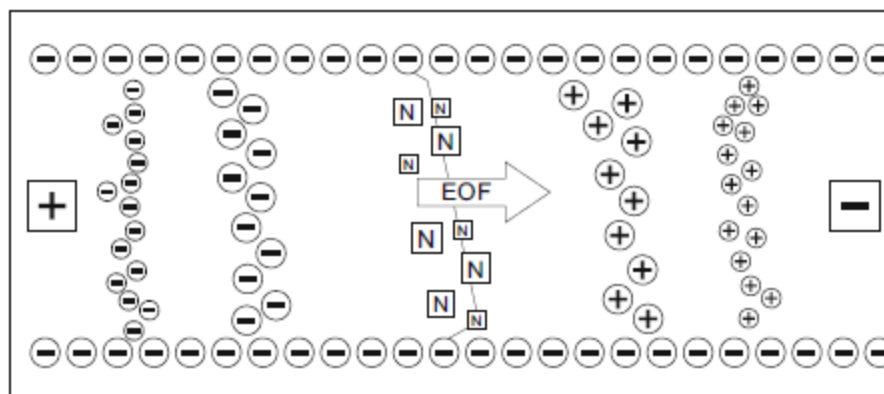


Figure 2.2: Diagrammatic representation of the CZE separation process

As shown in Figure 2.2, small, positively charged species with low mass to charge ratios will pass the detector at the cathodic end first, followed by cations with higher ratios and then unresolved neutral compounds which migrate under the forced influence of the EOF.

Next in the sequence are anions with high mass to charge ratios and finally, anionic species with low mass to charge ratios are dragged to the cathode by net bulk flow of the EOF and reach the detector last [4].

2.1.1.2 Micellar Electrokinetic Chromatography (MEKC)

MEKC is a hybrid of electrophoresis and chromatography and has the added advantage over CZE in that it is capable of separating both neutral and charged solutes within a single run. Here either an anionic or cationic surfactant is incorporated into the buffer solution in a concentration above the critical micelle concentration to form micelles. Micelles are spherical aggregates of surfactant molecules orientated with their polar heads towards the hydrophilic buffer phase and their hydrophobic tails closely associated within the micellar core [7]. The micellar phase in MEKC is often referred to as a pseudo-stationary phase and is likened to the stationary phase in conventional chromatography while the properties of the aqueous phase frequently corresponds to that of the mobile phase [8]. In an electrochromatographic system, the charged micelles migrate with or opposite to the

EOF depending on their charge. Cationic micelles migrate with the EOF while anionic micelles gravitate towards the anode. Under neutral or alkaline buffer conditions, the magnitude of the EOF is however greater than the migration velocity of the anionic micelles and there is a net movement in the direction of the cathode. Concurrently, complex interactions including hydrophobic, electrostatic and hydrogen bonding occur between the micelles and the analyte which facilitate separation.

In a system using a common anionic surfactant such as sodium dodecyl sulfate (SDS), charged analytes tend to migrate according to their electrophoretic mobilities in the aqueous phase while neutral analytes partition between the anionic micellar phase and aqueous phase, depending on their distribution coefficient. The more hydrophilic the analyte, the more it will partition into the aqueous phase and will be swept with the EOF towards the detection window while the hydrophobic compounds are more strongly associated with the negatively charged micelles and migrate at a slower rate. The MEKC separation process is depicted in Figure 2.3 [9].

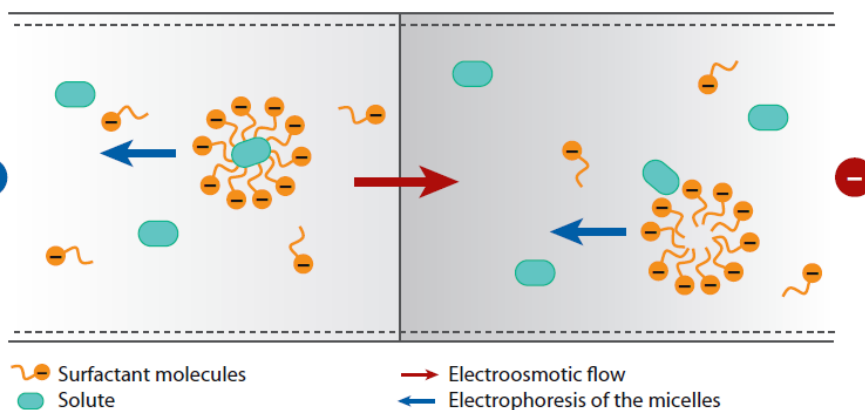


Figure 2.3: Schematic illustration of the separation principle of MEKC adapted from reference [9]

2.1.2 Analysis Parameters

The analyses were carried out on a Beckman P/ACE MDQ with P/ACE station software. The capillary used was of 50 μm internal diameter, with a length of 30 cm to the detector and a total length of 40.2 cm. The capillary was cooled to 30 $^{\circ}\text{C}$ throughout the analysis and the analyte was injected by pressure at 0.5 psi for 10 s. The samples were prepared in deionised water. A fixed voltage of 25 kV was applied to bring about separation of peaks. The detection was set at different

wavelengths in the visible spectrum, *i.e.* for Magenta at 542 nm, Yellow at 420 nm and Blue at 596 nm.

In this study, three different buffer systems were employed which are mentioned in Table 2.1. The buffers were replaced after every ten runs to minimise solvent evaporation effects that might cause irreproducible electroosmotic flow and migration times. The raw data were analysed and peaks were integrated using OriginPro 9.0.0.

Table 2.1: CE buffer systems for reactive dyes

Colour	Buffer System	pH
Magenta	6 mM Potassium Dihydrogen Phosphate in (acetonitrile–water; 10:90 v/v) ^[10]	9.0
Blue	15 mM Ammonium Acetate in (acetonitrile–water; 40:60 v/v) ^[11]	9.3
Yellow	20 mM Sodium Tetraborate, 50 mM Sodium Dodecyl Sulphate (SDS) ^[12]	9.3

2.2 Thin Layer Chromatography (TLC)

Chromatography is an analytical method that is widely used for the separation, isolation, identification, and quantification of components in a mixture. Components of the mixture are carried through the stationary phase by the flow of a mobile phase. Separations are based on differences in migration rates among the sample components ^[13].

Thin layer chromatography (TLC) was chosen over other chromatography methods because it is a simple, quick and inexpensive procedure that can be used for the analysis of mixtures.

TLC is a mode of liquid chromatography in which the sample is applied as a small spot or streak to the origin of a thin sorbent layer such as silica gel, alumina, or chemically bonded silica gel supported on a glass, plastic, or metal plate. This layer consists of finely divided particles and constitutes the stationary phase. The eluent or mobile phase is a solvent or a mixture of organic and/or aqueous solvents

in which the spotted plate is placed. The mobile phase moves through the stationary phase by capillary action, sometimes assisted by gravity or pressure ^[13, 14].

The basic TLC procedure is carried out by placing a spot of sample solution near one end of the stationary phase, a thin layer; the sample is then dried; and the end of stationary phase is placed into a mobile phase, usually a mixture of pure solvents, in a close chamber. The components of mixture migrate at different rates during movement of the mobile phase through the stationary phase, which is termed the development of the chromatogram. When the mobile phase has moved an appropriate distance, the stationary phase is removed, the mobile phase is rapidly dried, and if the compounds are not naturally coloured or fluorescent a visualisation reagent is applied to detect the zones ^[13, 15], and their retention factors, R_f values, are calculated by following formula:

$$R_f = \frac{\text{distance traveled by compound}}{\text{distance traveled by solvent}}$$

In TLC, the compounds roughly follow the elution order based on their polarity. Highly polar molecules interact fairly strongly with the polar SiOH groups (silica plate) and will tend to adsorb onto the fine particles of the adsorbent while weakly polar molecules are held less tightly. Weakly polar molecules generally tend to move through the adsorbent more rapidly than the polar molecules.

The larger an R_f value of a compound, the larger the distance it travels on the TLC plate. When comparing two different compounds run under identical chromatography conditions, the compound with the larger R_f is less polar because it interacts less strongly with the polar adsorbent on the TLC plate. Conversely, if you know the structures of the compounds in a mixture, you can predict that a compound of low polarity will have a larger R_f value than a polar compound run on the same plate.

TLC separations take place in the open layer, with each component having the same total migration time but different migration distances. Plates can be visualised, depending on the chemical structure of the compounds at visible light, UV-254 nm and 365 nm or by using spray reagents. The effectiveness of the separation depends on the mixture to be separated, the choice of the mobile phase and the adsorption layer ^[16].

The selection of a solvent for application of the sample can be a critical factor in achieving reproducible chromatography with distortion free zones. In general, the application solvent should be a good solvent for the sample and should be as volatile as possible and more nonpolar ^[13].

There are a number of advantages to the use of TLC for the analysis of dyes compared with other chromatographic techniques. The most obvious is that dyes are easily visualised on a chromatographic layer by their colour. Often slight differences in hue are more clearly seen on the layer than in solution and hence are easily distinguishable. It is therefore rarely necessary to employ detection reagents unless the area of interest is dye intermediates which may lack the conjugation needed in their molecular structure to be coloured in visible light.

2.2.1 Analysis Parameters

Thin layer chromatography (TLC) was used to follow the progress of the reaction by monitoring the consumption of starting materials and the appearance of the product. This technique was performed using aluminium plates coated with silica gel 60 F₂₅₄ (Merck) as stationary phase. Table 2.2 summarise the composition of eluents (mobile phase) that are used in this study.

The developed plates were visualised in visible light and also under both short and long wavelength ultraviolet light (254 nm, 365 nm) and retention factor (R_f) values are reported.

Table 2.2: TLC eluents for reactive dyes

Dyes	Eluents	Proportion (v/v)
Triazine	n-butanol–iso-propanol–ethyl acetate–water ^[17, 18]	2:4:1:3
Pyrimidine	iso-butanol–n-propanol–ethyl acetate–water ^[17, 18]	2:4:1:3

2.3 Infrared (IR) Spectroscopy

Infrared (IR) spectroscopy is one of the most common spectroscopic techniques used by organic and inorganic chemists. It is the absorption measurement of different IR frequencies by a sample positioned in the path of an IR beam. The

main goal of the IR spectroscopic analysis is to determine the chemical functional groups in the sample. Different functional groups absorb characteristic frequencies of IR radiation. Using various sampling accessories, IR spectrometers can accept a wide range of sample types such as gases, liquids, and solids. Thus, IR spectroscopy is an important and popular tool for structural elucidation and compound identification.

Infrared spectroscopy involves the interaction of the molecule with electromagnetic radiation. When an organic molecule is irradiated with infrared energy, certain energies are absorbed by the molecule. The energies absorbed correspond to the amount of energy needed to increase the amplitude of specific molecular vibrations such as bond stretching and bending. Every functional group has a characteristic set of infrared absorptions. By observing which frequencies of infrared radiation are absorbed by a molecule and which are not, it is possible to determine the functional group(s) a molecule contains ^[19].

In simple terms, IR spectra are obtained by detecting changes in transmittance (or absorption) intensity as a function of frequency. Most commercial instruments separate and measure IR radiation using dispersive spectrometers or Fourier transform spectrometers. In this study samples were run on Fourier Transform-Infrared Spectroscopy (FT-IR) with an Attenuated Total Reflection (ATR) attachment.

2.3.1 Fourier Transform-Infrared Spectroscopy (FT-IR) ^[20]

Fourier Transform-Infrared Spectroscopy (FT-IR) is an analytical technique used to identify organic (and in some cases inorganic) materials. This technique measures the absorption of infrared radiation by the sample material versus wavelength. The infrared absorption bands identify molecular components and structures.

The FT-IR spectrometer uses an interferometer to modulate the wavelength from a broadband infrared source. A detector measures the intensity of transmitted or reflected light as a function of its wavelength. The signal obtained from the detector is an interferogram, which must be analysed by a computer using Fourier transforms to obtain a single-beam infrared spectrum.

The FT-IR spectra are usually presented as plots of intensity versus wavenumber (in cm^{-1}). Wavenumber is the reciprocal of the wavelength. The intensity can be plotted as the percentage of light transmittance or absorbance at each wavenumber.

2.3.2 Attenuated Total Reflection (ATR) ^[21]

Attenuated Total Reflection (ATR) is an accessory of transmission IR spectrometers that significantly enhances surface sensitivity. An attenuated total reflection accessory operates by measuring the changes that occur in a totally internally reflected infrared beam when the beam comes into contact with a sample (shown in Figure 2.4).

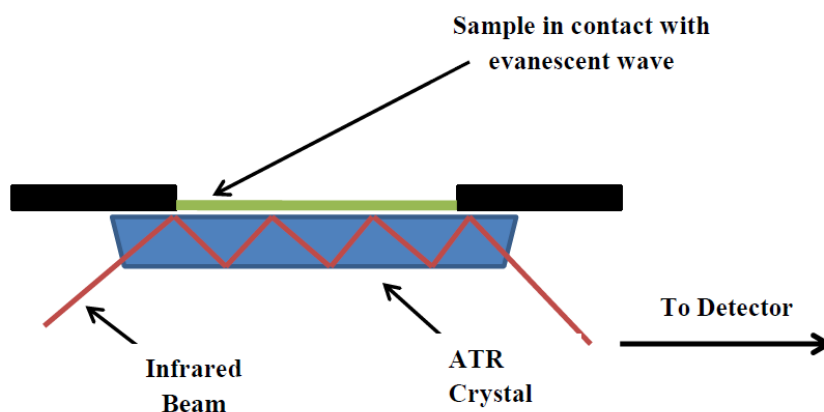


Figure 2.4: A multiple reflection ATR system adapted from reference ^[21]

An infrared beam is directed onto an optically dense crystal with a high refractive index at a certain angle. This internal reflectance creates an evanescent wave that extends beyond the surface of the crystal into the sample held in contact with the crystal. It can be easier to think of this evanescent wave as a bubble of infrared that sits on the surface of the crystal. This evanescent wave protrudes only a few microns ($0.5\mu - 5\mu$) beyond the crystal surface and into the sample. Consequently, there must be good contact between the sample and the crystal surface. In regions of the infrared spectrum where the sample absorbs energy, the evanescent wave will be attenuated or altered. The attenuated is passed back to the IR beam, which then exits the opposite end of the crystal and is passed to the detector in the IR spectrometer. The system then generates an infrared spectrum.

2.3.3 Analysis Parameters

In this study, infrared spectra were recorded on the Perkin Elmer Spectrum One spectrophotometer (Perkin Elmer, UK) using the PE Diamond Golden Gate sampling attachment for attenuated total reflection (ATR) measurement. Each spectrum was acquired using the following settings: 4 cm⁻¹ resolution, 100 scans per spectrum and a scan speed of 0.5 cm/s. The software used was a Perkin Elmer Spectrum 5.0.1 software. The raw data were analysed using OriginPro 9.0.0. The vibrational frequencies are reported in wavenumbers (cm⁻¹).

2.4 Elemental Analysis

Elemental analyses of modified dyes for carbon, hydrogen and nitrogen were performed using a FlashEA 1112 analyser from Thermo Scientific ¹.

Elemental analysis of poly sulfonated dyes may give misleading results since these dyes tend to crystallise with a varying number of water molecules in their crystal structure ^[22]. For triazine based dyes synthesised in this work, the dangers of drying at elevated temperatures leading to dye hydrolysis, were considered to be very significant; thus the presence of water of crystallisation was unavoidable and CHN analysis results were adjusted accordingly.

Moreover, any further disagreement between the calculated and found values could be attributed to the presence of traces of sodium chloride (used for crystallisation of dyes), traces of solvents or sodium phosphate buffer (used for stabilisation of dyes against hydrolysis during storage ^[23]) even after purification of crude dyes by solvent-non solvent method (see Section 2.5.2.1).

2.5 Inkjet Printing Procedure

Throughout this study, worsted 100% wool fabric, 1:1 twill, untreated, 200 g.m⁻² (Woolmark Co., UK) and 100% cotton fabric, plain weave, bleached, non-mercerised, 100 g.m⁻² (Whaleys, UK) were used for inkjet printing.

¹ Elemental analyses were performed by Mr. Ian Blakeley from School of Chemistry.

The sequence of wool substrate preparation and inkjet printing is shown in Figure 2.5.

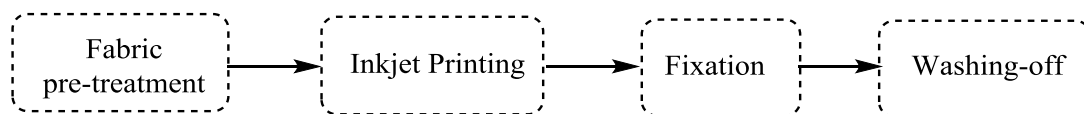


Figure 2.5: Sequence of substrate preparation and inkjet printing

2.5.1 Fabric Pre-Treatment

Pretreatment of textile substrates in inkjet printing is required to optimise the interaction between the low viscosity ink drops jetted from the print head and capillaries in fibres, yarns and fabric structures ^[24].

Therefore, wool fabric was padded at 100% wet pick-up using a Werner Mathis HVF padder with the pretreatment solution, mentioned in Table 2.3. Following padding the fabric was dried at 70 °C using a Werner Mathis dryer.

Table 2.3: Pre-treatment padding recipe

Sodium bisulfite ^[25, 26]	20 g.dm ⁻³
Carboxymethyl cellulose (CMC) ^[26]	20 g.dm ⁻³
Urea ^[25, 26]	300 g.dm ⁻³
Alcopol O 60 ^[26]	5 g.dm ⁻³
Water	X dm ³
	1 dm ³

2.5.2 Ink Preparation

2.5.2.1 Purification of Synthesised Dyes

Typically, synthesised dyes contain inorganic impurities such as electrolytes that prevent them from being used directly in the inkjet printing ink formulation. Purification is therefore required to remove inorganic impurity that can be detrimental to ink stability and ink performance in both print head and print quality.

Purification of parent and modified triazine based crude dyes and parent pyrimidine dyes was done, in accordance with the method described as *solvent–non-*

solvent mixtures for purification of dyes in references ^[27-29]. The crude dye was dissolved in a minimum quantity of cold *N,N*-dimethylformamide (DMF). The solution was stirred for 1 hour at room temperature and filtered to remove insoluble impurities. The residue was again extracted with DMF and filtered. The filtrates were combined, and refiltered. The dye was re-precipitated by adding non-solvent (see Table 2.4) to the filtrate. The pure dye was collected as a powder by filtration and dried *in vacuo*.

Table 2.4: Solvent–non-solvent mixtures used for the purification of dyes

Colour	Solvent–non-solvent
Magenta	DMF–Acetone (1:2, v/v)
Yellow	DMF–Acetone (1:2, v/v)
Blue	DMF–Diethyl ether (1:2, v/v)

Moreover, purification of pyrimidine based modified dyes were performed on Biotage Isolera Four system using Biotage Snap RP-C18 cartridge ².

2.5.2.2 Ink Formulation

The main function of an ink is to place functional molecules (dyes) on a substrate, after being jetted from a print head. Therefore, the ink should be liquid having, for most industrial print heads, a viscosity below 25 cP ^[24].

After purification, the dyes are formulated into ink according to the recipe mentioned in Table 2.5; and in following manner:

- 1 N-methylmorpholine N-oxide (NMMO), 2-pyrrolidone and propan-2-ol were accurately weighed up and mixed at 30 °C for 15 minutes.
- 2 Polysorbate 20 (0.1% w/v) was added to stirred deionised water.
- 3 The purified dye to be investigated, was weighed and then added to the mixture of tween 20 and water with constant stirring to made up a dye solution.

² Purification of pyrimidine based modified dyes were performed by Mr Martin Huscroft from School of Chemistry.

- 4 This dye solution was then added slowly to the mixture of N-methylmorpholine N-oxide, 2-pyrrolidone and propan-2-ol and stirred for 30 minutes.
- 5 The ink formulation was kept in an ultrasonic bath for 10 minutes and then filtered using a 1 μm filter to remove any larger elements of the ink.
- 6 After filtration viscosity and surface tension of the formulation were determined.
- 7 The ink formulation was then used to print the pre-treated wool fabric through an inkjet printer.

Table 2.5: Ink Recipe ^[30]

Dye	X % w/v
N-methylmorpholine N-oxide (NMMO) ^[31]	300 g.dm ⁻³
2-pyrrolidone ^[32]	20 g.dm ⁻³
Propan-2-ol	25 g.dm ⁻³
Polysorbate 20 (Tween 20) ^[33]	0.1% w/v
Water	X dm ³
	1 dm ³

2.5.2.2.1 Measurement of Surface Tension

The surface tension of the ink is a primary factor determining droplet formation and spreading on the substrate upon contact. It can be controlled by using surfactants and by selecting proper solvent compositions. Inks suitable for use in an inkjet printer preferably have surface tension in the range 25 – 60 dynes.cm⁻¹ ^[32, 34]

In this study, surface tension of ink formulation was measured by Du Nouy method in which the force required to pull the ring from the liquid surface is measured ^[35].

2.5.2.2.2 Measurement of Viscosity

The viscosity of the ink is of great importance for its performance during jetting and spreading on the substrate, and is affected by the presence of surfactants and also solvent composition. The viscosity of ink is preferably in the range 2 – 20 cP ^[32, 34].

In this study, viscosity of ink formulations was measured using a Brookfield Viscometer.

2.5.3 Application onto Wool Fabric

Inkjet printing was carried out on Hewlett-Packard (HP) Deskjet 6940 thermal drop on demand Colour Inkjet Printer with a single pass at a resolution of 600 dpi as a solid rectangle print pattern using the formulated inks. For the purpose of passing the fabric samples through the inkjet printer, they were glued to a sheet of A4 transparency by applying double sided tape to the fabric edges. Printed samples were allowed to air dry for 5 minutes and then subjected to selected fixation processes for the appropriate times. All the inks were applied twice through inkjet printing.

2.5.4 Fixation of Prints

After printing, the dye is deposited on the fibre surface within a thickener film in a highly aggregated form; therefore, an appropriate fixation step is necessary. In this study, the dyes were fixed onto wool fabric through;

1. Method 1: Batching at room temperature for 2 and 4 hours under moist conditions ³
2. Method 2: Batching at elevated temperature (see Table 2.6) for 30, 60, 90, 120, 150 and 180 minutes under moist conditions
3. Method 3: Saturated steam at 102 °C for 5, 10, 15, 20 and 25 minutes

Table 2.6: Batching temperatures for fixation

Reactive Group	Temperature
Triazine	65 °C ^[36, 37]
Pyrimidine	90 °C ^[36, 37]

The moist conditions for batching were provided by interleaving the printed wool fabric with a moist cotton fabric padded with distilled water at a wet pick-up of 80%. The moist cotton fabric was placed on the reverse side of the printed wool

³ Trichloropyrimidine based dyes (**d13_{mp}** and **d15_{bp}**) and their modifications (**d14_{mpm}** and **d16_{bpm}**) were not fixed through batching at room temperature.

fabric. The fabrics were rolled onto a plastic cylinder and wrapped in clingfilm to prevent moisture loss during batching.

2.5.5 Washing-off

Removal of hydrolysed and unreacted dye along with thickener and any residue chemical from the goods is a vital step after printing [38]. Washing-off conditions must minimise staining of the unprinted ground [39]. Therefore, an alkaline washing solution containing sodium bicarbonate and Sandozin NIE in the wash liquor were used.

The printed samples were washed according to the following three-step washing procedure:

1. 5 minutes cold rinsing until no colour could be removed;
2. 10 minutes hot washing at 80 °C [39-41] with the addition of 2 g.dm⁻³ Sandozin NIE and 5 g.dm⁻³ sodium bicarbonate;
3. 10 minutes rinsing with running tap water

After fixation and washing-off the printed samples were tested for light fastness and wash fastness following the procedures detailed in section 2.8.1 and 2.8.2.

2.6 Stability of Dye based Inks

In order to assess the stability of the dyes in ink formulations, each ink was allowed to stand at room temperature over a period of 1 to 12 months and the change in percent area of dye from fresh ink to stored ink was recorded through CE (CZE or MEKC).

Furthermore, for the ease of identification of dye peak in CE electropherogram, stored ink sample was tested against fresh ink sample made on that particular day. Therefore, the electropherograms presented in this research are of samples tested for stability at the same time under same CE conditions.

2.7 Determination of Percent Fixation (Fibre-Dye Bond)

UV/Vis spectroscopy is frequently used in the measurement of percent fixation of the dyes used in textile coloration [42-45].

2.7.1 Analysis Parameters

The percent fixation was determined using a Perkin Elmer Lambda 40 UV/Vis Spectrophotometer (UK) in order to calculate the dye concentration in the various wash-off solutions.

After printing, the first sample was washed off immediately to obtain the total amount of the dye printed on the fabric and the solution was diluted to 100 cm³; the remaining samples were used for fixation (steaming and batching) followed by washing to obtain the amount of the hydrolysed and unreacted dye after the fixation process; the washing solutions were diluted to the same volume of 100 cm³ individually. The absorbance of the printed dye solution A_0 and absorbance of the wash-off solution A_i at the wavelength of maximum absorption λ_{\max} were used to obtain the percent fixation (%F) according to Equation 2.2; and rounded to nearest tenth.

$$\%F = [(A_0 - A_i)/A_0] \times 100\% \dots\dots\dots [2.2]$$

2.8 Colour Fastness Testing

2.8.1 Light Fastness Testing

Light fastness relates to the ability of a textile to retain its colour under the influence of light. Light fastness test is carried out according to the BS EN ISO 105–B02 (Method 3) ^[46] by using Q-Sun 1000 Xenon test chamber with irradiance of 0.65 W/m² at a temperature of 45 °C.

The light fastness test is used to determine the resistance of the specimen to artificial light which has a spectrum close to that of daylight (D65). The specimen of printed fabric is exposed along with the appropriate dyed wool reference fabrics to the light from the Xenon arc lamp. The fastness is assessed by comparing the fading of specimen with that of the reference fabrics.

The test method ISO 105–B02:2013 method 3 is suitable where the test specimen is compared for conformity with a known performance specification. The basic feature is the control of exposure by inspection of the *target blue wool reference*. The method allows multiple test specimens to be tested using a reduced number of blue wool references, typically the target blue wool reference together with the two blue wool references immediately preceding the target blue wool

reference. This is to assist in quantifying a specimen which does not conform with the required performance specification. For this method, opaque covers masking approximately one-third and two-thirds of the test specimens and blue wool references are required.

2.8.2 Wash Fastness Testing

Wash fastness test is carried out according to the BS EN ISO 105-C06:2010 (A1S) ^[47] using Mathis WT laboratory machine.

A specimen of the wool substrate in contact with multi-fibre strip is laundered, rinsed and dried. Specimens are laundered under appropriate conditions shown in Table 2.7. The change in colour of the specimen and the staining of the adjacent fabrics was assessed by comparison with the greyscale.

Table 2.7: Test conditions for wash fastness ^[47]

Test #	Temperature	Liquor volume	Available chlorine	Sodium perborate	Time (min)	No. of Steel balls	Adjust pH to
A1S	40 °C	150 ml	None	None	30	<i>a</i>	Not adjusted

a: For delicate fabrics and articles of wool fibres, steel balls are not used in the test.

The washing liquor was prepared by dissolving 4g SDC ECE Phosphate Reference Detergent B in 1 L deionised water. The adjacent multi-fibre strip (100×40 mm) used in the testing contains the following fabrics: secondary cellulose acetate, bleached un-mercerised cotton, Nylon 6.6, polyester, acrylic and wool.

2.9 Microwave-Irradiated Synthesis

Microwave irradiation has gained popularity in the past decade as a powerful tool for rapid and efficient synthesis of a variety of compounds because of selective absorption of microwave energy by polar molecules. The microwave irradiation is quite successful in providing enhanced reaction rate and improved product yield in chemical synthesis of a variety of carbon-heteroatom bonds ^[48, 49]

During recent years, microwaves have been extensively used for carrying out chemical reactions and have become a useful non-conventional energy source for performing organic synthesis. This is supported by a great number of publications in recent years, related to the application of microwaves as a consequence of a great availability of dedicated and reliable microwave instrumentation ^[50, 51].

As it is known, microwave irradiation is a fast route in organic synthesis. However, the application of microwave irradiation for the synthesis of dyes is still limited to functional dyes such as cyanine dyes ^[52-55]. Furthermore, there is no report on the synthesis of reactive dyes under microwave irradiation.

Traditionally, organic reactions are heated using an external heat source and therefore heat is transferred by conductance. This is a relatively slow and inefficient method for transmitting energy into the system because it relies on the thermal conductivity of the various materials that must be penetrated, and results in the temperature of the reaction vessel being higher than that of the reaction mixture. In addition, a temperature gradient can develop within the sample and local overheating can lead to product, reactants or reagent decomposition ^[51, 56, 57].

In contrast, microwave irradiation produces efficient internal heating by direct coupling of microwave energy with the polar molecules of solvents, reagents or catalysts presented in the reaction mixture. Since the vessels or vials are typically made out of the microwave-transparent materials the radiation passes through the walls of the vessel directly into the whole reaction mixture volume and an inverted temperature gradient as compared to conventional thermal heating effects (see Figure 2.7); which is directly responsible for the enhancements in reaction rates and yields.

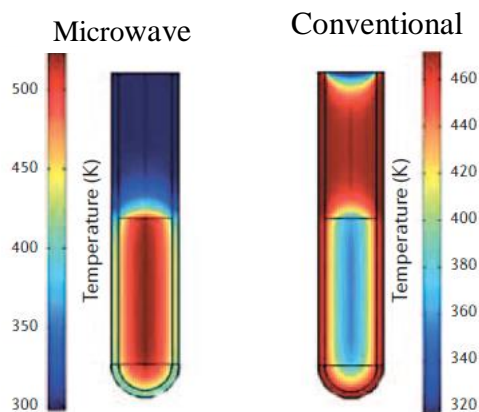


Figure 2.6: Inverted temperature gradients in microwave versus conventional heating adapted from reference ^[57]

2.9.1 Principle of Microwave-Irradiated Synthesis ^[57]

Microwave-irradiated synthesis is primarily based on the efficient heating of materials by microwave dielectric heating effects. Microwave dielectric heating is dependent on the ability of a specific material to absorb microwave energy and convert it to heat.

Microwave irradiation triggers heating by two main mechanisms: dipolar polarisation and ionic conduction ^[49].

2.9.1.1 Dipolar Polarisation

Dipolar polarisation is a process by which heat is generated in polar molecules. On exposure to an oscillating electromagnetic field of appropriate frequency, polar molecules try to follow the field and align themselves in phase with the field. However, owing to inter-molecular forces, polar molecules experience inertia and are unable to follow the field. This results in the random motion of particles (Figure 2.7), and this random interaction generates heat.



Figure 2.7: Dipolar interaction – dipolar molecules in reaction mixture will try to align with an oscillating electric field adapted from reference ^[49]

2.9.1.2 Conduction Mechanism

Due to the much stronger interaction of ions or even a single isolated ion with an electric field, the conduction mechanism leads to the heat generation. The ions will move under the influence of an electric field (Figure 2.8), resulting in expenditure of energy due to an increased collision rate, converting kinetic energy into heat. The heat generated by both mechanisms adds up resulting in a higher final temperature ^[51].



Figure 2.8: Ionic conduction – charged particles in reaction mixture will follow the applied electric field adapted from reference ^[49]

The conductivity mechanism is a much stronger interaction than the dipolar mechanism with regard to the heat generating capacity ^[49].

2.9.2 Advantages of Microwave-Irradiated Synthesis

- Higher reaction temperatures can be obtained by combining rapid microwave heating with sealed-vessel (autoclave) technology.
- Significantly reduced reaction times, higher yields and cleaner reaction profiles, allowing for more rapid reaction optimisation.
- Solvents with low boiling points can be used under pressure and be heated at temperatures considerably higher than their boiling point.
- Microwave heating allows direct in-core heating of the reaction mixture, which results in a faster and more even heating of the reaction mixture (see Figure 2.6).
- Easy on-line control of temperature and pressure profiles is possible, which leads to more reproducible reaction conditions.
- Microwave heating is more energy efficient than conventional heating because of direct molecular heating and inverted temperature gradients, see Figure 2.6.

2.9.3 Analysis Parameters

The microwave-irradiated syntheses were carried out in CEM Discover SP ^[58] using 35 ml CEM reactor vessel.

2.10 Miscellaneous Procedures

2.10.1 Completion of Diazotization

The completion of diazotization was determined by checking for the presence of excess nitrous acid using starch iodide paper ^[59]. When all the aromatic amine has reacted with sodium nitrite, then next portion (excess) of sodium nitrite added to the solution under test, converted to nitrous acid that remain in the solution and can be detected by the starch paper as an external indicator. This appearance of free nitrous acid in solution indicates that diazotization reaction is complete and equivalence point is attained.

2.10.2 Completion of Diazo-Coupling

In accordance with the method described in ^[59, 60], the endpoint of diazo-coupling reaction was determined by placing a few drops of the reaction mixture on a small heap of sodium chloride salt on filter paper. After 5 minutes, a drop of an alkaline solution of J-acid and drop of leftover diazonium salt solution were placed on both sides of the reaction mixture drop. Lines of colour appeared at the encounter of the migrating reagents thus showing the presence of coupling agent as well as diazonium salt. The coupling reaction was considered completed when a negative test is obtained on both sides of the reaction drop.

2.10.3 Freeze Drying

Reaction mixtures were freeze dried in Thermo Heto powerDry LL1500 freeze dryer ^[61].

2.11 References

1. Croft, S.N. and Hinks, D. Analysis of dyes by capillary electrophoresis. *Journal of the Society of Dyers and Colourists*, 1992, **108**, pp.546-551.

2. Croft, S.N. and Lewis, D.M. Analysis of reactive dyes and related derivatives using high-performance capillary electrophoresis. *Dyes and Pigments*, 1992, **18**, pp.309-317.
3. Hansa, A., Pillay, V. and Buckley, C. Analysis of reactive dyes using high performance capillary electrophoresis. *Water Science and Technology*, 1999, **39**, pp.169-172.
4. Terabe, S. *Micellar Electrokinetic Chromatography* [online]. [Accessed August 28,2012]. Available from: <http://pt7mdv.ceingebi.unam.mx/computo/pdfs/met/Electroforesis/Electroforesis/CE/MEKC/primer3.pdf>.
5. Heiger, D.N. *High performance capillary electrophoresis : an introduction* France: Hewlett Packard Co., 1992
6. Burkinshaw, S.M., Hinks, D. and Lewis, D.M. Capillary zone electrophoresis in the analysis of dyes and other compounds employed in the dye-manufacturing and dye-using industries. *Journal of Chromatography A*, 1993, **640**, pp.413-417.
7. Suntornsuk, L. Capillary electrophoresis of phytochemical substances. *Journal of Pharmaceutical and Biomedical Analysis*, 2002, **27**, pp.679-698.
8. Kim, J.-B. and Terabe, S. On-line sample preconcentration techniques in micellar electrokinetic chromatography. *Journal of Pharmaceutical and Biomedical Analysis*, 2003, **30**, pp.1625-1643.
9. Terabe, S. *Capillary Separation: Micellar Electrokinetic Chromatography* [online]. 2009. [Accessed August 28, 2012]. Available from: <http://www.annualreviews.org/doi/pdf/10.1146/annurev.anchem.1.031207.113005>.
10. Tapley, K.N. Capillary electrophoretic analysis of the reactions of bifunctional reactive dyes under various conditions including a study of the analysis of the traditionally difficult to analyse phthalocyanine dyes. *Journal of Chromatography A*, 1995, **706**, pp.555-562.
11. Stefan, A.R., Dockery, C.R., Nieuwland, A.A., Roberson, S.N., Baguley, B.M., Hendrix, J.E. and Morgan, S.L. Forensic analysis of anthraquinone, azo, and metal complex acid dyes from nylon fibers by micro-extraction and capillary electrophoresis. *Analytical and Bioanalytical Chemistry*, 2009, **394**, pp.2077-2085.

12. Ojstršek, A., Doliška, A. and Fakin, D. Analysis of reactive dyestuffs and their hydrolysis by capillary electrophoresis. *Analytical Sciences*, 2008, **24**, pp.1581-1587.
13. Fried, B. and Sherma, J. eds. *Handbook of thin-layer chromatography*. New York Marcel Dekker, 1996.
14. Skoog, D.A., West, D.M. and Holler, F.J. *Fundamentals of analytical chemistry*. New York: Saunders, 1988.
15. Fried, B. and Sherma, J. eds. *Thin-Layer Chromatography*. New York: Marcel Dekker, 1999.
16. Fritz, J.S. and George, H.S. *Quantitative analytical chemistry*. Boston: Allyn and Bacon, 1987.
17. Perkavac, J. and Perpar, M. Thin-layer chromatography of reactive dyes. *Fresenius' Zeitschrift für Analytische Chemie*, 1964, **206**, pp.356-9.
18. Perkavac, J. and Perpar, M. The analysis of reactive dyes by paper chromatography. *Kemija u Industriji*, 1964, **13**, pp.404-8.
19. McMurry, J. *Organic Chemistry*. 6 ed. London: Thomson Brooks/Cole, 2004.
20. Smith, B.C. *Infrared spectral interpretation: a systematic approach*. Florida: CRC, 1999.
21. Perkin Elmer. *FT-IR Spectroscopy: Attenuated Total Reflectance (ATR)* [online]. [Accessed July 12, 2012]. Available from: http://shop.perkinelmer.com/content/technicalinfo/tch_firatr.pdf.
22. Lewis, D.M. and Smith, S.M. Substituted thiol derivatives of vinyl sulphone dyes. *Dyes and Pigments*, 1995, **29**, pp.275-294.
23. Patent GB838337 (1960)
24. Ujiie, H. *Digital printing of textiles*. Cambridge: Woodhead Publishing Ltd., 2006.
25. Lewis, D.M. The Dyeing of Wool with Reactive Dyes. *Journal of the Society of Dyers and Colourists*, 1982, **98**, pp.165-175.
26. Clark, M., Yang, K. and Lewis, D.M. Modified 2,4-difluoro-5-chloropyrimidine dyes and their application in inkjet printing on wool fabrics. *Coloration Technology*, 2009, **125**, pp.184-190.
27. Chavan, R.B. The Use of Solvent-Nonsolvent Mixtures for the Purification of Anionic Dyes. *Textile Research Journal*, 1976, **46**, pp.435-437.

28. Hall, D.M. and Perkins, W.S. Practical Methods for Purification of Anionic Dyes as Their Sodium, Potassium and Lithium Salts. *Textile Research Journal*, 1971, **41**, pp.923-927.
29. Mehta, C.D. and Shah, K.H. Purification of Reactive dyes. *Indian Journal of Applied Chemistry*, 1966, **29**, pp.122-124.
30. Yang, K. *Reactive dye ink-jet printing on wool fabrics*. Ph.D. Thesis, University of Leeds, 2008.
31. Patent WO2002031067 (2002)
32. Patent WO2007045830 (2007)
33. Patent EP1853431 (2006)
34. Magdassi, S. Ink Requirements and Formulations Guidelines. In: S. Magdassi, ed. *Chemistry of Inkjet Inks*. New Jersey: World Scientific Publishing Ltd., 2012.
35. Du Noüy, P.L. A new apparatus for measuring surface tension. *The Journal of general physiology*, 1919, **1**, p.521.
36. Beech, W.F. *Fibre-Reactive Dyes* London: Logos Press Ltd., 1970.
37. Patent US20040081761 (2004)
38. Broadbent, A.D. *Basic principles of textile coloration*. Bradford: Society of Dyers and Colorists, 2001.
39. Broadbent, P.J. and Rigout, M.L. Wool Printing. *The Coloration of Wool and other Keratin Fibres*, 2013, pp.393-430.
40. Bell, V. Recent developments in wool printing. *Journal of the Society of Dyers and Colourists*, 1988, **104**, pp.159-172.
41. Christoe, J.R., Denning, R.J., Evans, D.J., Huson, M.G., Jones, L.N., Lamb, P.R., Millington, K.R., Phillips, D.G., Pierlot, A.P., Rippon, J.A. and Russell, I.M. Wool. In: *Kirk-Othmer Encyclopedia of Chemical Technology*. New York: An Interscience Publication, 2000.
42. Morris, K.F., Lewis, D.M. and Broadbent, P.J. Design and application of a multifunctional reactive dye capable of high fixation efficiency on cellulose. *Coloration Technology*, 2008, **124**, pp.186-194.
43. Mousa, A. Synthesis and application of a polyfunctional bis (monochlorotriazine/sulphatoethylsulphone) reactive dye. *Dyes and Pigments*, 2007, **75**, pp.747-752.

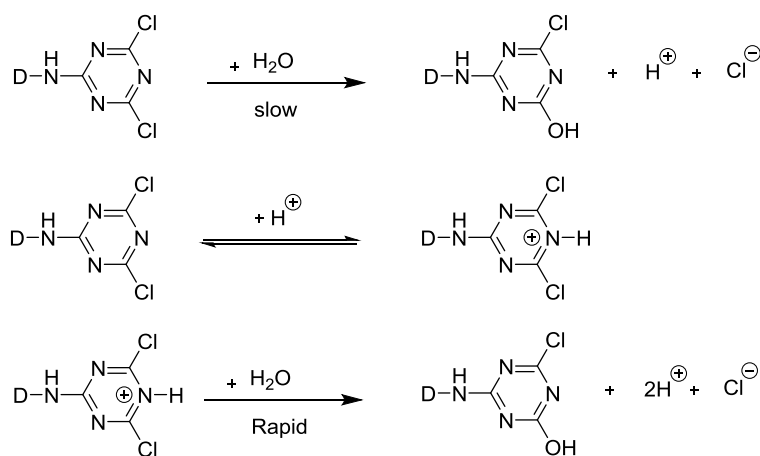
44. Li, Y., Zhang, S., Yang, J., Jiang, S. and Li, Q. Synthesis and application of novel crosslinking polyamine dyes with good dyeing performance. *Dyes and Pigments*, 2008, **76**, pp.508-514.
45. Smith, B., Berger, R. and Freeman, H.S. High affinity, high efficiency fibre-reactive dyes. *Coloration Technology*, 2006, **122**, pp.187-193.
46. British Standards Institution. *Colour fastness to artificial light: Xenon arc fading lamp test*, ISO 105-B02:2013.
47. British Standards Institution. *Textiles - Tests for colour fastness - Part C06: Colour fastness to domestic and commercial laundering*, BS EN ISO 105-C06:2010.
48. Ju, Y. and Varma, R.S. An efficient and simple aqueous N-heterocyclization of aniline derivatives: microwave-assisted synthesis of N-aryl azacycloalkanes. *Organic Letters*, 2005, **7**, pp.2409-2411.
49. Lidström, P., Tierney, J., Wathey, B. and Westman, J. Microwave assisted organic synthesis—a review. *Tetrahedron*, 2001, **57**, pp.9225-9283.
50. Mingos, D. The applications of microwaves in chemical syntheses. *Research on Chemical Intermediates*, 1994, **20**, pp.85-91.
51. Surati, M.A., Jauhari, S. and Desai, K. A brief review: Microwave assisted organic reaction. *Archives of Applied Science Research*, 2012, **4**, pp.645-661.
52. Baqi, Y. and Müller, C.E. Rapid and Efficient Microwave-Assisted Copper(0)-Catalyzed Ullmann Coupling Reaction: General Access to Anilinoanthraquinone Derivatives. *Organic Letters*, 2007, **9**, pp.1271-1274.
53. Baqi, Y. and Müller, C.E. Convergent Synthesis of the Potent P2Y Receptor Antagonist MG 50-3-1 Based on a Regioselective Ullmann Coupling Reaction. *Molecules*, 2012, **17**, pp.2599-2615.
54. Shaabani, A. Synthesis of metallophthalocyanines under solvent-free conditions using microwave irradiation. *Journal of Chemical Research, Synopses*, 1998, **10**, pp.672-673.
55. Lee, C.-C., Wang, J.-C. and Hu, A.T. Microwave-assisted synthesis of photochromic spirooxazine dyes under solvent-free condition. *Materials Letters*, 2004, **58**, pp.535-538.
56. Tierney, J.P. and Lidström, P. eds. *Microwave Assisted Organic Synthesis*. Oxford: Blackwell Publishing, 2005.

57. Kappe, C.O. and Dallinger, D. The impact of microwave synthesis on drug discovery. *Nature Reviews Drug Discovery*, 2005, **5**, pp.51-63.
58. CEM Corporation. *The latest in microwave synthesis technology* [online]. 2010. [Accessed January 10, 2013]. Available from: http://www.brs.be/pdf/DiscoverSPSynth_SinglePages.pdf.
59. Fierz-David, H.E. and Blangey, L. *Fundamental processes of dye chemistry*. New York: An Interscience Publication, 1949.
60. De Groot, R.A.M.C. and Neuman, M.G. Spot test for azo dye formation: An undergraduate laboratory experiment. *Journal of Chemical Education*, 1979, **56**, p.625.
61. Thermo Electron Cooperation. *Heto PowerDry® LL1500 Freeze Dryer* [online]. 2005. [Accessed March 01, 2013]. Available from: http://www.thermo.com.cn/Resources/200802/productPDF_27025.pdf.

3 Synthesis, Modification, Characterisation of Magenta Dichlorotriazine Dyes and Their Application onto Wool Fabric by Inkjet Printing

3.1 Introduction

Reactive dyes based on dichlorotriazine are the most reactive of all the reactive dyes available in the market ^[1-6]. Their tendency to undergo nucleophilic substitution is so pronounced that traces of moisture are sufficient to cause some hydrolysis of the dye and hence loss of reactivity. The liberated hydrogen chloride causes quaternisation of a nitrogen atom, thereby increasing its electrophilic character and hence accelerating the hydrolysis (shown in Scheme 3.1). The reaction is therefore autocatalytic which will inactivate even large batches in a very short time ^[7]. Therefore, dichlorotriazine dyes cannot be used in inkjet printing because of their low storage stability in inks ^[5]. Moreover, reactive inks should exhibit less than approximately 10% hydrolysis over a twelve months period ^[8].



Scheme 3.1: Hydrolysis of dichlorotriazine dye ^[7]

Replacement of one or both of the chlorine atoms of dichlorotriazine dye by other substituents can solve this problem by lowering the reactivity of this dye and hence stabilising it against hydrolysis.

Sulfophenoxy group has been claimed earlier as reactive group for cellulose ^[9, 10] and more recently for wool ^[11]. However, in earlier patented literature

sulfophenoxy is explored with other heterocyclic carrier systems such as 5-cyano-2,4,6-trichloropyrimidine ^[9, 12] and 2,4-difluoro-5-chloro-pyrimidine ^[11]. Moreover, sulfophenoxy group was also explored in cyanine dyes and high stability of sulfophenoxy cyanine dyes over its counterpart phenoxy dye was claimed ^[13].

Furthermore, in the presence of the sulfonic acid group (water-soluble group) in organic dyes, the unfixed dye is easily washed-off, resulting in improved wash fastness of dyes ^[14, 15].

On the basis of these earlier observations, it appeared that sulfophenoxy group might be compatible with chlorotriazine group and merit further investigation, especially in mono-substituted (sulfophenoxy/chlorotriazine) and also di-substituted (bis-sulfophenoxy group) dyes, since these appeared to be novel.

The sulfophenoxy group possesses some other potential attractions. It has a fairly low molecular weight (196.15) and thus does not dilute the chromophoric strength for the dye too drastically, and also it is readily incorporated, synthetically, into the dye molecules.

The agent used to modify the synthesised dichlorotriazine dye was sodium 4-hydroxybenzenesulfonate dihydrate (4HBSA), in the fibre-dye reaction, this then becomes the leaving group.

Moreover, the advantages targeted by replacing the halogen(s) with 4HBSA include a higher aqueous solubility, a lower chemical reactivity and hence a greater ink stability.

This chapter details the synthesis and characterisation of magenta dichlorotriazine dye **d2_{mt}**, modification of this dye by incorporating sulfophenoxy group to produce mono-substituted dye **d3_{mtm}** and also di-substituted dye **d4_{mtd}**.

This chapter also details the application of magenta dichlorotriazine dye and modified dyes based inks by inkjet printing onto wool fabrics along with performance evaluation of inks such as surface tension, viscosity, ink stability, percent fixation of the dye and colour fastness properties.

3.2 Experimental

3.2.1 Materials

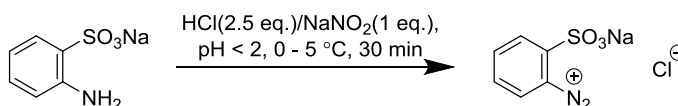
2-aminobenzenesulfonic acid (95%), sodium nitrite (98%), 4-amino-5-hydroxy-2,7-naphthalenedisulfonic acid monosodium salt hydrate (85%), cyanuric chloride (99%), sodium 4-hydroxybenzenesulfonate dihydrate (98%), sodium metabisulfite, carboxymethyl cellulose, polysorbate 20 (Tween 20) and N-methylmorpholine N-oxide (NMMO) were supplied by Sigma-Aldrich and used as received. Urea (MP Biomedicals), Alcopol O 60 (Acros organics), 2-pyrrolidone (Acros organics), 2-propanol (Fisher), Sandozin NIE (Clariant) were also purchased and used as received.

3.2.2 Synthesis and Characterisation of Magenta 5-Amino-4-Hydroxy-3-[(2-sulfophenyl)azo]-2,7-Naphthalenedisulfonic Acid Dye ($d1_m$)

3.2.2.1 Synthesis of $d1_m$

3.2.2.1.1 Diazotization

In accordance with the method described in reference [16], 2-aminobenzenesulphonic acid (18.2 g, 0.1 mol, 95%) was dissolved in water (100 cm³) which was then adjusted to pH 7 by the addition of 2N sodium carbonate solution followed by the addition of sodium nitrite (7.04 g, 0.1 mol, 98%), this formed a solution. This solution was then added dropwise, with good stirring to a mixture of concentrated hydrochloric acid (20 cm³, 0.25 mol, 36.6%), water (125 cm³) and ice (100 g) at 0 to 5 °C. The reaction mixture was stirred for further 30 min at 0 to 5 °C and pH < 2, excess nitrous acid was removed by adding sulfamic acid (confirmed by spotting a drop of reaction mixture on starch iodide paper). The reaction is shown in Scheme 3.2.

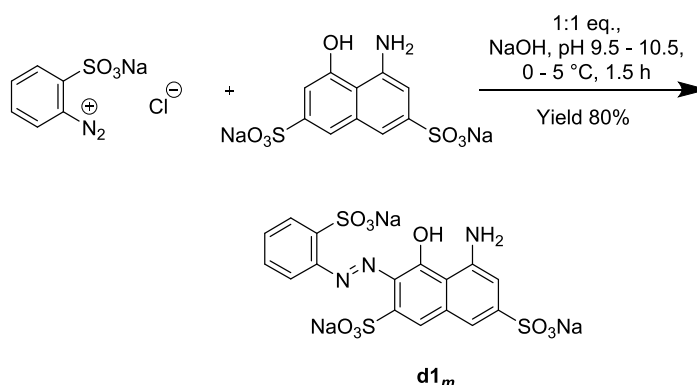


Scheme 3.2: Diazotisation of 2-aminobenzenesulfonic acid with nitrous acid leads to diazonium salt

3.2.2.1.2 Coupling

5-amino-4-naphthol-2,7-disulphonic acid (H-acid) (40.1 g, 0.1 mol, 85%) was suspended in water (100 cm³), sodium hydroxide solution (10% w/v) was added to raise the pH to 10, to allow the H-acid to dissolve. The temperature of the mixture was kept at 0 to 5 °C and pH was maintained at 9.5 to 10.5 by the addition of saturated sodium carbonate solution during the whole reaction period. The diazonium salt (0.1 mol) was added dropwise and with good stirring into the H-acid solution over 45 minutes, the reaction was continued for a further 1.5 hours (until the pH was stabilised), and was monitored by CZE, analytical TLC and spot test. Sodium chloride (8% w/v) was added in small portions to a stirred reaction mixture to precipitate the dye which was subsequently collected by filtration, washed with brine (10% w/v) and dried *in vacuo*.

The pure dye **d1_m** (40.27 g, 0.08 mol, yield 80%) was collected as magenta powder, after re-precipitation from DMF by acetone and dried *in vacuo* (Section 2.5.2.1). FT-IR analysis was conducted to confirm the presence of main functional groups in dye **d1_m**. The reaction is shown in Scheme 3.3.



Scheme 3.3: Azo coupling of diazonium salt with H-acid to form magenta dye chromophore **d1_m**

3.2.2.2 Characterisation of **d1_m**

The CZE electropherogram of the synthesised magenta dye chromophore **d1_m** at λ_{obs} , 542 nm is shown in Figure 3.1.

The synthesised **d1_m** was detected at 6.90 min with percent area of 100% indicating high purity of synthesised magenta dye chromophore.

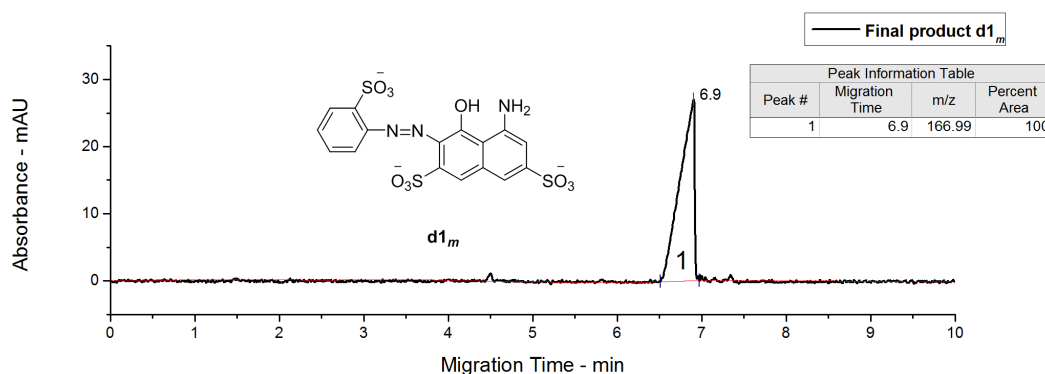


Figure 3.1: Electropherogram of magenta dye chromophore $d1_m$. CZE conditions: running buffer, 6mM potassium dihydrogen phosphate and acetonitrile (10% v/v) pH 9.0; pressure injection 0.5 psi for 10 s; voltage 25 kV; detection at 542 nm.

In TLC analysis, samples of the reaction mixture were taken at various time intervals during a reaction. At the start of the reaction, only the reactants (diazonium salt and H-acid) showed on the TLC plate. As the reaction progressed, the product $d1_m$ started to form and thus showed on the TLC plate. The $d1_m$ spot increased in intensity while the reactant spots decreased in intensity as more and more of the reactants were converted to product $d1_m$. The reaction was complete when the reactant spots were no longer showed on the TLC plate and the only product spot was visible. The R_f value of $d1_m$ was 0.68.

According to literature ^[17, 18], N–H bending vibration of primary amines is observed in the 1650 – 1580 cm^{-1} and medium to strong broad absorption in 909 – 666 cm^{-1} region of spectrum from N–H wagging. According to reference ^[19], the –N=N– stretch is likely to be weak and reported in the region 1450 – 1400 cm^{-1} region.

Analysis of FT-IR spectrum (Figure 3.2) of pure magenta powder suggested that the compound was $d1_m$ since peaks appeared at 1621 and 889 cm^{-1} and 1437 cm^{-1} attributed the presence of primary amine group and azo group on $d1_m$ respectively.

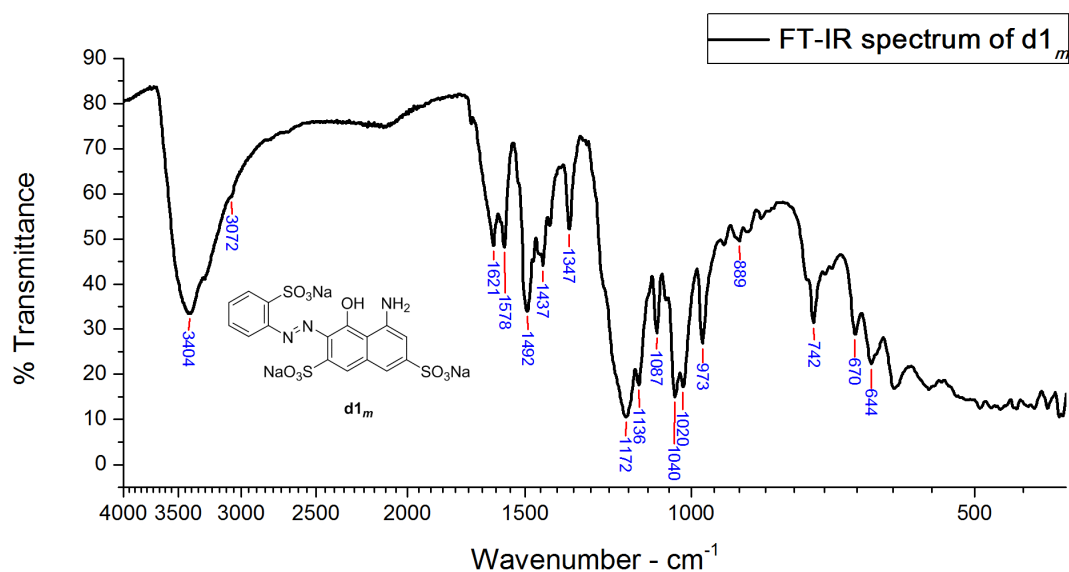


Figure 3.2: FT-IR spectrum of magenta dye chromophore $d1_m$

The detailed analysis of the spectrum (Figure 3.2) is as follows [17, 20-22]; broad intermolecular hydrogen bonded, O–H stretch, 3404 cm^{-1} ; overtone or combinational bands, $2000 - 1667\text{ cm}^{-1}$; N–H bending, 1621 cm^{-1} ; C=C ring stretch, $1578, 1492\text{ cm}^{-1}$; azo group stretch, 1437 cm^{-1} , C–N stretch (primary amine), 1347 cm^{-1} ; sulfonate, 1172 cm^{-1} ; in-plane C–H bend, $1040, 1020\text{ cm}^{-1}$; broad, N–H wag, 889 cm^{-1} ; out of plane aromatic C–H bend, 742 cm^{-1} .

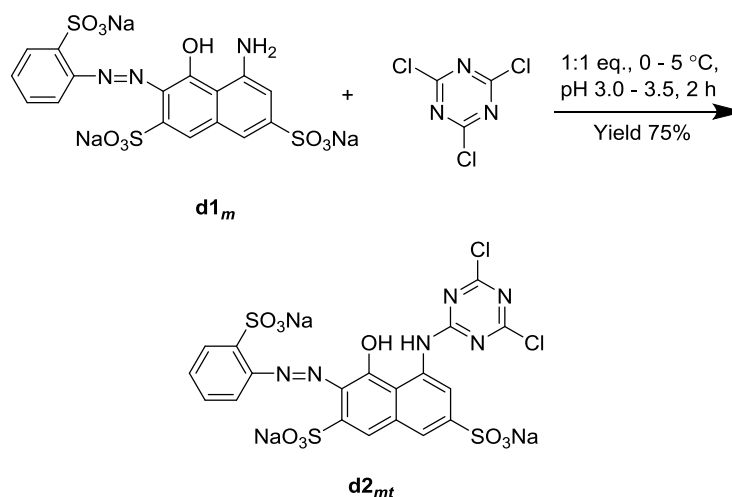
3.2.3 Synthesis and Characterisation of Magenta 5-[(4,6-Dichloro-1,3,5-triazin-2-yl)amino]-4-Hydroxy-3-[(2-Sulfophenyl)azo]-2,7-Naphthalenedisulfonic Acid Dye ($d2_{mt}$)

3.2.3.1 Synthesis of $d2_{mt}$

In accordance with the method described in references [1, 23, 24], 5-amino-4-hydroxy-3-[(2-sulfophenyl)azo]-2,7-naphthalenedisulfonic acid $d1_m$ (28.47 g, 0.05 mol) was dissolved in water (150 cm^3) which was adjusted to pH 3.0 by the addition of 2N hydrochloric acid solution at 0 to $5\text{ }^\circ\text{C}$. A solution of cyanuric chloride (9.22 g, 0.05 mol) in acetone (50 cm^3) was added dropwise to the dye $d1_m$ solution over 30 minutes. The reaction mixture was stirred and the pH was maintained at 3.0 to 3.5 by the addition of 2N sodium carbonate solution, while the temperature was kept at 0 to $5\text{ }^\circ\text{C}$. Once the addition of cyanuric chloride was complete, the reaction was stirred for further 2 hours (until the pH was stabilised) and was monitored with CZE

and TLC. When the mono condensation reaction of cyanuric chloride had gone to completion 2N sodium carbonate solution was added to raise the pH to 7.0 and phosphate buffer (0.2 mol, 10% v/v) was added to buffer the pH to 6.4 [1, 25]. Sodium chloride (8% w/v) was added to precipitate the dye. The crude dye **d2_{mt}** was collected by filtration and the filter cake was washed with brine (2 × 100 cm³) and dried *in vacuo*.

Purification of crude dye using solvent-nonsolvent technique (DMF–Acetone, 1:2 v/v) afforded the pure dye **d2_{mt}** (24.49 g, 3.75 mmol, yield 75%) as magenta powder. FT-IR analysis was conducted to confirm the presence of main functional groups in dye **d2_{mt}**. The reaction is shown in Scheme 3.4.



Scheme 3.4: Preparation of condensation product **d2_{mt} from magenta azo chromophore and cyanuric chloride**

3.2.3.2 Characterisation of **d2_{mt}**

Figure 3.3 shows the progression of the synthesis reactions of **d2_{mt}** from magenta starting material **d1_m** in a fused silica capillary at pH 9.0. Both analytes have a charge of -3 under these conditions. The EOF in this case is towards the cathode, while the analytes are moved electrophoretically towards the anode. The EOF contribution is larger than the electrophoretic mobility of analytes, so that the net movement of analytes will be toward the cathode. The analyte with the highest mass to charge ratio should elute first and the analyte with the lowest mass to charge ratio should elute last.

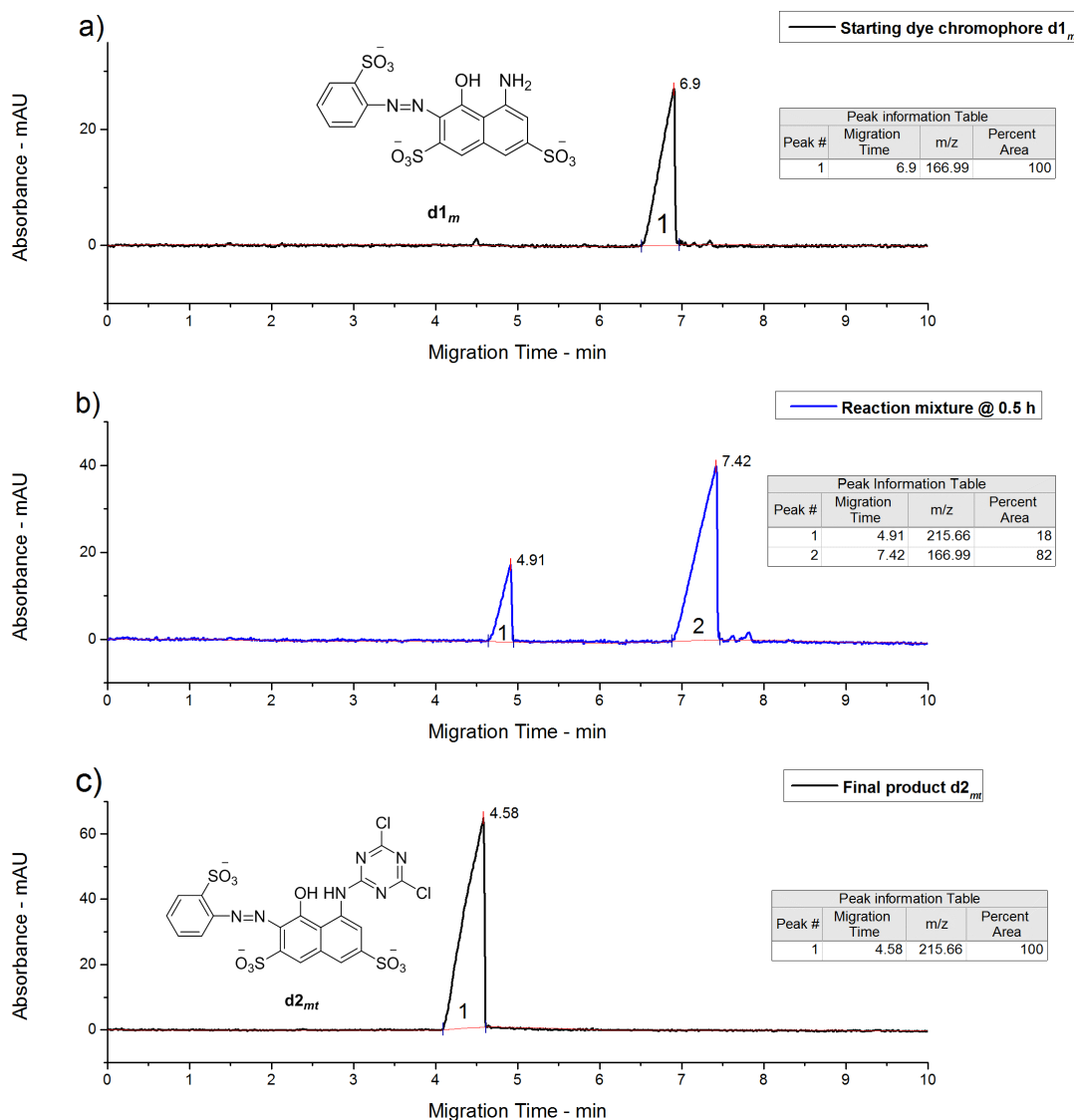


Figure 3.3: Electropherograms showing reaction progress of synthesis of $d2_{mt}$. (a) Starting dye chromophore $d1_m$; (b) $d1_m - d2_{mt}$ after 0.5 hour reaction time; (c) Final product $d2_{mt}$. CZE conditions: same as Figure 3.1.

The peaks observed in Figure 3.3b were as expected; the first peak to emerge was $d2_{mt}$ (4.91 min) which has the higher mass to charge ratio of the two analytes. This occurs because the addition of the triazine group onto the dye chromophore $d1_m$ increases the molecular weight of the dye $d2_{mt}$ without any additional sulfonic acid groups that would increase the negative charge.

Moreover, the percent area of the $d2_{mt}$ shown in Figure 3.3c, was 100% which indicates that there was no hydrolysed dye in the final product.

In TLC analysis the spots observed were as expected showing that reaction of dye chromophore $d1_m$ with cyanuric chloride occurs readily at 0 to 5 °C providing

that pH 3.0 to 3.5 is maintained. Analytical TLC showed gradual appearance of new magenta compound **d2_{mt}** (R_f value 0.71) of increased hydrophobicity compared to the magenta starting material **d1_m** (R_f value 0.68). This is because as the mobile phase ascends the plate, **d1_m** being polar interact more with the stationary phase while **d2_{mt}** being less polar interact more with the mobile phase. As a result, **d2_{mt}** ascend the plate faster than **d1_m** resulting in their separation ^[26]. Moreover, almost quantitative conversion to product (**d2_{mt}**) occurred in 2 hours.

Analysis of FT-IR spectrum (Figure 3.4) of pure magenta powder suggested that the compound has been **d2_{mt}** since peaks due to the presence of primary amine in **d1_m** (Figure 3.2) at 1621 cm^{-1} and 889 cm^{-1} are no longer present indicating that the primary amine had successfully reacted with cyanuric chloride. According to literature ^[17], triazine group have at least one strong band at $1580 - 1520\text{ cm}^{-1}$ and at least one band at $1450 - 1350\text{ cm}^{-1}$ corresponding to the stretching of the ring. The appearance of new peaks at 1540 cm^{-1} and 1397 cm^{-1} reflect the presence of the triazine group in **d2_{mt}**. Moreover, in accordance with literature ^[17, 22], the appearance of the peaks at the 1092 cm^{-1} and 794 cm^{-1} are attributed to the stretching vibrations of carbon chlorine bond on the triazine ring of the **d2_{mt}**.

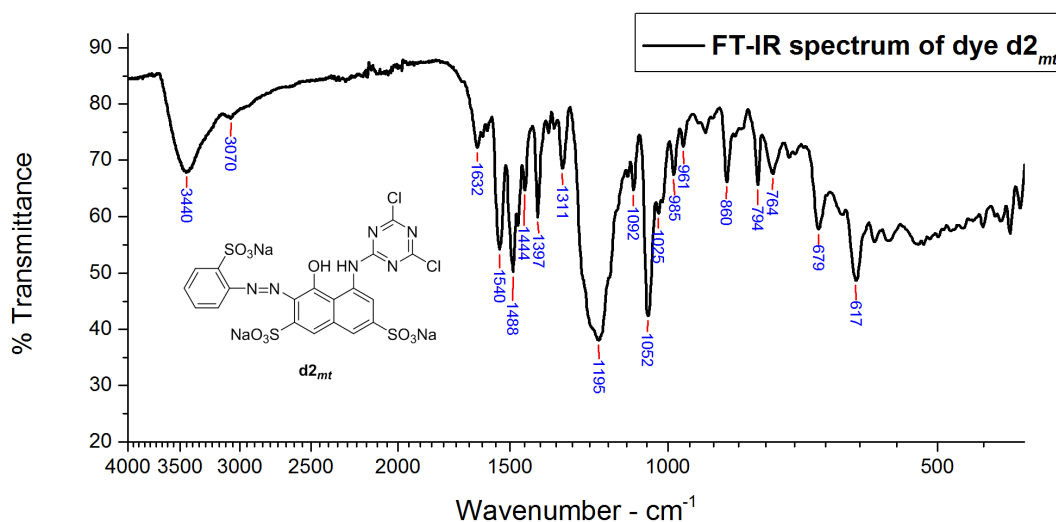


Figure 3.4: FT-IR spectrum of magenta dichlorotriazine dye **d2_{mt}**

The detailed analysis of spectrum (Figure 3.4) is as follows ^[17, 20-22]; N-H stretch, 3440 cm^{-1} ; overtone or combinational bands, $2000 - 1667\text{ cm}^{-1}$; C=C ring stretch, 1488 cm^{-1} ; azo group stretch, 1444 cm^{-1} ; C=N stretch, 1540 cm^{-1} , 1397 cm^{-1} ; C-N stretch (secondary amine), 1311 cm^{-1} ; sulfonate, 1195 cm^{-1} ; C-Cl stretch,

1092 cm^{-1} , 794 cm^{-1} ; in-plane C–H bend, 1052, 1025 cm^{-1} ; out of plane aromatic C–H bend, 764 cm^{-1} .

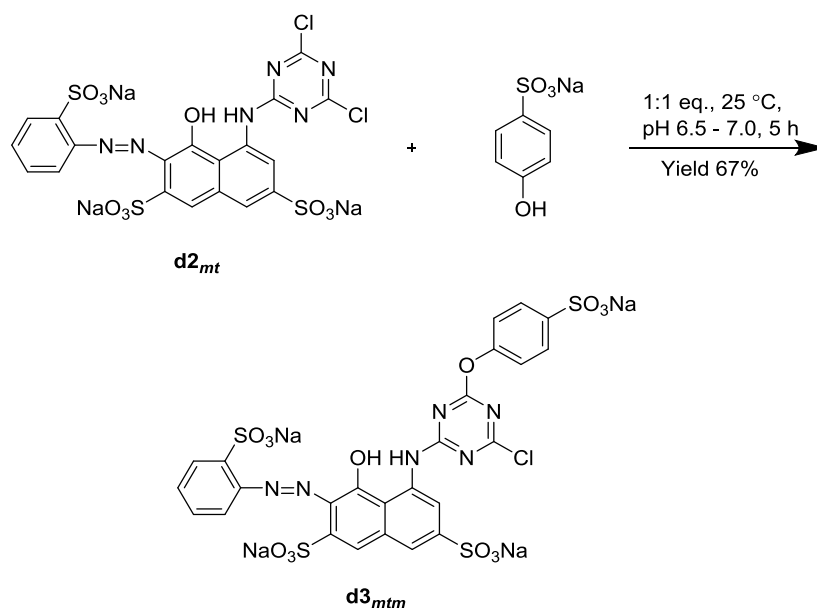
^1H NMR (D_2O , 500 MHz) δ 7.35 (1H, J = 10 Hz, t), 7.64 (1H, J = 10, t), 7.73 (1H, s), 7.82 (1H, J = 10 Hz, d), 7.88 (1H, s), 8.18 (1H, J = 10, d), 9.02 (1H, s)

3.2.4 Synthesis and Characterisation of Modified Magenta 5-[[4-Chloro-6-(4-sulfophenoxy)-1,3,5-triazin-2-yl]amino]-4-Hydroxy-3-[(2-sulfophenyl)azo]-2,7-Naphthalenedisulfonic Acid Dye ($\mathbf{d3}_{mtm}$)

3.2.4.1 Synthesis of $\mathbf{d3}_{mtm}$

Dye $\mathbf{d2}_{mt}$ (6.51 g, 0.01 mol, 1 eq.) and sodium bicarbonate ^[27] (1.23 g, 0.015 mol, 1.5 eq.) were dissolved in water (50 cm^3) at 25 °C. A solution of sodium 4-hydroxybenzenesulfonate dihydrate (4HBSA) (2.32 g, 0.01 mol, 1 eq.) in water (20 cm^3) was added dropwise over 15 minutes to the $\mathbf{d2}_{mt}$ solution; the pH was maintained at 6.5 to 7.0 by the addition of saturated sodium carbonate solution. Once the addition of 4HBSA solution was complete, the reaction mixture was stirred for a further 5 hours (until the pH was stabilised) and was monitored with CZE and TLC. Sodium chloride (10% w/v) was added to precipitate out the dye. The crude dye $\mathbf{d3}_{mtm}$ was collected by filtration and the filter cake was dried *in vacuo*.

Purification of crude dye $\mathbf{d3}_{mtm}$ using solvent-nonsolvent technique (DMF–Acetone, 1:2 v/v) yielded pure dye $\mathbf{d3}_{mtm}$ (5.45 g, 6.72 mmol, yield 67%) as magenta powder. The dye $\mathbf{d3}_{mtm}$ was characterised by FT-IR and elemental analysis (CHN). The reaction is shown in Scheme 3.5.



Scheme 3.5: Mono substitution of dye **d2_{mt} with 4HBSA to yield dye **d3_{mtm}****

3.2.4.2 Characterisation of **d3_{mtm}**

The electropherograms from CZE analysis are shown in Figure 3.5 which indicates the progression of the synthesis reaction from the starting dye **d2_{mt}** to the mono-substituted dye **d3_{mtm}** (peak 2 in Figure 3.5b).

As shown in Figure 3.5b, the first peak to emerge was **d2_{mt}** (4.57 min) which had the higher mass to charge ratio of the two analytes. The next peak to emerge was **d3_{mtm}** (5.89 min). This occurs because the mono substitution of **d2_{mt}** with HBSA not only increases the molecular weight of modified dye **d3_{mtm}** but also increase a negative charge on it, therefore the migration time of the dye **d3_{mtm}** increases.

In addition, CZE analysis also shows that starting material **d2_{mt}** was fully converted to modified dye **d3_{mtm}** in 5 hours.

Moreover, the percent area of the **d3_{mtm}** shown in Figure 3.5c indicates the purity of the final product.

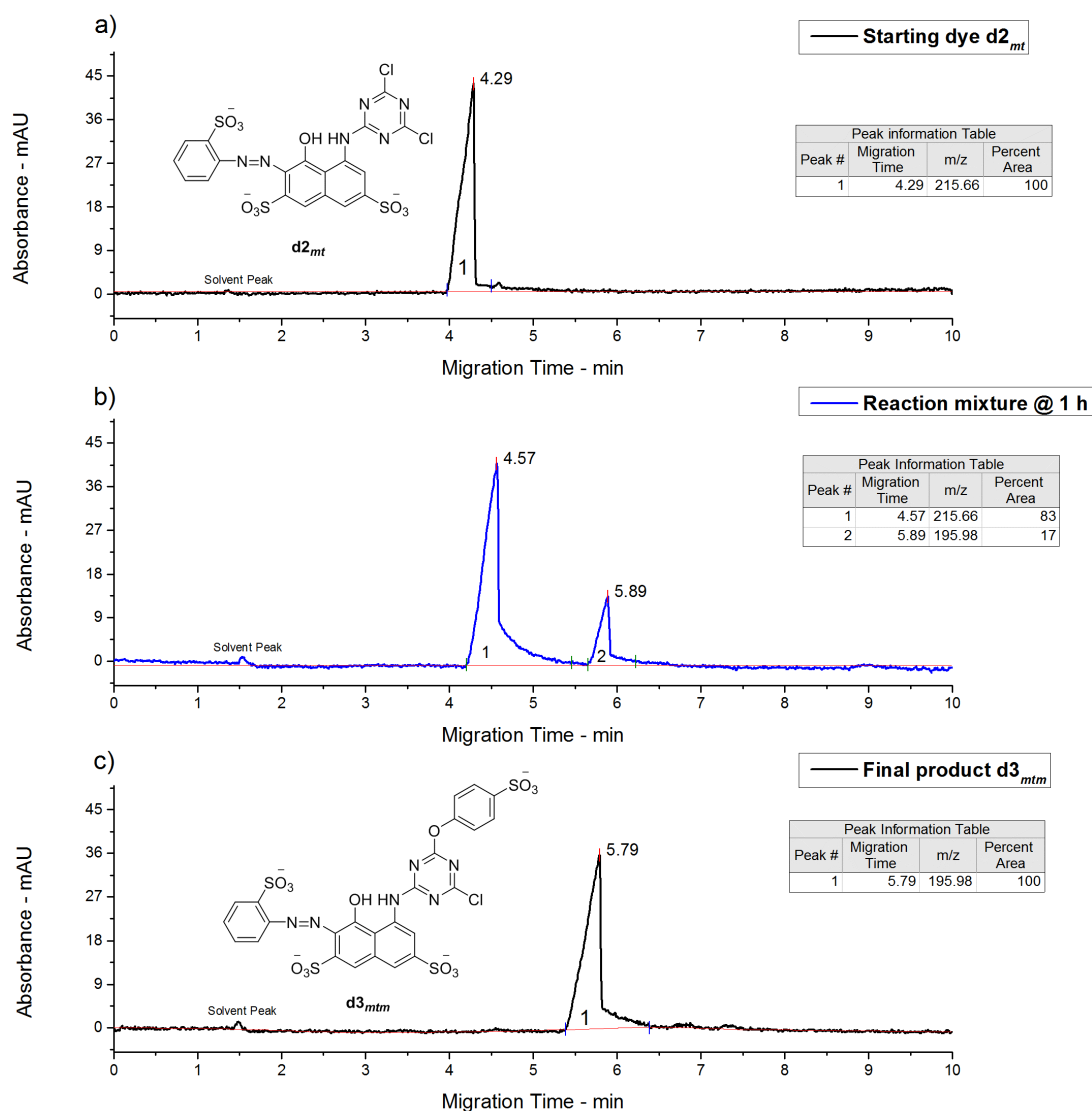


Figure 3.5: Electropherograms showing reaction progress of synthesis of $d3_{mtm}$. (a) Starting dye $d2_{mt}$; (b) $d2_{mt}$ – $d3_{mtm}$ after 1 hour reaction time; (c) Final product $d3_{mtm}$. CZE conditions: same as Figure 3.1.

In analytical TLC analysis, the spots appeared as expected, indicating that the primary condensation reaction of dye $d2_{mt}$ with HBSA taking place promptly at 25 °C provided that neutral pH was maintained. Analytical TLC showed the gradual appearance of new more polar magenta compound $d3_{mtm}$ (R_f value 0.67) compared to the magenta starting material $d2_{mt}$ (R_f value 0.71). Moreover, TLC showed that the starting material $d2_{mt}$ was fully converted to the $d3_{mtm}$ in 5 hours.

In accordance with the literature [17, 22], the appearance of new peak at 1124 cm^{-1} in Figure 3.6 can be attributed to the stretching vibration of C–O–C in the structure between the triazine and 4HBSA. The small peaks at 1092 cm^{-1} and 808

cm^{-1} can be attributed to the presence of aromatic C–Cl bond after the mono substitution of dye $\mathbf{d2}_{mt}$ with 4HBSA.

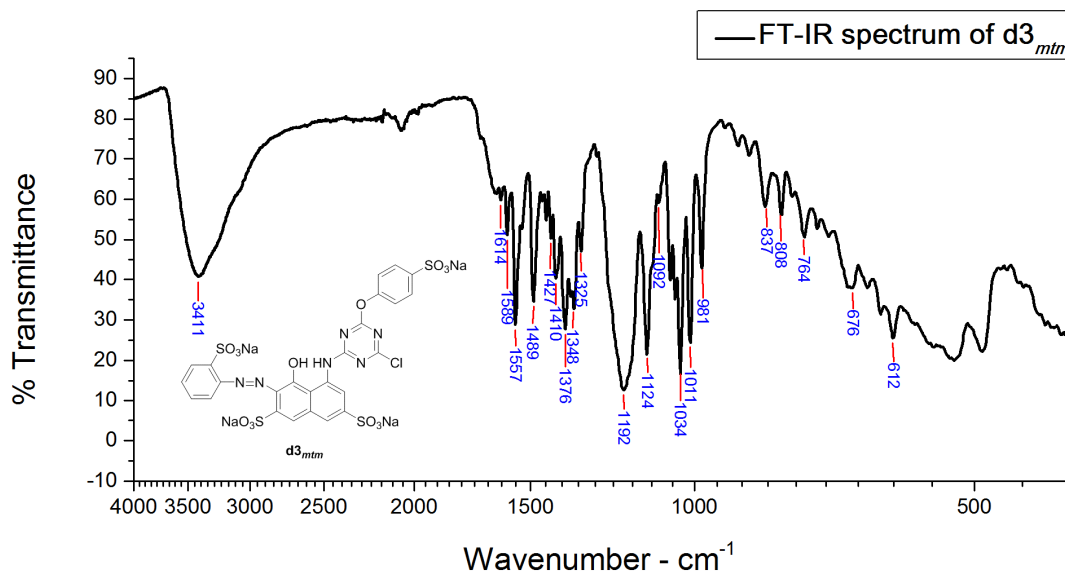


Figure 3.6: FT-IR spectrum of magenta mono-substituted modified dye $\mathbf{d3}_{mtm}$

The detailed analysis of the spectrum is as follows ^[17, 20-22]; N–H stretch, 3411 cm^{-1} ; overtone or combinational bands, $2000\text{--}1667 \text{ cm}^{-1}$; C=C ring stretch, 1489 , 1410 cm^{-1} ; azo group stretch, 1427 cm^{-1} ; C=N stretch, 1557 , 1376 cm^{-1} ; C–N stretch (secondary amine), 1325 cm^{-1} ; C–O–C stretching, 1124 cm^{-1} ; sulfonate, 1192 cm^{-1} ; C–Cl stretch, 1092 , 808 cm^{-1} ; in-plane C–H bend, 1034 , 1011 cm^{-1} ; out of plane aromatic C–H bend, 764 cm^{-1} .

Elemental analysis, Found: C, 30.98%; H, 2.38%; N, 8.79%. Calculated for $\text{C}_{25}\text{H}_{13}\text{ClN}_6\text{Na}_4\text{O}_{14}\text{S}_4 \cdot 4\text{H}_2\text{O}$: C, 31.65%; H, 2.32%; N, 8.86%. The results were adjusted due to the presence of water of crystallisation in the dye molecule.

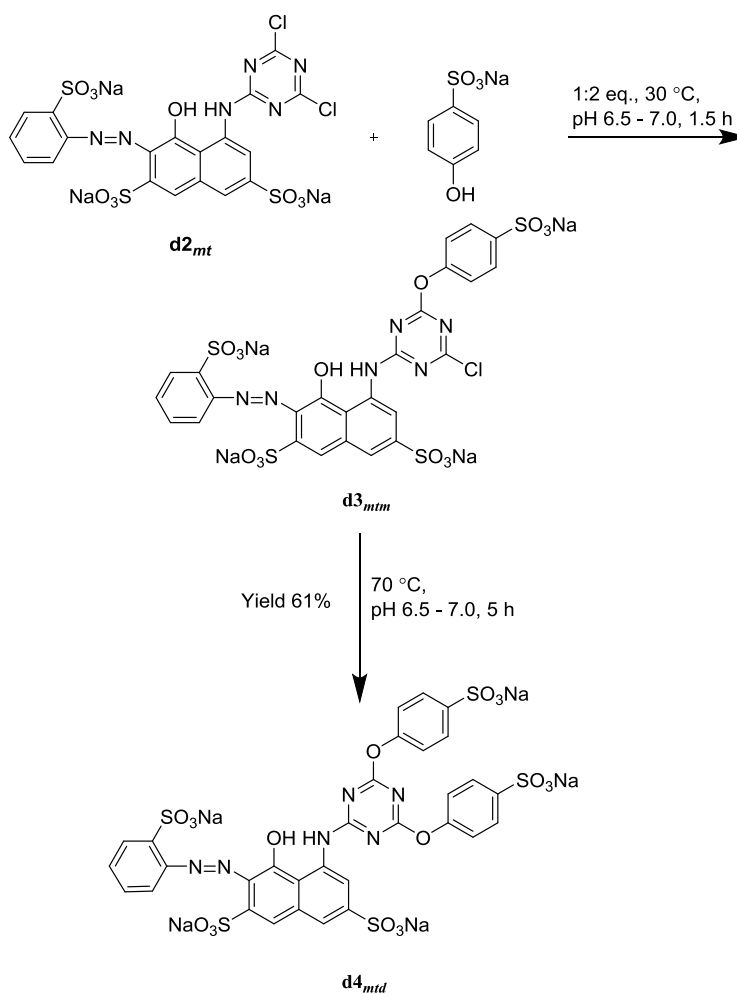
3.2.5 Synthesis and Characterisation of Modified Magenta 5-[[4,6-(4-Sulfophenoxy)-1,3,5-triazin-2-yl]amino]-4-Hydroxy-3-[(2-sulfophenyl)azo]-2,7-Naphthalenedisulfonic Acid Dye ($\mathbf{d4}_{mtd}$)

3.2.5.1 Synthesis of $\mathbf{d4}_{mtd}$

Dye $\mathbf{d2}_{mt}$ (6.51 g, 0.01 mol, 1 eq.) and sodium bicarbonate (1.23 g, 0.015 mol, 1.5 eq.) were dissolved in water (50 cm^3) and the temperature was raised to $30 \text{ }^\circ\text{C}$. A solution of sodium 4-hydroxybenzenesulfonate dihydrate (4HBSA) (4.86 g, 0.02 mol, 2 eq.) in water (30 cm^3) was added dropwise over 15 minutes to the dye $\mathbf{d2}_{mt}$

solution; the pH was maintained at 6.5 to 7.0 by the addition of saturated sodium carbonate solution. Once the addition of the 4HBSA solution was complete, the reaction was followed using CZE and TLC. The CZE and TLC analysis showed that the primary condensation of dye **d2_{mt}** was complete after 1.5 hours (pH has stabilised); after which the temperature of the reaction mixture was raised to 70 °C to enable the secondary condensation of dye **d2_{mt}** to occur. After 5 hours, the CZE and TLC analysis showed that the secondary condensation was complete. Sodium chloride (10% w/v) was added to precipitate out the dye. The crude dye **d4_{mtd}** was collected by filtration and the filter cake was dried *in vacuo*.

Purification of crude dye **d4_{mtd}** using solvent-nonsolvent technique (DMF–Acetone, 1:2 v/v) afforded pure dye **d4_{mtd}** (5.93 g, 6.11 mmol, yield 61%) as magenta powder. The dye **d4_{mtd}** was characterised by FT-IR and elemental analysis (CHN). The reaction is shown in Scheme 3.6.



Scheme 3.6: Preparation of di-substituted dye **d4_{mtd} from magenta dichlorotriazine dye **d2_{mt}** and 4HBSA**

3.2.5.2 Characterisation of $\mathbf{d4}_{mtd}$

The CZE electropherograms at different reaction times during the modification of dye $\mathbf{d2}_{mt}$ with 4HBSA are shown in Figure 3.7.

Dye $\mathbf{d2}_{mt}$ readily started to convert to the modified dye $\mathbf{d3}_{mtm}$ (peak 2 in Figure 3.7b) after 0.5 hour; moreover, small amount of modified dye $\mathbf{d4}_{mtd}$ (peak 3 in Figure 3.7b) was also formed. After 4.5 hours of reaction at 25 °C, all of the dye $\mathbf{d2}_{mt}$ had been converted to the dye $\mathbf{d3}_{mtm}$ or dye $\mathbf{d4}_{mtd}$ (peak 1 and peak 2 in Figure 3.7c). When the reaction temperature was raised to 70 °C and allowed to continue for a further 5 hours, the dye $\mathbf{d3}_{mtm}$ had been fully converted to modified dye $\mathbf{d4}_{mtd}$ as shown in Figure 3.7d. The peaks were eluted in the order of decreasing mass to charge ratio as expected.

Moreover, the percent area of the $\mathbf{d4}_{mtd}$ shown in Figure 3.7 indicates the purity of the final product.

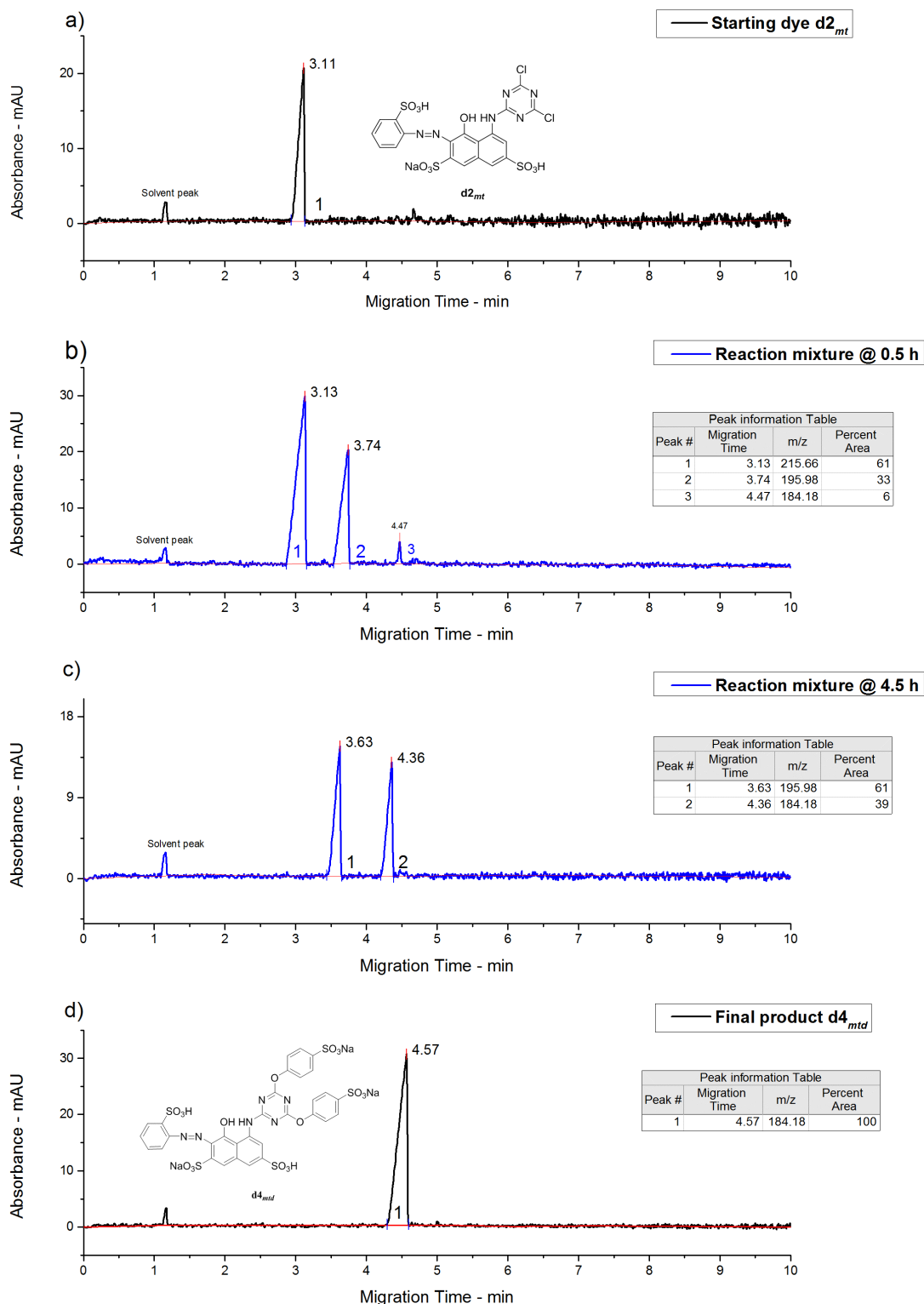


Figure 3.7: Electropherograms showing reaction progress of synthesis of $d4_{mtd}$. (a) Starting dye $d2_{mt}$; (b) $d2_{mt}$ – $d3_{mtm}$ – $d4_{mtd}$ after 0.5 hour reaction time; (c) $d3_{mtm}$ – $d4_{mtd}$ after 4.5 hours reaction time; (d) Final product $d4_{mtd}$. CZE conditions: same as Figure 3.1.

In analytical TLC analysis, the spots appeared as estimated, showing that the primary condensation reaction of dye $d2_{mt}$ with 4HBSA occur readily at 30 °C

provided that neutral pH was maintained. Analytical TLC showed the gradual appearance of new more polar magenta dye **d3_{mtm}** (R_f value 0.67) compared to the magenta starting material **d2_{mt}** (R_f value 0.71). Once the mono-substitution was completed, the di-substitution started and new more polar magenta dye **d4_{mtd}** (R_f value 0.60) appeared on TLC plate. TLC showed that mono-substituted dye **d3_{mtm}** was fully converted to the **d4_{mtd}** in 5 hours.

In the FT-IR spectrum of the dye **d4_{mtd}**, Figure 3.8, the appearance of new peak at 1123 cm^{-1} can be attributed to the stretching vibration of C–O–C in structure between the triazine and the 4HBSA. The C–Cl peaks at 1092 cm^{-1} and 794 cm^{-1} (Figure 3.4) are no longer present indicating that dye **d2_{mt}** has been successfully di-substituted with 4HBSA to yield dye **d4_{mtd}**.

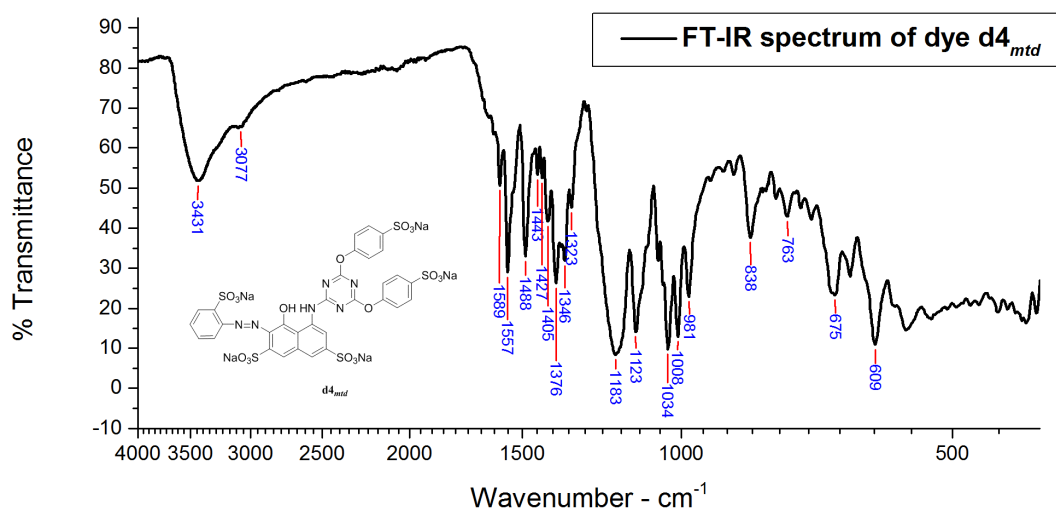


Figure 3.8: FT-IR spectrum of magenta di-substituted dye **d4_{mtd}**

The detailed analysis of spectrum (Figure 3.8) is as follows ^[17, 20-22]; N–H stretch, 3431 cm^{-1} ; aromatic C–H stretch, 3077 cm^{-1} ; overtone or combinational bands, $2000\text{--}1667\text{ cm}^{-1}$; C=C ring stretch, $1488, 1405\text{ cm}^{-1}$; azo group stretch, 1427 cm^{-1} ; C=N stretch, $1557, 1376\text{ cm}^{-1}$; C–N stretch (secondary amine), 1323 cm^{-1} ; C–O–C stretch, $1123, \text{cm}^{-1}$; sulfonate, 1183 cm^{-1} ; in-plane C–H bend, $1034, 1008\text{ cm}^{-1}$; out of plane aromatic C–H bend, 763 cm^{-1} .

Elemental analysis, Found: C, 30.80%; H, 3.06%; N, 6.79%. Calculated for $\text{C}_{31}\text{H}_{17}\text{N}_6\text{Na}_5\text{O}_{18}\text{S}_5 \cdot 10\text{H}_2\text{O}$: C, 30.61%; H, 3.07%; N, 6.91%. It should be noted that the results are adjusted due to the presence of water of crystallisation.

¹H NMR (D₂O, 500 MHz) δ 7.32 (2H, J = 10 Hz, t), 7.52 (2H,s), 7.62 (6H, m), 7.82 (2H, J = 10 Hz, d), 8.15 (2H, J = 10 Hz, d), 9.20 (2H, s)

3.2.6 Application of Magenta Dyes (**d_{2_{mt}}**, **d_{3_{mtm}}** and **d_{4_{mtd}}**) onto Wool Fabric by Inkjet Printing

The inks were prepared using 4% dye according to the procedure detailed in section 2.5.2, and then viscosity and surface tension of inks were measured.

The resulting ink formulation was then introduced in the cartridge and printed onto wool fabric using the HP 6940 Deskjet printer. Once printed, the printed wool samples were fixed by three methods detailed in section 2.5.4, and evaluated for percent fixation along with light fastness and wash fastness.

Moreover the inks were also evaluated for stability through CZE over twelve months storage time at room temperature.

3.2.7 Characteristics of Inks (**d_{2_{mt}}**, **d_{3_{mtm}}** and **d_{4_{mtd}}**)

3.2.7.1 Surface Tension and Viscosity of Inks

In terms of inkjet printing, aqueous inks are required to have a surface tension and viscosity of 25 – 60 dynes.cm⁻¹ and 2 – 20 cP respectively [28, 29]. It can be seen, from Table 3.1, that parent dye **d_{2_{mt}}** and both the modified dyes (**d_{3_{mtm}}** and **d_{4_{mtd}}**) based inks have a surface tension and viscosity within the operational range.

Table 3.1: Surface tension and viscosity of magenta inks

Ink formulation	Surface Tension (dynes.cm ⁻¹)	Viscosity (cP)
d_{2_{mt}} based ink	43.5	10
d_{3_{mtm}} based ink	44.0	10
d_{4_{mtd}} based ink	45.0	8

3.2.7.2 Stability of Dye (**d_{2_{mt}}**, **d_{3_{mtm}}** and **d_{4_{mtd}}**) Based Inks

As discussed earlier, dichlorotriazine dyes are susceptible to hydrolysis even with just traces of moisture. Moreover, reactive dyes can also react with

nucleophiles such as amino and hydroxyl groups present in ink during their storage. From this mechanism there are several unfavourable courses of reaction by reactive dyes during storage of inks. These reactions not only reduce the efficiency of coloration of dye (percent fixation) but also results in dye wastage [29]. Therefore, stability of dichlorotriazine dye along with new modified dyes in inks were also evaluated.

The results obtained from stability tests of magenta dyes are detailed in this section. The results of any change in the percent area of the peaks of the dyes **d2_{mt}**, **d3_{mtm}** and **d4_{mtd}** within inks stored at room temperature for 12 months can be seen in Figure 3.9, Figure 3.10 and Figure 3.11.

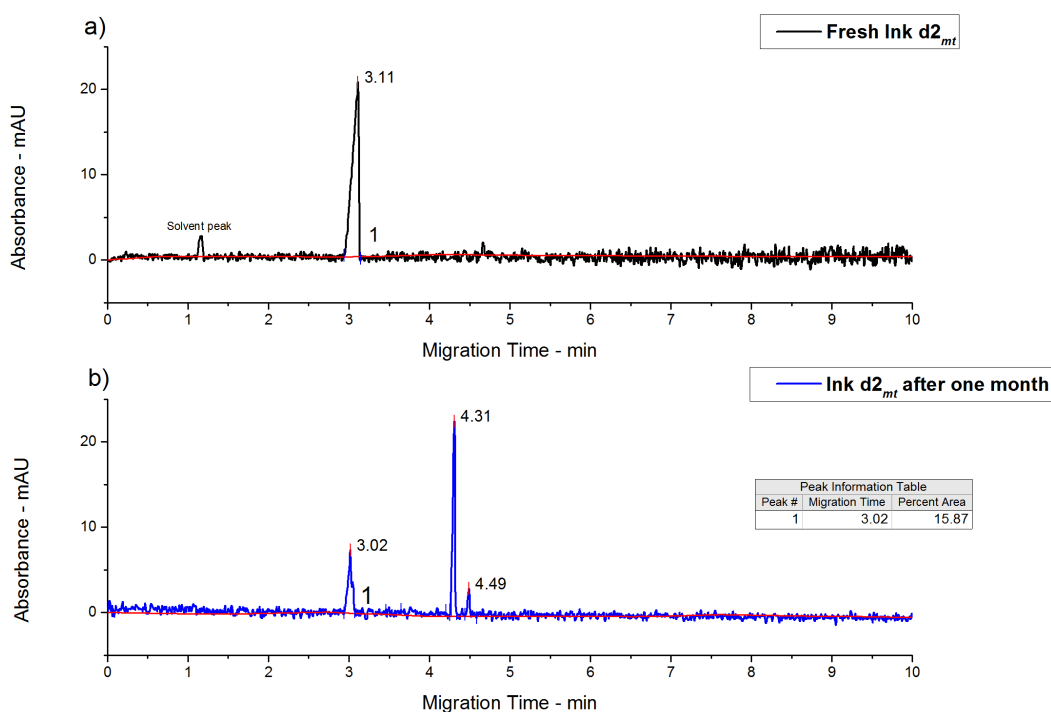


Figure 3.9: Electropherograms showing d2_{mt} based ink stability. (a) Fresh ink; (b) Ink after one month storage at room temperature.

The percent area of peaks on the CZE electropherogram is related to the concentration of specific compounds in the ink samples. As shown in Figure 3.9a, the effective component **d2_{mt}** in the fresh ink was 100%, which reduced to 16% (Figure 3.9b) after only one month storage, indicating that one or both of the labile chlorine atom(s) of triazine group got hydrolysed during storage at room temperature.

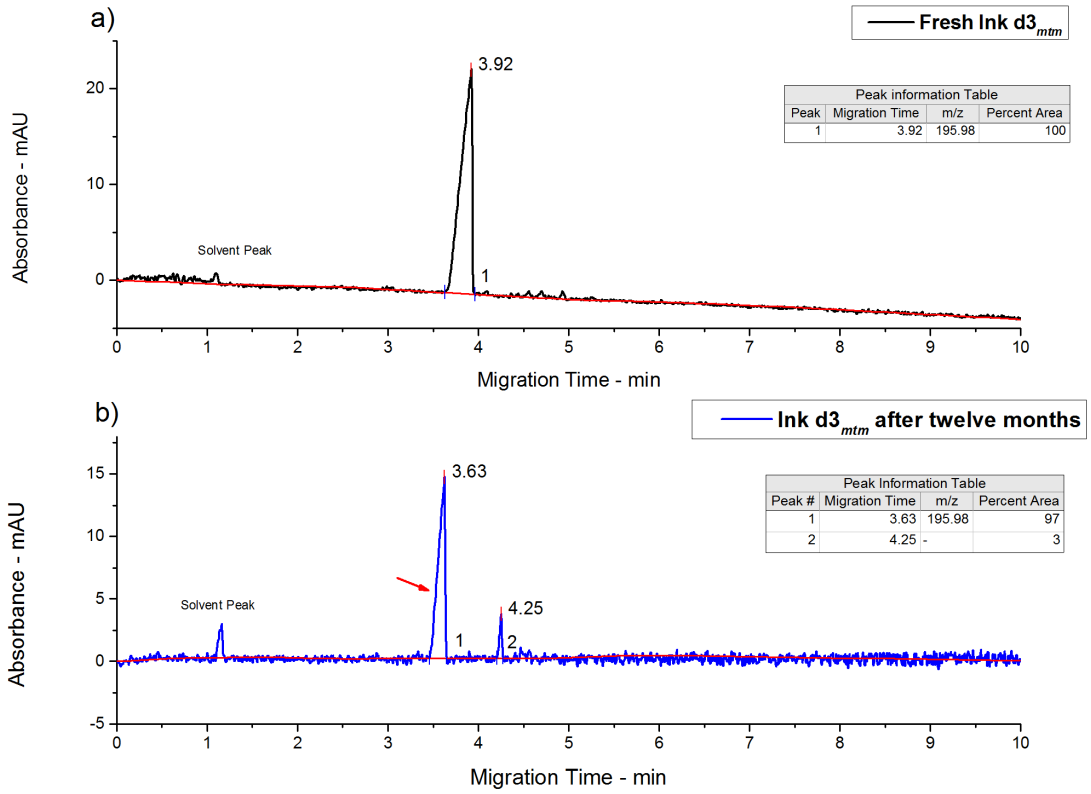


Figure 3.10: Electropherograms showing $d3_{mtm}$ based ink stability. (a) Fresh ink; (b) Ink after twelve months storage at room temperature.

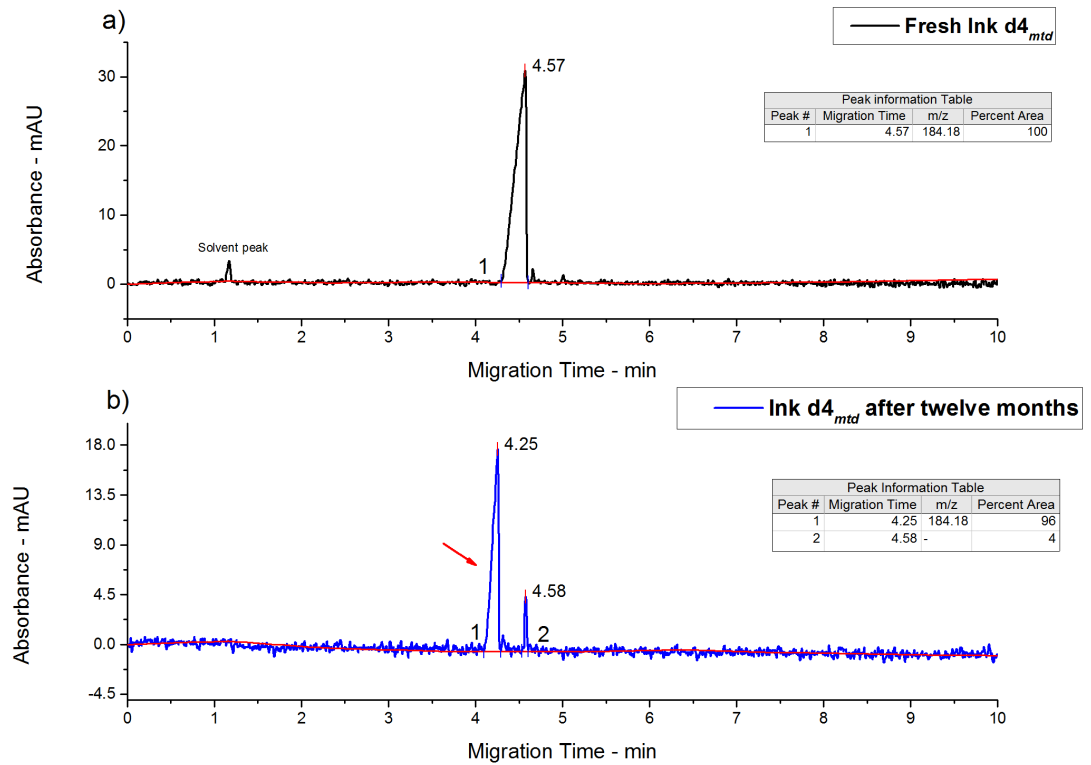


Figure 3.11: Electropherograms showing $d4_{mtd}$ based ink stability. (a) Fresh ink; (b) Ink after twelve months storage at room temperature.

As shown in Figure 3.10b and Figure 3.11b, no significant change in the percent area of peaks in modified dyes ($d3_{mtm}$ and $d4_{mtd}$) based inks were observed when the inks were stored for 12 months indicating that the modification of dichlorotriazine dye $d2_{mt}$ with 4HBSA is an effective method of improving the stability of inks by decreasing the reactivity of highly reactive dichlorotriazine reactive group.

3.2.8 Evaluation of Percent Fixation of Magenta Dyes ($d2_{mt}$, $d3_{mtm}$ and $d4_{mtd}$) by Different Fixation Methods

3.2.8.1 Method 1: Batching at Room Temperature

In accordance with literature ^[30-34], due to hydrophobic character of wool fibre, application of highly reactive dyes onto wool at room temperature is only possible in three cases: (1) the scaly structure of wool has been modified by chemical treatment; (2) organic solvents has been added to printing paste to accelerate the diffusion; (3) sodium metabisulfite along with urea has been added to the printing paste to accelerate the diffusion (discussed in Chapter 1).

In this study, urea and sodium metabisulfite were added in the pre-treatment liquor whereas, organic co-solvents such as propan-2-ol and 2-pyrrolidone were added into inks.

Table 3.2 shows the results obtained by batching the printed samples under moist conditions for 2 and 4 hours at room temperature (RT).

Table 3.2: Percent Fixation of $d2_{mt}$, $d3_{mtm}$ and $d4_{mtd}$. Fixation conditions: Batching at RT for 2 and 4 hours under moist conditions

Ink formulation	% Fixation (2 hours)	% Fixation (4 hours)
$d2_{mt}$	80	81
$d3_{mtm}$	80	82
$d4_{mtd}$	81	83

As shown in Table 3.2, high level of percent fixation was achieved when dichlorotriazine dye $d2_{mt}$ as well as modified dyes $d3_{mtm}$ and $d4_{mtd}$ were fixed through batching the printed samples at room temperature.

This significantly high percent fixation of reactive inks onto wool at room temperature can be attributed to the addition of co-solvents in inks as well as pre-treating the wool fabric by urea and sodium metabisulfite.

Organic co-solvents act mainly by being adsorbed as a surface phase in the wool fibres, the dye molecules than rapidly dissolved in this surface solvent phase and diffused from there into the fibre more rapidly than it would from the bulk aqueous phase which result in improved fixation. Whereas sodium metabisulfite increases the number of very reactive cysteine-thiol groups by breaking some of the disulfide bonds crosslinking the wool structure, hence, improvement in the dye fixation and colour strength is achieved (discussed in Chapter 1).

Additionally, it is also apparent from Table 3.2 that the modified dyes still have relatively high enough reactivity which enables fixation to occur even at low temperature conditions.

Furthermore, the application of dyes on wool at low temperatures leads to prints with low overall colour value (see Appendix B).

3.2.8.2 Method 2: Batching at 65 °C

Significant improvement in the extent of fibre–dye bond (percent fixation) was observed when the modified magenta dyes were applied by an Inkjet print–batch technique.

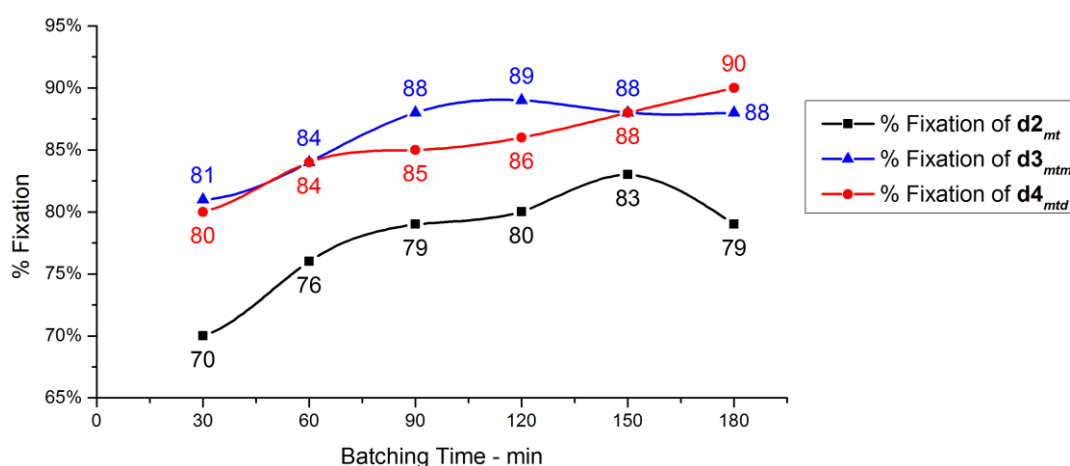


Figure 3.12: Percent fixation of $d2_{mt}$, $d3_{mtm}$ and $d4_{mtd}$. Fixation conditions: Batch at 65 °C for 30 to 180 minutes under moist conditions

Figure 3.12 shows the results obtained using $d2_{mt}$, $d3_{mtm}$ and $d4_{mtd}$ by batching the printed samples under moist conditions for 30 – 180 minutes at 30 minutes

interval. The highest level of percent fixation observed with ink based on magenta dichlorotriazine dye was 83% in 150 minutes batching time, and for longer batching times there was some evidence of the breakdown of fibre-dye bond. Whereas, for modified dyes **d3_{mtm}** and **d4_{mtd}** based inks they are 89% in 120 minutes and 90% in 180 minutes respectively. This shows an increase of approximately 7% and 8% improvement in the percent fixation of **d3_{mtm}** and **d4_{mtd}** onto wool respectively.

Moreover, di-substituted dye **d4_{mtd}** exhibit highest fixation due to the presence of more than one leaving group of same reactivity, which increases the chances of this dye (**d4_{mtd}**) to react with wool fibre, as every reactive group can cover another area of the fibre with the same probability.

3.2.8.3 Method 3: Steaming

The profile shown in Figure 3.13 reflects the effect of steaming and steaming time on the percent fixation of magenta dichlorotriazine (**d2_{mt}**) and modified dyes (**d3_{mtm}** and **d4_{mtd}**) printed on the wool fabric.

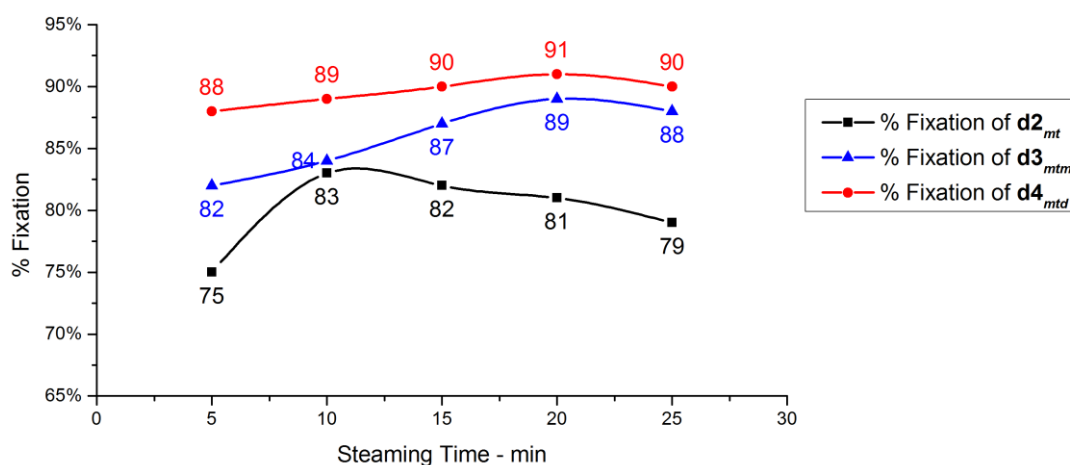


Figure 3.13: Percent fixation of **d2_{mt}, **d3_{mtm}** and **d4_{mtd}**. Fixation conditions: Steaming for 5, 10, 15, 20 and 25 minutes**

It can be seen from Figure 3.13 that, by steaming the samples at 102 °C, modified dyes (**d3_{mtm}** and **d4_{mtd}**) exhibited percent fixation which was clearly superior to that achieved with dichlorotriazine dye **d2_{mt}**. It is generally agreed that steam served as an effective source of both water and heat which allowed the wool fibres to open up for the inks to penetrate rapidly ^[35, 36], thus enabling the reaction of reactive group(s) with fibre to take place.

According to Figure 3.13, it was confirmed that the steaming times of 5 and 10 min were not sufficient to swell the pre-treated wool fibres, thereby greatly affecting the penetration of ink into the fibres. However, the fibres started to open well after 15 minutes and the percent fixation and colour yield even reached a higher level at the steaming time of 25 minutes.

3.2.9 Light Fastness

Light fastness testing was carried out according to the BS EN ISO 105-B02:2013 (Method 3) ^[37].

As shown in Table 3.3, all the inks passed target blue wool reference 6. However, modified dyes **d3_{mtm}** and **d4_{mtd}** showed even better light fastness than target wool reference 6, which can be attributed to a stable electron arrangement in dye molecules.

Table 3.3: Light fastness of magenta dyes (d2_{mt}, d3_{mtm} and d4_{mtd}) compared to target blue wool reference 6

Dye/Ink	Target blue wool reference 6	
d2_{mt}	Equal to 6 (6)	Satisfactory
d3_{mtm}	Better than 6 (6 ⁺)	Satisfactory
d4_{mtd}	Better than 6 (6 ⁺)	Satisfactory

3.2.10 Wash Fastness

Wash fastness was carried out according to the BS ISO 105-C06:2010 ^[38] and the results are shown in Table 3.4.

Magenta dichlorotriazine dye **d2_{mt}** showed a slight change in shade as well as slight staining in adjacent (cotton), whereas both the modified dyes **d3_{mtm}** and **d4_{mtd}** showed no evidence of any colour loss or staining of multifibre adjacents. Hence, the wash fastness tests showed that there had been no detrimental effect caused by modification of magenta dichlorotriazine dye.

Table 3.4: Wash fastness of magenta dyes ($d2_{mt}$, $d3_{mtm}$ and $d4_{mtd}$)

Dye/Ink	Change in shade	Staining					
		CA	C	N	P	A	W
$d2_{mt}$	4-5	5	4-5	5	5	5	5
$d3_{mtm}$	5	5	5	5	5	5	5
$d4_{mtd}$	5	5	5	5	5	5	5

CA: Cellulose Acetate; C: Cotton; N: Nylon; P: Polyester; A: Acrylic; W: Wool

3.3 Conclusions

In this study, the specificity of the reactivity of chlorine atoms of cyanuric chloride were explored in designing dyes for inkjet application of wool fabric with the aim to lower the chemical reactivity of magenta dichlorotriazine dye, increased solubility and increased stability.

Thus, one chlorine of cyanuric chloride was displaced by amino based magenta dye chromophore at 0 to 5 °C (pH 3.0 to 3.5) to produce magenta dichlorotriazine dye $d2_{mt}$ in pure form (without hydrolysed by-products).

The first modification of magenta dichlorotriazine dye was done by displacing the second chlorine atom by the sulfophenoxy group at 25 °C (5 hours) to produce mono-substituted dye $d3_{mtm}$ in pure form.

Second modification of magenta dichlorotriazine dye was done by displacing the second chlorine atom by using two equivalent sulfophenoxy group at 30 °C (1.5 hours) to produce intermediate dye $d3_{mtm}$ and then the third chlorine atom as displaced at 70 °C (5 hours) to produce di-substituted dye $d4_{mtd}$ in pure form.

The characteristic properties such as surface tension and viscosity of inks formulated by incorporating the synthesised dyes were found to be in the operational range.

As modified dyes are of low reactivity as such the inks can be stored for 12 months at room temperature without deterioration from hydrolysis of the reactive group(s).

Significant improvement in the extent of covalent dye fixation was observed when the modified magenta dyes were applied by both inkjet print–batch (elevated

temperature) and inkjet print–steaming methods. Moreover, when the inkjet print–batch (room temperature) method was used, although modified dyes along with dichlorotriazine dye gave high levels of fixation but there was no significant improvement in the extent of percent fixation of modified dyes as compared to dichlorotriazine dyes.

Furthermore, it is likewise evident from fixation results that reactive dyes with more than one leaving group of same reactivity have intrinsically better chances to react, since every reactive group can cover another area of the fibre with the same probability. Hence, showed increased percent fixation and considerable reduced washing-off.

Colour fastness properties of magenta dichlorotriazine dye-based ink was 0.5 grade lower when compared with the modified dyes-based inks for both the light fastness as well as wash fastness.

3.4 References

1. Beech, W.F. *Fibre-Reactive Dyes* London: Logos Press Ltd., 1970.
2. Zollinger, H. *Color Chemistry: Synthesis Properties, and Applications of Organic Dyes and Pigments*. Weinheim: Wiley-VCH, 2003.
3. Rattee, I.D. Historical Background. In: I.C.I. Ltd., ed. *Procion Dyestuffs in Textile Printing*. Leeds: Dyestuffs Division, 1960.
4. Imperial Chemical Industries Ltd. *Procion dyestuffs in textile printing*. London: The Division, 1960.
5. Hawkyard, C.J. Substrate preparation for inkjet printing. In: H. Ujiie, ed. *Digital printing of Textiles*. Cambridge: Woodhead Publishing Ltd, 2006.
6. Lewis, D.M. The Dyeing of Wool with Reactive Dyes. *Journal of the Society of Dyers and Colourists*, 1982, **98**, pp.165-175.
7. Hildebrand, D. Application and Properties. In: K. Venkataraman, ed. *The chemistry of synthetic dyes*. New York: Academic Press Ltd., 1978.
8. Patent US20040081761 (2004)
9. Patent FR1283172 (1961)
10. Patent CH464396 (1968)

11. Clark, M., Yang, K. and Lewis, D.M. Modified 2,4-difluoro-5-chloropyrimidine dyes and their application in inkjet printing on wool fabrics. *Coloration Technology*, 2009, **125**, pp.184-190.
12. Venkataraman, K. ed. *The chemistry of synthetic dyes*. New York: Academic Press Ltd., 1978.
13. Patent WO2002024815 (2002)
14. Mokhtari, J., Akbarzadeh, A., Phillips, D. and Taylor, J. Study of application properties of novel trisazo hetero bi-functional reactive dyes based on j-acid derivatives for cotton. *Arabian Journal for Science and Engineering*, 2009, **34**, pp.63-71.
15. Zuwang, W. Recent developments of reactive dyes and reactive dyeing of silk. *Review of Progress in Coloration and Related Topics*, 1998, **28**, pp.32-38.
16. Fierz-David, H.E. and Blangey, L. *Fundamental processes of dye chemistry*. New York: An Interscience Publication, 1949.
17. Socrates, G. *Infrared and Raman characteristic group frequencies : tables and charts*. Chichester: Wiley, 2001.
18. Lambert, J.B., Shurvell, H.E., Lightner, D.A. and Cooks, R.G. *Organic structural spectroscopy*. New Jersey: Prentice Hall, 1998.
19. Miller, R.K. Infrared Spectroscopy. In: K. Venkataraman, ed. *The Analytical Chemistry of Synthetic Dyes*. New York: Wiley & Sons, 1977.
20. Matlok, F., Gremlich, H.U., Bruker Analytische Meotechnik and Merck eds. *Merck FT-IR atlas : a collection of FT-IR spectra*. Weinheim: Vch, 1988.
21. Keller, R.J. and Sigma-Aldrich Corporation. *The Sigma library of FT-IR spectra*. Missouri: Sigma Chemical Company, 1986.
22. Silverstein, R.M., Webster, F.X. and Kiemle, D.J. *Spectrometric Identification of Organic Compounds*. 7th ed. New York: John Wiley and Sons, 2005.
23. Waring, D.R. and Hallas, G. eds. *The Chemistry and Application of Dyes*. New York: Plenum Press, 1994.
24. Patent GB785222 (1957)
25. Patent GB838337 (1960)

26. University of Colorado at Boulder. *Thin Layer Chromatography (TLC)* [online]. 2013. [Accessed December 10, 2011]. Available from: <http://orgchem.colorado.edu/Technique/Procedures/TLC/TLC.html>.
27. Patent DE2045086A (1971)
28. Magdassi, S. Ink Requirements and Formulations Guidelines. *In: S. Magdassi, ed. Chemistry of Inkjet Inks.* New Jersey: World Scientific Publishing Ltd., 2012.
29. Ujiie, H. *Digital printing of textiles.* Cambridge: Woodhead Publishing Ltd., 2006.
30. Beech, W.F. Reactive dyes for wool and synthetic fibres. *In: Fibre-Reactive Dyes* London: Logos Press Ltd., 1970.
31. Bell, V. Recent developments in wool printing. *Journal of the Society of Dyers and Colourists*, 1988, **104**, pp.159-172.
32. Peters, L. and Stevens, C.B. The Effect of Solvents in Dyeing. *Journal of the Society of Dyers and Colourists*, 1957, **73**, pp.23-23.
33. Hadfield, H.R. and Lemin, D.R. The use of Reactive Dyes for dyeing Wool and Wool Unions. *Journal of the Textile Institute Transactions*, 1960, **51**, pp.T1351-T1370.
34. Lewis, D.M. and Seltzer, I. Print-Batch (Cold)—A New Process for Wool. *Journal of the Society of Dyers and Colourists*, 1972, **88**, pp.327-329.
35. Chapman, K. Printing 2002: A digital odyssey. *AATCC Review*, 2002, **2**, pp.12-15.
36. Yuen, C., Ku, S., Choi, P. and Kan, C. The effect of the pretreatment print paste contents on colour yield of an ink-jet printed cotton fabric. *Fibers and Polymers*, 2004, **5**, pp.117-121.
37. British Standards Institution. *Colour fastness to artificial light: Xenon arc fading lamp test*, ISO 105-B02:2013.
38. British Standards Institution. *Textiles - Tests for colour fastness - Part C06: Colour fastness to domestic and commercial laundering*, BS EN ISO 105-C06:2010.

4 Synthesis, Modification, Characterisation of Yellow Dichlorotriazine Dyes and Their Application onto Wool Fabric by Inkjet Printing

This chapter details the synthesis and characterisation of yellow dichlorotriazine dye **d6_{yt}**, modification of this dye by incorporating sulfophenoxy group to produce mono-substituted dye **d7_{ym}** and also di-substituted dye **d8_{yt}**. CE (MEKC) and TLC were used to monitor above course of reactions and the structural changes were confirmed through FT-IR. Moreover, elemental analysis (CHN) of new modified dyes were also done.

This chapter also details the application of yellow dichlorotriazine dye and modified dyes based inks by inkjet printing on wool fabrics along with performance evaluation of inks such as surface tension, viscosity, ink stability, percent fixation of the dye and colour fastness properties.

4.1 Experimental

4.1.1 Materials

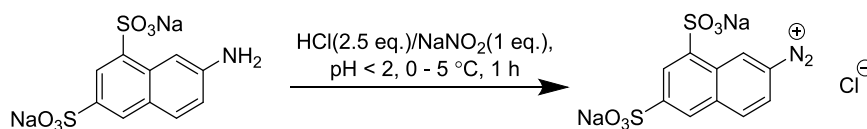
7-amino-1,3-naphthalenedisulfonic acid (88%), sodium nitrite (98%), *m*-toluidine (99%), cyanuric chloride (99%), sodium 4-hydroxybenzenesulfonate dihydrate (98%), sodium metabisulfite, carboxymethyl cellulose, polysorbate 20 (Tween 20) and N-methylmorpholine N-oxide (NMMO) were supplied by Sigma-Aldrich and used as received. Urea (MP Biomedicals), Alcopol O 60 (Acros organics), 2-pyrrolidone (Acros organics), 2-propanol (Fisher), Sandozin NIE (Clariant) were also purchased and used as received.

4.1.2 Synthesis and Characterisation of Yellow 7-[(4-Amino-2-methylphenyl)azo]-1,3-Naphthalenedisulfonic Acid Dye (d5_y)

4.1.2.1 Synthesis of d5_y

4.1.2.1.1 Diazotization

In accordance with the method described in references ^[1-4], 7-amino-1,3-naphthalenedisulfonic acid (17.22 g, 0.05 mol, 88%) was suspended in water (100 cm³) and then treated with concentrated hydrochloric acid (10 cm³, 0.125 mol, 36.6%) and cooled to 20 °C. The temperature was lowered to 0 to 5 °C by adding ice, and diazotization was carried out by adding 1N sodium nitrite solution (3.52 g, 0.05 mol, 98%). The reaction mixture was stirred at 0 to 5 °C and pH < 2. Diazotization was complete as soon as small amount withdrawn from a reaction mixture did not give a yellow colour when treated with 2N sodium acetate solution. Excess nitrous acid was removed by adding sulfamic acid (confirmed by spotting a drop of reaction mixture on starch iodide paper). The reaction is shown in Scheme 4.1.

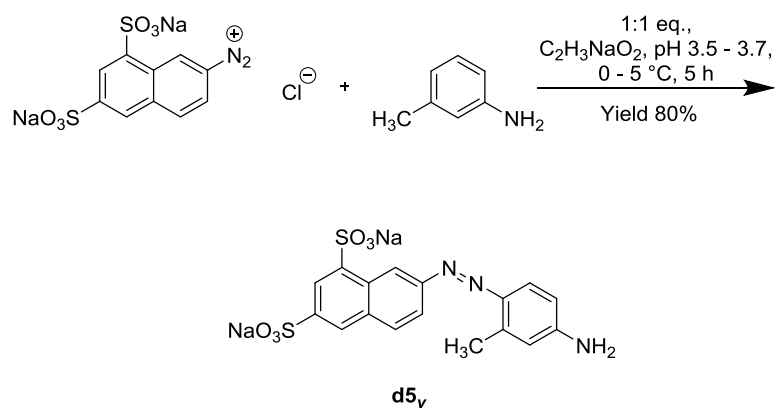


Scheme 4.1: Diazotization of 7-amino-1,3-naphthalenedisulfonic acid with nitrous acid to form diazonium salt

4.1.2.1.2 Coupling

Meta-toluidine (5.40 g, 0.05 mol, 99%) was dissolved in concentrated hydrochloric acid (5 cm³, strength 36.6%) and water (75 cm³) and then added dropwise with good stirring into the diazo solution (0.05 mol) at 0 to 5 °C over 45 minutes. The pH of the reaction mixture was then adjusted to pH 3.5 to 3.7 by the addition of 2N sodium acetate solution and the reaction mixture was stirred for further 4 hours at 0 to 5 °C; and was monitored by MEKC, analytical TLC and spot test for completion. Sodium chloride (8% w/v) was added in small portions to a stirred reaction mixture to precipitate the dye which was subsequently collected by filtration, washed with brine (10% w/v) and dried *in vacuo*.

Purification of crude dye **d5_y**, using solvent-nonsolvent technique (dimethylformamide–acetone, 1:2 v/v) yielded pure dye **d5_y** (18.62 g, 40.0 mmol, yield 80%) as redish yellow powder. FT-IR analysis was conducted to confirm the presence of main functional groups in dye **d5_y**. The reaction is shown in Scheme 4.2.



Scheme 4.2: Coupling of diazonium salt with m-toluidine to yield **d5_y**

4.1.2.2 Characterisation of **d5_y**

Although most charged analytes are easily separated by CZE on the basis of differences in electrophoretic mobility or velocity, MEKC provides added separation selectivity and sometimes the necessary separation power for charged analytes that cannot be separated by CZE. Charged analytes in MEKC are separated on the basis of differences in analyte affinities between the pseudostationary phase (micelle) and aqueous phase and electrophoretic migration of the analyte ^[5, 6].

The MEKC electropherogram of the synthesised azo based yellow dye chromophore **d5_y** at λ_{obs} . 420 nm is shown in Figure 4.1. The synthesised **d5_y** was detected at 4.55 min with percent area of 100% indicating high purity of synthesised yellow dye chromophore.

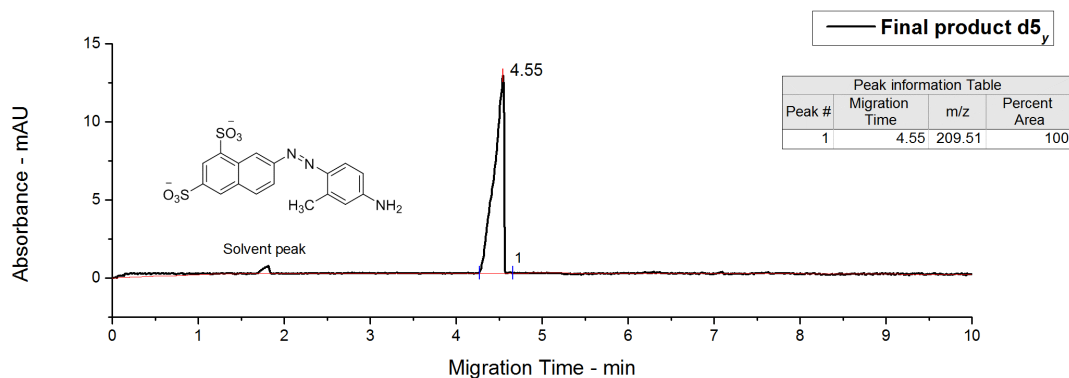


Figure 4.1: Electropherogram of yellow dye chromophore $d5_y$. MEKC conditions: running buffer, 20 mM sodium tetraborate, 50 mM sodium dodecyl sulphate (SDS), pH 9.3; pressure injection 0.5 psi for 10 s; voltage 25 kV; detection at 420 nm

Only a single spot with R_f value of 0.63 was detected on a chromatogram in n-butanol–iso-propanol–ethyl acetate–water (2:4:1:3 v/v).

According to literature ^[7, 8], primary amines display two absorption bands near $3400 - 3200 \text{ cm}^{-1}$, these bands represent the asymmetrical and symmetrical N–H stretching modes respectively. Also, strong to medium N–H bending vibration of primary amines is observed in the $1650-1580 \text{ cm}^{-1}$ and medium to strong broad absorption in $909 - 666 \text{ cm}^{-1}$ region of spectrum from N–H wagging.

Analysis of FT-IR spectrum (Figure 4.2) of pure redish yellow powder suggested that the compound was $d5_y$, since peaks appeared at $3328, 3227 \text{ cm}^{-1}$ (stretching); 1588 cm^{-1} (bending) and 881 cm^{-1} (wagging) attributed the presence of primary amine group on $d5_y$.

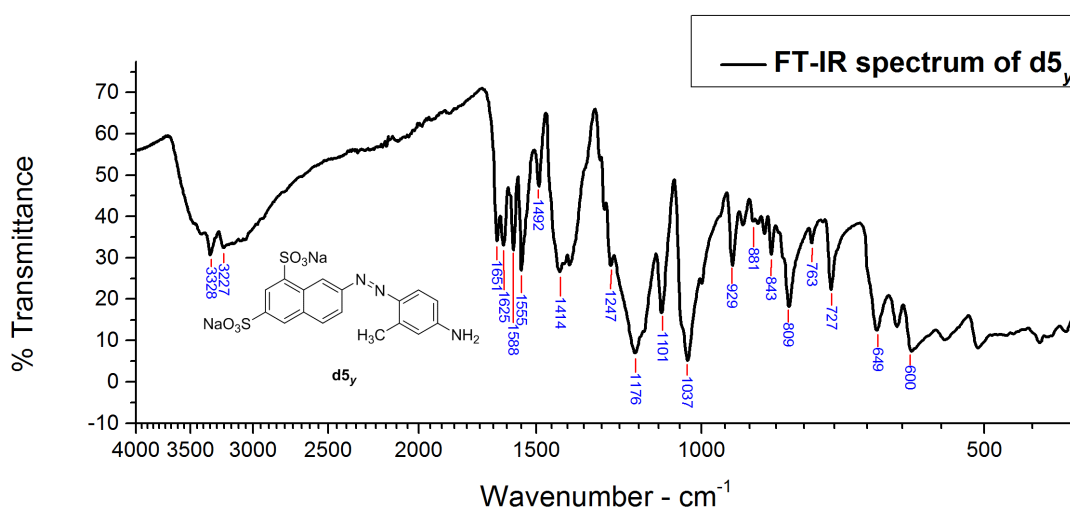


Figure 4.2: FT-IR spectrum of yellow dye chromophore $d5_y$

The detailed analysis of spectrum (Figure 4.2) is as follows ^[7-10]; N–H stretch, primary amine, 3328 cm⁻¹ and 3227 cm⁻¹; overtone or combinational bands, 2000–1667 cm⁻¹; C=C stretch, 1651 cm⁻¹; N–H bending, 1625 cm⁻¹; C=C ring stretch, 1555, 1492; azo group stretch, 1414 cm⁻¹; C–N stretch (primary amine), 1247 cm⁻¹; sulfonate salts, 1176 cm⁻¹; in-plane C–H bend, 1037 cm⁻¹; broad, N–H wag, 881 cm⁻¹; out of plane aromatic C–H bend, 809, 763 cm⁻¹; CH₃ rock, 727 cm⁻¹.

¹H NMR (D₂O, 500 MHz) δ 2.30 (3H, s), 6.38 (1H, s), 6.41 (1H, J = 10 Hz, d), 7.30 (1H, J = 10 Hz, d), 7.77 (1H, J = 10 Hz, d), 7.91 (1H, J = 10, d), 8.22 (1H, s), 8.29 (1H, s), 8.68 (1H, s)

4.1.3 Synthesis and Characterisation of Yellow 7-[(4,6-Dichloro-1,3,5-triazin-2-yl)amino -2-methylphenyl]azo]-1,3-Naphthalenedisulfonic Acid Dye (**d6_{yt}**)

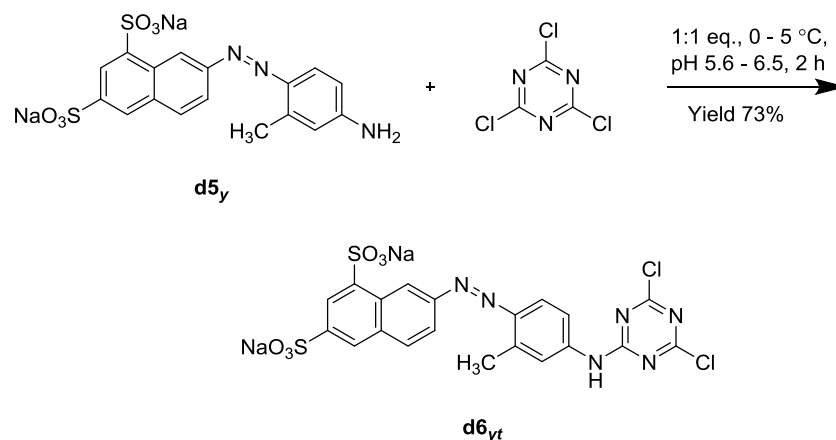
4.1.3.1 Synthesis of **d6_{yt}**

In accordance with the method described in references ^[11-14], a solution of cyanuric chloride (9.22 g, 0.05 mol) in acetone (50 cm³) was poured into a stirred mixture of water (125 cm³) and ice (125 cm³) at a temperature below 5 °C. Dye chromophore **d5_y** (0.05 M, 23.37 g) was dissolved in water (250 cm³) and the pH was adjusted to 7.0 by the addition of 2N sodium carbonate solution and then added dropwise to the cyanuric chloride solution over 30 minutes. The pH of the reaction mixture was maintained at pH 5.6 to 6.5 by the addition of 2N sodium carbonate solution, while the temperature was kept at 0 to 5 °C.

Once the addition of the dye chromophore solution was complete, the reaction was stirred for a further 2 hours and monitored by MEKC and analytical TLC. When the reaction had gone to completion, the 2N sodium carbonate solution was added to raise the pH to 7.0. Phosphate buffer (30 cm³, NaH₂PO₄ 0.12 M, Na₂HPO₄ 0.2 M, pH 6.4) was added to buffer the reaction mixture. The dye was precipitated by the addition of sodium chloride (10% w/v). The crude dye **d6_{yt}** was collected by filtration and the filter cake was washed with brine (2 × 50 cm³) and dried *in vacuo*.

Purification of crude dye using solvent–nonsolvent technique (DMF–acetone, 1:2 v/v) yielded the pure dye **d6_{yt}** (9.98 g, 14.6 mmol, yield 73%) as yellow powder.

FT-IR analysis was conducted to confirm the presence of main functional groups in dye **d6_{yt}**. The reaction is shown in Scheme 4.3.



Scheme 4.3: Preparation of condensation product **d6_{yt} from yellow azo chromophore and cyanuric chloride**

4.1.3.2 Characterisation of **d6_{yt}**

It has previously been mentioned that the micelles used in MEKC are charged on the surface, therefore an analyte with the opposite charge of the micelle will strongly interact with the micelle through electrostatic forces and an analyte with the same charge as the micelle will interact weakly, due to the electrostatic repulsion [15]. When anionic micelle such as sodium dodecyl sulfate (SDS) is employed, the general migration order will be exactly the opposite as in CZE: anions, neutral analytes and cations. Anions will remain mostly in the bulk solution due to electrostatic repulsions from the micelle; neutral molecules will be separated exclusively due to their hydrophobicity; while cations will migrate last due to the strong electrostatic attraction [16].

As anionic analytes spend more of their time in the bulk phase due to electrostatic repulsions from the SDS micelle. Therefore, the greater the anionic charge, the more rapid the elution [17].

As SDS micelle was used in this study for the separation of yellow dichlorotriazine dye and modified dyes, therefore they will interact weakly due to electrostatic repulsion, resulting in separation in the order of decreasing anionic charge.

Figure 4.3 shows the reaction progression of synthesis of **d6_{yt}** in a fused silica capillary at pH 9.3. Both analytes have a charge of -2 under these conditions. As

shown in Figure 4.3b, water migrates quickly at the EOF velocity followed by **d5_y** (4.87 min) and then **d6_{yt}** (5.49 min), this is because dye **d6_{yt}** has an increased molecular weight compared to dye **d5_y** but no additional sulfonate groups that would increase the solubility or hydrophilicity of the dye **d6_{yt}**.

Moreover, the percent area of the **d6_{yt}** shown in Figure 4.3c, was 100% which indicates that there was no hydrolysed dye in the final product.

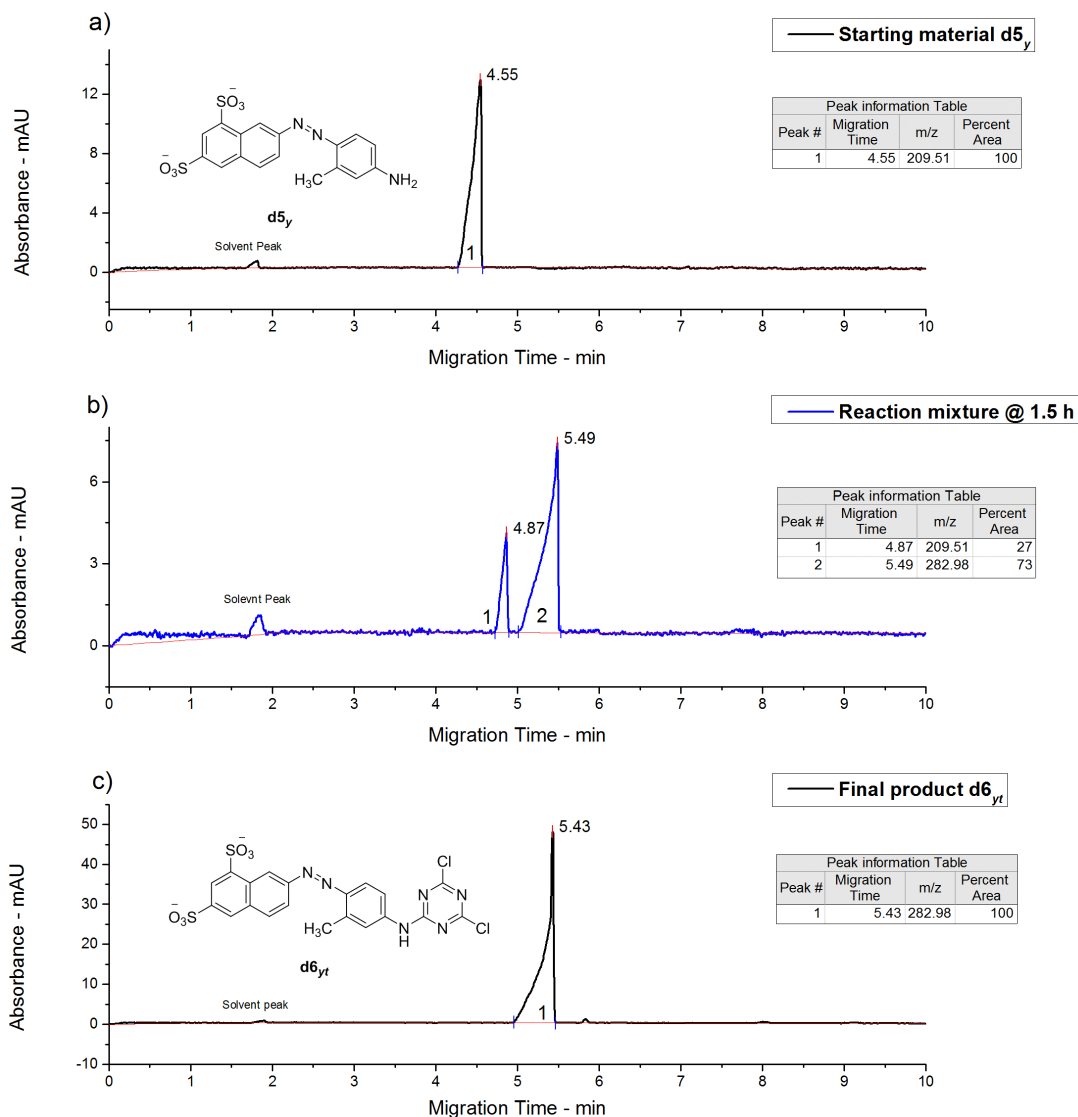


Figure 4.3: Electropherograms showing reaction progress of synthesis of **d6_{yt}. (a) Starting yellow dye chromophore **d5_y**; (b) **d5_y**-**d6_{yt}** after 1.5 hours reaction; (c) Final product **d6_{yt}**. MEKC conditions: same as Figure 4.1.**

Being weakly polar as compared to the yellow starting material **d5_y** (R_f value 0.63) the new dichlorotriazine dye **d6_{yt}** (R_f value 0.70) move through the adsorbent more rapidly. Moreover, almost quantitative conversion to product occurred in 2 hours.

Analysis of FT-IR spectrum (Figure 4.4) of pure powder suggested that the compound is **d6_{yt}** since peaks due to the presence of primary amine in **d5_y** (Figure 4.2) at 1588 cm⁻¹ no longer present indicating that the primary amine had successfully reacted with cyanuric chloride. According to literature [7], triazine group have at least one strong band at 1580 – 1520 cm⁻¹ and at least one band at 1450 – 1350 cm⁻¹ corresponding to the stretching of the ring. The appearance of new peaks at 1542 cm⁻¹ and 1386 cm⁻¹ reflects the presence of the triazine group in **d6_{yt}**. Moreover, in accordance with literature [7, 8], the appearance of the peaks at the 1097 cm⁻¹ and 791 cm⁻¹ are attributed to the stretching vibrations of carbon chlorine bond on the triazine ring of the **d6_{yt}**.

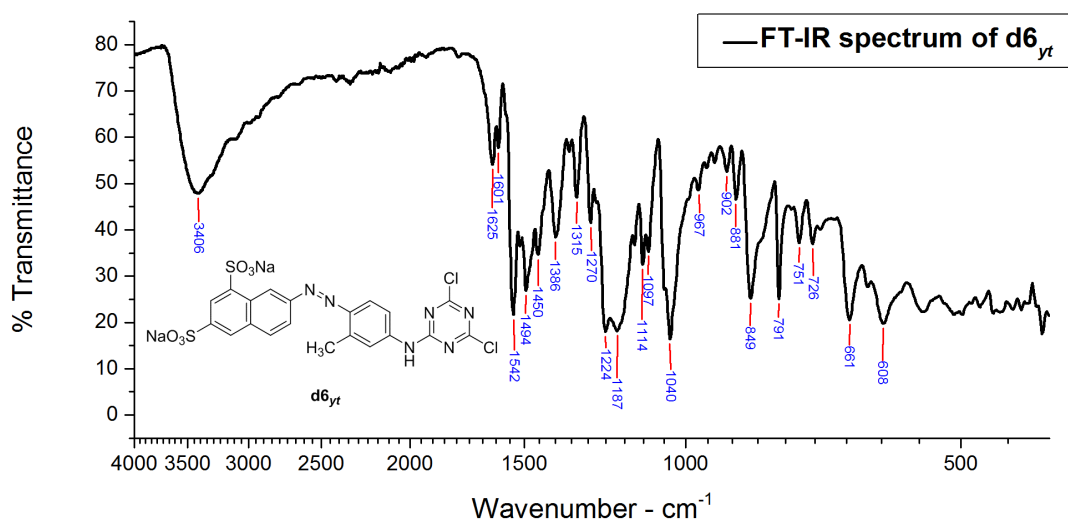


Figure 4.4: FT-IR spectrum of yellow dichlorotriazine dye **d6_{yt}**

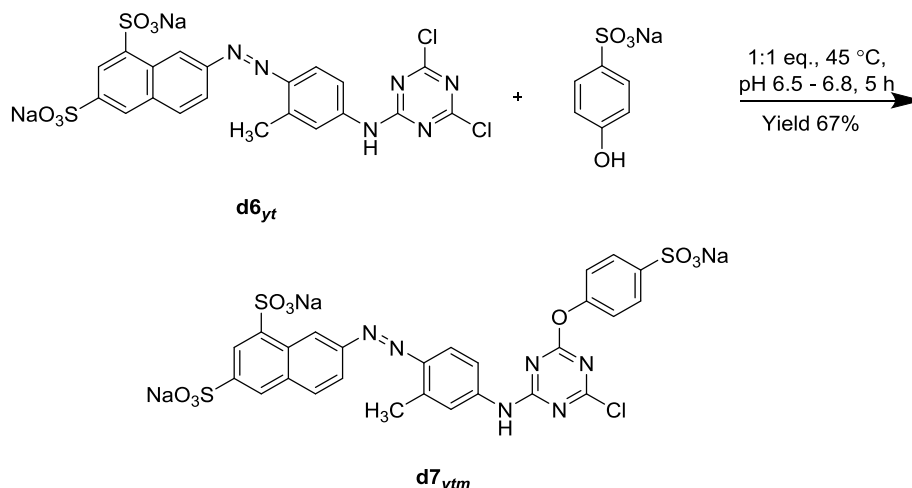
The detailed analysis of the spectrum (Figure 4.4) is as follows [7-10]; N-H stretch, 3406 cm⁻¹; overtone or combination bands, 2000–1667 cm⁻¹; N-H bending, 1625 cm⁻¹; C=C ring stretch, 1601, 1494; azo group stretch, 1450 cm⁻¹; C=N stretch, 1542 cm⁻¹, 1386 cm⁻¹; C-N stretch (secondary amine), 1315 cm⁻¹; sulfonate salts, 1187 cm⁻¹; C-Cl stretch, 1097 cm⁻¹, 791 cm⁻¹; in-plane C-H bend, 1040 cm⁻¹; out of plane aromatic C-H bend, 751 cm⁻¹; CH₃ rock 726 cm⁻¹.

4.1.4 Synthesis and Characterisation of Modified Yellow 7-[(4-Chloro-6-(4-sulfophenoxy)-1,3,5-triazin-2-yl)amino-2-methylphenyl]azo]-1,3-Naphthalenedisulfonic Acid, Dye (**d7_{ym}**)

4.1.4.1 Synthesis of **d7_{ym}**

Dye **d6_{yt}** (6.51 g, 0.01 mol, 1 eq.) and sodium bicarbonate (1.23 g, 0.015 mol, 1.5 eq.) were dissolved in water (50 cm³) at 45 °C. A solution of sodium 4-hydroxybenzenesulfonate dihydrate (4HBSA) (2.32 g, 0.01 mol, 1 eq.) in water (20 cm³) was added dropwise over 15 minutes to the dye **d6_{yt}** solution; the pH was maintained at 6.5 to 6.8 by the addition of saturated sodium carbonate solution. Once the addition of 4HBSA solution was complete, the reaction was stirred for further 5 hours (until the pH was stabilised) and was monitored with MEKC and TLC. Sodium chloride (10% w/v) was added to precipitate out the dye. The crude dye **d7_{ym}** was collected by filtration and the filter cake was dried *in vacuo*.

Purification of crude dye **d7_{ym}** using solvent-nonsolvent technique (DMF–Acetone, 1:2 v/v) afforded pure dye **d7_{ym}** (5.45 g, 6.72 mmol, yield 67%) as yellow powder. The dye **d7_{ym}** was characterised by FT-IR and elemental analysis. The reaction is shown in Scheme 4.4.



Scheme 4.4: Mono substitution of dye **d6_{yt} with 4HBSA to yield dye **d7_{ym}****

4.1.4.2 Characterisation of **d7_{ym}**

The electropherograms from MEKC analysis are shown in Figure 4.5, which indicates the progression of the synthesis reaction from the starting dye **d6_{yt}** to the mono-substituted dye **d7_{ym}** (peak 2 in Figure 4.5b).

As shown in Figure 4.5b, after reacting with 4HBSA the resultant dye **d7_{ym}** migrates more quickly than the **d6_{yt}**. This occurs because the mono substitution of **d6_{yt}** with 4HBSA not only increases the molecular weight of modified dye **d7_{ym}** but also increase a negative charge on it, therefore increasing the hydrophilicity of modified dye.

In addition, MEKC analysis also shows that starting material **d6_{yt}** was fully converted to modified dye **d7_{ym}** in 5 hours.

Moreover, the percent area of the **d7_{ym}** shown in Figure 4.5c, was 100% which indicates the purity of the final product.

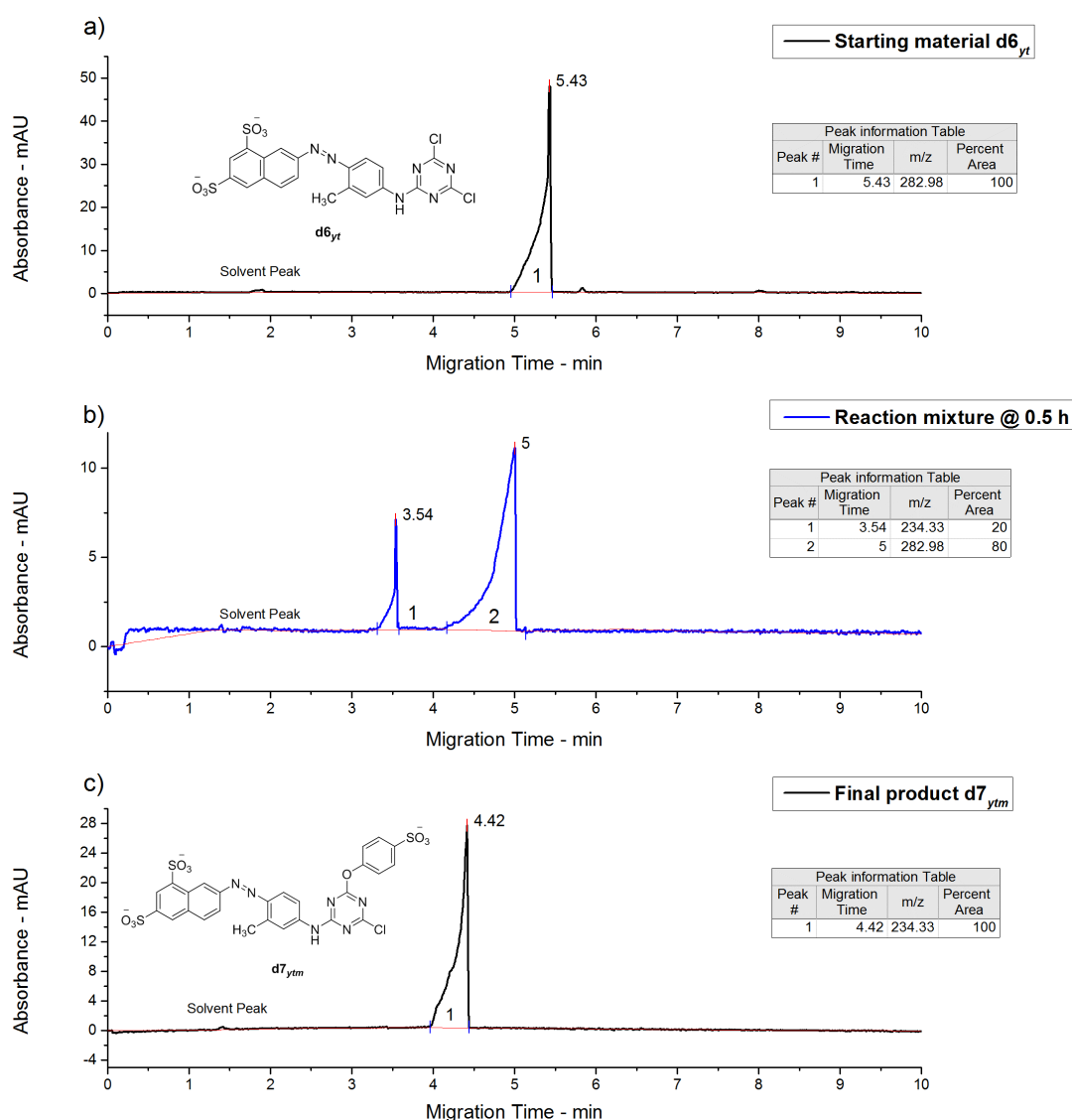


Figure 4.5: Electropherograms showing reaction progress of synthesis of **d7_{ym}. (a) yellow dichlorotriazine dye **d6_{yt}**; (b) **d6_{yt}** – **d7_{ym}** after 0.5 hour reaction; (c) Final product **d7_{ym}**. MEKC conditions: same as Figure 4.1**

R_f values were 0.70 and 0.67 for starting material (**d6_{yt}**) and product (**d7_{ym}**) respectively.

In FT-IR spectrum of the **d7_{ym}**, Figure 4.6, the new peak at 1120 cm^{-1} is evident which can be attributed to the stretching vibration of C–O–C in its structure between the triazine and the 4HBSA. The peak at 797 cm^{-1} can be attributed to the presence of C–Cl after the mono-substitution of **d6_{yt}** with 4HBSA.

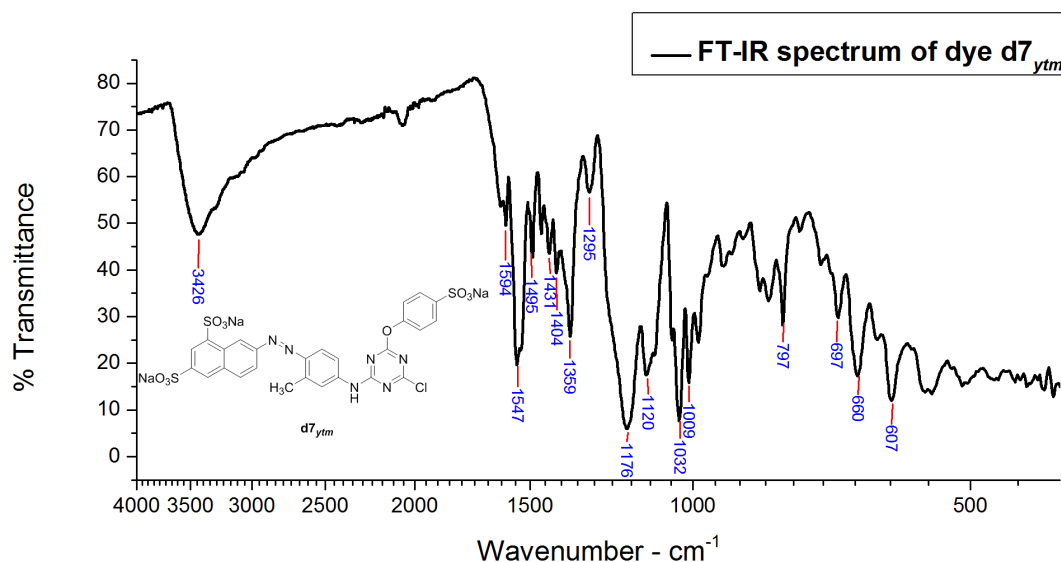


Figure 4.6: FT-IR spectrum of mono-substituted yellow dye **d7_{ym}**

The detailed analysis of spectrum (Figure 4.6) is as follows ^[7-10]; N–H stretch, 3426 cm^{-1} ; overtone or combinational bands, 2000–1667 cm^{-1} ; C=C ring stretch, 1594, 1495, 1404 cm^{-1} ; azo group stretch, 1431 cm^{-1} ; triazine stretch, 1547 cm^{-1} , 1359 cm^{-1} ; C–N stretch (secondary amine), 1295 cm^{-1} ; sulfonate salts, 1176 cm^{-1} ; C–O–C stretch, 1120 cm^{-1} ; in-plane C–H bend, 1032, 1009 cm^{-1} ; C–Cl stretch, 797 cm^{-1} ; out of plane aromatic C–H bend, 760 cm^{-1} .

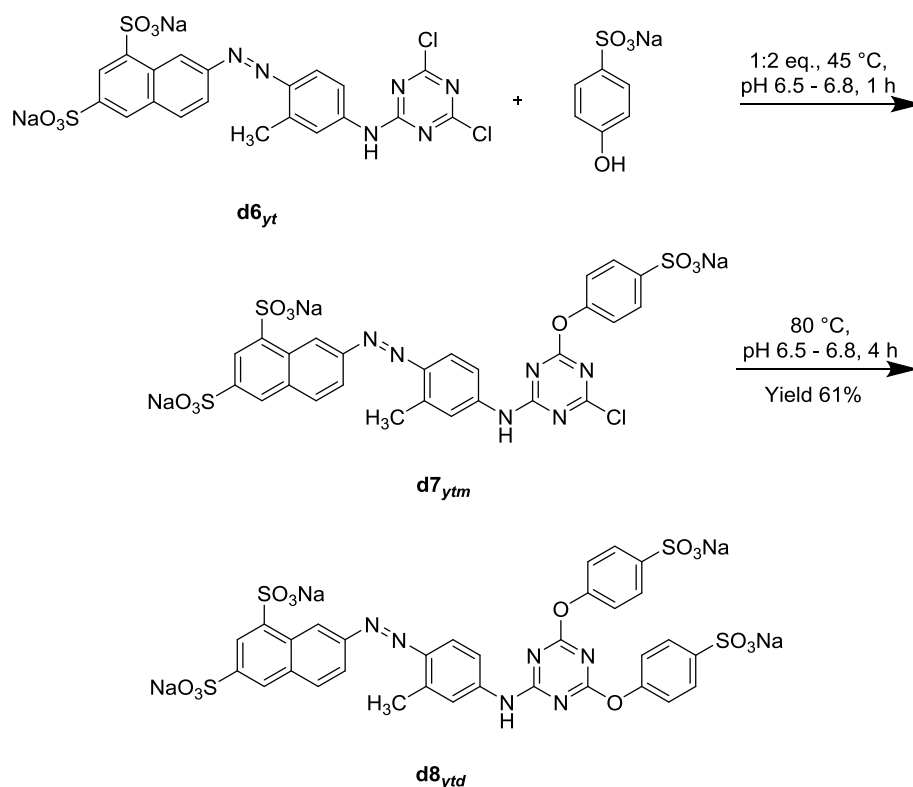
Elemental analysis, Found: C, 35.58%; H, 3.10%; N, 8.87%. Calculated for $\text{C}_{26}\text{H}_{16}\text{ClN}_6\text{Na}_3\text{O}_{10}\text{S}_3 \cdot 6\text{H}_2\text{O}$: C, 35.46%; H, 3.20%; N, 9.54%. The results were adjusted due to the presence of water of crystallisation in the dye molecule. Further disagreement could be attributed to the presence of traces of salt.

4.1.5 Synthesis and Characterisation of Modified Yellow 7-[(4,6-(4-Sulfophenoxy)-1,3,5-triazin-2-yl)amino-2-methylphenyl]azo]-1,3-Naphthalenedisulfonic Acid Dye (**d8_{ytd}**)

4.1.5.1 Synthesis of **d8_{ytd}**

Dye **d6_{yt}** (6.51 g, 0.01 mol, 1 eq.) and sodium bicarbonate (1.23 g, 0.015 mol, 1.5 eq.) were dissolved in water (50 cm³) and temperature is raised to 45 °C. A solution of sodium 4-hydroxybenzenesulfonate dihydrate (4HBSA) (4.86 g, 0.02 mol, 2 eq.) in water (30 cm³) was added dropwise over 15 minutes to the dye **d6_{yt}** solution; the pH was maintained at 6.5 to 6.8 by the addition of 2N sodium carbonate solution. Once the addition of the 4HBSA solution was complete, the reaction was followed using MEKC and TLC. The MEKC and TLC analysis showed that the mono substitution of dye **d6_{yt}** was complete after 1 h (pH had stabilised); after that the temperature of the reaction mixture was raised to 80 °C to enable the secondary di-substitution of dye **d6_{yt}** to occur. After 4 hours, the MEKC and TLC analysis showed that the di-substitution was also complete. Sodium chloride (10% w/v) was added to precipitate out the dye. The crude dye **d8_{ytd}** was collected by filtration and the filter cake was dried *in vacuo*.

Purification of crude dye **d8_{ytd}** using solvent-nonsolvent technique (DMF–Acetone, 1:2 v/v) yielded pure dye **d8_{ytd}** (5.93 g, 6.11 mmol, yield 61%) as yellow powder. The dye **d8_{ytd}** was characterised by FT-IR and elemental analysis (CHN). The reaction is shown in Scheme 4.5.



Scheme 4.5: Preparation of di-substituted $d8_{ytd}$ from yellow dichlorotriazine dye $d6_{yt}$ and 4HBSA

4.1.5.2 Characterisation of $d8_{ytd}$

The pattern of the migration times for the dyes $d6_{yt}$, $d7_{ym}$ and $d8_{ytd}$, Figure 4.7, was as expected for dyes of this sort when analysed with MEKC. The addition of 4HBSA onto the triazine group of dye $d6_{yt}$ to form $d7_{ym}$ and $d8_{ytd}$ increases the hydrophilic character of the dye at pH 9.3 (the pH conditions in the capillary with buffer employed for MEKC analysis), therefore the mono and di-substituted dyes ($d7_{ym}$ and $d8_{ytd}$), migrates more quickly than dye $d6_{yt}$. Moreover, $d8_{ytd}$ (2.95 min) migrating more quickly than $d7_{ym}$ (3.77 min), shown in Figure 4.7b.

The sequence being attributed to the more hydrophilic nature of the modified dyes and therefore their preference to be in the bulk solution in the capillary rather than in the micelle.

Additionally, the percent area of the $d8_{ytd}$ shown in Figure 4.7c, was 100% which indicates the purity of the final product.

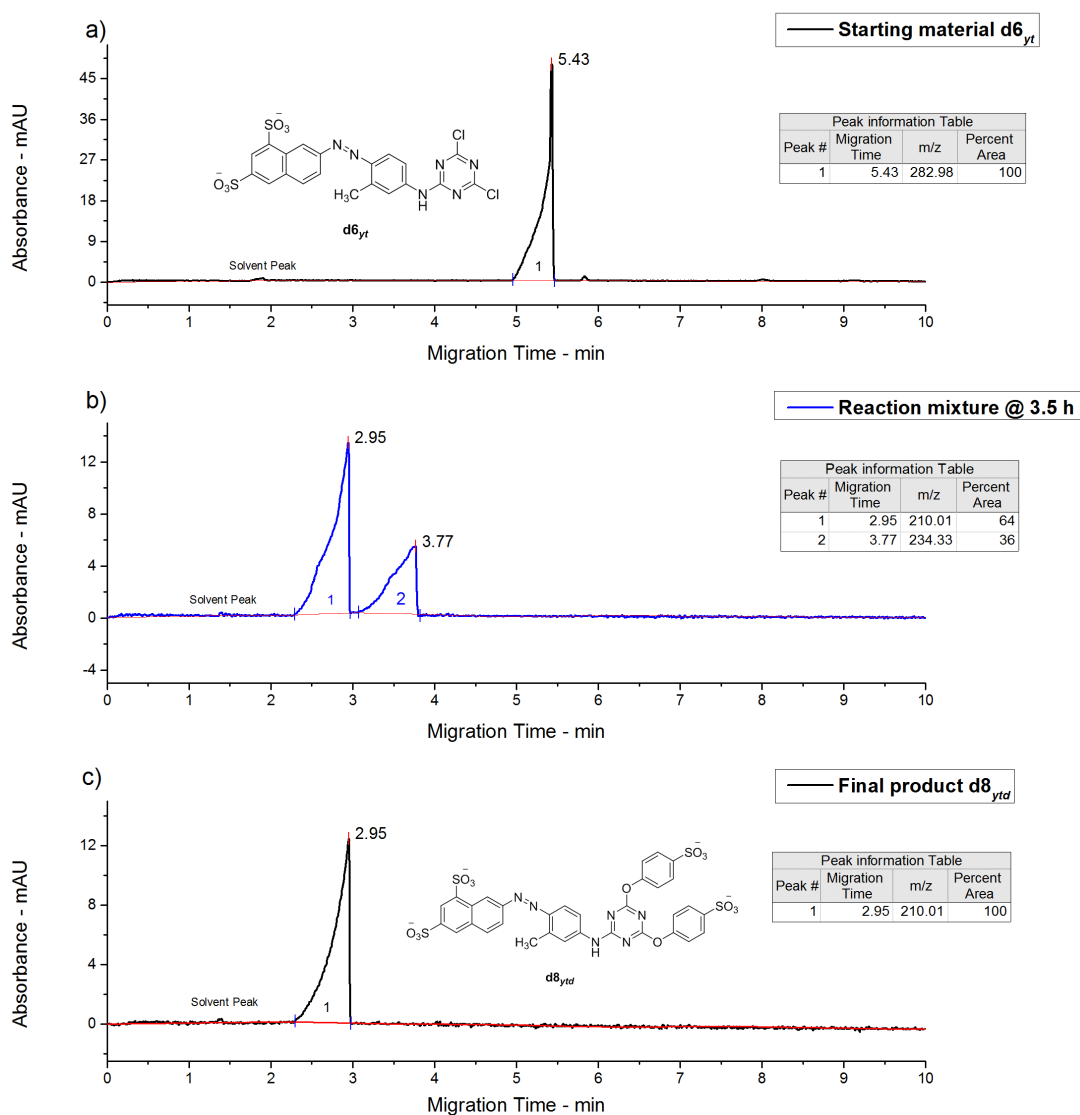


Figure 4.7: Electropherograms showing reaction progress of synthesis of $d8_{ytd}$. (a) yellow dichlorotriazine dye $d6_{yt}$; (b) $d7_{ytm}$ – $d8_{ytd}$ after 3.5 hours reaction; (c) Final product $d8_{ytd}$. MEKC conditions: same as Figure 4.1

In TLC analysis, once the mono substitution of $d6_{yt}$ (R_f value 0.70) was completed, the di substitution started and new highly polar yellow compound $d8_{ytd}$ (R_f value 0.64) started to appeared on TLC plate. This sequence can be attributed due to fairly strong interaction of highly polar compound $d8_{ytd}$ with the surface of adsorbents, as a result $d8_{ytd}$ tends to stick or adsorb onto the fine particles of the adsorbent and move slowly^[18]. TLC showed that the product of mono substitution $d7_{ytm}$ was fully converted to the $d8_{ytd}$ in 4 hours.

In the FT-IR spectrum of the dye $d8_{ytd}$, Figure 4.8, shows the new peak at 1120 cm^{-1} which can be attributed to the stretching vibration of C–O–C in its structure between the triazine and the 4HBSA. The C–Cl peaks at 1097 and 791 cm^{-1} (Figure

4.4) are no longer present indicating that dye **d6_{yt}** has been successfully di-substituted with 4HBSA to yield dye **d8_{ytd}**.

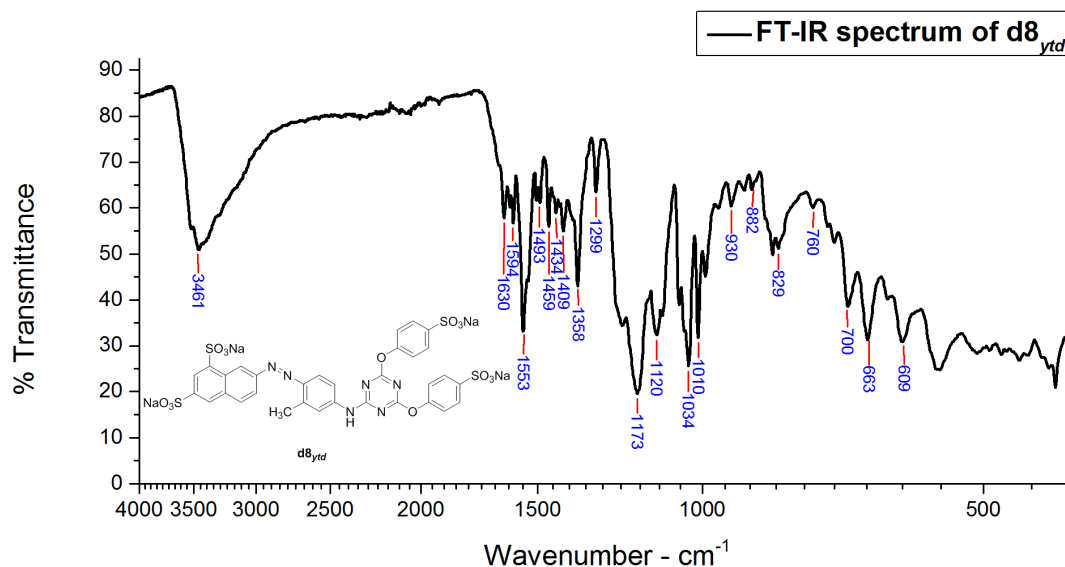


Figure 4.8: FT-IR spectrum of di-substituted yellow dye **d8_{ytd}**

The detailed analysis of spectrum (Figure 4.8) is as follows [7-10, 191]; N-H stretch, 3461 cm⁻¹; overtone or combination bands, 2000–1667 cm⁻¹; N-H bending, 1630 cm⁻¹; C=C ring stretch, 1594, 1493, 1459 cm⁻¹; azo group stretch, 1434 cm⁻¹; C=N stretch, 1553, 1358 cm⁻¹; C-N stretch (secondary amine), 1299 cm⁻¹; sulfonate salts, 1173 cm⁻¹; C-O-C stretching, 1120 cm⁻¹; in-plane C-H bend, 1040, 1010 cm⁻¹; out of plane aromatic C-H bend, 760 cm⁻¹.

Elemental analysis, Found: C, 30.88%; H, 3.30%; N, 7.86%. Calculated for C₃₂H₂₀N₆Na₄O₁₄S₄·7H₂O: C, 36.32%; H, 3.24%; N, 7.94%. The results were adjusted due to the presence of water of crystallisation in the dye molecule. Further disagreement could be attributed to the presence of traces of salt.

4.1.6 Application of Yellow Dyes (**d6_{yt}**, **d7_{ytm}** and **d8_{ytd}**) onto Wool Fabric by Inkjet Printing

The inks were prepared using 5% dye according to the procedure detailed in section 2.5.2, and then viscosity and surface tension of inks were measured.

The resulting ink formulation was then introduced in the cartridge and printed onto wool fabric using HP 6940 deskjet printer. Once printed, the printed wool samples were fixed by three methods detailed in section 2.5.4, and evaluated for percent fixation along with light fastness and wash fastness.

Moreover the inks were also evaluated for stability through MEKC over six months storage time at room temperatures.

4.1.7 Characteristics of Formulated Inks (**d6_{yt}**, **d7_{ym}** and **d8_{yt}**)

4.1.7.1 Surface Tension and Viscosity of Inks

In terms of inkjet printing, aqueous inks are required to have a surface tension and viscosity of 25 – 60 dynes.cm⁻¹ and 2 – 20 cP respectively [20, 21]. It can be seen, from Table 4.1, that parent dye **d6_{yt}** and both the modified dyes (**d7_{ym}** and **d8_{yt}**) based inks had a surface tension and viscosity within the operational range.

Table 4.1: Surface tension and viscosity of yellow inks

Ink formulation	Surface Tension (dynes.cm⁻¹)	Viscosity (cP)
d6_{yt} based Ink	44.5	8
d7_{ym} based Ink	44.5	6
d8_{yt} based Ink	45.5	8

4.1.7.2 Stability of Dye (**d6_{yt}**, **d7_{ym}** and **d8_{yt}**) Based Inks

As discussed earlier, dichlorotriazine dyes are susceptible to hydrolysis even in traces of moisture. Therefore, stability of yellow dichlorotriazine dye along with new modified dyes in inks were also evaluated.

The results of any change in percent area of the peaks of the dyes **d6_{yt}**, **d7_{ym}** and **d8_{yt}** within inks stored at room temperature for six months can be seen in Figure 4.9, Figure 4.10 and Figure 4.11.

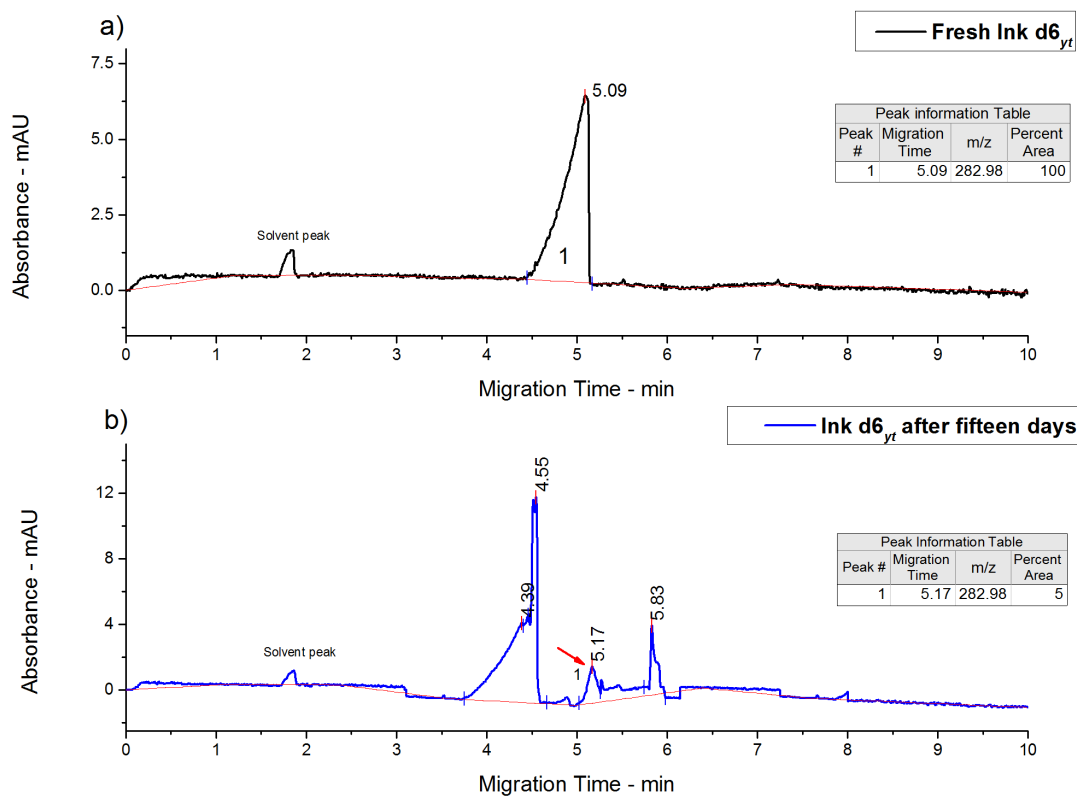


Figure 4.9: Electropherograms showing $d6_{yt}$ based ink stability. (a) Fresh ink; (b) Ink after fifteen days storage at room temperature.

The percent area of peaks on the MEKC electropherogram is related to the concentration of specific compounds within the samples. As shown in Figure 4.9a, the effective component $d6_{yt}$ reduced to 5% (Figure 4.9b) after only fifteen days storage, indicating that one or both of the labile chlorine atom(s) of triazine system got hydrolysed or reacted with other components of inks during storage at room temperature.

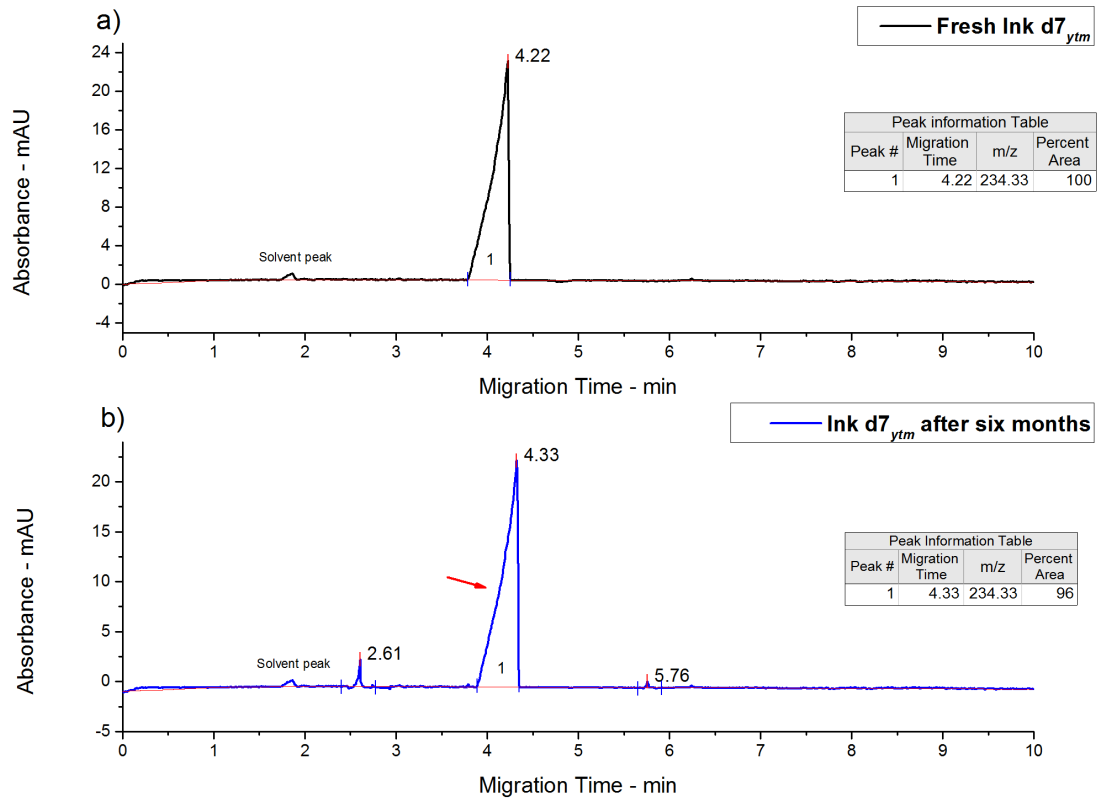


Figure 4.10: Electropherograms showing $d7_{ym}$ based ink stability. (a) Fresh ink; (b) Ink after six months storage at room temperature

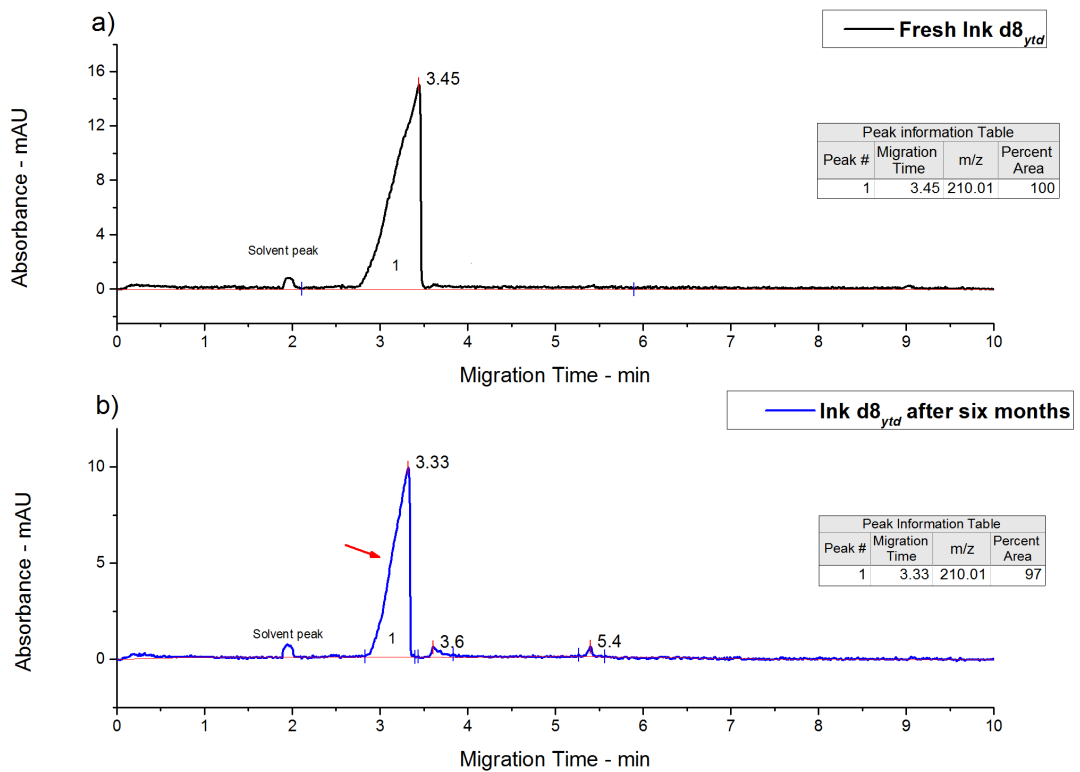


Figure 4.11: Electropherograms showing $d8_{ytd}$ based ink stability. (a) Fresh ink; (b) Ink after six months storage at room temperature

As shown in Figure 4.10b and Figure 4.11b, no significant change in the percent area of peaks in modified dyes **d7_{ytm}** and **d8_{ytd}** based yellow inks were observed when stored for six months indicating that the decreased reactivity of both the modified dyes increased the overall stability of inks.

4.1.8 Evaluation of Percent Fixation of Yellow Dyes (**d6_{yt}**, **d7_{ytm}** and **d8_{ytd}**) by Different Fixation Methods

4.1.8.1 Method 1: Batching at Room Temperature

Table 4.2 shows the results obtained by batching the printed samples under moist conditions for 2 and 4 hours at room temperature.

Table 4.2: Percent fixation of **d6_{yt}, **d7_{ytm}** and **d8_{ytd}**. Fixation conditions: Batching at 25 °C for 2 and 4 hours under moist conditions**

Ink formulation	% Fixation (2 hours)	% Fixation (4 hours)
d6_{yt}	69	73
d7_{ytm}	76	79
d8_{ytd}	76	80

As discussed earlier that the addition of urea and sodium metabisulfite in the pretreatment liquor is advantageous in promoting the dye penetration under the room temperature conditions and increases the extent of percent fixation. In accordance with literature ^[12], this effect is more prominent in case of moderate reactivity dyes and high molecular weight dyes.

As moderate level of fixation (73%) was achieved with yellow dichlorotriazine dye **d6_{yt}** as being low weight but highly reactive dye whereas comparatively moderate to high level of fixation, *i.e.*, 79% and 80% was achieved for **d7_{ytm}** and **d8_{ytd}** respectively as being high weight and moderately reactive as compared to dichlorotriazine dye.

Therefore, modification of **d6_{yt}** with 4HBSA proved to be advantageous as the modified yellow multifunctional dyes **d7_{ytm}** and **d8_{ytd}** gave better fixation results than dichlorotriazine dye **d6_{yt}** even at room temperature.

4.1.8.2 Method 2: Batching at 65 °C

Significant improvement in the extent of dye–fibre bond (percent fixation) was observed when the modified yellow dyes were applied by a print (Inkjet)–batch technique.

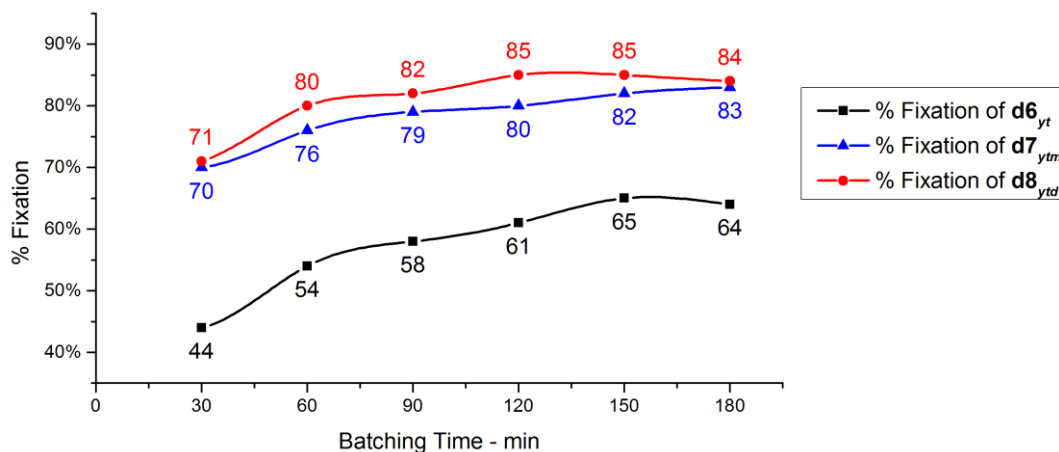


Figure 4.12: Percent fixation of $d6_{yt}$, $d7_{ytm}$ and $d8_{ytd}$. Fixation conditions: Batch at 65 °C for 30 to 180 minutes under moist conditions

Figure 4.12 shows the results obtained using $d6_{yt}$, $d7_{ytm}$ and $d8_{ytd}$ by batching the printed samples under moist conditions for 30 – 180 minutes at 30 minutes interval.

It is observed that yellow dichlorotriazine dye $d6_{yt}$, being highly reactive dye not only react with wool but also got hydrolysed under selected conditions of fixation. Therefore, resulted in moderate fixation results of 65%.

Moreover, modified dyes $d7_{ytm}$ and $d8_{ytd}$ based inks show remarkable improvement in percent fixation as $d7_{ytm}$ gave 83% in 180 minutes and $d8_{ytd}$ gave 85% in 120 minutes. This shows an increase of approximately 22% and 23% improvement in the percent fixation of $d7_{ytm}$ and $d8_{ytd}$ onto wool respectively as compared to yellow dichlorotriazine dye.

It is also evident from the Figure 4.12, that incorporating two sulfophenoxy groups on dichlorotriazine dye gave better results. It could be due to the better stability of sulfophenoxy group at the fixation temperature used.

4.1.8.3 Method 3: Steaming

Figure 4.13 shows the effect of steaming temperature and steaming time, on the fixation results of printed wool.

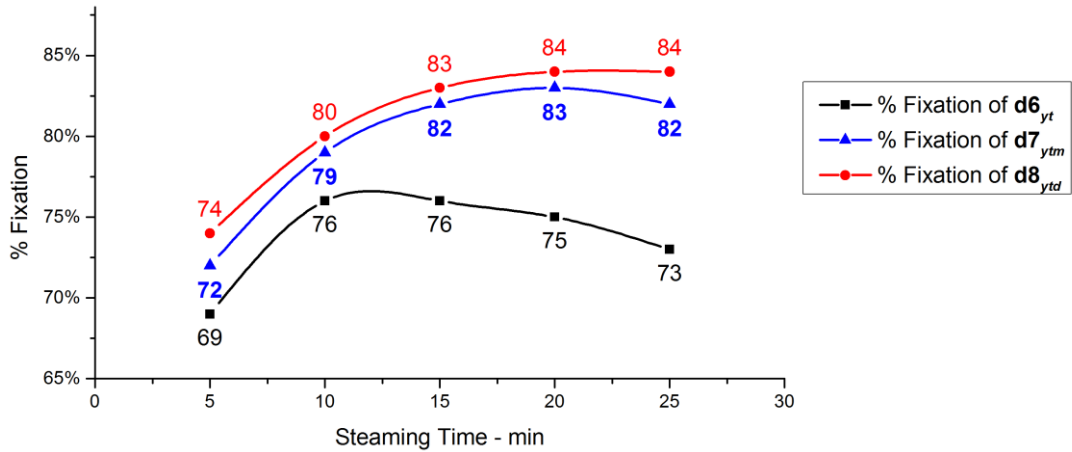


Figure 4.13: Percent fixation of d6_{yt}, d7_{ytm} and d8_{ytd}. Fixation conditions: Steaming for 5, 10, 15, 20 and 25 minutes

From Figure 4.13, it is evident that increasing the steaming time from 5 min to 25 min at 102 °C, brings about an increase in percent fixation of printed dyes, reflecting the positive impact of proper steaming time on releasing the dye molecules from the thickener film to the fabric phase, transfer of dye molecules across the fabric structure, diffusion into the fibre structure to its active groups and a consequent reaction with and fixation at those reactive sites, thereby increasing the percent fixation ^[22].

A maximum percent fixation is expected when steaming is carried out for 20 min at 102 °C. These results clearly reflect the difference in reactivity of parent and modified dyes used. Further lengthening of steam fixation time up to 25 min at 102 °C has practically slight or no effect on the fixation of the dyes, most probably due to the shortage in and/or inaccessibility of the dye-sites ^[23].

It is also evident from Figure 4.13 that steaming the printed samples at 102 °C has a positive impact on fixation as well as depth of shade regardless of any reactive dyes used, most probably due to the enhancement in fabric swellability, the extent of dye release from the thickener film and diffusion within the swelled structure to appropriate active centres; and binding at those sites thereby gives rise to a darker depth of shade (see Appendix B – steamed samples).

It can be concluded from Figure 4.13 that 10 min at 102 °C is an ideal time for yellow dichlorotriazine dye **d6_{yt}** fixation owing to its high reactivity, whereas 20 min is an ideal time for modified dyes fixation owing to their lower reactivity that needs longer time to achieve higher dye fixation.

4.1.9 Light Fastness

The light fastness of wool printed with printing paste using yellow dye **d6_{yt}** and modified dyes **d7_{ytm}** and **d8_{ytd}** were tested and evaluated according to BS EN ISO 105-B02:2013 (Method 3) ^[24], and the results are shown in Table 4.3.

All the dyes passed target wool reference 6. However, modified dyes **d3_{mtm}** and **d4_{mta}** shows even better light fastness than target wool reference 6.

Table 4.3: Light fastness of yellow dyes (d6_{yt}, d7_{ytm} and d8_{ytd}) compared to target blue wool reference 6

Dye/Ink	Target blue wool reference 6	
d6_{yt}	Equal to 6 (6)	Satisfactory
d7_{ytm}	Better than 6 (6 ⁺)	Satisfactory
d8_{ytd}	Better than 6 (6 ⁺)	Satisfactory

4.1.10 Wash Fastness

Wash fastness was carried out according to the BS ISO 105-C06:2010 ^[25] and the results are shown in Table 4.4. Yellow dichlorotriazine dye **d6_{yt}** showed a small change in shade resulting in a grade 4-5; and also there was light staining on cotton (adjacent fabrics) whereas both the modified dyes **d7_{ytm}** and **d8_{ytd}** showed no change in colour or staining, hence, showed excellent wash fastness. This excellent wash fastness is because of the strong covalent bonding between the dye and the wool fibre.

Table 4.4: Wash fastness of yellow dyes ($d6_{yt}$, $d7_{ytm}$ and $d8_{ytd}$)

Dye/Ink	Change in shade	Staining					
		CA	C	N	P	A	W
$d6_{yt}$	4-5	5	4-5	5	5	5	5
$d7_{ytm}$	5	5	5	5	5	5	5
$d8_{ytd}$	5	5	5	5	5	5	5

CA: Cellulose Acetate; C: Cotton; N: Nylon; P: Polyester; A: Acrylic; W: Wool

4.2 Conclusions

With the aim of designing a series of yellow dyes for inkjet inks for wool with lower chemical reactivity, increased solubility and increased stability, one chlorine of cyanuric chloride was displaced by amino based yellow dye chromophore at 0 – 5 °C (pH 5.6 – 6.5) to produce yellow dichlorotriazine dye $d6_{yt}$ in pure form (without hydrolysed by-products).

Modification of yellow dichlorotriazine was done by the same sequence as done for magenta dyes, however, the parameters for modification were optimised.

The first modification of yellow dichlorotriazine dye was done by displacing the second chlorine atom by the sulfophenoxy group at 45 °C (5 hours) to produce mono-substituted dye $d7_{ytm}$ in pure form.

Second modification of yellow dichlorotriazine dye was done by displacing the second chlorine atom by using two equivalent sulfophenoxy group at 45 °C (1 hours) to produce intermediate dye $d4_{ytm}$ and then the third chlorine atom as displaced at 80 °C (4 hours) to produce homobifunctional dye $d8_{ytd}$ in pure form.

The characteristic properties such as surface tension and viscosity of inks formulated by incorporating the synthesised dyes were found to be in operation range.

The stability of modified dyes based inks increased significantly due to the lower reactivity of the modified dyes, which make them ideally suited to inkjet printing processes.

Significant improvement in the extent of covalent dye fixation was observed when the modified yellow dyes were applied by all methods. However, noteworthy

enhancement observed when the samples were fixed through batch at 65 °C and steaming at 102 °C.

With respect to the fastness properties, the yellow dichlorotriazine dye was 0.5 grade lower when compared with the modified dyes for light fastness test. Moreover, modified dyes showed excellent wash fastness properties whereas dichlorotriazine dye showed a small change in shade as well as staining on adjacent fabrics (cotton).

4.3 References

1. David, H.E.F. and Blangey, L. *Fundamental processes of dye chemistry*. New York: Interscience Publishers, 1949.
2. Cain, J.C. *The chemistry of the diazo-compounds*. London: Edward Arnold Publishers Ltd., 1908.
3. Patent GB1165661 (1969)
4. Patent WO2007012828 (2007)
5. Terabe, S. Capillary Separation: Micellar Electrokinetic Chromatography. *Annual Review of Analytical Chemistry*, 2009, **2**, pp.99-120.
6. Quirino, J.P. and Terabe, S. Sample stacking of cationic and anionic analytes in capillary electrophoresis. *Journal of Chromatography A*, 2000, **902**, pp.119-135.
7. Socrates, G. *Infrared and Raman characteristic group frequencies : tables and charts*. Chichester: Wiley, 2001.
8. Silverstein, R.M., Webster, F.X. and Kiemle, D.J. *Spectrometric Identification of Organic Compounds*. 7th ed. New York: John Wiley and Sons, 2005.
9. Matlok, F., Gremlich, H.U., Bruker Analytische Meotechnik and Merck eds. *Merck FT-IR atlas : a collection of FT-IR spectra*. Weinheim: Vch, 1988.
10. Keller, R.J. and Sigma-Aldrich Corporation. *The Sigma library of FT-IR spectra*. Missouri: Sigma Chemical Company, 1986.
11. Beech, W.F. *Fibre-Reactive Dyes* London: Logos Press Ltd., 1970.
12. Waring, D.R. and Hallas, G. eds. *The Chemistry and Application of Dyes*. New York: Plenum Press, 1994.
13. Patent WO2006103414 (2006)

14. Patent GB774925 (1957)
15. Li, S.F.Y. *Capillary electrophoresis: principles, practice and applications*. Amsterdam: Elsevier Science Publishers, 1992.
16. Hancu, G., Simon, B., Rusu, A., Mircia, E. and Gyéresi, Á. Principles of Micellar Electrokinetic Capillary Chromatography Applied in Pharmaceutical Analysis. *Advanced Pharmaceutical Bulletin*, 2013, **9**, pp.1-8.
17. Coulter, B. *Introduction to Capillary Electrophoresis* [online]. [Accessed]. Available from:
<https://www.google.co.uk/url?sa=t&rct=j&q=&esrc=s&source=web&cd=1&cad=rja&ved=0CDsQFjAA&url=https%3A%2F%2Fwww.beckmancoulter.com%2Fwsrportal%2Fbibliography%3Fdocname%3D360643-CEPrimer1.pdf&ei=6upWUp7ALcu10QWUioCABw&usq=AFQjCNEDEtGGHzNUfJbcnwFbcKYb9FNdLw>.
18. University of Colorado at Boulder. *Thin Layer Chromatography (TLC)* [online]. 2013. [Accessed December 10, 2011]. Available from:
<http://orgchem.colorado.edu/Technique/Procedures/TLC/TLC.html>.
19. Miller, R.K. Infrared Spectroscopy. In: K. Venkataraman, ed. *The Analytical Chemistry of Synthetic Dyes*. New York: Wiley & Sons, 1977.
20. Magdassi, S. Ink Requirements and Formulations Guidelines. In: S. Magdassi, ed. *Chemistry of Inkjet Inks*. New Jersey: World Scientific Publishing Ltd., 2012.
21. Ujiie, H. *Digital printing of textiles*. Cambridge: Woodhead Publishing Ltd., 2006.
22. Kongliang, X. and Aiqin, H. Application of a reactive cationic dye to wool. *Journal of the Society of Dyers and Colourists*, 1998, **114**, pp.20-23.
23. Ibrahim, N., El Zairy, M., El-Gamal, A. and Tolba, S. Printing of nylon-6 fabric with anionic dyes in presence of thiourea/ammonium persulphate redox system. *Colourage*, 2001, **48**, pp.19-26.
24. British Standards Institution. *Colour fastness to artificial light: Xenon arc fading lamp test*, ISO 105-B02:2013.
25. British Standards Institution. *Textiles - Tests for colour fastness - Part C06: Colour fastness to domestic and commercial laundering*, BS EN ISO 105-C06:2010.

5 Synthesis, Modification, Characterisation of Blue Dichlorotriazine Dyes and Their Application onto Wool Fabric by Inkjet Fabric

This chapter details the synthesis and characterisation of blue dichlorotriazine dye **d10_{bt}** from anthraquinone based chromophore, modification of this dye by incorporating sulfophenoxy group to produce mono-substituted dye **d11_{btm}** and also di-substituted dye **d12_{btid}**. CE (CZE) and TLC were used to monitor course of reactions and the structural changes were confirmed through FT-IR.

This chapter also details the application of blue dichlorotriazine dye and modified dyes based inks by inkjet printing on wool fabrics along with performance evaluation of inks such as surface tension, viscosity, ink stability, percent fixation of the dye and colour fastness properties.

5.1 Experimental

5.1.1 Materials

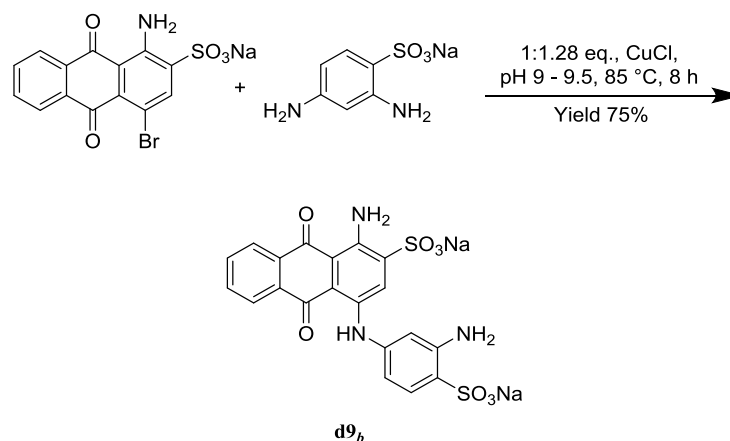
Bromaminic acid sodium salt, 2,4-diamino-benzenesulfonic acid, copper(I) chloride, cyanuric chloride (99%), and sodium 4-hydroxybenzenesulfonate dihydrate (98%), sodium metabisulfite, carboxymethyl cellulose, polysorbate 20 (Tween 20) and N-methylmorpholine N-oxide (NMMO) were purchased from Sigma-Aldrich and used as received. Urea (MP Biomedicals), Alcopol O 60 (Acros organics), 2-pyrrolidone (Acros organics), 2-propanol (Fisher), Sandozin NIE (Clariant) were purchased and used as received. All other chemicals were of reagent grade unless otherwise stated.

5.1.2 Synthesis and Characterisation of Blue 1-Amino-4-[(3-amino-4-sulfophenyl)amino]-Anthraquinone-2-Sulfonic Acid Dye (d9_b)

5.1.2.1 Synthesis of d9_b

In accordance with the method described in reference ^[1], bromaminic acid (12.13 g, 0.03 mol, 1 eq.) dissolved in water (300 cm³) and stirred for 1 hour at 60 °C. 2,4-diamino-benzenesulfonic acid (7.15 g, 0.038 mol, 1.28 eq.), sodium

carbonate (5.82 g, 0.055 mol), sodium bicarbonate (1.84 g, 0.022 mol) and copper(I) chloride (1.26 g, 0.013 mol) were added to a stirred solution of bromaminic acid and temperature was raised to 85 °C. The reaction mixture was stirred until the bromaminic acid was no longer detectable by CZE and analytical TLC. These analyses showed that the Ullmann coupling was completed in 8 hours; after which the reaction mixture was diluted to 500 cm³ and temperature of the reaction mixture was raised to 95 °C for 2 hours. The reaction mixture was filtered hot to remove copper and other impurities. The filtrate was cooled to room temperature and dye **d9_b** was precipitated by careful addition of concentrated hydrochloride solution along with sodium chloride (8% w/v). The dye was collected by filtration and the filter cake was washed with brine (2 × 100 cm³) and dried *in vacuo* (50 °C, 12 hours) to yield dye **d9_b** (12.00 g, 0.023 mol, yield 75%) as blue powders. FT-IR analysis was conducted to confirm the presence of main functional groups in dye **d9_b**. The reaction is shown in Scheme 5.1.



Scheme 5.1: Synthesis of d9_y by Ullmann coupling reaction

5.1.2.2 Characterisation of d9_b

The CZE electropherogram of the synthesised anthraquinone based blue dye chromophore **d9_b** at λ_{obs} , 592 nm is shown in Figure 5.1. The synthesised **d9_b** was detected at 6.75 min with percent area of 100% indicating high purity of synthesised blue dye chromophore.

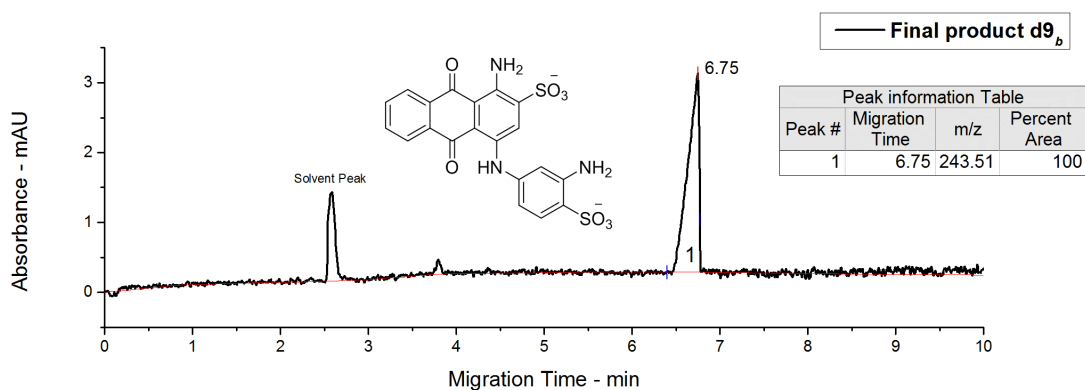


Figure 5.1: Electropherogram of blue dye chromophore $d9_b$. CZE conditions: running buffer, 15mM ammonium acetate and acetonitrile (40% v/v) pH 9.3; pressure injection 0.5 psi for 10 s; voltage 25 kV; detection at 596 nm

The R_f value of $d9_b$ was 0.63. The single spot indicates that the product was pure.

In FT-IR spectrum of the blue dye chromophore $d9_b$ (Figure 5.2), the connecting bond between anthraquinone structure and the 2,4-diaminesulfonic acid can be evident by the appearance of the intense peak at 1279 cm^{-1} for C–N aromatic group [2-4]. The band at 1736 cm^{-1} , which was responsible for the combination of stretching vibration of C=O conjugated with C=C of the anthraquinone structure is also present [2], confirming the structure of $d9_b$.

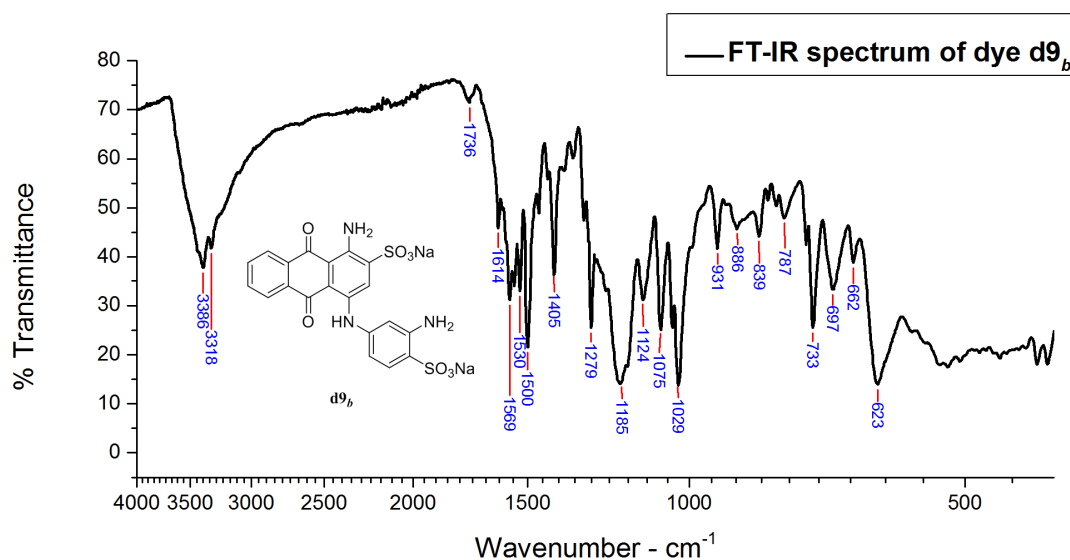


Figure 5.2: FT-IR spectrum of blue dye chromophore $d9_b$

The detailed analysis of the spectrum (Figure 5.2) is as follows [3-6]; N–H stretch, primary amine, 3386 cm^{-1} and 3318 cm^{-1} ; overtone or combinational bands,

2000–1700 cm^{-1} ; C=O, 1736 cm^{-1} ; N–H bending, 1614 cm^{-1} ; C=C ring stretch, 1569, 1500, 1405 cm^{-1} ; C–N stretch, 1279 cm^{-1} ; sulfonate, 1185 cm^{-1} ; in-plane C–H bend, 1020 cm^{-1} ; broad, N–H wag, 886 cm^{-1} ; out of plane aromatic C–H bend, 733 cm^{-1} ; out of plane ring C=C bend, 697 cm^{-1} .

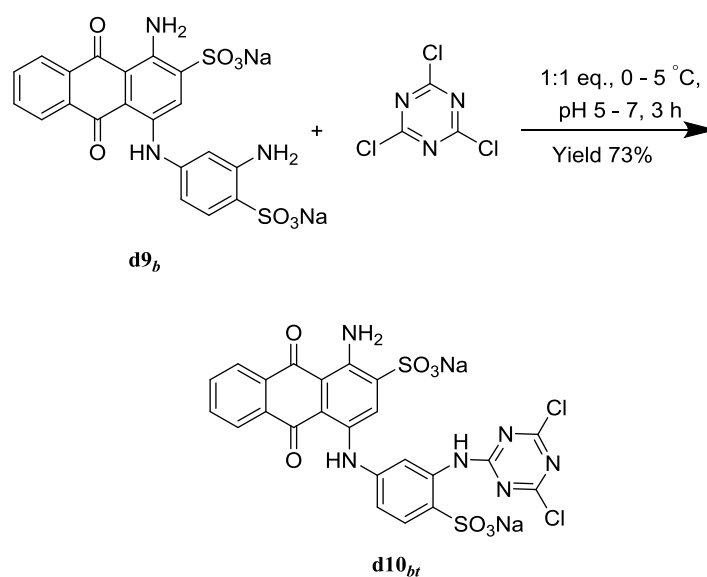
5.1.3 Synthesis and Characterisation of Blue 1-Amino-4-[[3-(4,6-dichloro)-1,3,5-triazin-2-yl]amino]-4-(sulfophenylamino)]-Anthraquinone-2-Sulfonic Acid Dye (**d10_{bt}**)

5.1.3.1 Synthesis of **d10_{bt}**

In accordance with the method described in reference [7], a solution of cyanuric chloride (3.63 g, 0.02 mol) in acetone (30 cm^3) was added dropwise to a mixture of ice–water (50 cm^3). The dye chromophore **d9_b** (10.67 g, 0.02 mol) as dissolved in water (150 cm^3) which was then adjusted to pH 7.0 by the addition of 2N sodium carbonate solution and then added to the stirred cyanuric chloride suspension at 0 to 5 °C, to form a reaction mixture.

Once the addition of dye chromophore **d9_b** was complete, the reaction was stirred for further 3 hours (until the pH had stabilised) and was monitored with CZE and analytical TLC. When the reaction had gone to completion 2N sodium carbonate solution was added to raise the pH to 7.0 and phosphate buffer (0.2 mol, 10% v/v) was added to buffer the pH to 6.4. Sodium chloride (10% w/v) was added to precipitate the dye. The crude dye **d10_{bt}** was collected by filtration and the filter cake was washed with brine (2 × 100 cm^3) and dried *in vacuo*.

Purification of crude dye using solvent–nonsolvent technique (1:2, DMF–diethyl ether) afforded the pure dye **d10_{bt}** (9.98 g, 14.6 mmol, yield 73%) as blue powders. FT-IR analysis was conducted to confirm the presence of main functional groups in dye **d10_{bt}**. The reaction is shown in Scheme 5.2.



Scheme 5.2: Preparation of condensation product **d10_{bt} from blue anthraquinone chromophore and cyanuric chloride**

5.1.3.2 Characterisation of **d10_{bt}**

Figure 5.3 shows the reaction progression of synthesis of **d10_{bt}** in a fused silica capillary at pH 9.3. Both dyes have a charge of -2 under these conditions. The peak labelled solvent peak (see Figure 5.3) represents the water in which the samples were dissolved. This water plug does not have any electrophoretic mobility; the movement of this plug is due solely to electroosmotic flow, and it is the first peak to pass the detector. The next peak to emerge, **d10_{bt}** at 5.74 min, which has the higher mass to charge ratio of the two analytes. This is because dye **d10_{bt}** has an increased molecular weight compared to dye **d9_b** but no additional sulfonate groups that would increase the negative charge; therefore dye **d10_{bt}** (5.74 min) elutes faster than dye **d9_b** (6.75 min), see Figure 5.3b.

Moreover, the percent area of the **d10_{bt}** shown in Figure 5.3c, was 100% which indicates that there was no hydrolysed dye in the final product.

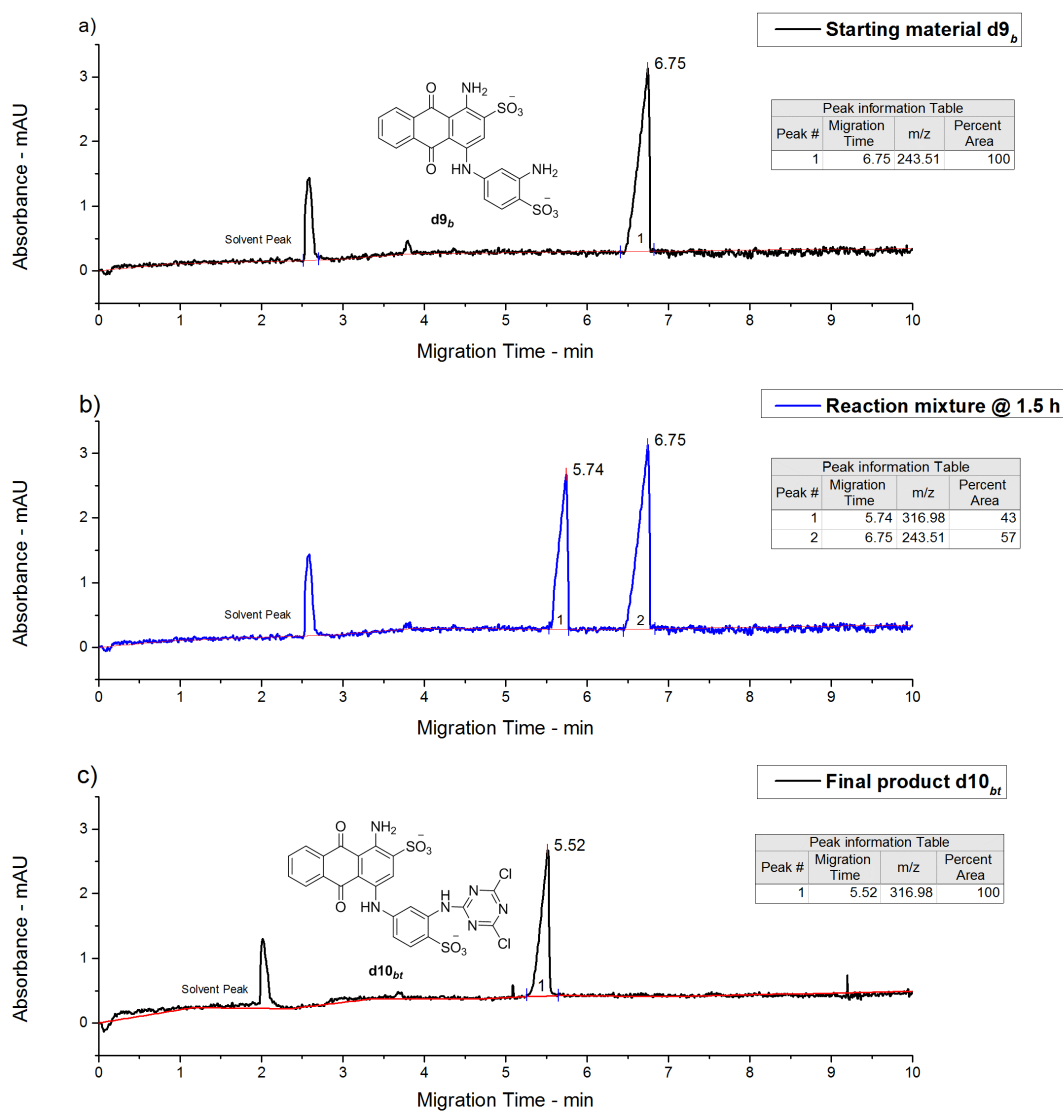


Figure 5.3: Electropherograms showing reaction progress of synthesis of $d10_{bt}$. (a) blue dye chromophore $d9_b$; (b) $d9_b - d10_{bt}$ after 1.5 hours reaction time; (c) Final product $d10_{bt}$. CZE conditions: same as Figure 5.1

The R_f values of starting material and product were found to be 0.63 and 0.73 respectively. Moreover, almost quantitative conversion to product occurred in 3 hours.

In FT-IR spectrum of blue dichlorotriazine dye $d10_{bt}$, the appearance of new peaks at 1546 and 1404 cm^{-1} reflect the presence of the triazine ring in dye $d10_{bt}$. Also the presence of the peaks at the 1086 and 792 cm^{-1} are attributed to the C–Cl stretching vibration on the triazine ring of the dye.

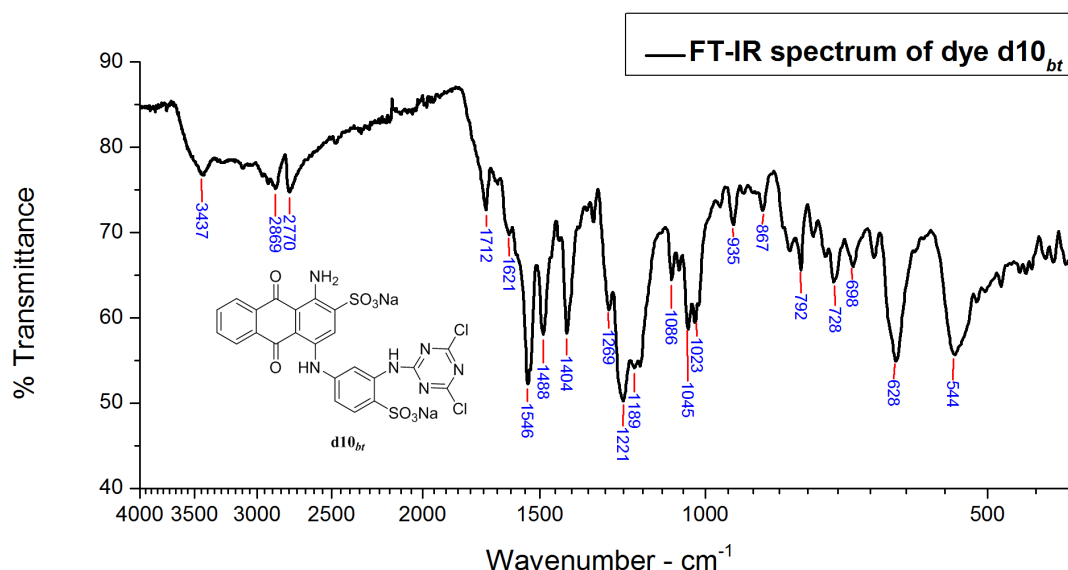


Figure 5.4: FT-IR spectrum of blue dichlorotriazine dye $d10_{bt}$

The detailed analysis of the spectrum (Figure 5.4) is as follows ^[3-6]; N–H stretch, 3437 cm^{-1} ; aromatic C–H stretch, $2866, 2770\text{ cm}^{-1}$; overtone or combinational bands, $2000 - 1700\text{ cm}^{-1}$; C=O, 1712 cm^{-1} ; N–H bend, 1621 cm^{-1} ; C=C ring stretch, 1488 cm^{-1} ; triazine stretch, $1546, 1404\text{ cm}^{-1}$; C–N stretch, 1269 cm^{-1} ; C–CO–C, 1221 cm^{-1} ; sulfonate, 1189 cm^{-1} ; C–Cl stretch, $1086\text{ cm}^{-1}, 792\text{ cm}^{-1}$; in-plane C–H bend, $1045, 1023\text{ cm}^{-1}$; out of plane aromatic C–H bend, 728 cm^{-1} .

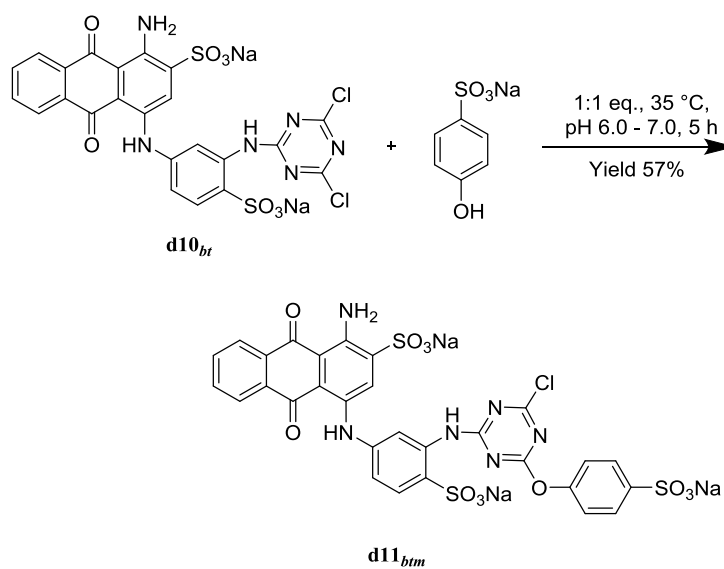
5.1.4 Synthesis and Characterisation of Modified Blue 1-Amino-4-[3-(4-chloro-6-(4-sulfophenoxy)-1,3,5-triazin-2-yl)amino]-4-(sulfophenyl)amino]-Anthraquinone-2-Sulfonic Acid Dye ($d11_{btm}$)

5.1.4.1 Synthesis of $d11_{btm}$

Dye $d10_{bt}$ (6.81 g, 0.01 mol, 1 eq.) and sodium bicarbonate (1.23 g, 0.015 mol, 1.5 eq.) were dissolved in water (50 cm^3) and the temperature was raised to $35\text{ }^\circ\text{C}$. A solution of sodium 4-hydroxybenzenesulfonate dihydrate (4HBSA) (2.32 g, 0.01 mol, 1 eq.) in water (20 cm^3) was added dropwise over 15 minutes to the dye $d10_{bt}$ solution; the pH was maintained at 6.0 to 7.0 by the addition of saturated sodium carbonate solution. Once the addition of 4HBSA solution was complete, the reaction was stirred for further 5 hours (until the pH was stabilised) and was monitored with CZE and analytical TLC. The reaction mixture was cooled to room temperature and

sodium chloride (10% w/v) was added to precipitate out the dye. The crude dye **d11_{btm}** was collected by filtration and the filter cake was dried *in vacuo*.

Purification of crude dye **d11_{btm}** using solvent–nonsolvent technique (DMF–diethyl ether, 1:2 v/v) afforded pure dye **d11_{btm}** (4.80 g, 5.7 mmol, yield 57%) as blue powders. FT-IR analysis was conducted to confirm the synthesis of the dye. The reaction is shown in Scheme 5.3.



Scheme 5.3: Condensation of dye **d10_{bt} with 4HBSA to yield dye **d11_{btm}****

5.1.4.2 Characterisation of **d11_{btm}**

The electropherograms from CZE analyses are shown in Figure 5.5 which indicates the progression of the synthesis reaction from the starting dye **d10_{bt}** to the mono-substituted dye **d11_{btm}** (peak 3 in Figure 5.5b). After the modification, the mass to charge ratio of the dye **d11_{btm}** decreases compared to the parent dye **d10_{bt}**, therefore the migration time of the dye **d11_{btm}** (6.65 min) increases as compared to **d10_{bt}** (5.69 min).

Furthermore, the percent area of modified dye **d11_{btm}** was 100% which indicates there was only one colour component in the synthesised dye (see Figure 5.5c).

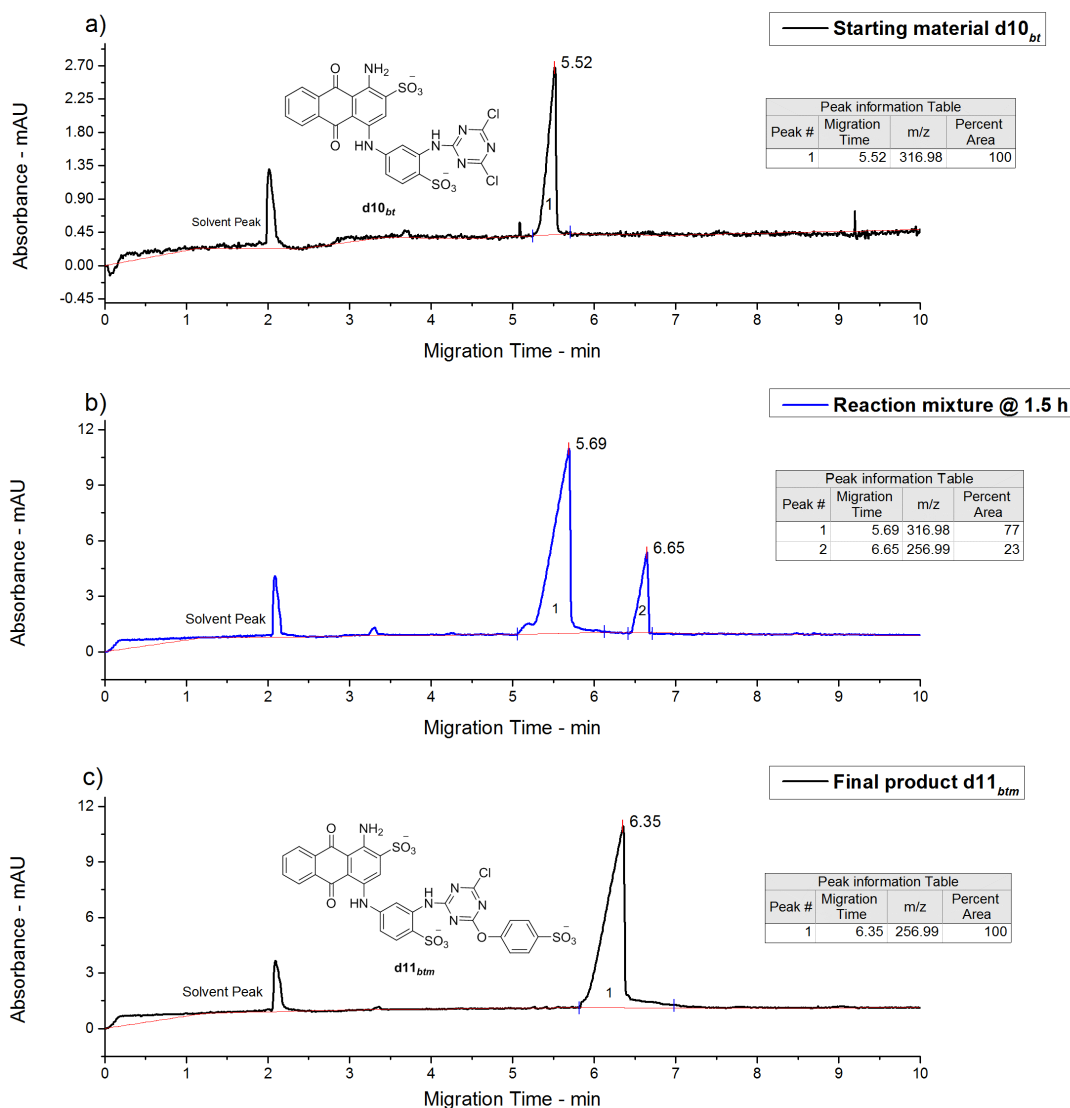


Figure 5.5: Electropherograms showing reaction progress of synthesis of $d11_{btm}$. (a) blue dichlorotriazine dye $d10_{bt}$; (b) $d10_{bt}$ – $d11_{btm}$ after 1.5 hours reaction; (c) Final product $d11_{btm}$. CZE conditions: same as Figure 5.1

In analytical TLC analysis, the spots appeared as estimated, showing that the primary condensation reaction of dye $d10_{bt}$ with 4HBSA take place readily at 35 °C provided that neutral pH was maintained. Analytical TLC showed the gradual appearance of new more polar blue compound $d11_{btm}$ (R_f value 0.69) compared to the starting material $d10_{bt}$ (R_f value 0.73). Moreover, TLC showed that the starting material $d10_{bt}$ was fully converted to the $d11_{btm}$ in 5 hours.

In FT-IR spectrum of the mono substituted dye $d11_{btm}$, Figure 5.6, the new peak at 1126 cm^{-1} is evident which can be attributed to the stretching vibration of C–O–C in its structure between the triazine and the 4HBSA. The peaks at 1077 and

803 cm^{-1} can be attributed to the presence of C–Cl after the mono substitution of dye **d10_{bt}** with 4HBSA.

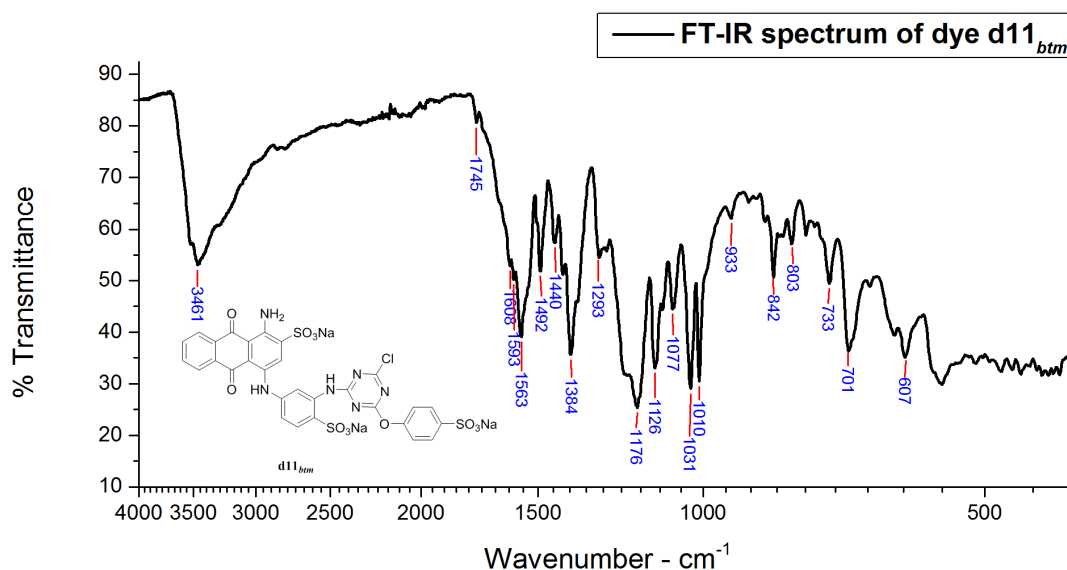


Figure 5.6: FT-IR spectrum of blue mono-substituted dye **d11_{btm}**

The detailed analysis of the spectrum (Figure 5.6) is as follows [3-6]; N–H stretch, 3461 cm^{-1} ; overtone or combinational bands, 2000–1700 cm^{-1} ; C=O stretching, 1745 cm^{-1} ; N–H bending, 1608 cm^{-1} ; C=C ring stretch, 1593, 1492, 1440 cm^{-1} ; triazine stretch, 1563, 1384 cm^{-1} ; C–N stretch, 1283 cm^{-1} ; C–O–C stretching, 1126 cm^{-1} ; sulfonate, 1176 cm^{-1} ; C–Cl stretch, 1077, 803 cm^{-1} ; in-plane C–H bend, 1031, 1010 cm^{-1} ; out of plane aromatic C–H bend, 733 cm^{-1} .

Elemental analysis, Found: C, 38.08%; H, 2.30%; N, 9.10%. Calculated for $\text{C}_{29}\text{H}_{16}\text{ClN}_6\text{Na}_3\text{O}_{12}\text{S}_3 \cdot 5\text{H}_2\text{O}$: C, 37.42%; H, 2.82%; N, 9.03%. The results were adjusted due to the presence of water of crystallisation in the dye molecule. Further disagreement could be attributed to the presence of traces of salt.

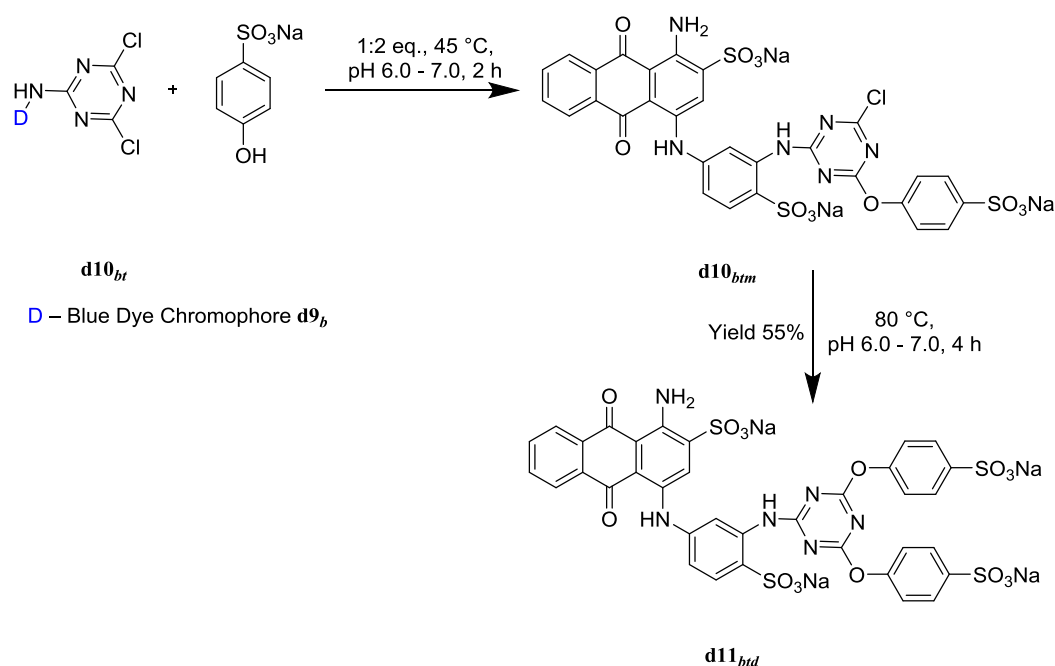
5.1.5 Synthesis and Characterisation of Modified Blue 1-Amino-4-[3-(4,6-(4-sulfophenoxy)-1,3,5-triazin-2-yl)amino]-4-(sulfophenyl)amino]-Anthraquinone-2-Sulfonic Acid Dye (**d12_{btd}**)

5.1.5.1 Synthesis of **d12_{btd}**

Dye **d10_{bt}** (6.51 g, 0.01 mol, 1 eq.) and sodium bicarbonate (1.23 g, 0.015 mol, 1.5 eq.) were dissolved in water (50 cm^3) and temperature was raised to 45 °C. A solution of sodium 4-hydroxybenzenesulfonate dihydrate (4HBSA) (4.86 g, 0.02

mol, 2 eq.) in water (30 cm³) was added dropwise over 15 minutes to the dye **d10_{bt}** solution; the pH was maintained at 6.0 to 7.0 by the addition of saturated sodium carbonate solution. Once the addition of the 4HBSA solution was complete, the reaction was followed using CZE and analytical TLC. The CZE and TLC analysis showed that the primary condensation of dye **d10_{bt}** was complete after 2 hours (pH has stabilised); after which the temperature of the reaction mixture was raised to 80 °C to enable the secondary condensation of dye **d10_{bt}** to occur. After 4 hours, the CZE and analytical TLC analysis showed that the secondary condensation was complete. The reaction mixture was cooled to room temperature and sodium chloride (10% w/v) was added to precipitate out the dye. The crude dye **d12_{btd}** was collected by filtration and the filter cake was dried *in vacuo*.

Purification of crude dye **d12_{btd}** using solvent–nonsolvent technique (DMF–diethyl ether, 1:2 v/v) afforded pure dye **d12_{btd}** (5.5 g, 5.49 mmol, yield 55%) as blue powders. The dye **d12_{btd}** was characterised by FT-IR and elemental analysis. The reaction is shown in Scheme 5.4.



Scheme 5.4: Preparation of di substituted dye **d12_{btd} from blue dichlorotriazine dye **d10_{bt}** and 4HBSA**

5.1.5.2 Characterisation of **d12_{btd}**

The CZE electropherograms at different reaction times during the modification of dye **d10_{bt}** with 4HBSA are shown in Figure 5.7. After 4 hours of reaction all of

the dye **d10_{bt}** had been converted to the dye **d11_{btm}** and dye **d12_{btd}**, see Figure 5.7b. When the reaction temperature was raised to 80 °C and allowed to continue for a further 4 hours, all of the dye **d11_{btm}** had been converted to dye **d12_{btd}** as shown in Figure 5.7c.

After the modification, the mass to charge ratio of the dye decreases compared to the parent dye **d10_{bt}** (5.52 min), therefore the migration time of the dye **d12_{btd}** (6.73 min) increases.

Additionally, the percent area of the **d12_{btd}** shown in Figure 5.7 indicates the purity of final product.

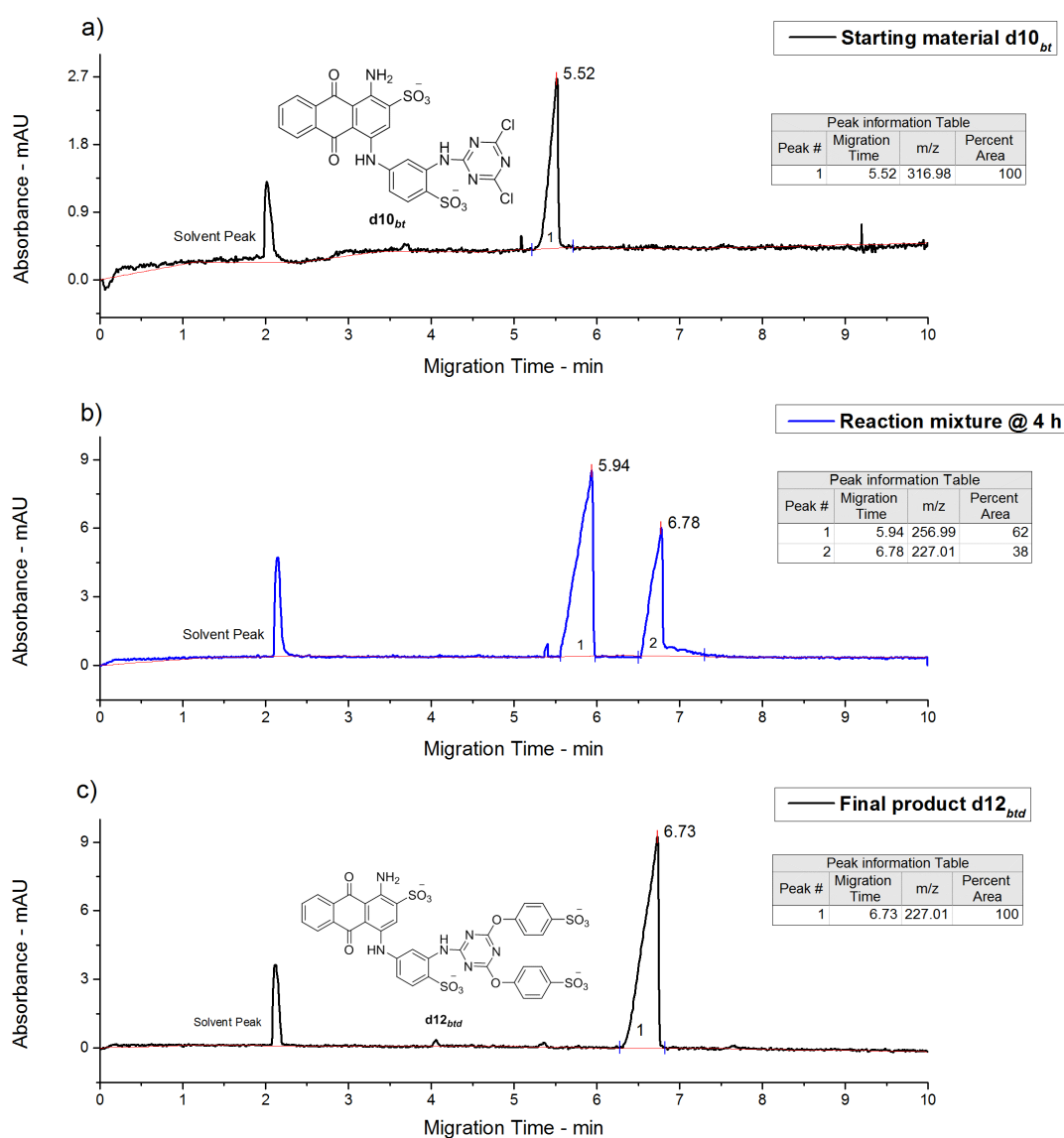


Figure 5.7: Electropherograms showing reaction progress of synthesis of d12_{btd}. (a) blue dichlorotriazine dye d10_{bt}; (b) d11_{btm} – d12_{btd} after 4 hours reaction; (c) Final product d12_{btd}. CZE conditions: same as Figure 5.1

In analytical TLC analysis, the spots appeared as estimated, showing that once the mono substitution was completed, the di substitution started and new more polar blue dye **d12_{btd}** (R_f value 0.65) started to appear on TLC plate. TLC showed that the product of mono substitution **d11_{btm}** was fully converted to the **d12_{btd}** in 4 hours.

In the FT-IR spectrum of the di-substituted dye **d12_{btd}**, Figure 5.8, shows the new peak at 1127 cm^{-1} which can be attributed to the stretching vibration of C–O–C in its structure between the triazine and the 4HBSA. The C–Cl stretching peaks at 1086 and 792 cm^{-1} (Figure 5.4) are no longer present indicating that dichlorotriazine dye **d10_{bt}** has been successfully di-substituted with 4HBSA to yield dye **d12_{btd}**.

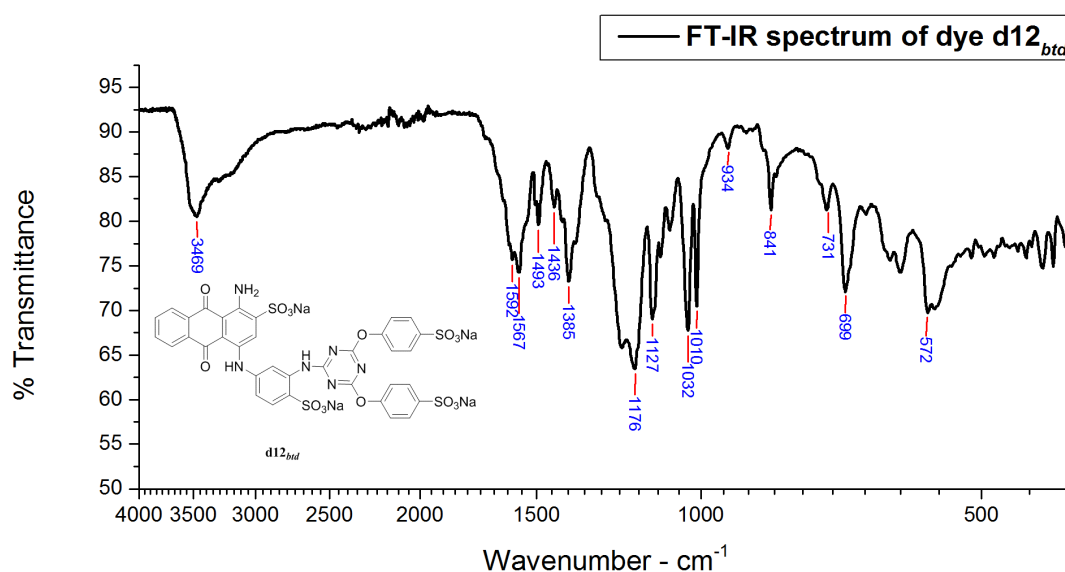


Figure 5.8: FT-IR spectrum of blue di-substituted dye **d12_{btd}**

The detailed analysis of spectrum (Figure 5.8) is as follows ^[3-6]; N–H stretch, 3469 cm^{-1} ; overtone or combinational bands, $2000\text{--}1667\text{ cm}^{-1}$; C=C ring stretch, $1592, 1493, 1436\text{ cm}^{-1}$; triazine stretch, $1567, 1385\text{ cm}^{-1}$; C–O–C stretching, 1127 cm^{-1} ; sulfonate, 1176 cm^{-1} ; in-plane C–H bend, $1032, 1010\text{ cm}^{-1}$; out of plane aromatic C–H bend, 731 cm^{-1} .

Elemental analysis, Found: C, 36.36%; H, 3.20%; N, 7.45%. Calculated for $\text{C}_{35}\text{H}_{20}\text{N}_6\text{Na}_4\text{O}_{16}\text{S}_4 \cdot 8\text{H}_2\text{O}$: C, 36.73%; H, 3.17%; N, 7.34%. The results were adjusted due to the presence of water of crystallisation in the dye molecule. Further disagreement could be attributed to the presence of traces of salt.

5.1.6 Application of Blue Dyes (**d10_{bt}**, **d11_{btm}** and **d12_{btd}**) onto Wool Fabric by Inkjet Printing

The inks were prepared using 5% dye according to the procedure detailed in section 2.5.2, and then viscosity and surface tension of inks were measured.

The resulting ink formulation was then introduced in the cartridge and printed onto wool fabric using HP 6940 deskjet printer. Once printed, the printed wool samples were fixed by three methods detailed in section 2.5.4, and evaluated for percent fixation along with light fastness and wash fastness.

Moreover the inks were also evaluated for stability through CZE over one month storage time at room temperatures.

5.1.7 Characteristics of Formulated Inks (**d10_{bt}**, **d11_{btm}** and **d12_{btd}**)

5.1.7.1 Surface Tension and Viscosity of Inks

As mentioned earlier, in terms of inkjet printing aqueous inks are required to have a surface tension and viscosity of 25 – 60 dynes.cm⁻¹ and 2 – 20 cP respectively ^[8, 91]. It can be seen, from Table 5.1, that blue dichlorotriazine dye **d10_{bt}** and both the modified dyes (**d11_{btm}** and **d12_{btd}**) based inks had a surface tension and viscosity within the operational range.

Table 5.1: Surface tension and viscosity of blue Inks

Ink formulation	Surface Tension (dynes.cm⁻¹)	Viscosity (cP)
d10_{bt} based Ink	44.5	8
d11_{btm} based Ink	43.5	8
d12_{btd} based Ink	43.0	8

5.1.7.2 Stability of Dye (**d10_{bt}**, **d11_{btm}** and **d12_{btd}**) Based Inks

As discussed earlier, dichlorotriazine dyes are susceptible to hydrolysis even in traces of moisture. Therefore, stability of blue dichlorotriazine dye along with new modified dyes in inks were also evaluated.

The results of any change in percent area of peaks of the dyes **d10_{bt}**, **d11_{btm}** and **d12_{bt}** within inks stored at room temperature for one month can be seen in Figure 5.9, Figure 5.10 and Figure 5.11 respectively.

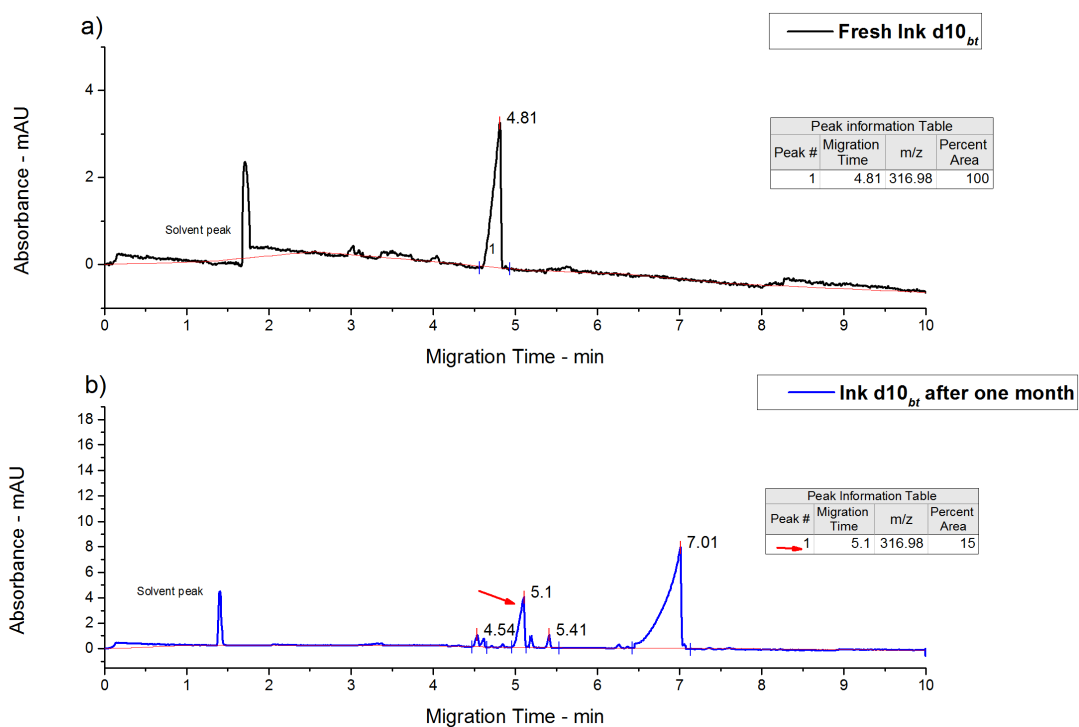


Figure 5.9: Electropherograms showing d10_{bt} based ink stability. (a) Fresh ink; (b) Ink after one month storage at room temperature.

From Figure 5.9, it can be seen that the reactive group of dye molecule underwent hydrolysis under the storage conditions. The percent area of the effective component **d10_{bt}** of the ink was reduced from 100% to 15 % (Figure 5.9b) after one month storage.

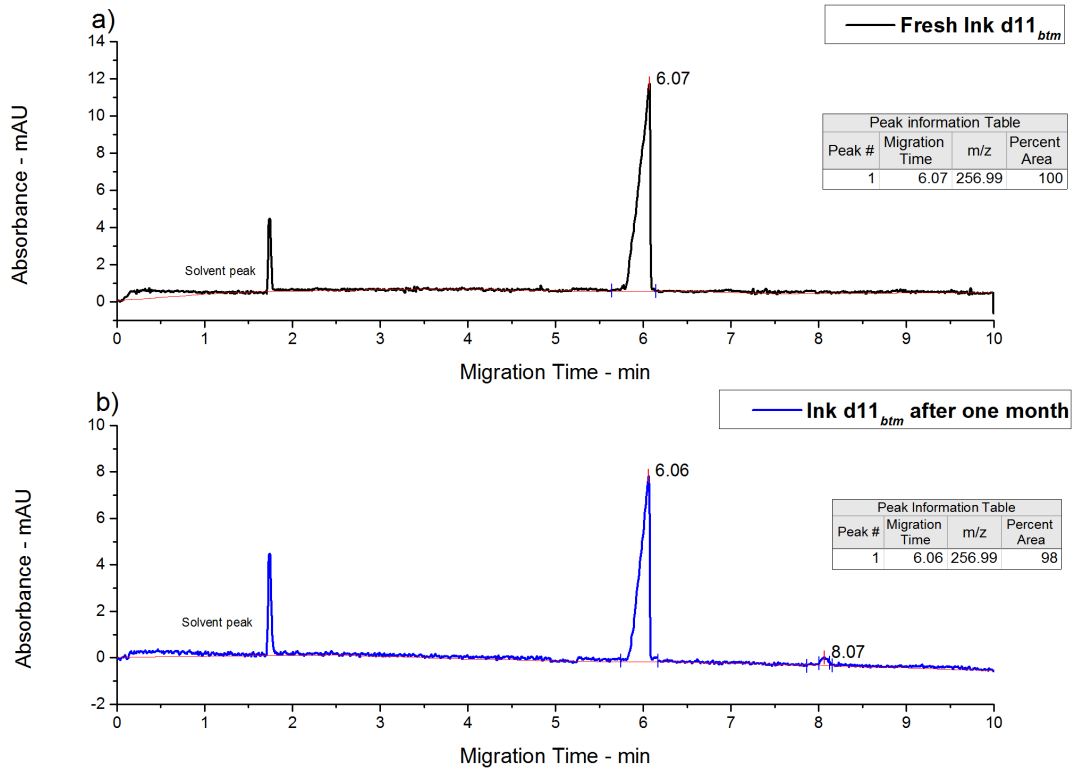


Figure 5.10: Electropherograms showing d11_{btm} based ink stability. (a) Fresh ink; (b) Ink after one month storage at room temperature

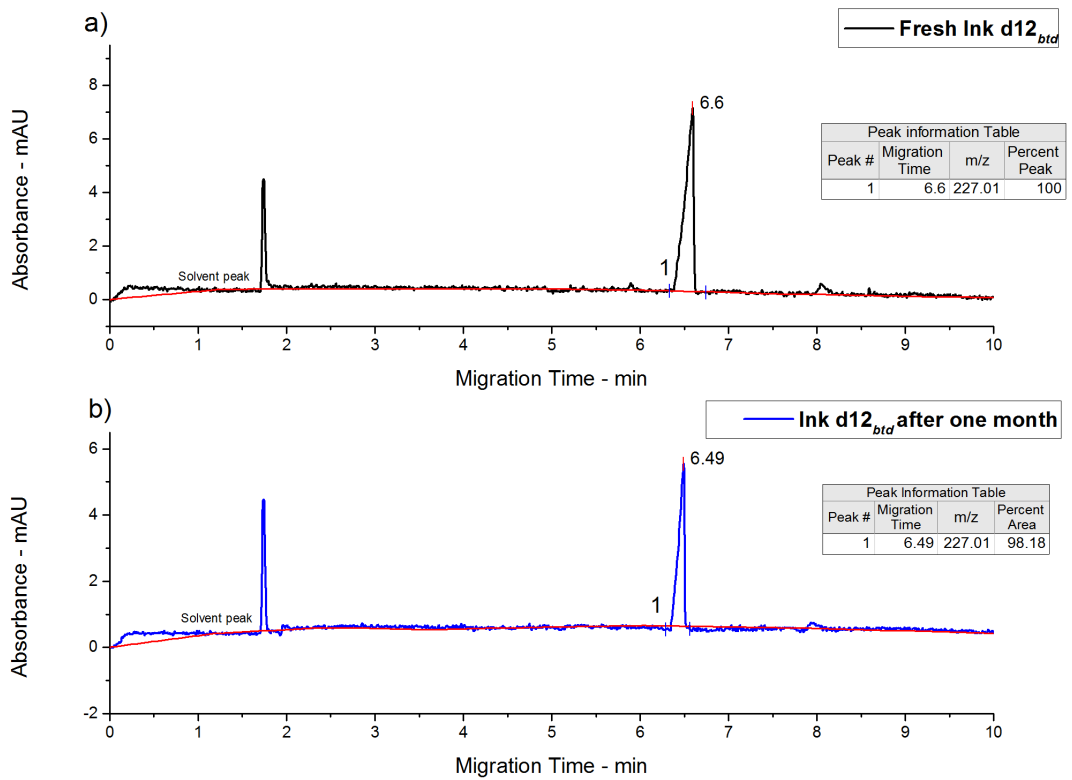


Figure 5.11: Electropherograms showing d12_{btd} based ink stability. (a) Fresh ink; (b) Ink after one month storage at room temperature

As shown in Figure 5.10b and Figure 5.11b, for the blue modified dyes based inks, **d11_{btm}** and **d12_{btd}**, there was no significant change in the percent area of peaks observed in CZE electropherograms.

Thus, modification of blue dichlorotriazine dye by incorporating sulfophenoxy group onto triazine is an effective method of improving the stability of dyes in inks by decreasing the reactivity of highly reactive dichlorotriazine reactive group.

5.1.8 Evaluation of Percent Fixation of Blue Dyes (**d10_{bt}**, **d11_{btm}** and **d12_{btd}**) by Different Fixation Methods

5.1.8.1 Method 1: Batching at Room Temperature

Table 5.2 shows the results obtained by batching the printed samples under moist conditions for 2 and 4 hours at room temperature.

Table 5.2: Percent fixation of d10_{bt}, d11_{btm} and d12_{btd}. Fixation conditions: Batching at RT for 2 and 4 hours under moist conditions

Ink formulation	% Fixation (2 hours)	% Fixation (4 hours)
d10_{bt}	46%	48%
d11_{btm}	54%	68%
d12_{btd}	54%	66%

For the results shown in Table 5.2, it is clear that blue dichlorotriazine dye **d10_{bt}** exhibit low level of fixation, *i.e.*, 48% whereas modified dyes **d11_{btm}** and **d12_{btd}** exhibit marginally better level of fixations 68% and 66% respectively.

Therefore, modification of **d10_{bt}** with sulfophenoxy group proved to be advantageous.

5.1.8.2 Method 2: Batching at 65 °C

Significant improvement in the extent of dye–fibre bond (percent fixation) was observed when the modified blue dyes were applied by a print (Inkjet)–batch technique.

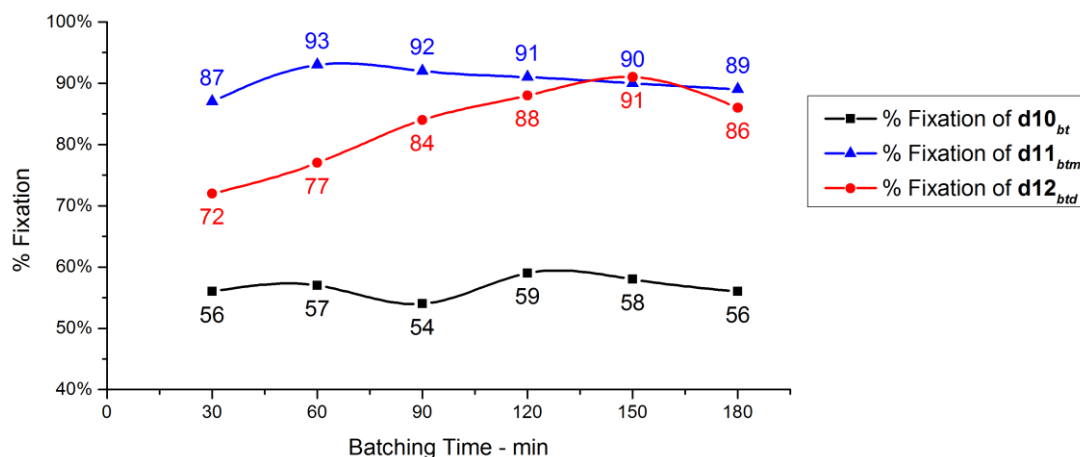


Figure 5.12: Percent fixation of ($d10_{bt}$, $d11_{btm}$ and $d12_{btd}$). Fixation conditions: Batch at 65 °C for 30 to 180 minutes under moist conditions

Figure 5.12 shows the results obtained using $d10_{bt}$, $d11_{btm}$ and $d12_{btd}$ by batching the printed samples under moist conditions for 30 – 180 minutes at 30 minutes interval.

As shown in Figure 5.12, blue dichlorotriazine dye $d10_{bt}$ exhibit low to moderate fixation, *i.e.* 59%. This could be because of its high reactivity and susceptibility towards hydrolysis that one chlorine atom reacts with wool fibre and the other hydrolysed readily under selected conditions.

Moreover, it is also evident from Figure 5.12 that blue modified dyes $d11_{btm}$ and $d12_{btd}$ based inks show remarkable improvement in percent fixation. This could be due to the alteration of leaving group(s) attached to triazine ring which effect the reactivity of the resulting dye and because of the lower reactivity of these dyes they give better fixation at higher temperatures.

It is also evident from Figure 5.10, that mono substituted dye $d11_{btm}$ gave better results initially, however, later di-substituted dye $d12_{btd}$ levelled off the results. It could be due to the better stability of the sulfophenoxy group at the fixation temperature used.

5.1.8.3 Method 3: Steaming

Figure 5.13 shows the effect of steaming on the percent fixation of blue dichlorotriazine and modified dyes printed on the wool fabric.

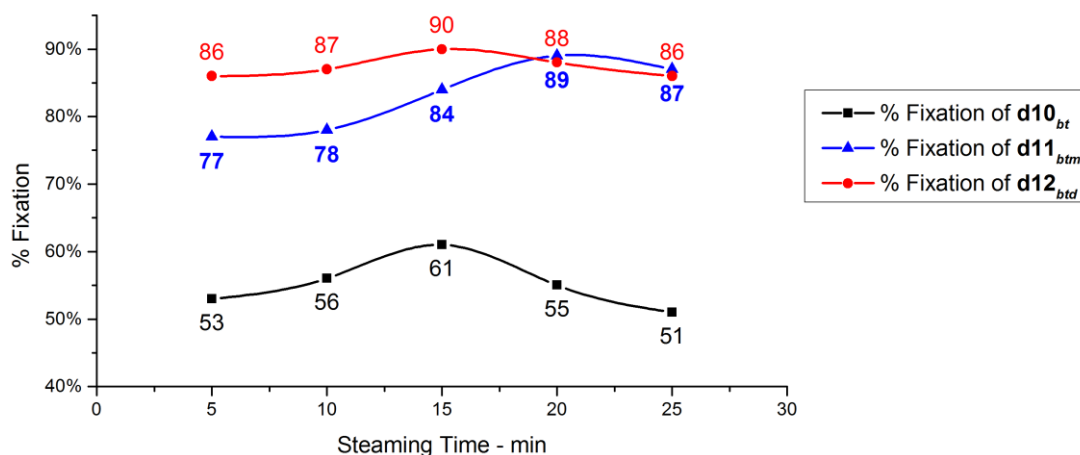


Figure 5.13: Percent fixation of ($d10_{bt}$, $d11_{btm}$ and $d12_{btd}$). Fixation conditions: Steaming for 5, 10, 15, 20 and 25 minutes

As shown in Figure 5.13, significant improvement in percent fixation was observed after blue dichlorotriazine dye was modified with sulfophenoxy group. The highest fixation achieved with blue dichlorotriazine dye $d10_{bt}$ was 61% whereas with mono-substituted dye $d11_{btm}$ it was 89% in 20 minutes and 90% in 15 minutes with di-substituted dye $d12_{btd}$.

5.1.9 Light Fastness

Light fastness testing was carried out according to the BS EN ISO 105-B02:2013 (Method 3) ^[10] detailed in section 2.8.1.

As shown in Table 5.3, modified dyes pass target wool reference 6 whereas blue dichlorotriazine dye failed target wool reference 6. However, it pass then blue wool reference 5.

It is also observed that modified dyes $d11_{btm}$ and $d12_{btd}$ shows even better light fastness than target wool reference 6.

Table 5.3: Light fastness of blue dyes ($d10_{bt}$, $d11_{btm}$ and $d12_{btd}$) compared to target blue wool reference 6

Dye/Ink	Target blue wool reference 6	
$d10_{bt}$	*Less than 6	Unsatisfactory
$d11_{btm}$	Better than 6 (6^+)	Satisfactory
$d12_{btd}$	Better than 6 (6^+)	Satisfactory

*: However, for textile applications light fastness of target wool reference 5 is also satisfactory.

5.1.10 Wash Fastness

Wash fastness was carried out according to the BS ISO 105-C06:2010 ^[11] and the results are shown in Table 5.4. Blue dichlorotriazine dye $d6_{yt}$ showed a small change in shade resulting in a grade 4-5; and also there was light staining on cotton (adjacent fabrics) whereas both the modified dyes $d7_{ytm}$ and $d8_{ytd}$ showed no change in colour or staining, hence, showed excellent wash fastness. This excellent wash fastness is because of the strong covalent bonding between the dye and the wool fibre and also due to the high stability of this bond under washing conditions.

Table 5.4: Wash fastness of blue dyes ($d10_{bt}$, $d11_{btm}$ and $d12_{btd}$)

Dye/Ink	Change in shade	Staining					
		CA	C	N	P	A	W
$d10_{bt}$	4-5	5	4-5	5	5	5	5
$d11_{btm}$	5	5	5	5	5	5	5
$d12_{btd}$	5	5	5	5	5	5	5

CA: Cellulose Acetate; C: Cotton; N: Nylon; P: Polyester; A: Acrylic; W: Wool

5.2 Conclusions

With the aim of designing a series of blue dyes for inkjet inks for wool with lower chemical reactivity, increased solubility and increased stability, one chlorine of cyanuric chloride was displaced by anthraquinone based blue dye chromophore at

0 to 5 °C (pH 5.0 to 7.0) to produce blue dichlorotriazine dye **d10_{bt}** in pure form (without hydrolysed by-products).

Modification of blue dichlorotriazine was done by same sequence as done for magenta and yellow dyes, however, the parameters for modification were optimised.

First modification of blue dichlorotriazine dye was done by displacing the second chlorine atom by sulfophenoxy group at 35 °C (5 hours) to produce heterobifunctional dye **d11_{btm}** in pure form.

Second modification of blue dichlorotriazine dye was done by displacing the second chlorine atom by using two equivalent sulfophenoxy group at 45 °C (2 hours) to produce intermediate dye **d11_{btm}** and then the third chlorine atom as displaced at 80 °C (4 hours) to produce homobifunctional dye **d12_{btm}** in pure form.

The characteristic properties such as surface tension and viscosity of inks formulated by incorporating the synthesised dyes were found to be in operational range.

The stability of modified dyes based inks increased significantly due to the lower reactivity of the modified dyes, which make them ideally suited to inkjet printing processes.

Significant improvement in the extent of covalent dye fixation was observed when the modified blue dyes were applied by inkjet printing and fixed through batching and steaming.

With respect to colour fastness, the blue dichlorotriazine dye was 1.0 grade lower when compared with the modified dye ink prints for light fastness test. Moreover, modified dyes showed excellent wash fastness properties whereas dichlorotriazine dye showed a small change in shade as well as staining on adjacent fabrics (cotton).

5.3 References

1. Patent CN101575456 (2009)
2. Liu, J.L., Luo, H.J. and Wei, C.H. Degradation of anthraquinone dyes by ozone. *Transactions of Nonferrous Metals Society of China*, 2007, **17**, pp.880-886.

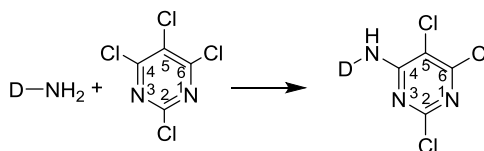
3. Silverstein, R.M., Webster, F.X. and Kiemle, D.J. *Spectrometric Identification of Organic Compounds*. 7th ed. New York: John Wiley and Sons, 2005.
4. Socrates, G. *Infrared and Raman characteristic group frequencies : tables and charts*. Chichester: Wiley, 2001.
5. Matlok, F., Gremlich, H.U., Bruker Analytische Meotechnik and Merck eds. *Merck FT-IR atlas : a collection of FT-IR spectra*. Weinheim: Vch, 1988.
6. Keller, R.J. and Sigma-Aldrich Corporation. *The Sigma library of FT-IR spectra*. Missouri: Sigma Chemical Company, 1986.
7. Beech, W.F. *Fibre-Reactive Dyes* London: Logos Press Ltd., 1970.
8. Magdassi, S. Ink Requirements and Formulations Guidelines. In: S. Magdassi, ed. *Chemistry of Inkjet Inks*. New Jersey: World Scientific Publishing Ltd., 2012.
9. Ujiie, H. *Digital printing of textiles*. Cambridge: Woodhead Publishing Ltd., 2006.
10. British Standards Institution. *Colour fastness to artificial light: Xenon arc fading lamp test*, ISO 105-B02:2013.
11. British Standards Institution. *Textiles - Tests for colour fastness - Part C06: Colour fastness to domestic and commercial laundering*, BS EN ISO 105-C06:2010.

6 Synthesis, Modification, Characterisation of Magenta Trichloropyrimidine Dyes and Their Application onto Wool Fabric by Inkjet Printing

6.1 Introduction

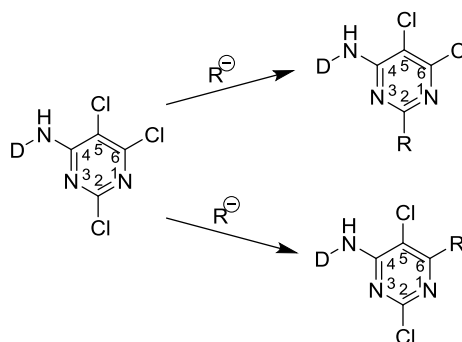
As discussed in Chapter 1, pyrimidine is technically the most important heterocyclic carrier system in addition to triazine. Depending on the leaving groups, substituents and bridging group, pyrimidine permits wider range of variations with regard to the required properties in application (reactivity, ease of washing-off and fastness properties) as compared to triazine ^[1]. Pyrimidines bearing halogen substituents at activated positions 2, 4, and 6 are the cornerstone to diverse modifications of the pyrimidine ring. The polyhalogenated pyrimidine compounds undergo regioselective and stepwise substitutions with common nucleophiles such as amines ^[2]. Thus, Geigy and Sandoz claimed almost simultaneously water-soluble trichloropyrimidine dyes in 1959 and marketed them together under the trade names Reactone (Geigy) and Drimaren (Sandoz). This technically important group of dyes are slightly less reactive than monochlorotriazine dyes and also because of ease of removal of unfixed dye and the high stability of the paste this group is well suited for textile printing ^[3,4].

It was at one time thought possible that the comparatively high solubility and low substantivity of chloropyrimidine dyes might be associated with isomer formation during condensation of polychloropyrimidines with amino chromophores; however, Ackermann and Dussy ^[5] found that in the condensation with the bridging group of the dye chromophore, replacement of the chlorine atom in the 4-position occurs exclusively (see Scheme 6.1). For this reason they are synthesised in this study as compounds in which the amino group of the dye chromophore becomes attached to the 4-position of the pyrimidine ring.



Scheme 6.1: Condensation of 2,4,5,6-tetrachloropyrimidine with dye chromophore ^[6]

Ackermann and Dussy also found that any further substitution of 4-aminotrichloropyrimidine produces 2 or 6 substituted pyrimidines (See Scheme 6.2) ^[6].



Scheme 6.2: Substitution of 2,5,6-trichloropyrimidine dye ^[6]

Furthermore, on account of their low reactivity, chloropyrimidine react less readily with amines than do the corresponding chlorotriazines, and this restricts the methods available for preparing some dyes of pyrimidine series. Thus, the substitution of tetrachloropyrimidine with the amino-containing chromophore is much more difficult than the cyanuric chloride which is analogue in the triazine series and generally requires vigorous reaction conditions such as high temperatures and long reaction times (hours or days). Moreover, the reaction is difficult to bring to completion and suffers from mostly poor yield ^[4].

According to the literature ^[5, 7-10], two synthesis routes were used for the preparation of trichloropyrimidine dyes.

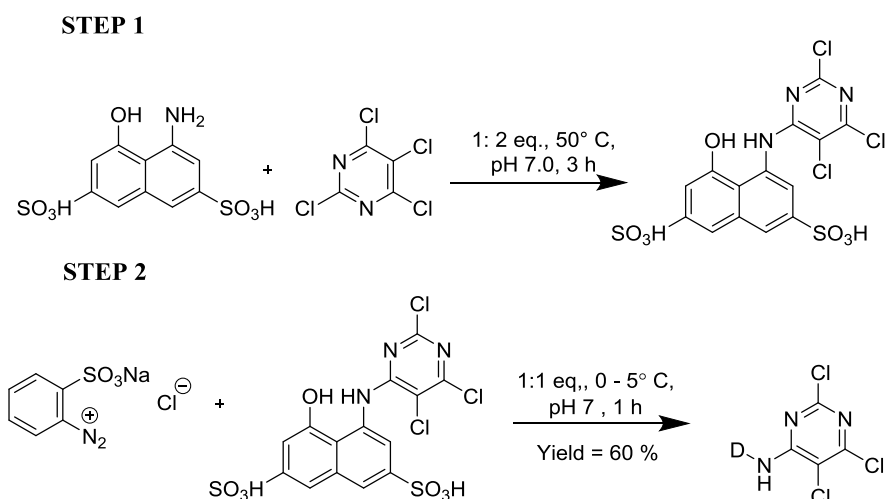
6.1.1 Synthesis Route 1

Ackermann and Dussy ^[5] dissolve equimolar amount of reactants in a mixture of equal volumes of water and acetone and added alkali to maintain the pH at 6.0 to 7.0 and the reaction mixture was subsequently heated to 50 °C. However, the

described synthesis did not report the percent conversion to product nor the yield of the product. The reaction is shown in Scheme 6.1.

6.1.2 Synthesis Route 2

In another approach [4, 7-9], it is recommended to react chloropyrimidine group with one of the components prior to azo coupling. The suggested synthesis route is shown in Scheme 6.3.



Scheme 6.3: Route 2 for the synthesis of trichloropyrimidine dyes [7]

In this study, initially both the published approaches were investigated for reacting tetrachloropyrimidine with amino chromophore to synthesis a series of *magenta*, *yellow* and *blue* dyes as outlined in Scheme 6.1 and Scheme 6.3. In many cases, no products or only poor yields could be obtained with significant amount to by-product even for prolonged reaction times (days).

In comparison to the conventional methods, route 1 appeared to be superior over route 2. Therefore, after six failed attempts route 2 was not investigated further. Nevertheless, not only the route 2 but also route 1, despite its superiority is still unsatisfactory.

Recently, microwave irradiated synthesis has emerged as an efficient tool in organic synthesis, and its benefits are well documented [11] and has previously been mentioned in Chapter 2. In a number of studies, it has been shown that microwave-irradiated synthesis can circumvent the need of prolong heating and it generally accelerates the rate of chemical reactions often with increased yields [12]. The use of

microwave irradiation for the formation of carbon-carbon, carbon-oxygen as well as carbon-nitrogen has been successfully demonstrated ^[13].

Thus, in this study, it was expected that microwave irradiation could improve the condensation reaction of 2,4,5,6-tetrachloropyrimidine with amino chromophore. Moreover, substitution reaction of synthesised trichloropyrimidine dyes by 4HBSA can also be done.

Therefore, microwave-irradiated synthesis, a novel strategy for the preparation of the target dyes *magenta* trichloropyrimidine **d13_{mp}**, *blue* trichloropyrimidine dye **d15_{bp}**, *yellow* trichloropyrimidine dye **d17_{yp}** was developed which resulted in high yields of products along with high percent conversion and shorter reaction times.

After the successful syntheses of parent trichloropyrimidine dyes (*magenta* **d13_{mp}**, *blue* **d15_{bp}** and *yellow* **d17_{yp}**), modification of these dyes with sulfophenoxy group was also investigated, initially, with conventional heating method. However, these trials were completely failed in terms of achieving satisfactory yields of products. Later, microwave-irradiated method was used which results in high yields along with shorter reaction times.

This chapter details the synthesis, modification and characterisation of magenta dyes based on the pyrimidine reactive group by the conventional heating method as well as microwave irradiation and the results were evaluated.

Moreover, the synthesised magenta parent and specially modified reactive dye were applied to wool fabric through inkjet printing in order to evaluate their percent fixation, stability of inks along with colour fastness (light and wash) properties.

6.2 Experimental

6.2.1 Materials

Magenta dye chromophore **d1_m** (100%); 2,4,5,6-tetrachloropyrimidine (97%), sodium 4-hydroxybenzenesulfonate dihydrate (98%), sodium bisulfite, carboxymethyl cellulose, polysorbate 20 (Tween 20) and N-methylmorpholine N-oxide (NMMO) were purchased from Sigma-Aldrich and used as received. Urea (MP Biomedicals), Alcopol O 60 (Acros organics), 2-pyrrolidone (Acros organics), 2-propanol (Fisher), Sandozin NIE (Clariant) were also purchased and used as received.

6.2.2 Conventional Heating Methods for the Synthesis of Magenta 5-[(2,5,6-trichloro-4-pyrimidinyl)amino]-4-Hydroxy-3-[(2-sulfophenyl)azo]-2,7-Naphthalenedisulfonic Acid Dye ($d13_{mp}$)

6.2.2.1 Conventional Heating Method (Route 1)

In accordance with the literature ^[5, 10], amino based dye chromophore $d1_m$ was dissolved in water and adjusted to the pH 6.0 to 7.0 by the addition to 2N hydrochloric acid at 35 °C. A solution of investigated molar ratio of 2,4,5,6-tetrachloropyrimidine in acetone was added as thin stream to the dye chromophore solution. The reaction mixture was refluxed to the investigated temperature and percent conversion were monitored through CZE. The percent conversion can be obtained from percent area of target dye on the CZE electropherogram.

The target magenta trichloropyrimidine dye was synthesised using a molar ratio of 1:1 and 1:2 at a temperature range of 50, 60, 70, 85 and 100 °C.

6.2.2.2 Conventional Heating Method (Route 2)

In accordance with the literature ^[7], 5-amino-4-naphthol-2,7-disulphonic acid (H-acid) (4 g, 0.011 mol, 1 eq.) was dissolved in water (50 cm³) and acetone (37.5 cm³) at 50 °C and the pH adjusted to 7 with 2N sodium hydroxide. 2,4,5,6-tetrachloropyrimidine (5 g, 0.02 mol, 2 eq.) in acetone (12.5 cm³) was added dropwise and the solution was stirred under reflux at 50 °C for three hours. The pH was maintained between 6 and 8 by addition of 2N sodium hydroxide and the reaction is monitored through CZE. The product was precipitated by pouring the solution into acetone, and filtered.

However, after six unsuccessful attempts conventional heating method (route 2) was not attempted further.

6.2.3 Investigation of Conventional Heating Method (Route 1) for the Synthesis of Magenta Trichloropyrimidine Dye ($d13_{mp}$)

6.2.3.1 Percent Conversion to $d13_{mp}$ Under Various Temperature

The percent conversion of $d1_m$ to yield $d13_{mp}$ at temperatures 50, 60, 70, 85 and 100 °C were investigated provided that the reactants were used in equal molar ratios (1:1) and pH of reaction mixture was maintained at 6.0 to 7.0 throughout with

2N sodium carbonate solution. The reactions were stirred until the pH had stabilised (50 hours) and prolonged reaction times did not have any effect on percent conversion to **d13_{mp}**. The reactions were monitored through CZE.

The percent conversion to magenta dye **d13_{mp}** achieved at different temperatures are shown in Figure 6.1 and isolated yields are listed in Table 6.1.

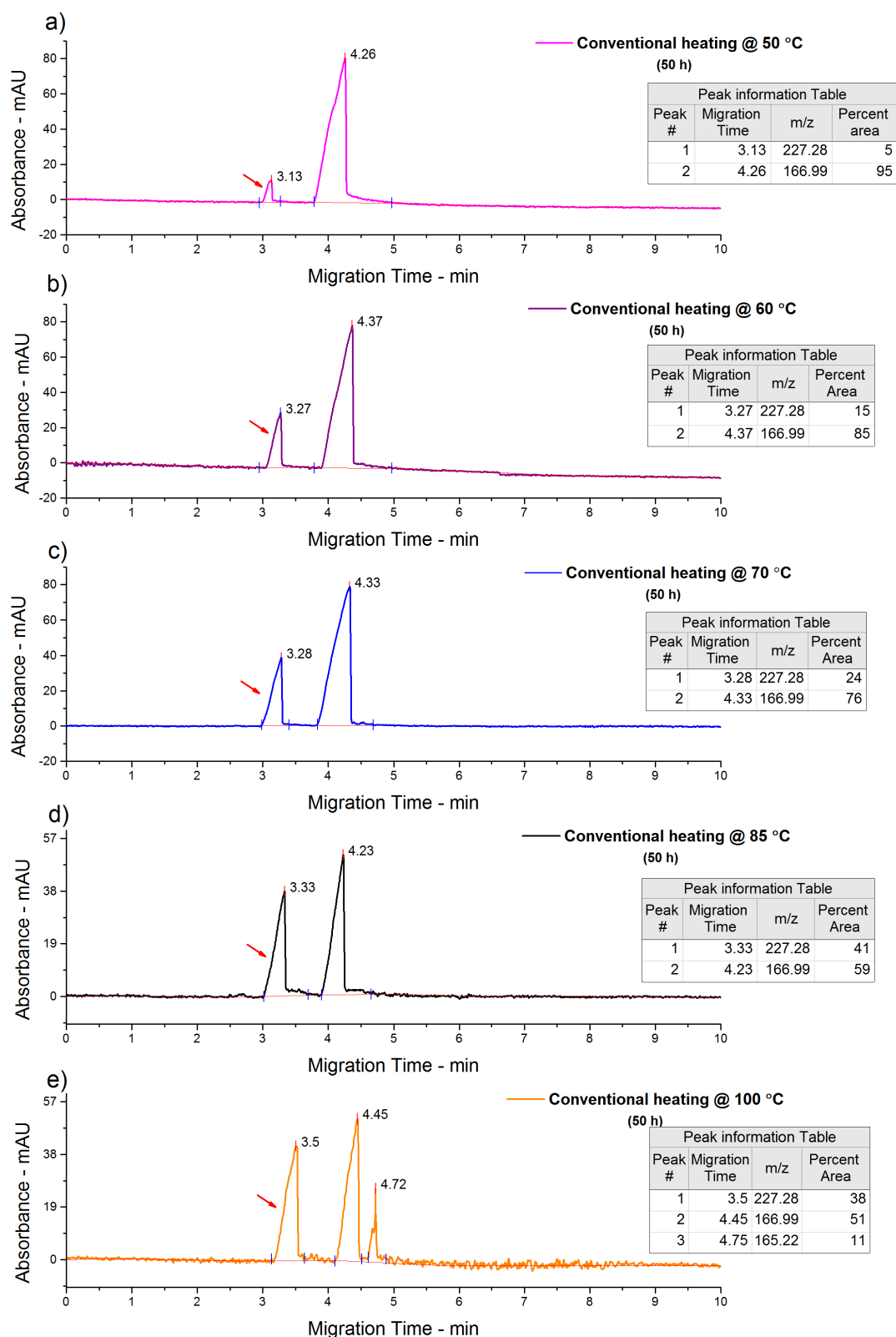


Figure 6.1: Electropherograms showing conversion of reactants to d13_{mp} using conventional heating method (route 1) at; (a) 50 °C; (b) 60 °C; (c) 70 °C; (d) 85 °C; (e) 100 °C. CZE conditions: running buffer, 6mM potassium dihydrogen phosphate and acetonitrile (10% v/v) pH 9.0; pressure injection 0.5 psi for 10 s; voltage 25 kV; detection at 542 nm.

When an initial reaction was performed under literature conditions ^[5] (1:1 eq., Na₂CO₃, pH 6.0 to 7.0, water–acetone, 50 °C) to first establish the conversion to product at a reaction time of 50 hours, poor conversion (5%) was seen (Figure 6.1a, peak 1; Table 6.1, entry 1).

Table 6.1: Summary of results with conventional heating (route 1) at various temperatures

Entry	Parameters	Time (hours)	Conversion ^a (%)	Yield (%)
1	1:1 eq., Na ₂ CO ₃ , pH 6.0 – 7.0, water–acetone, 50 °C ^[5]	50	5	*
2	1:1 eq., Na ₂ CO ₃ , pH 6.0 – 7.0, water–acetone, 60 °C	50	15	*
3	1:1 eq., Na ₂ CO ₃ , pH 6.0 – 7.0, water–acetone, 70 °C ^[10]	50	24	6
4	1:1 eq., Na ₂ CO ₃ , pH 6.0 – 7.0, water–acetone, 85 °C	50	41	13
5	1:1 eq., Na ₂ CO ₃ , pH 6.0 – 7.0, water–acetone, 100 °C	50	38 _b	15 _c

^a: Determined by CZE analysis; ^b: significant amount of by-product; ^c: isolated **d13_{mp}** not pure; *: Dye **d13_{mp}** was not isolated from the reaction mixture due to low percent conversion

Adjustments of 10 – 15 °C per run provide a way to identify the optimal reaction temperature of a conventional reaction. The percent conversion was seen to increase as higher temperatures were screened as it accelerates the rate of reaction (Figure 6.1 b, c, and d; Table 6.1, entries 2, 3 and 4) until significant amounts of an by-product appeared in the CZE electropherogram of entry 5 (Figure 6.1e).

The reactions were carried out by conventional heating at a range of temperatures, but the reactions generally proceeded sluggishly. Therefore, it is concluded that by using conventional heating method (route 1) for the synthesis of magenta trichloropyrimidine dye **d13_{mp}**, the maximum percent conversion to the product was 41% at 85 °C in 50 hours giving a poor yield of 13%.

6.2.3.2 Percent Conversion to **d13_{mp}** Under Different Molar Ratio

The percent conversion of **d1_m** to yield **d13_{mp}** using 1:1 and 1:2 molar ratio at 85 °C were investigated provided that the pH of the reaction mixture was maintained at 6.0 to 7.0 throughout with 2N sodium carbonate solution. The reactions were

stirred until the pH had stabilised and prolonged reaction times did not have any effect on percent conversion to **d13_{mp}**. The reactions were monitored through CZE.

The percent conversions achieved are shown in Figure 6.2 and isolated yields are listed in Table 6.2.

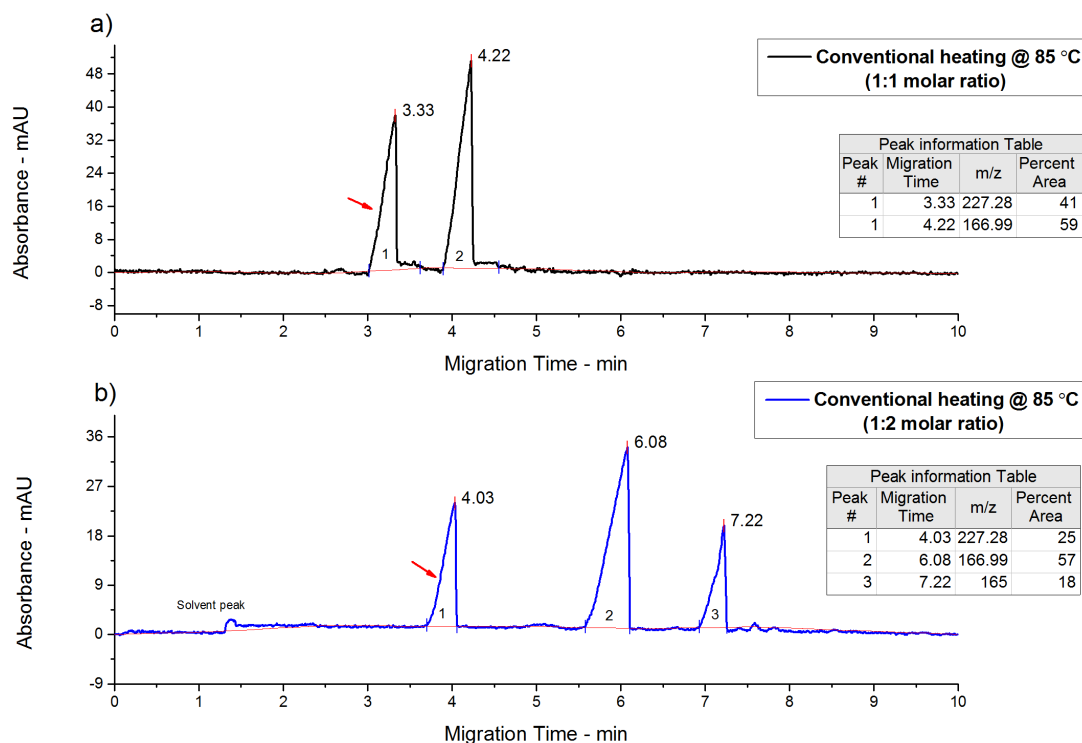


Figure 6.2: Electropherograms showing conversion of reactants to **d13_{mp}** using conventional heating method (route 1); (a) 1:1 molar ratio; (b) 1:2 molar ratio. CZE conditions: same as Figure 6.1.

Table 6.2: Summary of results from conventional heating (route 1) at different molar ratios

Entry	Parameters	Time (hours)	Conversion ^a (%)	Yield (%)
1	1:1 eq., Na ₂ CO ₃ , pH 6.0 – 7.0, water–acetone, 85 °C	50	41	13
2	1:2 eq., Na ₂ CO ₃ , pH 6.0 – 7.0, water–acetone, 85 °C	18	25	8 _b

^a: Determined by CZE analysis; _b: isolated **d13_{mp}** not pure

As shown in Figure 6.2, when reactants are used in equal moles, percent conversion of 41% was achieved at 85 °C in 50 hours. However, when the molar ratio of 1:2 was used the rate of reaction accelerated, though after 18 hours of reaction the product begins to hydrolyse (Figure 6.2b). Therefore, increasing the

molar ratio does not prove beneficial in the synthesis of **d13_{mp}** under the reaction conditions adopted.

The reaction conditions for the synthesis of **d13_{mp}** using conventional heating method (route 1) were investigated in detail and concluded that the current conventional heating method for the synthesis of **d13_{mp}** gave a poor yield of only 13%. Therefore, the documented conventional heating methods for the synthesis of **d13_{mp}** are unsatisfactory and insufficient.

6.2.4 Optimisation of Microwave-Irradiated Synthesis of Dye d13_{mp}

For the optimisation of microwave-irradiated synthesis, the reaction should initially run with the conditions used for conventional synthesis. However, if the reaction is not successful, a change in temperature and reaction time is recommended. Moreover, other conditions for example solvent and reagents can also be varied when appropriate.

For this study, an initial reaction was performed under literature conditions [1:1 eq., Na₂CO₃ (1 eq.), water–acetone, 50 °C; Table 6.3, entry 1] to first establish the conversion to product at a typical microwave reaction conditions. Poor conversion (9%) was seen at literature temperature (Table 6.3, entry 1; Figure 6.3a), and no pressure increase was noted as the reaction proceeded.

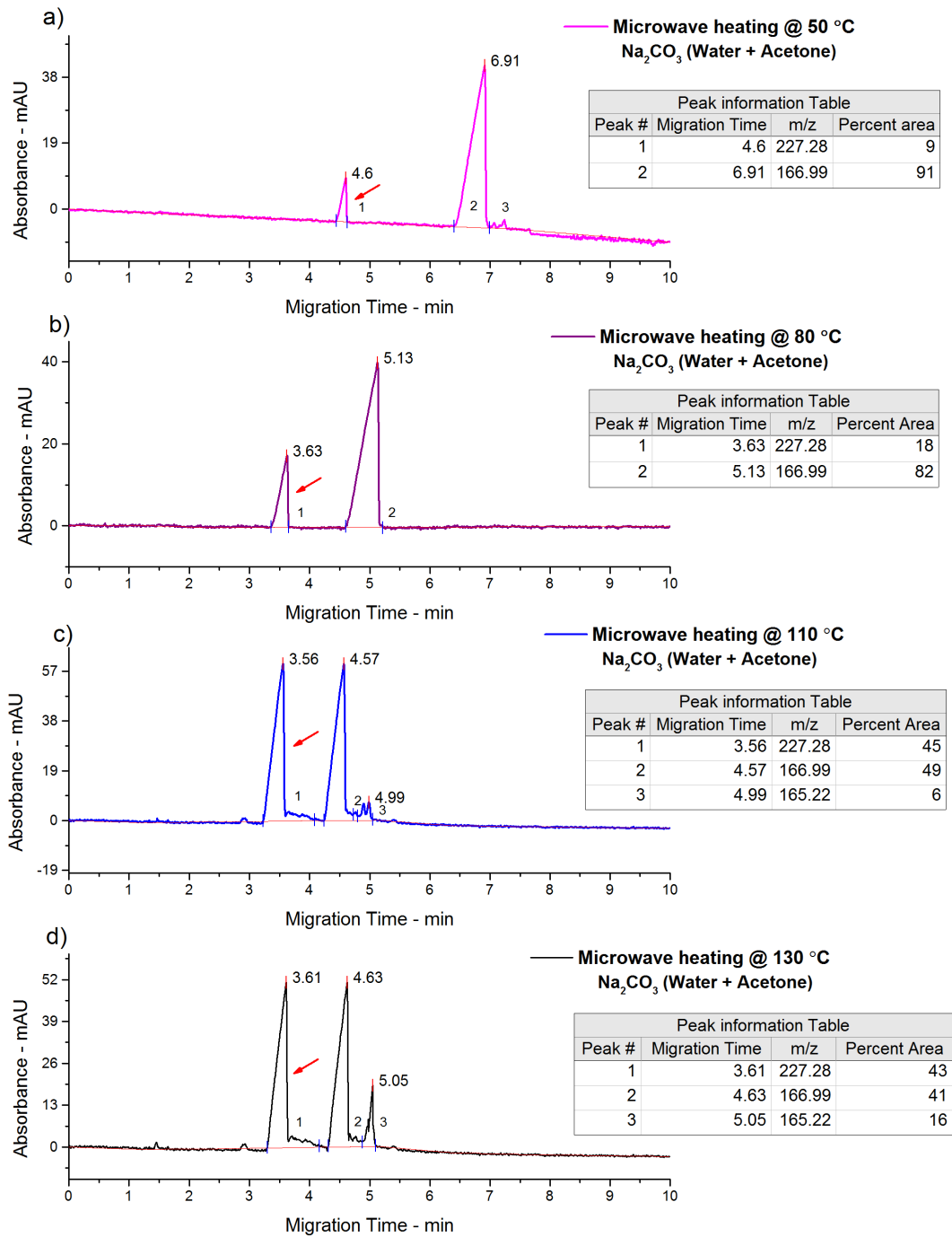


Figure 6.3: Electropherograms showing conversion of reactants to $d13_{mp}$ using microwave irradiation at; (a) 50 °C; (b) 80 °C; (c) 110 °C; (d) 130 °C. CZE conditions: same as Figure 6.1.

Table 6.3: Optimisation of reaction temperature for microwave-irradiated condensation reaction

Entry	Solvent	Alkali	Temperature (°C)	Time (hours)	Conversion (%)
1	Water–Acetone	Na ₂ CO ₃	50	8	9
2	Water–Acetone	Na ₂ CO ₃	80	8	18
3	Water–Acetone	Na ₂ CO ₃	110	10	45 _a
4	Water–Acetone	Na ₂ CO ₃	130	10	43 _a

a: significant amount of hydrolysed dye (by-product)

Adjustments of 20 - 40 °C per run provide an efficient way to identify the optimal reaction temperature of a microwave-irradiated reaction. The percent conversion was seen to increase as higher temperatures were screened (entries 2, 3) until significant amounts of hydrolysed by-product appeared in the CZE electropherograms of entry 3 and 4 (Figure 6.3c and Figure 6.3d). However, it is evident from Figure 6.3 and Table 6.3 that microwave irradiation is advantageous for the synthesis of trichloropyrimidine dyes but needs further optimisation of conditions to minimise side reactions, such as hydrolysis.

Since the hydrolysis of halogenated pyrimidines in water is fairly easy, there are two competing reactions in the synthesis of trichloropyrimidine dyes; (1) the condensation reaction with the amino group of dye chromophore and (2) the formation of hydroxyl substituted pyrimidine by-product by nucleophilic displacement of chlorine with water.

A thorough search of the patent literature yielded hints that during the course of the reaction of chloropyrimidine and amino chromophore the reaction turn acidic due to the formation of hydrogen chloride, therefore, use of buffer ^[14, 15] (sodium phosphate buffer) might be advantageous to control the pH of reaction mixture and to avoid or minimise side reactions, i.e. hydrolysis of halogen.

Furthermore, Mueller and Baqi ^[16] patented microwave irradiated synthesis of anilinoanthraquinone derivatives in the presence of different mixtures of phosphate buffer (neutral to basic) as a solvent system and they concluded that the reaction went to completion with excellent yields.

Therefore, a new set of reactions were performed using sodium phosphate buffer [Na_2HPO_4 (0.20 M, 2 ml) and NaH_2PO_4 (0.12 M, 8 ml), pH 7.0] instead of sodium carbonate at 130 and 100 °C, because acidic to neutral pH conditions are recommended for the condensation reaction of tetrachloropyrimidine with amino group [5, 7, 8, 10]. The percent conversion to magenta dye **d13_{mp}** achieved at different temperatures are shown in Figure 6.4 (peak 1), and isolated yields are listed in Table 6.1.

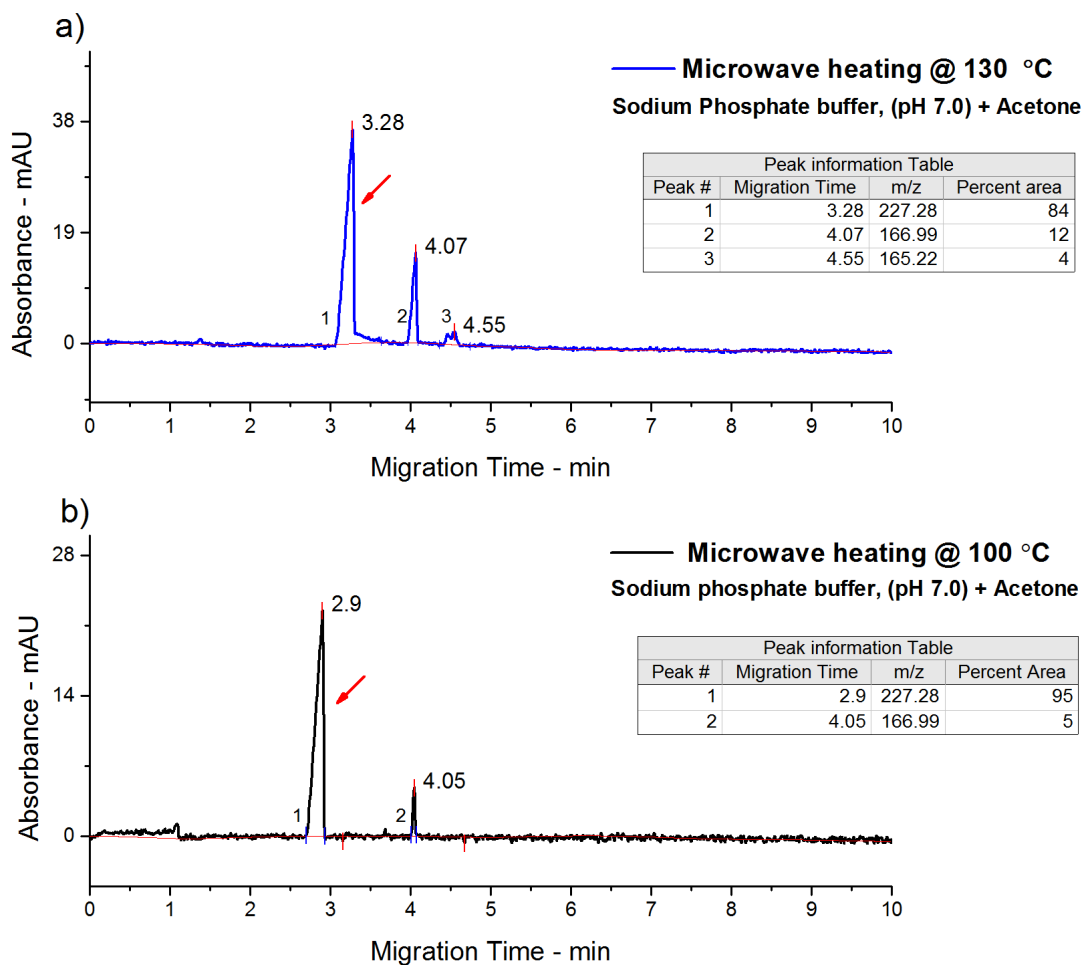


Figure 6.4: Electropherograms showing conversion of reactants to d13_{mp} using microwave-irradiated method (sodium phosphate buffer, pH 7.0); (a) 130 °C; (b) 100 °C. CZE conditions: same as Figure 6.1

Table 6.4: Modification of reaction conditions for microwave irradiated condensation reaction

Entry	Solvent (equal volumes)	Temperature (°C)	Time (hours)	Conversion (%)
1	Sodium phosphate buffer pH (7.0) –Acetone	130	2	84 _a [63 _c] ^b
2	Sodium phosphate buffer pH (7.0) –Acetone	100	4	95 [83] ^b

_a: hydrolysed dye (by-product); _b: isolated yield; _c: isolated **d13_{mp}** not pure.

Although the conversion to **d13_{mp}** was 84% at 130 °C in 2 hours, however, only 63% yield of expected product was gained, which possibly suggested that higher temperature might result in more by-products. Therefore, decreasing the reaction temperature to 100 °C and increasing the time to 4 hours resulted in both a significant increase in the initial rate of reaction and in the overall conversion of 95% with a pure 83% yield.

The microwave irradiation condensation of tetrachloropyrimidine with amino chromophore worked very well with aqueous sodium phosphate buffer and acetone at moderate temperature (100 °C), yielding the desired magenta trichloropyrimidine dye **d13_{mp}** in more than 80% yield. The desired dye **d13_{mp}** was formed almost exclusively, and only traces of **d1_m** were detected with CZE (Figure 6.4b). The product was isolated by salting-out with sodium chloride (10% v/v) at 55 °C.

6.2.5 Comparative Study of Conventional and Microwave-Irradiated Synthesis of Dye **d13_{mp}**

As shown in Figure 6.5, microwave-irradiated reaction was completed in only 4 hours with a dramatic increase in the rate of reaction and conversion of reactants to **d13_{mp}** in comparison to conventional heating which takes 50 hours until only 41% conversion and resulted with a significant amount of hydrolysed by-product.

Moreover, dye **d13_{mp}** of high purity was obtained in excellent yield of 83% with microwave irradiated synthesis, whereas, a poor yield of 13% was achieved with conventional heating method.

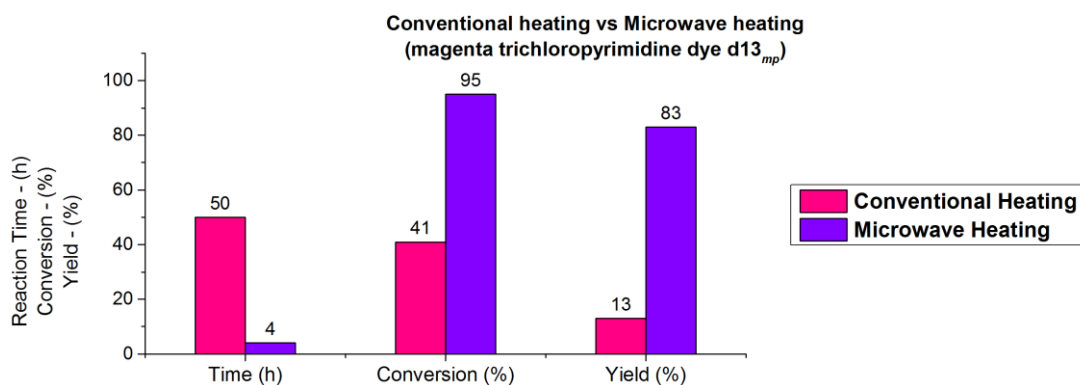


Figure 6.5: Comparison of reaction times, conversions and yields obtained by conventional heating and microwave irradiation (d13_{mp}**)**

This enhancement in the rate of reaction, conversion to product and high yield is due to higher microwave temperatures as high microwave temperatures have led to reaction times up to three orders of magnitude shorter than those for the same preparations carried out conventionally ^[17].

This is because, with conventional heating, reactants are slowly activated by external heat source which passes first through the walls of the vessel in order to reach the solvent and reactants. This is a slow and inefficient method for transferring energy into the reacting system. Whereas, in the microwave irradiation, microwaves couple directly with the molecules of the entire reaction mixture, leading to a rapid rise in temperature. Since the process is not limited by the thermal conductivity of the vessel, the result is an instantaneous localised superheating of any substance that will respond to either dipole rotation or ionic conduction.

Moreover, in conventional heating due to the developed temperature gradient and localised overheating the product, reactants or reagent can be decomposed.

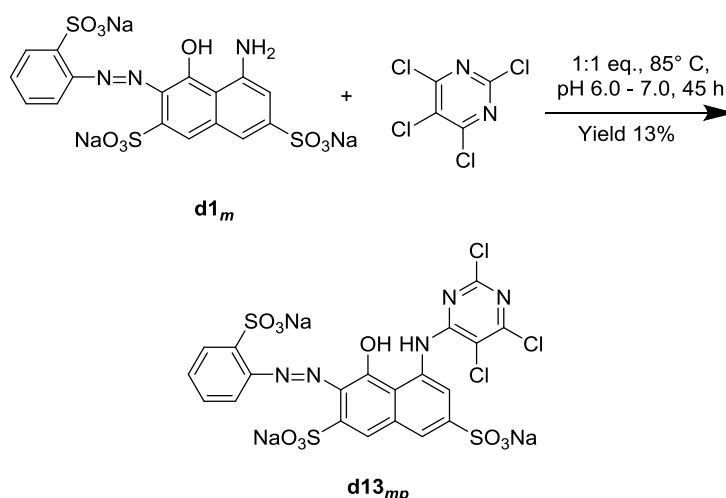
Therefore, in this study the novel, fast, efficient, and high-yielding procedure for the synthesis of magenta trichloropyrimidine dye **d13_{mp}** was developed, which is superior to previously published methods in all aspects, including yields, reaction time, and versatility.

6.2.6 Synthesis of Magenta 5-[(2,5,6-Trichloro-4-pyrimidinyl)amino]-4-Hydroxy-3-[(2-sulfophenyl)azo]-2,7-Naphthalenedisulfonic Acid Dye (**d13_{mp}**)

6.2.6.1 Optimised Conventional Heating Method (Route 1)

In accordance with optimised synthesis parameters discussed in section 6.2.3.1 and 6.2.3.2, magenta dye chromophore **d1_m** (11.39 g, 0.02 mol, 1 eq.) was dissolved in water (100 cm³) which was adjusted to pH 7.0 by the addition of 2N hydrochloric acid solution at 35 °C. A solution of 2,4,5,6-tetrachloropyrimidine (4.34 g, 0.02 mol, 1 eq.) in acetone (100 cm³) was added as thin stream to the dye **d1_m** solution. Once the addition of tetrachloropyrimidine was complete, the reaction mixture was stirred and the pH was maintained at 6.0–7.0 by the addition of 2N sodium carbonate solution, while the temperature was raised and maintained at 85 °C (reflux). The reaction was stirred for further 50 hours (until the pH had stabilised) and was monitored with CZE and analytical TLC. When CZE and TLC show no more conversion of **d1_m** to **d13_{mp}**, 2N sodium carbonate solution was added to raise the pH to 7.0 and sodium chloride (8% w/v) was added to precipitate the dye. The reaction mixture was filtered hot (55 °C) and the crude dye was collected and was washed with brine (2 × 100 cm³) and dried *in vacuo* (40 °C, 12 hours).

Purification of crude dye **d13_{mp}** using solvent-nonsolvent technique (1:2, DMF–Acetone) afforded the pure dye **d13_{mp}** (0.82 g, 1.09 mmol, yield 13%) as magenta powder. The reaction is shown in Scheme 6.4.



Scheme 6.4: Condensation of tetrachloropyrimidine with magenta dye chromophore **d1_m to yield **d13_{mp}** by conventional heating method**

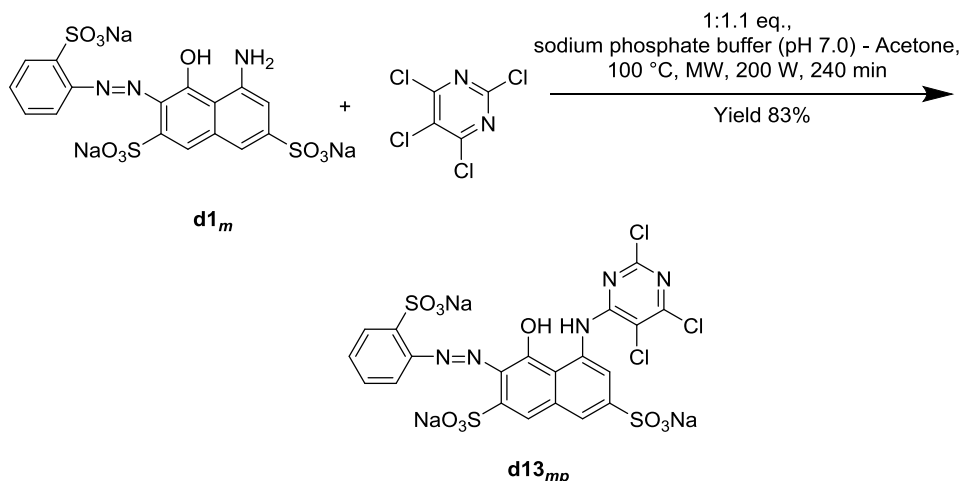
6.2.6.2 Optimised Microwave-Irradiated Method

Magenta dye chromophore **d1_m** (0.569 g, 1 mmol, 1 eq.) and 2,4,5,6-tetrachloropyrimidine (0.238 g, 1.1 mmol, 1.1 eq.) were added to each of the ten 35 ml microwave reaction vials equipped with a magnetic stirring bars followed by addition of 10 ml of sodium phosphate buffer [Na_2HPO_4 (0.20 M, 2 ml) and NaH_2PO_4 (0.12 M, 8 ml), pH 7.0] and 10 ml of acetone.

The mixtures were capped and irradiated in the microwave oven (200 W) for 4 hours at 100 °C. Then the reaction mixture were transferred from the vials to a beaker and sodium chloride (8% w/v) was added to precipitate the dye. The reaction mixture was filtered hot (55 °C) and the crude dye was collected and was washed with brine ($2 \times 100 \text{ cm}^3$) and dried *in vacuo* (40 °C, 12 hours).

Purification of crude dye **d13_{mp}** using solvent-nonsolvent technique (1:2, DMF–Acetone) afforded the pure dye **d13_{mp}** (5.91 g, 7.87 mmol, yield 83%) as magenta powder.

FT-IR analysis was conducted to confirm the presence of main functional groups in dye **d13_{mp}**. The reaction is shown in Scheme 6.5.



Scheme 6.5: Condensation of tetrachloropyrimidine with magenta dye chromophore **d1_m to yield **d13_{mp}** by microwave-irradiated method**

6.2.6.3 Characterisation of Magenta 5-[(2,5,6-Trichloro-4-pyrimidinyl)amino]-4-Hydroxy-3-[(2-Sulfophenyl)azo]-2,7-Naphthalenedisulfonic Acid Dye (**d13_{mp}**)

The electropherograms (Figure 6.6) showing the progression of synthesis reaction of **d13_{mp}** with microwave irradiations. The peaks observed were as expected (Figure 6.6b); the first peak to emerge was **d13_{mp}** (2.9 min) which has the higher mass to charge ratio of the two analytes. This occurs because the addition of the pyrimidine group on to the dye chromophore **d1_m** increases the molecular weight of the dye **d13_{mp}** without any additional sulfonic acid groups that would increase the negative charge.

Moreover, the percent area of the **d13_{mp}** shown in Figure 6.6c, was 100% which indicates that there was no hydrolysed dye in the final product.

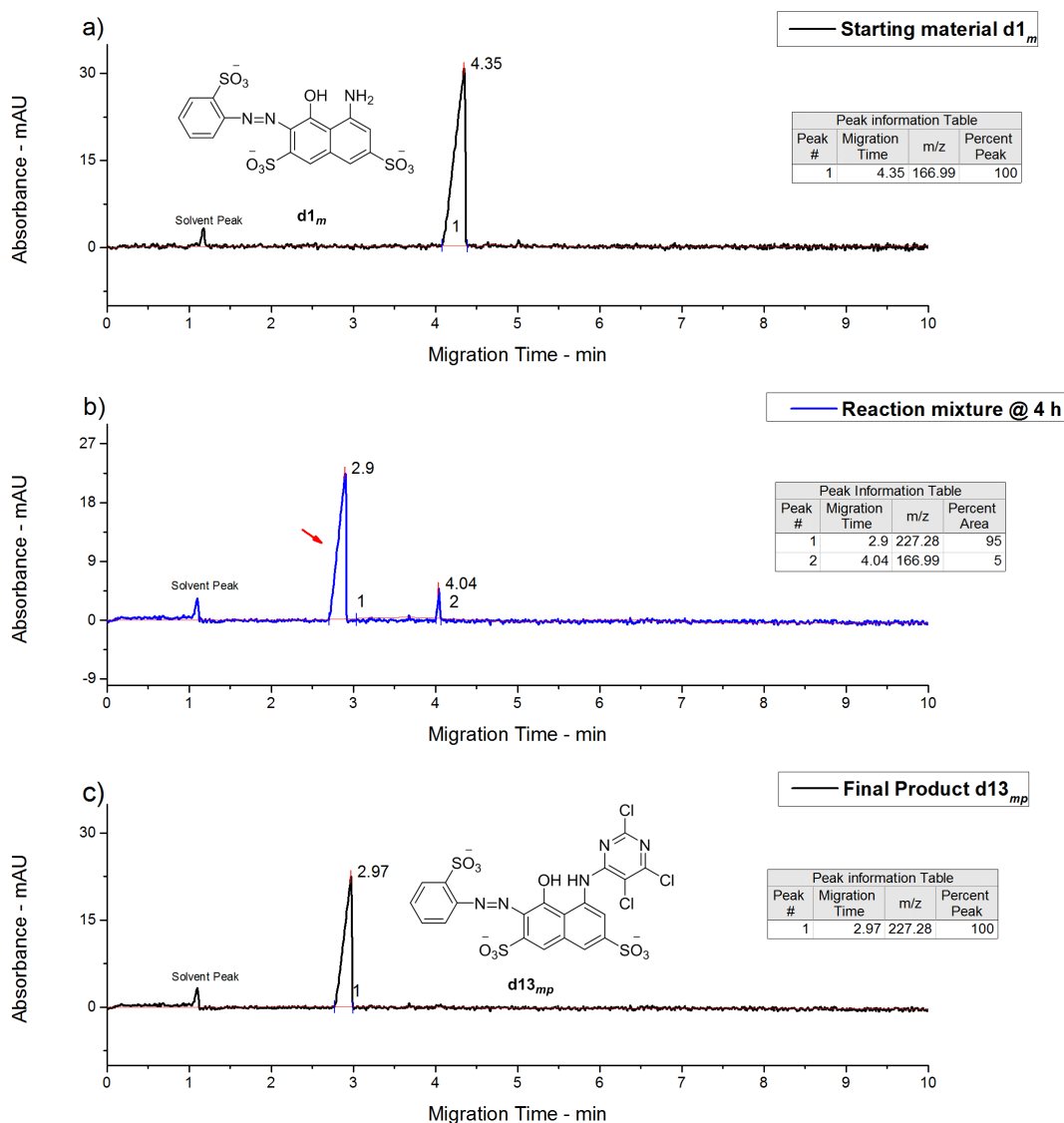


Figure 6.6: Electropherograms showing reaction progress of synthesis of $d13_{mp}$. (a) magenta dye chromophore $d1_m$; (b) $d1_m - d13_{mp}$ after 4 hours reaction; (c) Final product $d13_{mp}$. CZE conditions: same as Figure 6.1

Analytical TLC show gradual appearance of new magenta less polar compound $d13_{mp}$ (R_f value 0.65) compared to the magenta starting material $d1_m$ (R_f value 0.62) Moreover, almost quantitative conversion occurred in 4 hours with microwave irradiated synthesis.

Analysis of FT-IR spectrum (Figure 6.7) of pure magenta powder suggested that the compound has been $d13_{mp}$ since peaks due to the presence of primary amine in $d1_m$ (Figure 3.2, page 70) at 1621 cm^{-1} and 889 cm^{-1} are no longer present indicating that the primary amine had successfully reacted with 2,4,5,6-tetrachloropyrimidine. According to literature [18, 19], C=N have at least one strong band at $1580\text{-}1520\text{ cm}^{-1}$ and at least one band at $1450\text{-}1350\text{ cm}^{-1}$ corresponding to

the stretching of the ring. The appearance of new peaks at 1542 cm^{-1} and 1393 cm^{-1} reflects the presence of the C=N in **d13_{mp}**. Moreover, in accordance with literature [18, 20], the appearance of the peaks at the 1091 cm^{-1} and 849 cm^{-1} [21, 22] is attributed to the stretching vibrations of carbon chlorine bond on the diazine ring of the **d13_{mp}**.

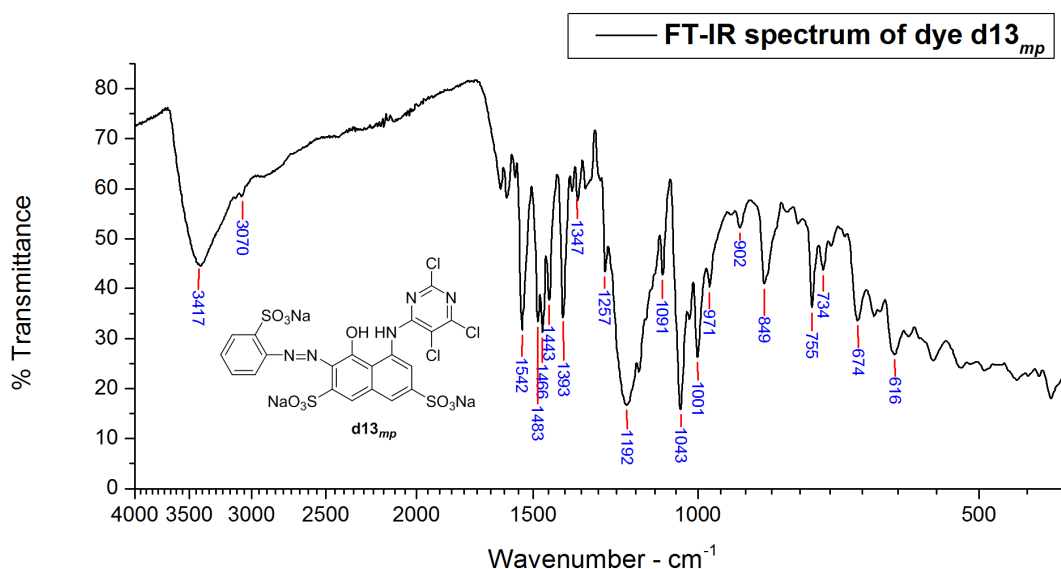


Figure 6.7: FT-IR spectrum of magenta trichloropyrimidine dye **d13_{mp}**

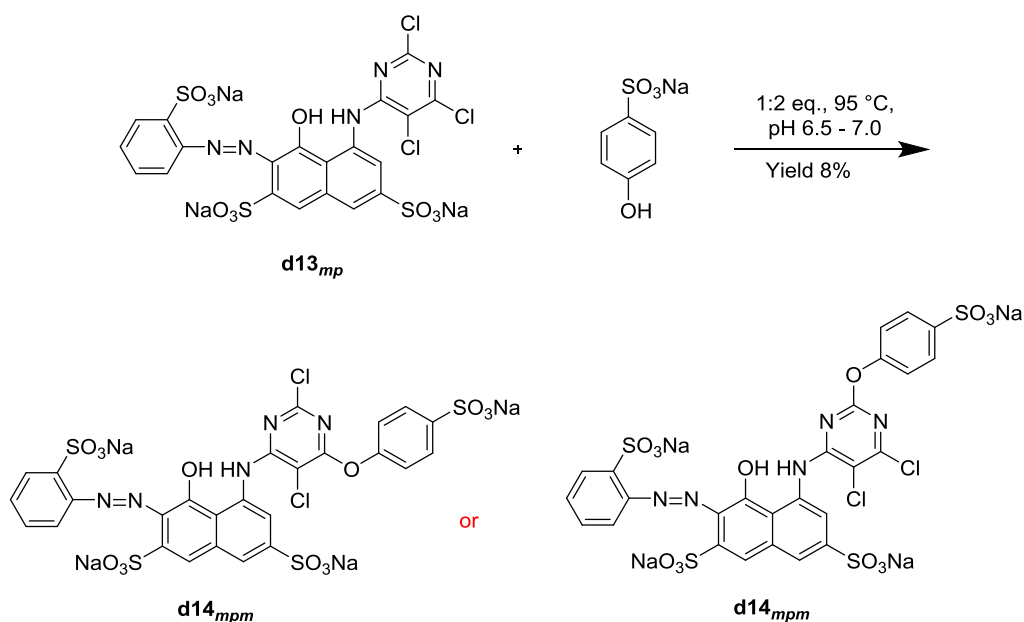
The detailed analysis of the spectrum (Figure 6.7) is as follows [18, 20, 23, 24], N–H stretch, 3417 cm^{-1} ; aromatic C–H stretch, 3070 cm^{-1} ; overtone or combinational bands, $2000\text{--}1667\text{ cm}^{-1}$; C=C ring stretch, 1483 cm^{-1} , 1466 cm^{-1} ; azo group stretch, 1443 cm^{-1} ; C=N ring stretch, 1542 cm^{-1} , 1393 cm^{-1} ; C–N stretch (secondary amine), 1347 cm^{-1} ; sulfonate 1192 cm^{-1} ; C–Cl stretch, 1091 cm^{-1} , 849 cm^{-1} ; in-plane C–H bend, 1043 cm^{-1} , 1001 cm^{-1} ; out of plane aromatic C–H bend, 755 cm^{-1} .

6.2.7 Synthesis of Modified Magenta 5-[(2-(4-Sulfophenoxy)-5,6-dichloro-4-pyrimidinyl)amino]-4-Hydroxy-3-[(2-sulfophenyl)azo]-2,7-Naphthalenedisulfonic Acid Dye (**d14_{mpm}**)

6.2.7.1 Conventional Heating Method

Dye **d13_{mp}** (3.74 g, 0.005 mol, 1 eq.) was dissolved in water (50 cm^3) at $25\text{ }^\circ\text{C}$. A solution of sodium 4-hydroxybenzenesulfonate dihydrate (4HBSA) (2.32 g, 0.01 mol, 2 eq.) in water (20 cm^3) was added to the **d13_{mp}** solution; pH was maintained at 7.0 to 7.5 by the addition of saturated sodium carbonate solution. Once the addition

of 4HBSA solution was complete, the reaction mixture was refluxed at 95 °C and stirred until the pH had stabilised and was monitored with CZE and TLC. The reaction is shown in Scheme 6.6 and the CZE electropherograms showing the reaction progression is shown in Figure 6.8.



Scheme 6.6: Mono substitution of dye **d13_{mp} with 4HBSA to yield dye **d14_{mpm}** by conventional heating**

The reaction mixture was freeze dried and then was subsequently submitted to flash column chromatography using RP-18 silica gel and water as an eluent. The polarity of the eluent was then gradually decreased by the addition of methanol in 5 - 95% gradient and was applied at a relatively slow flow rate (10 ml·min⁻¹). The fractions containing magenta product **d14_{mpm}** were collected. The pooled product-containing fractions were evaporated under vacuum to remove the methanol, and the remaining water was subsequently removed by freeze drying to yield the pure **d14_{mpm}** dye (95.2 mg, yield 8%) as a magenta powder.

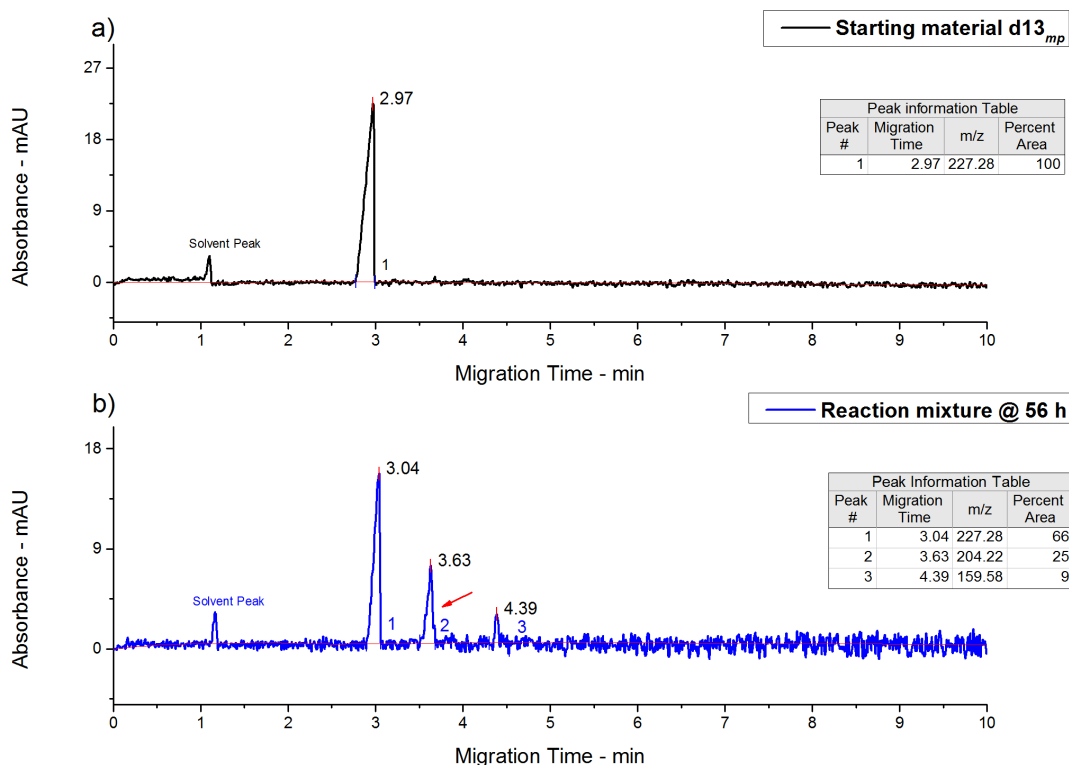


Figure 6.8: Electropherograms showing reaction progress of synthesis of **d14_{mpm} by conventional heating (a) magenta dye **d13_{mp}**; (b) **d13_{mp}** – **d14_{mpm}** after 56 hours reaction time. CZE conditions: same as Figure 6.1**

As shown in Figure 6.8b, the percent conversion to modified dye **d14_{mpm}** was only 25% in 56 hours of reaction time with small amount of by-product.

The conventional heating method resulted in poor conversion (25%), longer reaction time and poor yield of (8%). Therefore, microwave-irradiated synthesis was adopted for the modification of **d13_{mp}**.

6.2.7.2 Optimising Microwave-Irradiated Method

For the optimisation of substitution reaction of magenta trichloropyrimidine dye **d13_{mp}** with 4HBSA, sodium phosphate buffer pH 7.4 was used. The reaction showed an excellent conversion (79.13%) to product along with a high yield (68.09%) as compared to conventional heating method. However, the rate of reaction was sluggish (10 hours) (shown in Table 6.5).

Table 6.5: Optimisation of reaction conditions for microwave-irradiated synthesis of d14_{mpm}

Solvent	Concentration of reactants	Temperature (°C)	Time (hours)	Conversion (%)	Yield (%)
Sodium phosphate buffer pH (7.4)	0.02 (0.1 mM/5 ml)	100	10	79	68

Because for bimolecular reactions such as S_NAr, rate of reaction is highly dependent on the concentration of reactants, therefore, for improving the reaction rate, concentration of reaction mixture was increased to 0.05.

Table 6.6: Modification of reaction conditions for microwave irradiated synthesis of d14_{mpm}

Solvent	Concentration of reactants	Temperature (°C)	Time (hours)	Conversion (%)	Yield (%)
Sodium phosphate buffer pH (7.4)	0.05 (0.1 mM/2 ml)	100	2.5	89	70

As shown in Table 6.6 and Figure 6.9, the rate of reaction increased dramatically by increasing the concentration of reactants in the reaction. This is because as the concentration of reactants increased the reactant particles become more crowded and there are more successful particle collisions and hence the rate of reaction increases.

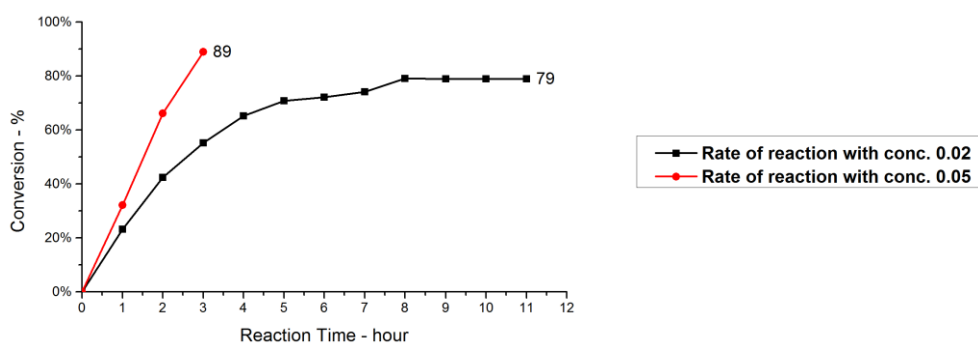


Figure 6.9: Effect of reactant concentration on rate of reaction (d14_{mpm})

6.2.8 Comparative Study of Conventional and Microwave-Irradiated Synthesis of Dye $d14_{mpm}$

A comparison between the results obtained under conventional heating and microwave-irradiated synthesis for the reaction times, conversions and isolated yields for the synthesis of $d14_{mpm}$ are shown in Figure 6.10.

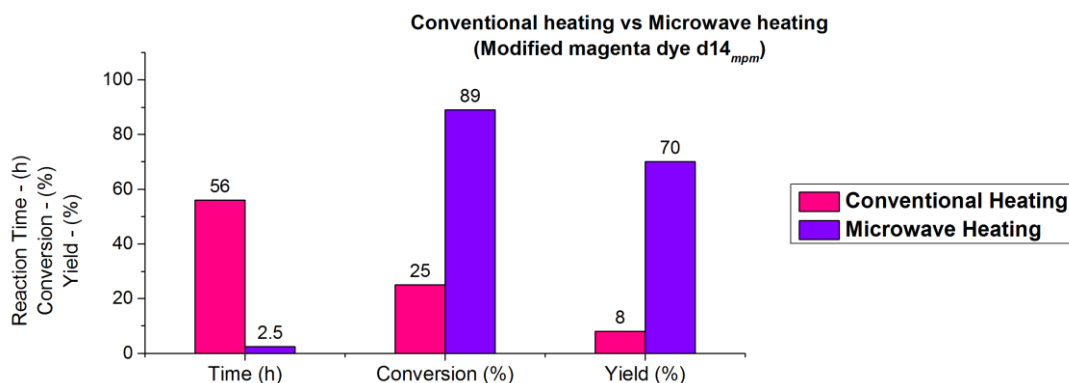


Figure 6.10: Comparison of reaction times, conversions and yields obtained by conventional heating and microwave irradiation ($d14_{mpm}$)

As can be seen in Figure 6.10, microwave irradiation effectively reduced the reaction time from 56 hours to a few hours (2.5 hours) with significant enhancement in the conversion from only 25% to 89%.

Moreover, by using microwave irradiation, the modified mono-substituted dye $d14_{mpm}$ was prepared in high yield (70%) and purity in contrast to low yield obtained (8%) after 56 hours of conventional heating at 95 °C.

This is because, incorporation of sodium phosphate buffer not only maintain the required pH of the reaction mixture, but also behave as ions that heats up rapidly when exposed to microwave irradiation and hence enhances the rate of reaction.

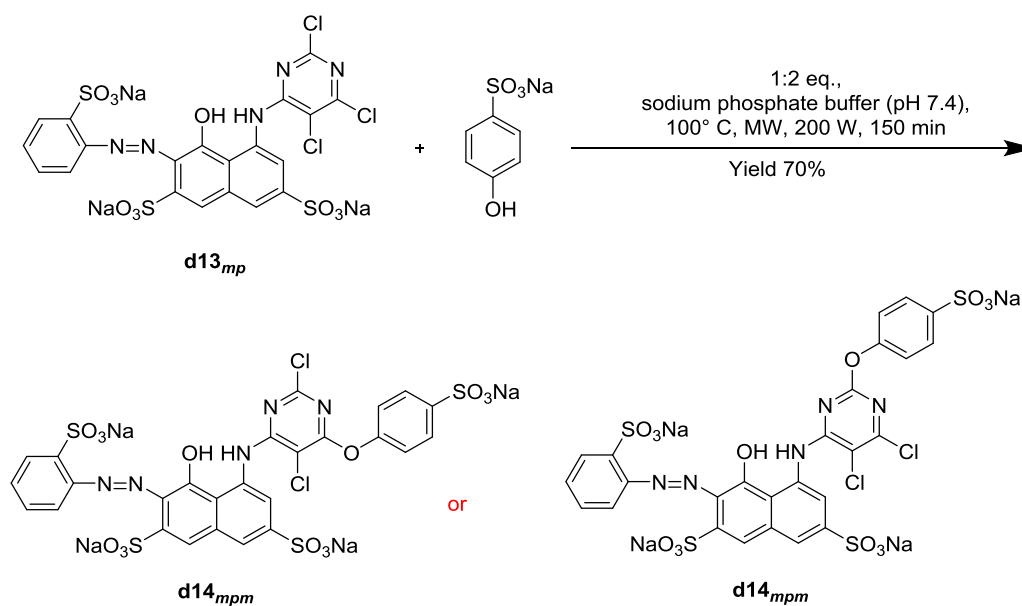
Therefore, it is concluded that the microwave irradiated method is an efficient, fast and easy method for the synthesis of $d14_{mpm}$. In addition, the yield is also increased.

6.2.9 Synthesis of Modified Magenta 5-[(2-(4-Sulfophenoxy)-5,6-dichloro-4-pyrimidinyl)amino]-4-Hydroxy-3-[(2-sulfophenyl)azo]-2,7-Naphthalenedisulfonic Acid Dye ($d14_{mpm}$)

Magenta trichloropyrimidine dye $d13_{mp}$ (0.748 g, 1 mmol, 1 eq.) and 4HBSA (0.464 g, 2 mmol, 2 eq.) were added to each of the five 35 ml microwave reaction vials equipped with a magnetic stirring bars followed by the addition of 20 ml of

sodium phosphate buffer [Na_2HPO_4 (0.20 M, 8 ml) and NaH_2PO_4 (0.12 M, 12 ml), pH 7.4].

The mixtures were capped and irradiated in the microwave oven (200 W) for 2.5 hours at 100 °C. The reaction mixtures were combined and purified through flash column chromatography as discussed in section 2.5.4 to yield a pure **d14_{mpm}** dye (2.84 g, 3.12 mmol, yield 70%) as a magenta powder. The optimal conditions of reaction are shown in Scheme 6.7.



Scheme 6.7: Mono substitution of dye **d13_{mp} with 4HBSA to yield dye **d14_{mpm}** with microwave irradiation**

6.2.9.1 Characterisation of Modified Magenta 5-[(2-(4-Sulfophenoxy)-5,6-dichloro-4-pyrimidinyl)amino]-4-Hydroxy-3-[(2-sulfophenyl)azo]-2,7-Naphthalenedisulfonic Acid Dye (**d14_{mpm}**)

The electropherograms from CZE analysis are shown in Figure 6.11 which indicates the progression of the synthesis reaction from the starting dye **d13_{mp}** to the mono-substituted dye **d14_{mpm}** (peak 2 in Figure 6.11b).

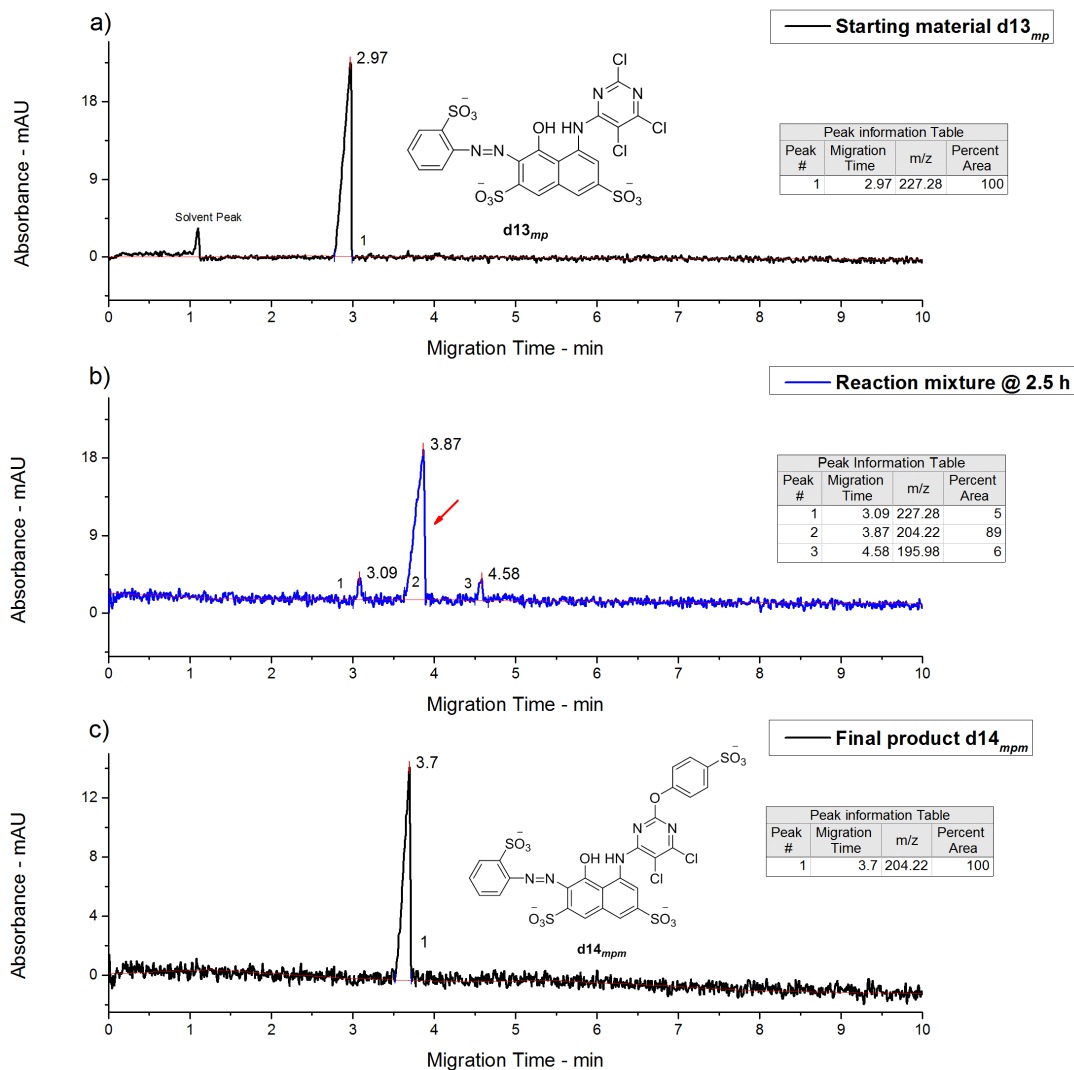


Figure 6.11: Electropherograms showing reaction progress of synthesis of **d14_{mpm}. (a) magenta dye **d13_{mp}**; (b) **d13_{mp}** – **d14_{mpm}** after 2.5 hours reaction time; (c) Final product **d14_{mpm}**. CZE conditions: same as Figure 6.1**

As shown in Figure 6.11, as the mono substitution of **d13_{mp}** with 4HBSA increases the molecular weight of modified dye **d14_{mpm}** as well as increases a negative charge on it. Hence the dye **d13_{mpm}** with the highest mass to charge ratio elute first (Figure 6.11b, peak 1) and the dye **d14_{mpm}** with the second least mass to charge ratio eluted second (Figure 6.11b, peak 2). Moreover, the last peak to emerge in the Figure 6.11b could be the hydrolysed dye or di-substitution product as by-product of reactions.

Furthermore, Figure 6.11c shows that the final product **d14_{mpm}** was pure after flash column chromatography.

The R_f values were found to be 0.65 and 0.62 for starting material (**d1_m**) and product (**d13_{mp}**) respectively.

In accordance with the literature [18, 20], the appearance of new peaks at 1125 cm^{-1} in Figure 6.12 can be attributed to the stretching vibration of C–O–C in structure between the diazine and 4HBSA. The small peaks at 1091 cm^{-1} and 834 cm^{-1} can be attributed to the presence of aromatic C–Cl bond after the mono substitution of dye **d13_{mp}** with 4HBSA.

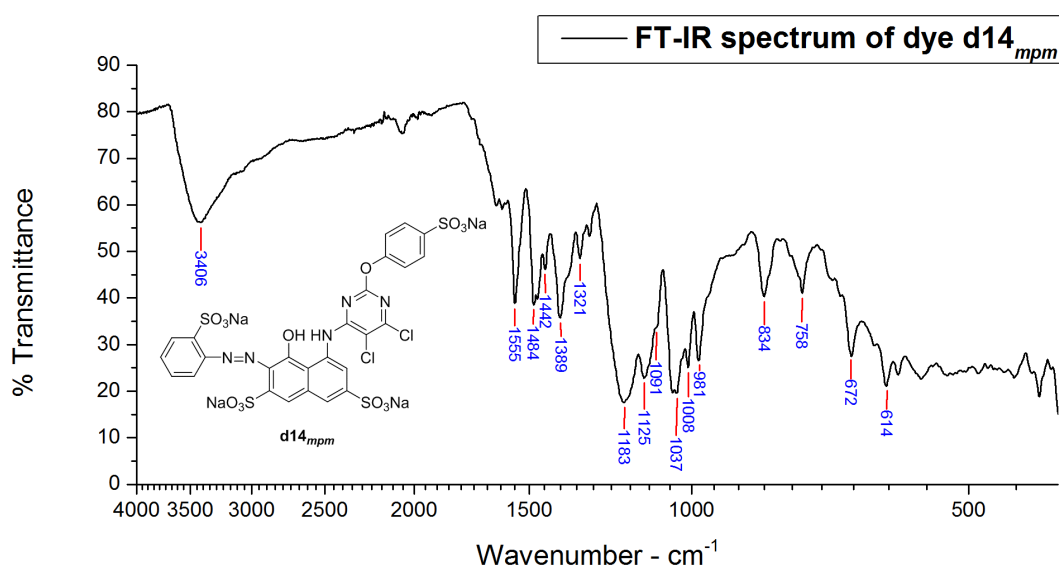


Figure 6.12: FT-IR spectrum of magenta mono-substituted dye d14_{mpm}

The detailed analysis of spectrum (Figure 6.12) is as follows [18, 20, 23, 24]; N–H stretch, 3406 cm^{-1} ; overtone or combinational bands, 2000–1667 cm^{-1} ; C=C ring stretch, 1484 cm^{-1} , azo group stretch, 1442 cm^{-1} ; C=N ring stretch, 1555 cm^{-1} , 1389 cm^{-1} ; C–N stretch (secondary amine), 1321 cm^{-1} ; C–O–C stretching, 1125 cm^{-1} ; sulfonate, 1183 cm^{-1} ; C–Cl stretch, 1091 cm^{-1} , 834 cm^{-1} ; in-plane C–H bend, 1037 cm^{-1} , 1008 cm^{-1} ; out of plane aromatic C–H bend, 758 cm^{-1} .

Elemental analysis, Found: C, 33.18%; H, 1.59%; N, 7.27%. Calculated for $\text{C}_{26}\text{H}_{13}\text{Cl}_2\text{N}_5\text{Na}_4\text{O}_{14}\text{S}_4 \cdot \text{H}_2\text{O}$: C, 33.65%; H, 1.63%; N, 7.51%. It should be noted that the results are adjusted due to the presence of water of crystallisation.

6.2.10 Application of Magenta Dyes ($d13_{mp}$ and $d14_{mpm}$) onto Wool Fabric by Inkjet Printing

The inks were prepared using 4% dye according to the procedure detailed in section 2.5.2, and then tested for viscosity and surface tension.

The resulting ink formulation was then introduced in the cartridge and printed onto wool fabric using HP 6940 deskjet printer. Once printed, the printed wool samples were fixed by two methods detailed in section 2.5.4, and evaluated for percent fixation along with light fastness and wash fastness.

Moreover the inks were also evaluated for stability through CZE over eight months storage time at room temperatures.

6.2.11 Characteristics of Formulated Inks ($d13_{mp}$ and $d14_{mpm}$)

6.2.11.1 Surface Tension and Viscosity of Inks

It can be seen, from Table 6.7, that parent dye $d13_{mp}$ and the modified dye $d14_{mpm}$ based inks had a surface tension and viscosity within the operational range.

Table 6.7: Ink properties

Ink formulation	Surface Tension (dynes.cm ⁻¹)	Viscosity (cP)
$d13_{mp}$ based Ink	49.0	12
$d14_{mpm}$ based Ink	46.5	10

6.2.11.2 Stability of Dye ($d13_{mp}$ and $d14_{mpm}$) Based Inks

As discussed earlier, due to the low reactivity of trichloropyrimidine dyes, they are not prone to hydrolysis. However, they can react with nucleophiles, such as amino and hydroxyl present in ink during storage. Therefore, stability of trichloropyrimidine dye $d13_{mp}$ along with new modified dye $d14_{mpm}$ in inks were also evaluated.

The results of any change in percent area of the peaks of the dyes within inks stored at room temperature for eight months can be seen in Figure 6.13 and Figure 6.14.

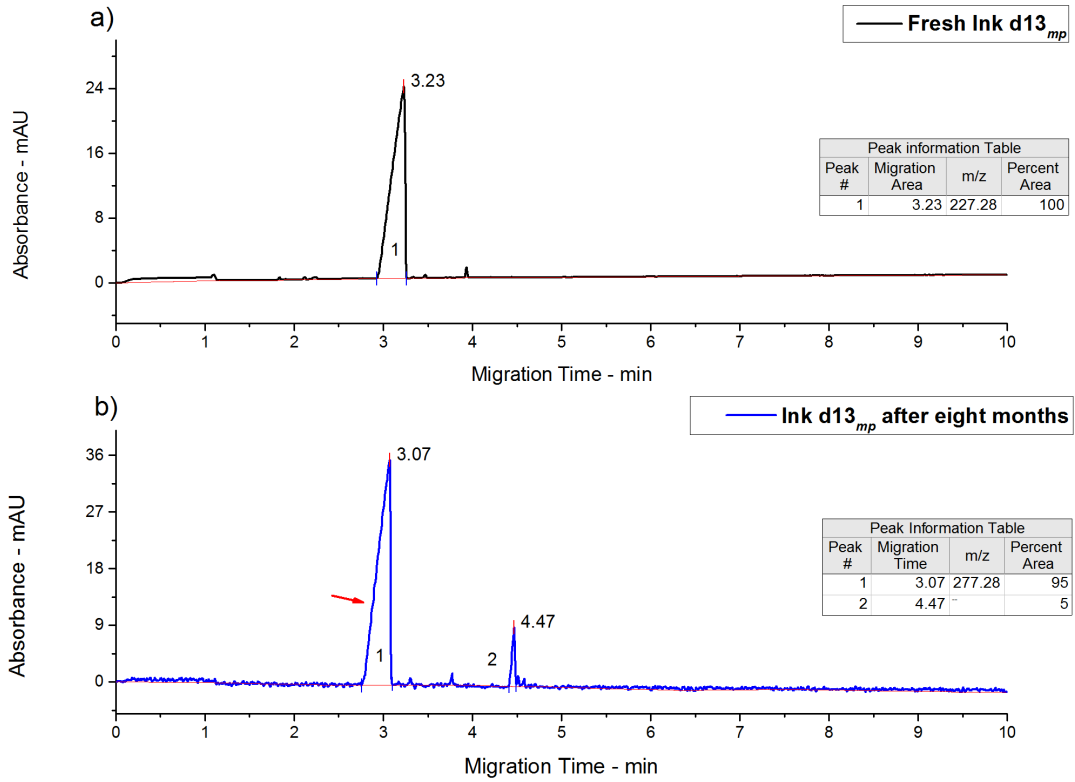


Figure 6.13: Electropherograms showing $d13_{mp}$ based ink stability. (a) Fresh ink; (b) Ink after eight months storage at room temperature.

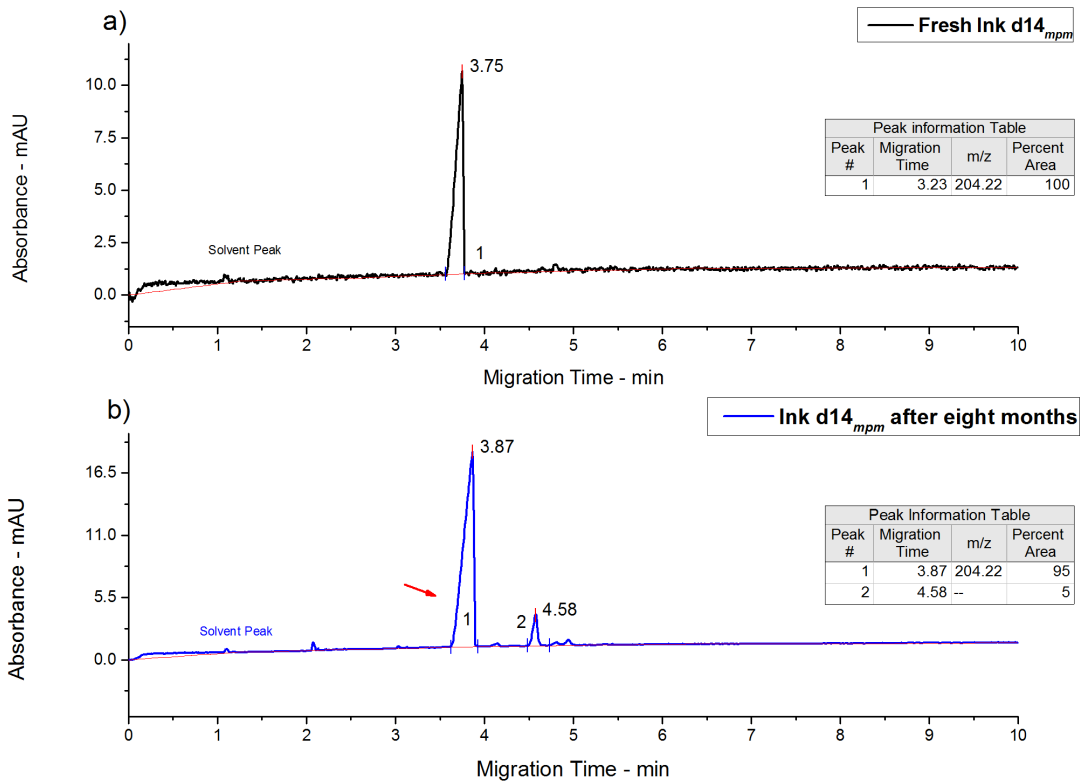


Figure 6.14: Electropherograms showing $d14_{mpm}$ based ink stability. (a) Fresh ink; (b) Ink after eight months storage at room temperature.

As shown in Figure 6.13 and Figure 6.14, no significant change in the percent area of peaks of both, *i.e.*, magenta trichloropyrimidine dye **d13_{mp}** and modified dye **d14_{mpm}** based ink were observed indicating that there had been no detrimental effect caused by the modification of magenta trichloropyrimidine dye with 4HBSA.

6.2.12 Evaluation of Percent Fixation of Magenta Pyrimidine based Dyes (**d13_{mp}** and **d14_{mpm}**) by Various Fixation Methods

The maximum percent fixations of magenta trichloropyrimidine dye **d13_{mp}** and magenta modified dye **d14_{mpm}** for batching at 90 °C and steaming at 102 °C are shown in Figure 6.15.

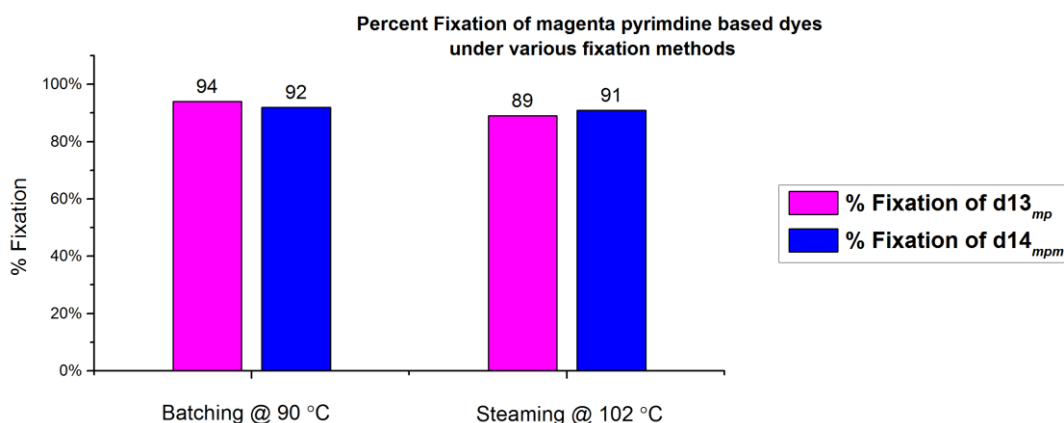


Figure 6.15: Percent fixation of d13_{mp} and d14_{mpm} under various fixation methods

As shown in Figure 6.15, inkjet printing with magenta **d13_{mp}** and **d14_{mpm}** based inks carried out using a pad–batch (90 °C) process showed exceptionally high levels of dye fixations *i.e.* 94% and 92% respectively.

Moreover, Figure 6.15 also reflects the effect of steaming on the percent fixation of magenta trichloropyrimidine and modified dye printed on the wool fabric. The magenta mono-substituted dye **d14_{mpm}** (91%) showed the highest percent fixation followed by trichloropyrimidine dye **d13_{mp}** (89%).

This could be due to bifunctional behavior of both dyes under the fixation conditions used, as Ackermann and Dussy^[5, 25, 26] found evidence that dyes based on tetrachloropyrimidine can exchange more than one chlorine with fibre under drastic reaction conditions. Also in case of steaming, mono substituted dye being less reactive than the parent trichloropyrimidine dye allowed more controlled formation of covalent bonds between the dye molecule and the wool fibre.

Moreover, it is noted the effect of addition of urea and sodium bisulfite in pretreatment liquor is more pronounced in the inkjet printing of wool fabric with low reactivity pyrimidine dyes as compared to analogous triazine based dyes .

6.2.13 Light Fastness

Light fastness testing was carried out according to the BS EN ISO 105-B02:2013 (Method 3) [27].

The printed samples were tested against blue wool reference 6. As shown in Table 6.8, both the dyes pass target wool reference 6.

Table 6.8: Light fastness of magenta dyes ($d13_{mp}$ and $d14_{mpm}$) compared to target blue wool reference 6

Dye/Ink	Target blue wool reference 6	
$d13_{mp}$	Better than 6 (6^+)	Satisfactory
$d14_{mpm}$	Better than 6 (6^+)	Satisfactory

6.2.14 Wash Fastness

Wash fastness was carried out according to the BS ISO 105-C06:2010 [28] and the results are shown in Table 6.9.

The tested fabric samples showed no evidence of any colour loss or staining of multifibre adjacents. Hence, the wash fastness tests showed that there had been no detrimental effect caused by modification of dye $d13_{mp}$.

Table 6.9: Wash fastness of magenta dyes ($d13_{mp}$ and $d14_{mpm}$)

Dye/Ink	Change in shade	Staining					
		CA	C	N	P	A	W
$d13_{mp}$	5	5	5	5	5	5	5
$d14_{mpm}$	5	5	5	5	5	5	5

CA: Cellulose Acetate; C: Cotton; N: Nylon; P: Polyester; A: Acrylic; W: Wool

6.3 Conclusions

By using microwave irradiation both the dyes **d13_{mp}** and **d14_{mpm}** were prepared in yields that were appreciable higher than conventional heating method (Figure 6.5 and Figure 6.10).

Optimal reaction conditions time for the synthesis of **d13_{mp}** and **d14_{mpm}** were 4 hours and 2.5 hours at 200W of microwave irradiation power at 100 °C in the presence of sodium phosphate buffer as energy transfer medium respectively.

The modification of magenta trichloropyrimidine dye **d13_{mp}** with 4HBSA did not have a detrimental effect on the stability of dye in the ink when stored for eight months at room temperature.

When inkjet printed both the dyes exhibit excellent fixation properties. Moreover, there is no significant difference in the percent fixation between parent and modified dye although the reactivity of modified dye was lowered by the incorporation of sulfophenoxy group.

Printed wool sample showed outstanding colour fastness to light and wash.

6.4 References

1. Siegel, E. Reactive Dyes: Reactive Groups. *In*: K. Venkataraman, ed. *The chemistry of synthetic dyes*. New York ; London: Academic Press, 1978.
2. Brown, D.J. *The pyrimidines*. The Chemistry of heterocyclic compounds. New York: Wiley and Sons, 1993.
3. Venkataraman, K. ed. *The chemistry of synthetic dyes*. New York: Academic Press Ltd., 1978.
4. Beech, W.F. *Fibre-Reactive Dyes* London: Logos Press Ltd., 1970.
5. Ackermann, H. and Dussy, P. Cellulose-reactive chloropyrimidinyl dyes-chemical reactivity and stabilizing ability. *Melliand Textilber*, 1961, **42**, pp.1167-72.
6. Stamm, O.A. Mechanisms of Reaction of Reactive Dyes with Cellulosic and other Fibres. *Journal of the Society of Dyers and Colourists*, 1964, **80**, pp.416-422.
7. Rocha Gomes, J.I.N. *Studies in the stability of bonds between fibre-reactive dyes and cellulose*. Ph.D. Thesis, University of Leeds, 1983.

8. Patent EP221013 (1987)
9. Patent US4766206 (1988)
10. Patent DE4231537A1 (1993)
11. Lidström, P., Tierney, J., Wathey, B. and Westman, J. Microwave assisted organic synthesis—a review. *Tetrahedron*, 2001, **57**, pp.9225-9283.
12. Galema, S.A. Microwave chemistry. *Chemical Society Reviews*, 1997, **26**, pp.233-238.
13. Baqi, Y. and Müller, C.E. Rapid and Efficient Microwave-Assisted Copper(0)-Catalyzed Ullmann Coupling Reaction: General Access to Anilinoanthraquinone Derivatives. *Organic Letters*, 2007, **9**, pp.1271-1274.
14. Patent GB838337 (1960)
15. Patent BE578933 (1959)
16. Patent WO2008107211 (2008)
17. Tierney, J.P. and Lidström, P. eds. *Microwave Assisted Organic Synthesis*. Oxford: Blackwell Publishing, 2005.
18. Socrates, G. *Infrared and Raman characteristic group frequencies : tables and charts*. Chichester: Wiley, 2001.
19. Ito, M., Shimada, R., Kuraishi, T. and Mizushima, W. Vibrational Spectra of Diazines. *The Journal of Chemical Physics*, 1956, **25**, pp.597-598.
20. Silverstein, R.M., Webster, F.X. and Kiemle, D.J. *Spectrometric Identification of Organic Compounds*. 7th ed. New York: John Wiley and Sons, 2005.
21. Lewis, D.M. and Wang, J.C. The use of fourier transform infrared (FT-IR) spectroscopy to study the state of heterobifunctional reactive dyes. *Dyes and Pigments*, 1998, **39**, pp.111-123.
22. Daimay, L.-V., Colthup, N.B., Fateley, W.G. and Grasselli, J.G. *The handbook of infrared and Raman characteristic frequencies of organic molecules*. London: Academic Press Ltd., 1991.
23. Matlok, F., Gremlich, H.U., Bruker Analytische Meotechnik and Merck eds. *Merck FT-IR atlas : a collection of FT-IR spectra*. Weinheim: Vch, 1988.
24. Keller, R.J. and Sigma-Aldrich Corporation. *The Sigma library of FT-IR spectra*. Missouri: Sigma Chemical Company, 1986.

25. Ackermann, H. and Dussy, P. Constitution and reactivity of trichloropyrimidylamino derivatives. *Helvetica Chimica Acta*, 1962, **45**, pp.1683-98.
26. Hildebrand, D. Application and Properties. *In: K. Venkataraman, ed. The chemistry of synthetic dyes*. New York: Academic Press Ltd., 1978.
27. British Standards Institution. *Colour fastness to artificial light: Xenon arc fading lamp test*, ISO 105-B02:2013.
28. British Standards Institution. *Textiles - Tests for colour fastness - Part C06: Colour fastness to domestic and commercial laundering*, BS EN ISO 105-C06:2010.

7 Synthesis, Modification, Characterisation of Blue Trichloropyrimidine Dyes and Their Application onto Wool Fabric by Inkjet Printing

This chapter details the synthesis, modification and characterisation of blue dyes based on pyrimidine reactive group by the conventional heating method as well as microwave irradiation. The syntheses progression were monitored through CZE and TLC and the structural changes was confirmed by FT-IR.

Moreover, the synthesised blue trichloropyrimidine dye **d15_{bp}** and specially modified dye **d16_{bpm}** were applied to wool fabric through inkjet printing in order to evaluate their percent fixation, stability of inks along with colour fastness (light and wash) properties.

7.1 Experimental

7.1.1 Materials

Blue dye chromophore **d9_b** (100%), 2,4,5,6-tetrachloropyrimidine (97%), sodium 4-hydroxybenzenesulfonate dihydrate (98%), sodium metabisulfite, carboxymethyl cellulose, polysorbate 20 (Tween 20) and N-methylmorpholine N-oxide (NMO) were purchased from Sigma-Aldrich and used as received. Urea (MP Biomedicals), Alcopol O 60 (Acros organics), 2-pyrrolidone (Acros organics), 2-propanol (Fisher), Sandozin NIE (Clariant) were also purchased and used as received.

7.1.2 Conventional Heating Method for the Synthesis of Blue 1-Amino-4-[3-[(2,5,6-trichloro-4-pyrimidinyl)amino]-4-(Sulfohenyl)amino]-Anthraquinone-2-Sulfonic Acid Dye (**d15_{bp}**)

7.1.2.1 Conventional Heating Method

In accordance with the literature ^[1-3], amino based dye chromophore **d9_b** (1 eq.) was dissolved in water and adjusted to the pH 6.0 to 7.0 by the addition to 2N sodium carbonate solution at 35 °C. A solution of 2,4,5,6-tetrachloropyrimidine (1.1eq.) in investigated solvent was added as thin stream to the dye chromophore

solution. The reaction mixture was refluxed to the investigated temperature and percent conversion were monitored through CZE. The percent conversion can be obtained from percent area of target dye on the CZE electropherogram.

The target blue trichloropyrimidine dye **d15_{bp}** was synthesised using acetone and ethanol as co-solvents at a temperature range of 50, 70, 80 and 90 °C.

7.1.3 Investigation of Conventional Heating Method for the Synthesis of Blue Trichloropyrimidine Dye (d15_{bp})

7.1.3.1 Percent Conversion to d15_{bp} Under Various Temperature

The percent conversion of **d9_b** to yield **d15_{bp}** at temperatures 50, 70, 80 and 90 °C were investigated provided that the reactants were used in 1:1.1 molar ratio and pH of reaction mixture was maintained at 6.0 to 7.0 throughout with 2N sodium carbonate solution. The reactions were stirred until the pH had stabilised and prolonged reaction times do not increase conversion to **d15_{bp}**. The reactions were monitored through CZE.

The percent conversion to blue dye **d15_{bp}** achieved at different temperatures are shown in Figure 7.1 and isolated yields are listed in Table 7.1.

As shown in Figure 7.1a, using 1:1 eq. of reactants, Na₂CO₃ acid-binding agent to maintain pH at 6.0 to 7.0 and water–acetone as solvent system at 50 °C, did not lead to detectable conversion to **d15_{bp}** even after 15 hours, however, by-products were detectable in CZE electropherogram.

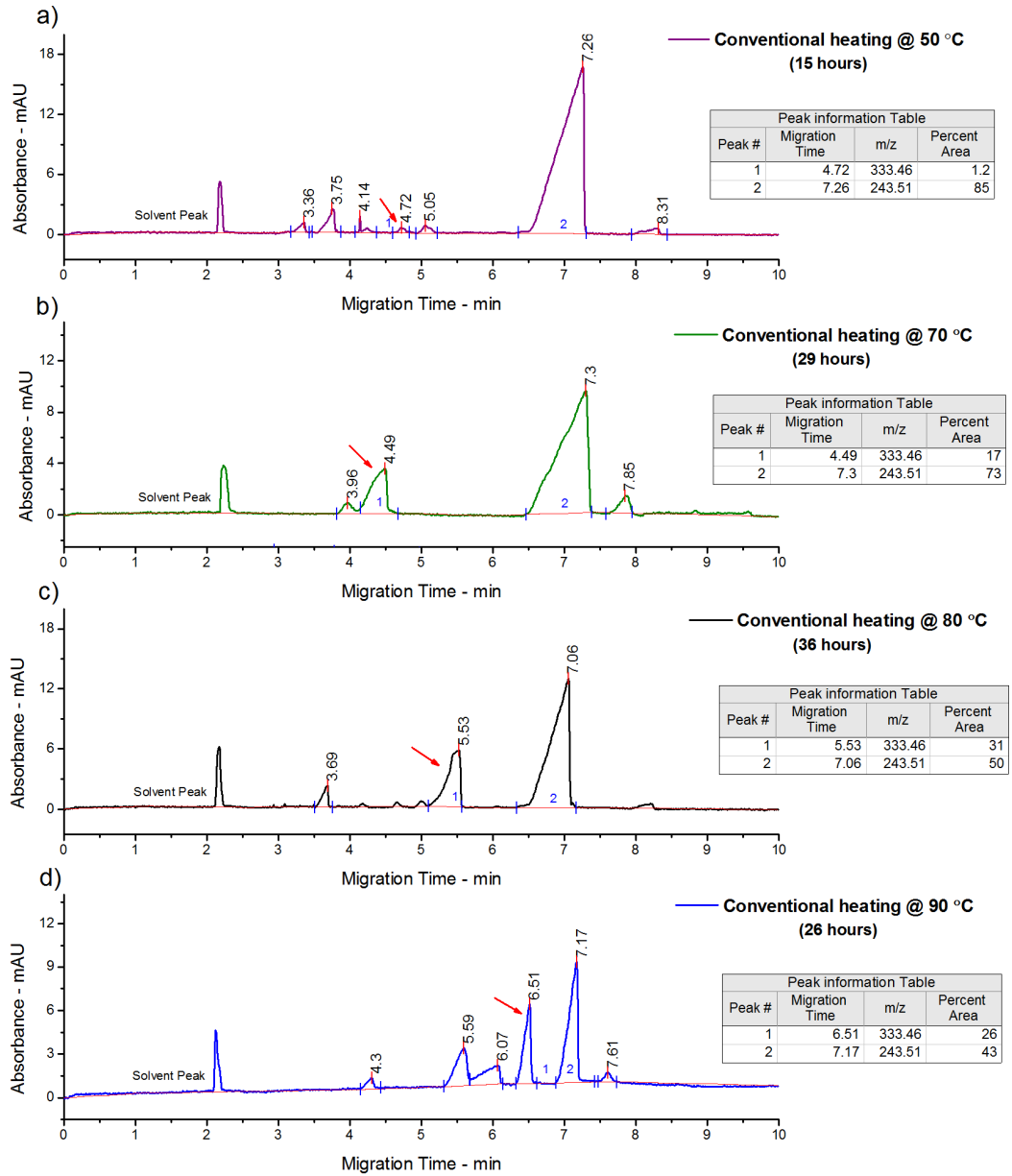


Figure 7.1: Electropherograms showing conversion to $d15_{bp}$ using conventional heating method at: (a) 50 °C; (b) 70 °C; (c) 80 °C; (d) 90 °C. CZE conditions: running buffer, 15 mM ammonium acetate and acetonitrile (40% v/v) pH 9.3; pressure injection 0.5 psi for 10 s; voltage 25 kV; detection at 596 nm

Table 7.1: Summary of results with conventional heating at various temperatures

Entry	Parameters	Time (hours)	Conversion ^a (%)	Yield ^c (%)
1	1:1.1 eq., Na ₂ CO ₃ , pH 6.0 – 7.0, water–acetone, 50 °C	15	1.2	*
2	1:1.1 eq., Na ₂ CO ₃ , pH 6.0 – 7.0, water–acetone, 70 °C	29	17	4.6
3	1:1.1 eq., Na ₂ CO ₃ , pH 6.0 – 7.0, water–acetone, 80 °C	36	31	12
4	1:1.1 eq., Na ₂ CO ₃ , pH 6.0 – 7.0, water–acetone, 90 °C	26	26 _b	10

^a: Determined by CZE analysis; _b: significant amount of by-product; ^c: isolated product; *: Product was not isolated from the reaction mixture due to low conversion

The reactions were carried out by conventional heating at a range of temperatures, but the reactions generally proceeded sluggishly and resulted in more by-products as shown in Figure 7.1. Therefore, it is concluded that by using conventional heating method for the synthesis of blue trichloropyrimidine dye **d15_{bp}**, the reaction proceeded sluggishly, and an isolated yield of 12% of **d15_{bp}** could be obtained after a total reaction time of 36 hours at 80 °C.

7.1.3.2 Percent Conversion to **d15_{bp}** Under Different Co-Solvents

In general terms, the choice of solvent can have a significant effect on the performance of a reaction. Therefore, percent conversion of **d9_b** to yield **d15_{bp}** using acetone and ethanol at 80 °C were investigated provided that pH of reaction mixture was maintained at 6.0 to 7.0 throughout with 2N sodium carbonate solution. The reactions were stirred until the pH had stabilised and prolonged reaction times did not have any effect on percent conversion to **d15_{bp}**. The reactions were monitored through CZE.

The percent conversions achieved are shown in Figure 7.2 and isolated yields are listed in Table 7.2.

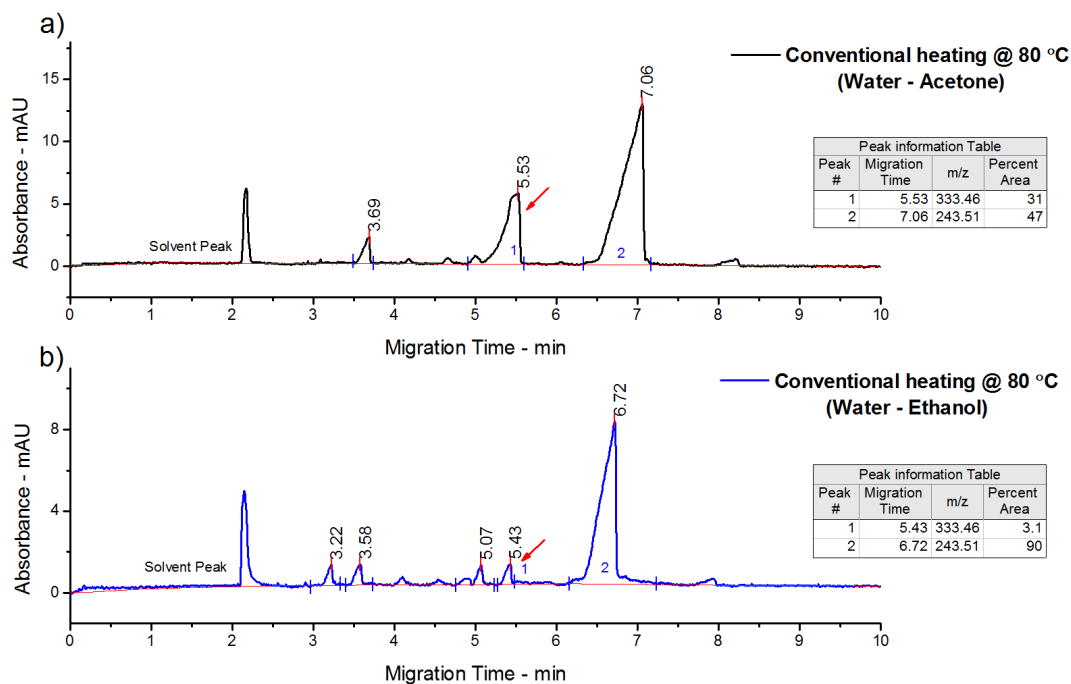


Figure 7.2: Electropherograms showing percent conversion to $d15_{bp}$ using conventional heating method: (a) Water-acetone; (b) Water-ethanol. CZE conditions: same as Figure 7.1.

Table 7.2: Summary of results from conventional heating using different co-solvents

Entry	Parameters	Time (hours)	Conversion ^a (%)	Yield ^b (%)
1	1:1 eq., Na ₂ CO ₃ , pH 6.0 – 7.0, water–acetone , 80 °C	36	31	12
2	1:2 eq., Na ₂ CO ₃ , pH 6.0 – 7.0, water–ethanol , 80 °C	9	3.1	*

^a: Determined by CZE analysis; ^b: isolated product; *: Product was not isolated from the reaction mixture due to low conversion

As shown in Figure 7.2, the optimal co-solvent was found to be acetone whereas ethanol was found to be less effective in improving any of the results (conversion, reaction time and yield) in the synthesis of $d15_{bp}$ by conventional heating method.

The effects of various experimental conditions (temperature and solvent) on conversion, reaction times and yield were investigated and concluded that the conventional heating method for the synthesis of blue trichloropyrimidine dye $d15_{bp}$ is unsatisfactory and insufficient.

For these reasons, microwave irradiation was used for the syntheses of blue trichloropyrimidine dye **d15_{bp}** as well as for the modification of this dye.

7.1.4 Optimisation of Microwave-Irradiation Method for the Synthesis of Blue Trichloropyrimidine Dye **d15_{bp}**

For the optimisation of microwave irradiated synthesis of **d15_{bp}** several modifications and improvements have been sought. However, high yield was achieved by performing the reaction with sodium phosphate buffer pH 7.0 for 1.5 hours at 100 °C.

The percent conversion to blue trichloropyrimidine dye **d15_{bp}** are shown in Figure 7.3 and isolated yield are listed in Table 7.3.

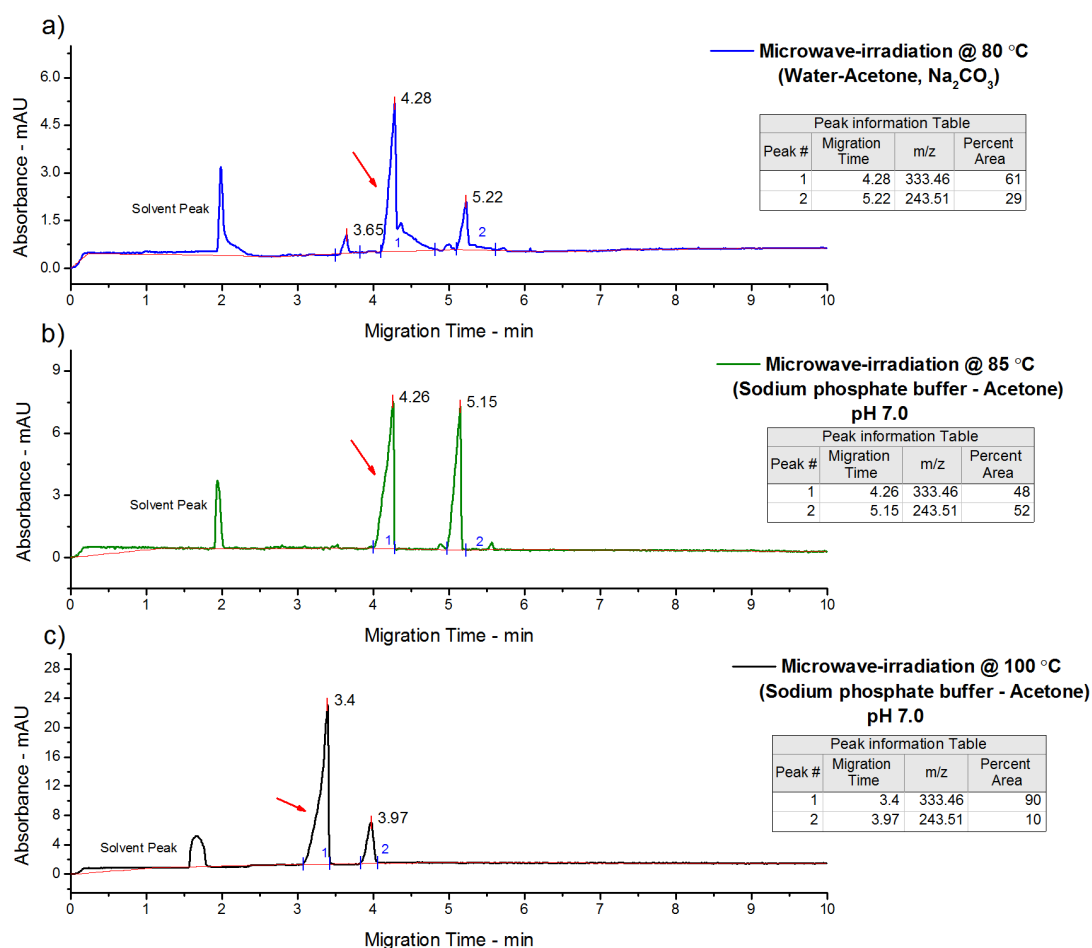


Figure 7.3: Electropherograms showing percent conversion to **d15_{bp} using microwave-irradiation method: (a) Water-acetone (Na₂CO₃) at 80 °C; (b) Sodium phosphate buffer pH 7.0 at 85 °C; (c) Sodium phosphate buffer pH 7.0 at 100 °C. CZE conditions: same as Figure 7.1.**

Table 7.3: Optimisation of reaction conditions for microwave-irradiated condensation reaction

Entry	Solvent (equal volumes)	Temperature (°C)	Time (hours)	Conversion (%)
1	Water – Acetone	80	7.5	61
2	Sodium phosphate buffer pH (7.0) –Acetone	85	1.5	48
3	Sodium phosphate buffer pH (7.0) –Acetone	100	1.5	90 [80] ^b
4	Sodium phosphate buffer pH (7.0) –Acetone	120	0.5	<i>a</i>

a: decomposition of product occur ; *b*: isolated yield

Using water-acetone as energy transfer medium in the presence of Na₂CO₃ (1 eq.), 61% conversion of **d9_b** to **d15_{bp}** was achieved after 7.5 hours at 80 °C (Figure 7.3a). However, substantial amount of by-product was also observed.

Therefore, sodium phosphate buffer pH 7.0 was used as energy transfer medium, 48% conversion of **d9_b** to **d15_{bp}** was achieved after 1.5 hours at 85 °C. Increasing the reaction temperature to 100 °C resulted in both a significant increase in the initial rate of reaction and in the overall conversion (90%), although further increments in the reaction temperature to 120 °C gave rise to much smaller changes to either the rate or final conversion; discolouration of the reaction mixtures was observed, indicating the start of undesirable decomposition.

7.1.5 Comparative Study of Conventional and Microwave-Irradiated Synthesis of Dye **d15_{bp}**

It can be seen in Figure 7.4, that the microwave irradiated reaction was completed in 1.5 hours (90 min) with 90% conversion, which signifies the dramatic acceleration of the condensation reaction of blue amino chromophore with 2,4,5,6-tetrachloropyrimidine in comparison to conventional heating which took 36 hours until only 31% conversion along with significant amount of hydrolysed by-products. This approach represents a much more efficient method of the synthesis compared to the traditional procedure discussed previously.

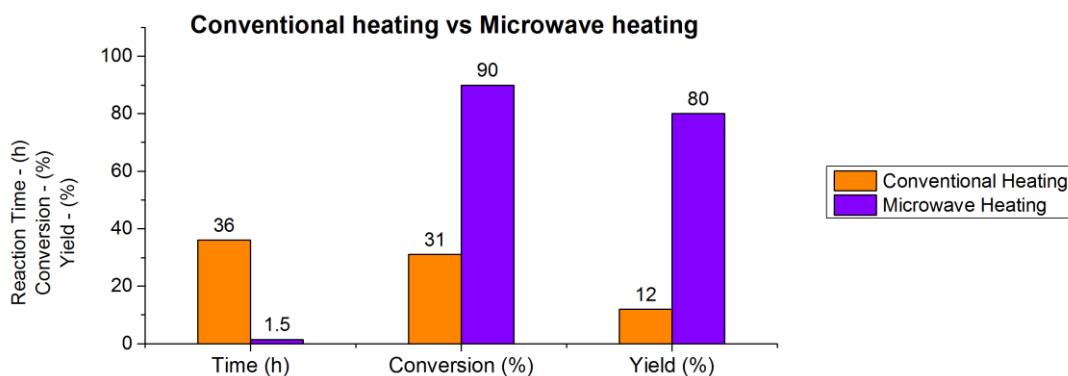


Figure 7.4: Comparison of reaction times, conversions and yields obtained by conventional heating and microwave heating

A comparison of yields obtained by conventional and microwave irradiated synthesis is shown in Figure 7.4. It was noted that time required for microwave irradiated synthesis was less and yield was high (80%) against conventional synthesis. The conventional synthesis of blue trichloropyrimidine dye **d15_{bp}** requires long reaction time at reflux temperature and obtain poor yield (12%).

From the above results, it could be concluded that the microwave irradiated method is an efficient, fast, simple method for the synthesis of blue trichloropyrimidine dye **d15_{bp}**. In addition the yield is also increased. Hence it is a viable and feasible method for the synthesis of dyes and intermediates.

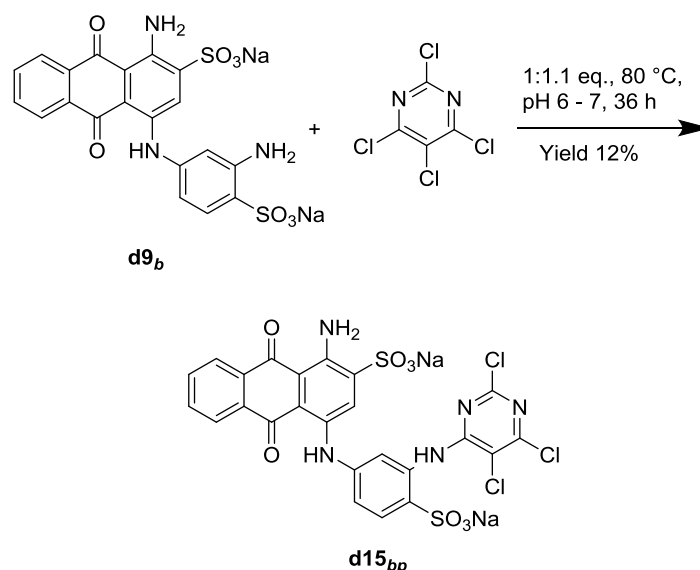
7.1.6 Synthesis of Blue 1-Amino-4-[3-[(2,5,6-Trichloro-4-pyrimidinyl)amino]-4-(sulfohenyl)amino]-Anthraquinone-2-Sulfonic Acid Dye (**d15_{bp}**)

7.1.6.1 Optimised Conventional Heating Method

In accordance with preparation method discussed in section 7.1.3, **d9_b** (10.67 g, 0.02 mol) was dissolved in water (50 cm³) which was adjusted to pH 7.0 by the addition of 2N sodium carbonate solution at 35 °C. A solution of 2,4,5,6-tetrachloropyrimidine (4.36 g, 0.02 mol) in acetone (50 cm³) was added as thin stream to the dye **d9_b** solution. Once the addition of tetrachloropyrimidine was complete, the reaction mixture was stirred and the pH was maintained at 6.0 to 7.0 by the addition of 2N sodium carbonate solution, while the temperature was raised and maintained at 80 °C (reflux). The reaction was stirred for further 36 hours (until the pH had stabilised) and was monitored with CZE and analytical TLC. When CZE

and TLC show no more conversion of **d9_b** to **d15_{bp}**, 2N sodium carbonate solution was added to raise the pH to 7.0 and sodium chloride (8% w/v) was added to precipitate the dye. The reaction mixture was filtered hot (55 °C) and the crude dye was collected and was washed with brine (2 × 100 cm³) and dried *in vacuo* (40 °C, 12 hours).

Purification of crude dye **d15_{bp}** using solvent-nonsolvent technique (1:2, DMF–diethyl ether) afforded the pure dye **d15_{bp}** (0.54 g, 0.75 mmol, yield 12%) as blue powder. The reaction is shown in Scheme 7.1.



Scheme 7.1: Condensation of 2,4,5,6-tetrachloropyrimidine with blue dye chromophore **d9_b to yield **d15_{bp}** by conventional heating method**

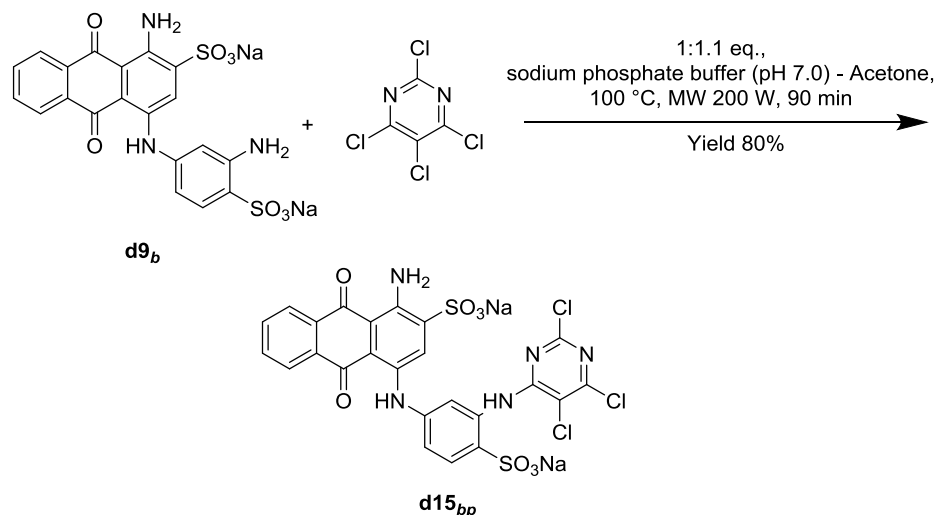
7.1.6.2 Optimised Microwave Irradiation Method

Blue dye chromophore **d9_b** (0.533 g, 1 mmol, 1 eq.) and 2,4,5,6-tetrachloropyrimidine (0.238 g, 1.1 mmol, 1.1 eq.) were added to each of the ten 35 ml microwave reaction vials equipped with a magnetic stirring bars followed by addition of 10 ml of sodium phosphate buffer [Na₂HPO₄ (0.20 M, 2 ml) and NaH₂PO₄ (0.12 M, 8 ml), pH 7.0] and 10 ml of acetone.

The mixtures were capped, mixed and irradiated in the microwave oven (200 W) for 1.5 hours (90 minutes) at 100 °C. Then the reaction mixtures were transferred from the vials to beaker and sodium chloride (8% w/v) was added to precipitate the dye. The reaction mixture was filtered hot (55 °C) and the crude dye was collected and was washed with brine and dried *in vacuo* (40 °C, 12 hours).

Purification of crude dye **d15_{bp}** using solvent-nonsolvent technique (1:2, DMF– diethyl ether) afforded the pure dye **d15_{bp}** (5.14 g, 7.10 mmol, yield 80%) as blue powder.

FT-IR analysis was conducted to confirm the presence of main functional groups in dye **d15_{bp}**. The reaction is shown in Scheme 7.2.



Scheme 7.2: Condensation of 2,4,5,6-tetrachloropyrimidine with blue dye chromophore **d9_b to yield **d15_{bp}** by microwave irradiation method**

7.1.6.3 Characterisation of Blue 1-Amino-4-[3-[(2,5,6-Trichloro-4-pyrimidinyl)amino]-4-(sulfophenyl)amino]-Anthraquinone-2-Sulfonic Acid Dye (**d15_{bp}**)

The peaks observed were as expected (Figure 7.5b); the first peak to emerge was **d15_{bp}** (3.39 min) which has the higher mass to charge ratio of the two analytes. This occurs because the addition of the pyrimidine group onto the dye chromophore **d9_b** increases the molecular weight of the dye **d15_{bp}** without any additional sulfonic acid groups that would increase the negative charge.

Moreover, the percent area of the **d15_{bp}** after isolation (Figure 7.5c) was 100% which indicates that there was no hydrolysed dye in the final product.

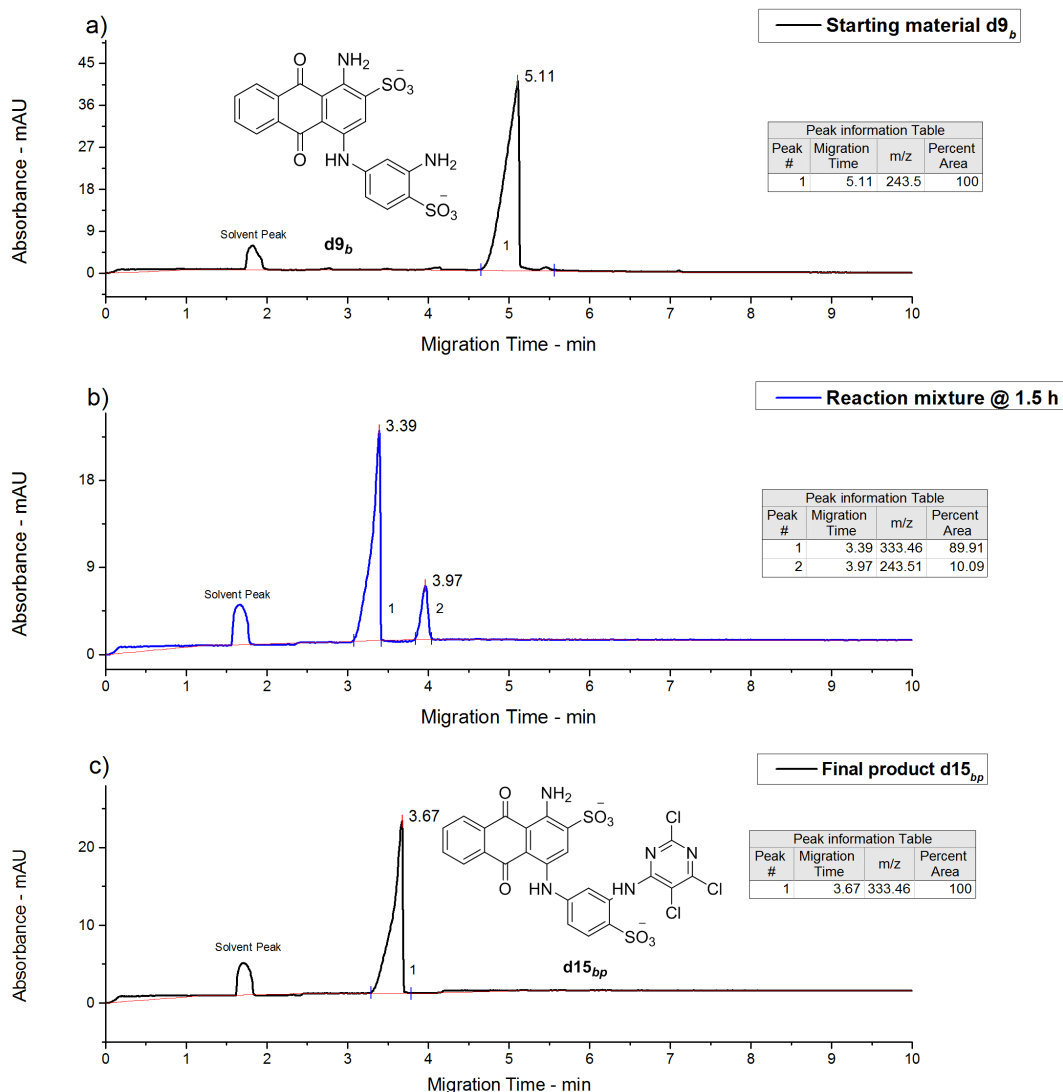


Figure 7.5: Electropherograms showing reaction progress of synthesis of $d15_{bp}$. (a) blue dye chromophore $d9_b$; (b) $d9_b$ – $d15_{bp}$ after 1.5 hours reaction time; (c) final product $d15_{bp}$. CZE conditions: same as Figure 7.1

R_f values were found to be 0.63 and 0.76 for starting material and product respectively.

In FT-IR spectrum of blue trichloropyrimidine dye $d15_{bp}$, the appearance of new peaks at 1531 cm^{-1} and 1416 cm^{-1} reflect the presence of the C=N group in dye $d15_{bp}$. Also the presence of the peaks at the 1093 cm^{-1} and 847 cm^{-1} [4, 5] are attributed to the C–Cl stretching vibration on the diazine ring of the dye.

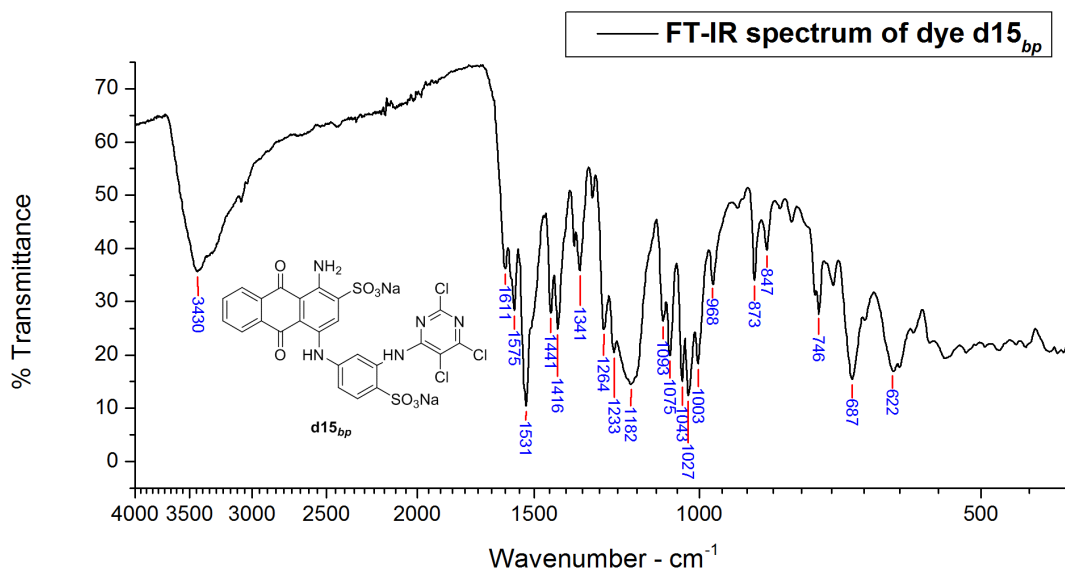


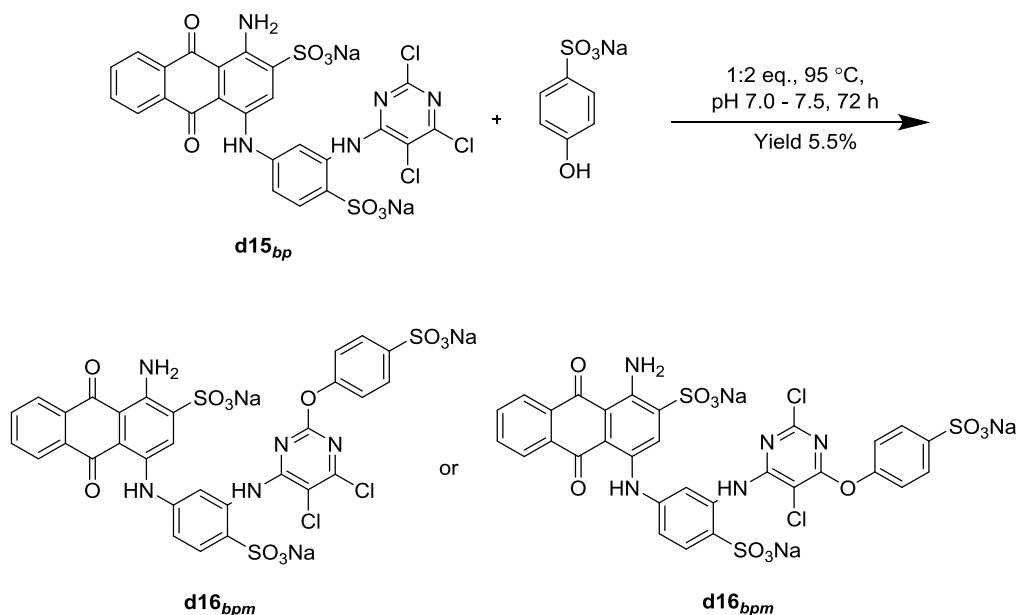
Figure 7.6: FT-IR spectrum of blue trichloropyrimidine dye **d15_{bp}**

The detailed analysis of spectrum (Figure 7.6) is as follows ^[6-9]; N–H stretch, 3430 cm^{-1} ; overtone or combinational bands, 2000 – 1700 cm^{-1} ; N–H bend, 1611 cm^{-1} ; C=C ring stretch, 1575 cm^{-1} , 1441 cm^{-1} , 1341 cm^{-1} ; C=N stretch, 1531 cm^{-1} , 1416 cm^{-1} ; C–N stretch, 1264 cm^{-1} ; C–CO–C, 1233 cm^{-1} ; sulfonate, 1182 cm^{-1} ; C–Cl stretch, 1093 cm^{-1} , 847 cm^{-1} ; in-plane C–H bend, 1043 cm^{-1} , 1027 cm^{-1} ; out of plane aromatic C–H bend, 746 cm^{-1} .

7.1.7 Synthesis of Modified Blue 1-Amino-4-[3-[[2-(4-Sulfophenoxy)-5,6-trichloro-4-pyrimidinyl]amino]-4-(sulfophenyl)amino]-Anthraquinone-2-Sulfonic Acid Dye (**d16_{bpm}**)

7.1.7.1 Conventional Heating Method

Dye **d15_{bp}** (7.14 g, 0.01 mol, 1 eq.) was dissolved in water (50 cm^3) at 25 °C. A solution of sodium 4-hydroxybenzenesulfonate dihydrate (4HBSA) (4.64 g, 0.02 mol, 2 eq.) in water (50 cm^3) was added to the **d15_{bp}** solution; pH was maintained at 7.0 to 7.5 by the addition of saturated sodium carbonate solution. Once the addition of 4HBSA solution was complete, the reaction mixture was refluxed at 95 °C and stirred until the pH had stabilised and was monitored with CZE and TLC. The reaction is shown in Scheme 7.3 and the CZE electropherograms showing the reaction progression is shown in Figure 7.7.



Scheme 7.3: Mono substitution of dye $d15_{bp}$ with 4HBSA to yield dye $d16_{bpm}$ by conventional heating

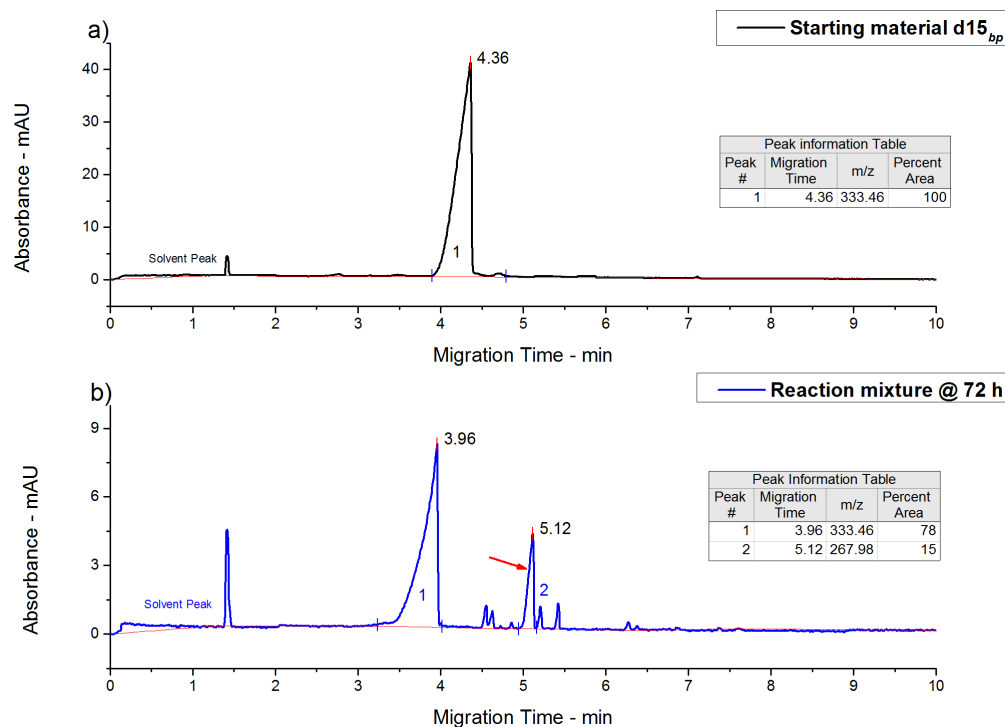


Figure 7.7: Electropherograms showing reaction progress of synthesis of $d16_{bpm}$. (a) blue dye $d15_{bp}$; (b) $d15_{bp}$ – $d16_{bpm}$ after 72 hours reaction time. CZE conditions: same as Figure 7.1

After the modification, the mass to charge ratio of the dye $d15_{bpm}$ decreases compared to the parent dye $d15_{bp}$, therefore the migration time of the dye $d16_{bpm}$ (5.12 min) (Figure 7.7b, peak 2) increases as compared to $d15_{bp}$ (3.96 min) (Figure

7.7b, peak 1). Furthermore, the percent conversion to modified dye **d16_{bpm}** was only 15% in 72 hours of reaction time with significant amount of by-products.

The reaction mixture was freeze dried and then was subsequently submitted to flash column chromatography using RP-18 silica gel and water as an eluent. The polarity of the eluent was then gradually decreased by the addition of methanol in 5 - 95% gradient and was applied at a relatively slow flow rate (10 ml·min⁻¹). The fractions containing blue product **d16_{bpm}** were collected. The pooled product-containing fractions were evaporated under vacuum to remove the methanol, and the remaining water was subsequently removed by freeze drying to yield the pure **d16_{bpm}** dye (71.2 mg, 0.08 mmol, yield 5.5%) as blue powder.

The conventional heating method resulted in poor conversion (14.71%), longer reaction time and poor yield of 5.5%. Therefore, microwave irradiated synthesis was adopted for the modification of **d15_{bp}**.

7.1.7.2 Optimisation of Microwave-Irradiation Method

For the optimisation of microwave irradiated synthesis of **d16_{bpm}** several modifications and improvements have been sought. However, high yield (74%) was achieved by performing the reaction with sodium phosphate buffer pH 7.4 for 3.5 hours at 100 °C. The percent conversion to modified dye **d16_{bpm}** and isolated yields are listed in Table 7.4.

Table 7.4: Optimisation of reaction conditions for microwave-irradiated condensation reaction

Entry	Solvent	Temperature (°C)	Time (hours)	Conversion (%)	Yield (%)
1	Water	130	1.5	≥ 50 ^{a,b}	43 _c
2	Water	100	6.5	≥ 50 ^{a,b}	38 _c
3	Sodium phosphate buffer pH (7.4)	100	2.5	≥70 ^a	-
4	Sodium phosphate buffer pH (7.4)	100	3.5	94	74 ^e

^a: Determined by analytical TLC; ^b: significant amount of by-product (di-substituted dye) ; ^c: product not pure; ^d: determined by CZE; ^e: isolated yield after flash column chromatography.

To optimise the reaction conditions, a mixture of reactants in water was initially exposed to microwave irradiation at 130 °C for 1.5 hours. TLC analysis indicated the reaction as uncompleted (conversion ≥ 50) with significant amount of di-substituted dye.

Therefore, sodium phosphate buffer pH 7.4 (neutral to alkaline) ^[10] was used as energy transfer medium, $\geq 70\%$ conversion of **d15_{bp}** to **d16_{bpm}** was observed after 2.5 hours at 100 °C. Increasing the reaction time to 3.5 hours resulted in significant increase in the overall conversion (94%), although further increments in the reaction time gave rise to much smaller changes to either the rate or final conversion.

7.1.8 Comparative Results of Conventional and Microwave-Assisted Synthesis of **d16_{bpm}**

A comparison between the results obtained under conventional heating and microwave-irradiated synthesis for the reaction times, conversions and yield are shown in Figure 7.8.

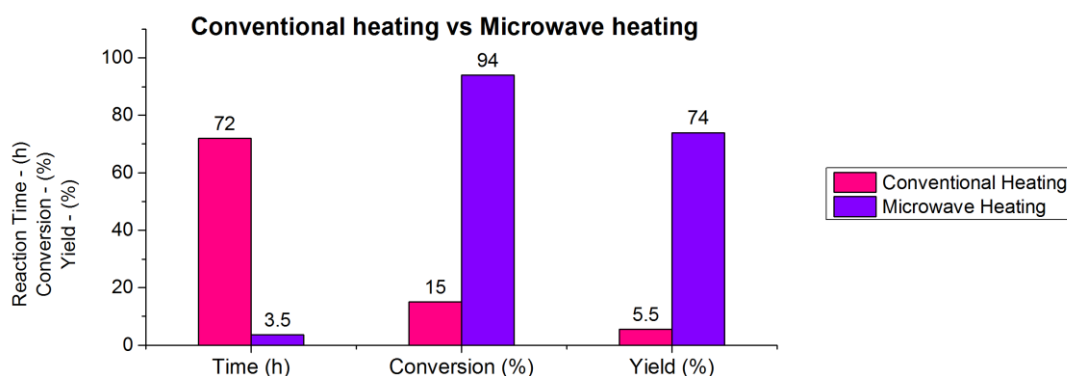


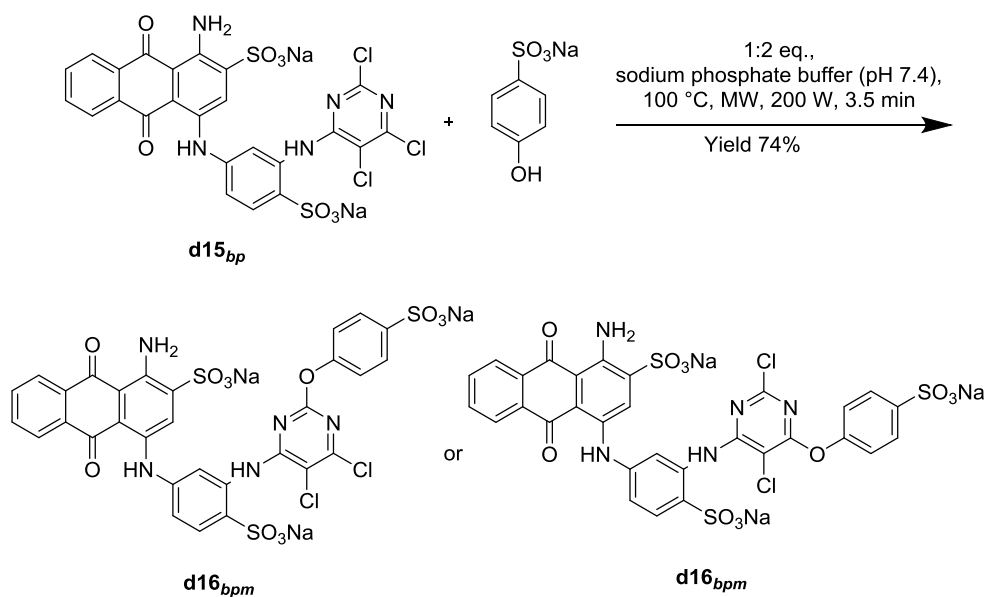
Figure 7.8: Comparison of reaction times, conversions and yields obtained by conventional heating and microwave irradiation (d16_{bpm}**)**

As can be seen in Figure 7.8, microwave heating effectively reduced the reaction time from 72 hours to a few hours (3.5 hours) with significant enhancement in the conversions percent from only 15% to 94%. By using microwave radiation for heating, the modified mono-substituted dye **d16_{bpm}** was prepared in yield (74%) that was appreciably higher than the conventional method (5.5%) in high purity (see Figure 7.9c).

7.1.9 Synthesis of Modified Blue 1-Amino-4-[3-[[2-(4-sulfophenoxy)-5,6-trichloro-4-pyrimidinyl]amino]-4-(sulfophenyl)amino]-Anthraquinone-2-Sulfonic Acid Dye (**d15_{bp}**) using Optimised Microwave-irradiation Method

Blue trichloropyrimidine dye **d15_{bp}** (0.714 g, 0.1 mmol, 1 eq.) and sodium 4-hydroxybenzenesulfonate dihydrate (4HBSA) (0.464 g, 0.2 mmol, 2 eq.) were added to each of the five 35 ml microwave reaction vials equipped with magnetic stirring bars followed by addition of 20 ml of sodium phosphate buffer [Na_2HPO_4 (0.20 M, 8 ml) and NaH_2PO_4 (0.12 M, 12 ml), pH 7.4].

The mixtures were capped and irradiated in the microwave oven (200 W) for 3.5 hours at 100 °C. The reaction mixtures were combined and purified through flash column chromatography as discussed in section 2.5.4 to yield pure **d16_{bpm}** dye (3.03 g, 3.46 mmol, yield 74%) as blue powder. The optimal conditions of reaction are shown in Scheme 7.4.



Scheme 7.4: Mono substitution of dye **d15_{bp} with 4HBSA to yield dye **d16_{bpm}** by microwave irradiation**

7.1.9.1 Characterisation of Modified Blue 1-Amino-4-[3-[[2-(4-sulfophenoxy)-5,6-trichloro-4-pyrimidinyl]amino]-4-(sulfophenyl)amino]-Anthraquinone-2-Sulfonic Acid Dye (**d16_{bpm}**)

The electropherograms from CZE analysis are shown in Figure 7.9 which indicates the progression of the synthesis reaction from the starting dye **d15_{bp}** to the mono-substituted dye **d16_{bpm}** (peak 2 in Figure 7.9b).

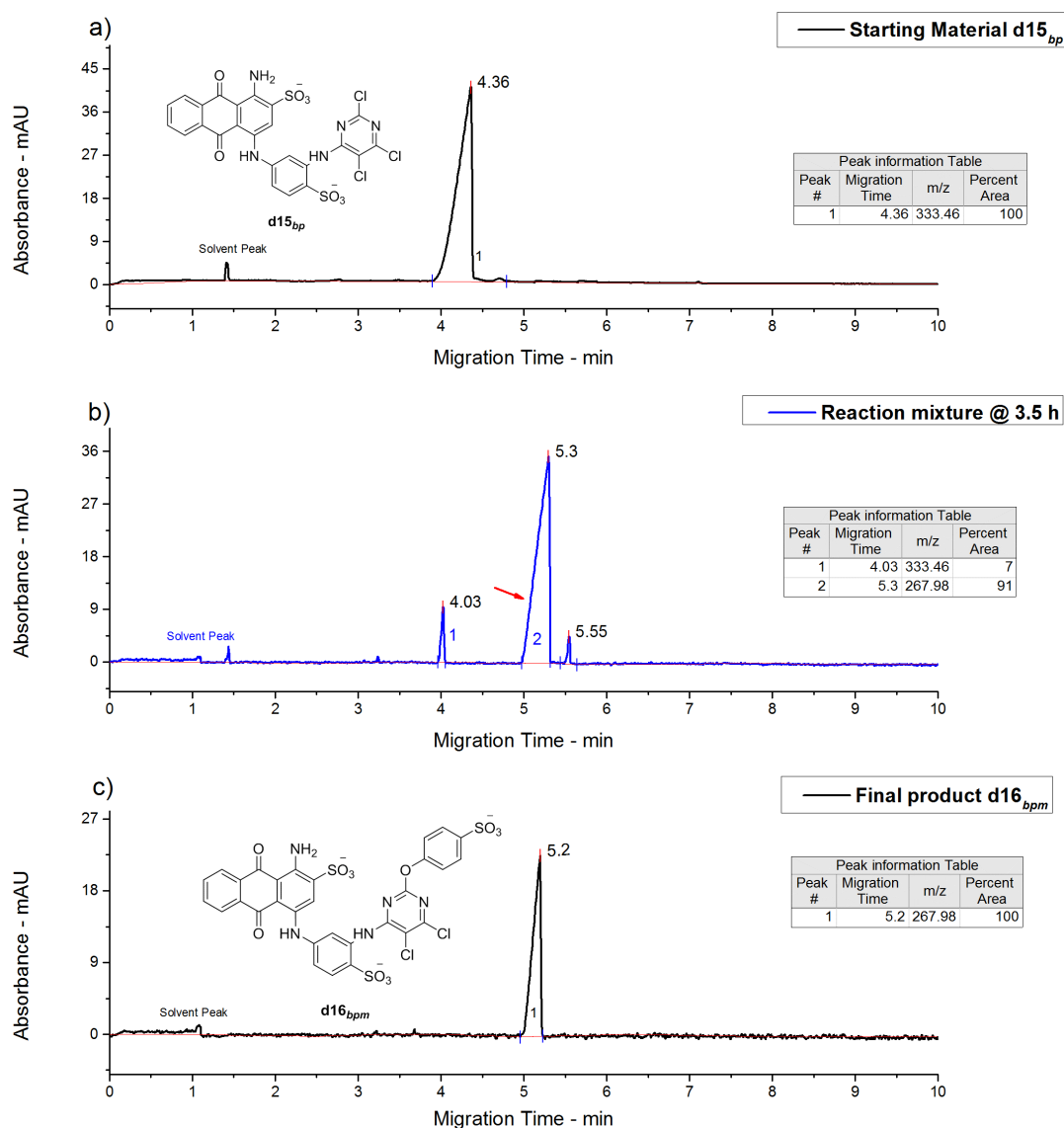


Figure 7.9: Electropherograms showing reaction progress of synthesis of **d16_{bpm}. (a) blue dye **d16_{bpm}**; (b) **d15_{bp}** – **d16_{bpm}** after 3.5 hours reaction time; (c) Final product **d16_{bpm}**. CZE conditions: same as Figure 7.1**

As shown in Figure 7.9b, after the modification, the mass to charge ratio of the dye **d16_{bpm}** decreases compared to the parent dye **d15_{bp}**, therefore the migration time of the modified dye **d16_{bpm}** (5.3 min) increases as compared to **d15_{bp}** (4.03 min).

In analytical TLC analysis, the spots appeared as expected, and R_f values were 0.76 and 0.70 for the starting material **d15_{bp}** and product **d16_{bpm}** respectively.

In FT-IR spectrum of the mono-substituted dye **d16_{bpm}**, Figure 7.10, the new peak at 1123 cm^{-1} is evident which can be attributed to the stretching vibration of C–O–C in its structure between the diazine and the 4HBSA. The peaks at 1091 cm^{-1} and 828 cm^{-1} can be attributed to the presence of C–Cl after the mono substitution of dye **d15_{bp}** with 4HBSA.

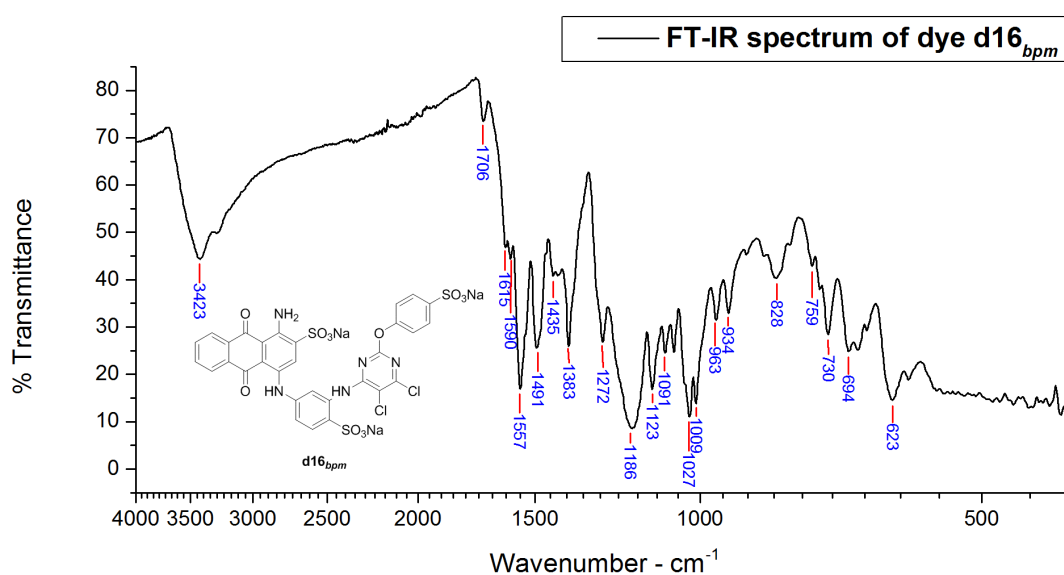


Figure 7.10: FT-IR spectrum of blue mono-substituted dye **d16_{bpm}**

The detailed analysis of the spectrum (Figure 7.10) is as follows ^[6-9]; N–H stretch, 3423 cm^{-1} ; overtone or combinational bands, $2000\text{--}1700\text{ cm}^{-1}$; C=O stretching, 1706 cm^{-1} ; N–H bending, 1615 cm^{-1} ; C=C ring stretch, 1590 cm^{-1} , 1491 cm^{-1} , 1435 cm^{-1} ; C=N stretch, 1557 cm^{-1} , 1383 cm^{-1} ; C–N stretch, 1272 cm^{-1} ; C–O–C stretching, 1123 cm^{-1} ; sulfonate, 1186 cm^{-1} ; C–Cl stretch, 1091 cm^{-1} , 828 cm^{-1} ; in-plane C–H bend, 1027 cm^{-1} , 1009 cm^{-1} ; out of plane aromatic C–H bend, 730 cm^{-1} .

Elemental analysis, Found: C, 39.88%; H, 1.99 %; N, 7.59%. Calculated for $\text{C}_{30}\text{H}_{16}\text{Cl}_2\text{N}_5\text{Na}_3\text{O}_{12}\text{S}_3 \cdot \text{H}_2\text{O}$: C, 40.39%; H, 2.03%; N, 7.85%. It should be noted that the results are adjusted due to the presence of water of crystallisation.

7.1.10 Application of Blue Dyes ($d15_{bp}$ and $d16_{bpm}$) onto Wool Fabric by Inkjet Printing

The inks were prepared using 4% dye according to the procedure detailed in section 2.5.2, and then tested for viscosity and surface tension.

The resulting ink formulation was then introduced in the cartridge and printed onto wool fabric using HP 6940 deskjet printer. Once printed, the printed wool samples were fixed by two methods detailed in section 2.5.4, and evaluated for percent fixation along with light fastness and wash fastness.

Moreover the inks were also evaluated for stability through CZE over three months storage time at room temperatures.

7.1.11 Characteristics of Formulated Inks ($d15_{mp}$ and $d16_{bpm}$)

7.1.11.1 Surface Tension and Viscosity of Inks

It can be seen, from Table 7.5, that parent dye $d15_{bp}$ and the modified dye $d15_{bpm}$ based inks had a surface tension and viscosity within the operational range.

Table 7.5: Ink measured properties

Ink formulation	Surface Tension (dynes.cm ⁻¹)	Viscosity (cP)
$d15_{bp}$	42.3	6
$d16_{bpm}$	40.5	8

7.1.11.2 Stability of Dye ($d15_{bp}$ and $d16_{bpm}$) Based Inks

Stability of blue trichloropyrimidine dye $d15_{bp}$ along with new modified dye $d16_{bpm}$ in inks were also evaluated.

The results of any change in percent area of peaks of the dyes within inks stored at room temperature for three month can be seen in Figure 7.11.

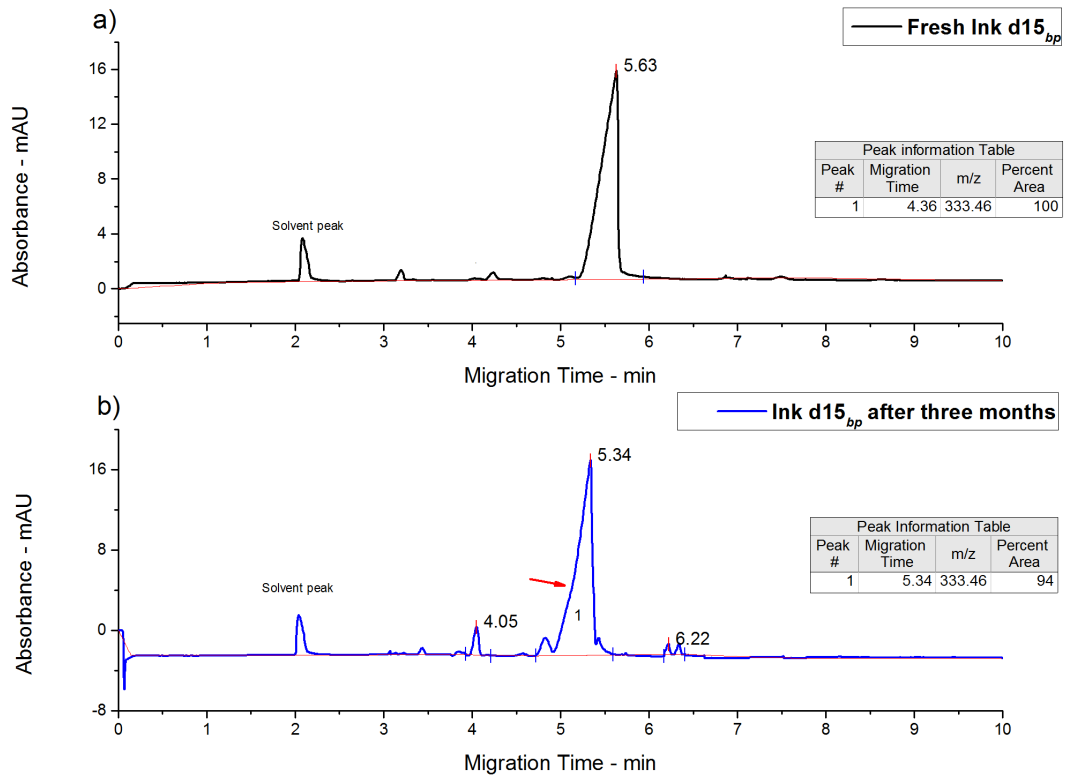


Figure 7.11: Electropherograms showing d15_{bp} based ink stability. (a) Fresh ink; (b) Ink after three months storage at room temperature

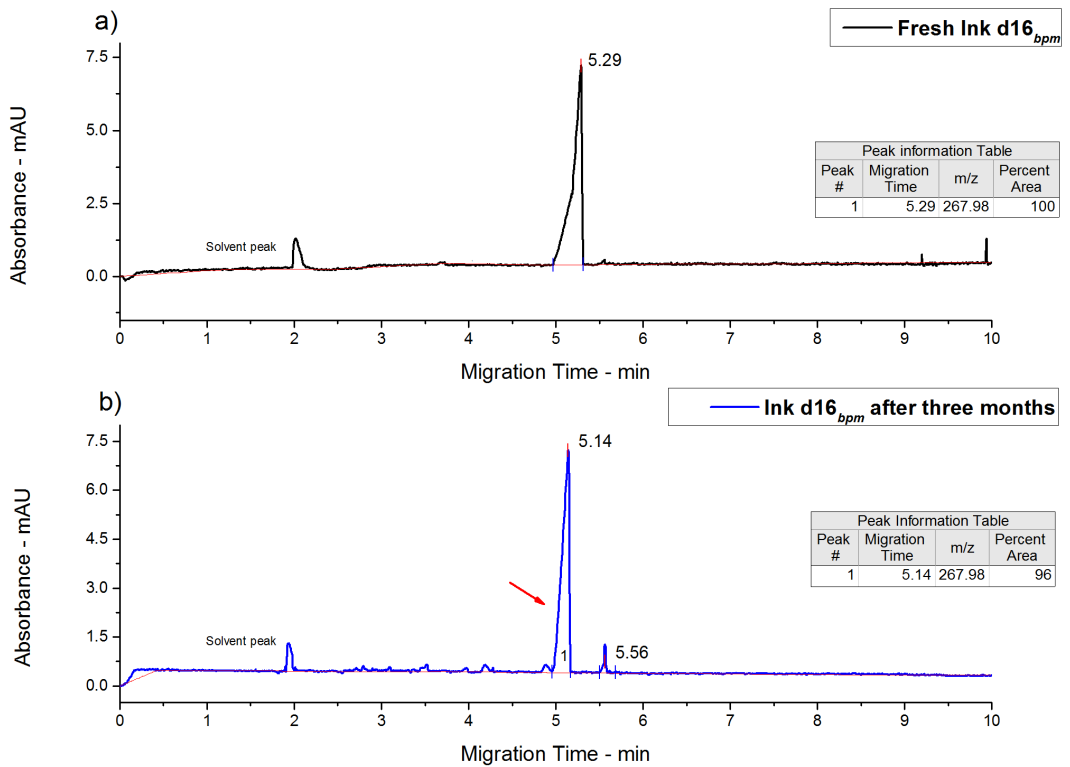


Figure 7.12: Electropherograms showing d16_{bpm} based ink stability. (a) Fresh ink; (b) Ink after three months storage at room temperature

As shown in Figure 7.11 and Figure 7.12, no significant changes in the percent area of peaks of both, *i.e.*, blue trichloropyrimidine dye **d15_{bp}** and modified dye **d16_{bpm}** based ink were observed signifying that there had been no detrimental effect caused by the modification of blue trichloropyrimidine dye with 4HBSA.

Moreover, the good stability of parent trichloropyrimidine could be associated with its low reactivity.

7.1.12 Evaluation of Percent Fixation of Blue Dyes (**d15_{bp}** and **d16_{bpm}**) by Different Fixation Methods

The maximum percent fixations of blue trichloropyrimidine dye **d15_{bp}** and blue modified dye **d16_{bpm}** for batching at 90 °C and steaming at 102 °C are shown in Figure 7.13.

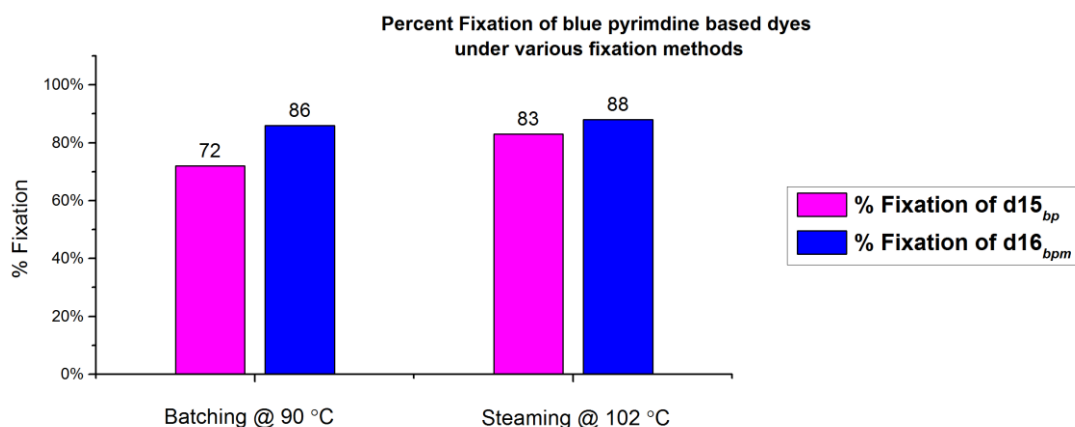


Figure 7.13: Percent fixation of **d15_{bp} and **d16_{bpm}** under various fixation methods**

As shown in Figure 7.13, inkjet printing with **d15_{bp}** based ink carried out using a print–batch (high temperature) process showed medium level of percent fixation (72% for **d15_{bp}**) along with unlevelled prints. Whereas, modified blue dye **d16_{bpm}** gave marginally high fixation with leveled prints. This is due to the low reactivity of modified dye. The lower reactivity of the new dye would be viewed as advantageous as it allows greater control of the absorption phase and thus leads to increased leveling properties.

Figure 7.13 also reflects the effect of steaming on the percent fixation of blue trichloropyrimidine and modified dye printed on the wool fabric. The blue mono-substituted dye **d16_{bpm}** (88%) showed the best percent fixation followed by

trichloropyrimidine dye **d15_{bp}** (83%). This is because mono-substituted dye being less reactive than the parent trichloropyrimidine dye allowed more controlled formation of covalent bonds between the dye molecule and the wool fibre.

7.1.13 Light Fastness

Light fastness testing was carried out according to the BS EN ISO 105-B02:2013 (Method 3) ^[11].

The printed samples were tested against blue wool reference 6. As shown in Table 7.6, both the dyes pass target wool reference 6. However, modified dye **d16_{bpm}** shows even better light fastness than target wool reference 6.

Table 7.6: Light fastness of blue dyes (d15_{bp} and d16_{bpm}) compared to target blue wool reference 6

Dye/Ink	Target blue wool reference 6	
	d15_{bp}	Equal to 6 (6)
d16_{bpm}	Better than 6 (6 ⁺)	Satisfactory

7.1.14 Wash Fastness

Wash fastness was carried out according to the BS ISO 105-C06:2010 ^[12] and the results are shown in Table 7.7. The tested fabric sample printed with modified blue dye **d16_{bpm}** showed no evidence of any colour loss or staining of multifibre adjacents. Hence, the wash fastness tests showed that there had been no detrimental effect caused by modifying the dye. However, parent trichloropyrimidine dye show slight change in shade (4-5) and slight staining on cotton.

Table 7.7: Wash fastness of blue dyes (d15_{bp} and d16_{bpm})

Dye/Ink	Change in shade	Staining					
		CA	C	N	P	A	W
d15_{bp}	4-5	5	4-5	5	5	5	5
d16_{bpm}	5	5	5	5	5	5	5

CA: Cellulose Acetate; C: Cotton; N: Nylon; P: Polyester; A: Acrylic; W: Wool

7.2 Conclusions

With the help of microwave irradiation, the blue trichloropyrimidine dye **d15_{bp}** and modified dye **d16_{bpm}** were prepared. By using the new method, the reaction time was shortened, conversion to product was significantly increased with high yields of dyes in pure form were achieved in comparison with conventional synthesis at elevated temperatures.

By employing the microwave irradiation method difficultly synthesised **d15_{bp}** dye was successfully synthesised in pure 80% yield in 1.5 hours at 100 °C with 90% conversion.

Moreover, the modification of **d15_{bp}** was successfully done by using microwave irradiation. at 100 °C, virtually quantitative conversion could be achieved within 3.5 hours.

In addition, for these syntheses reactions performed under microwave irradiation, sodium phosphate buffer was found to be the solvent of choice, provided temperatures were kept below 110 °C. At higher reaction temperatures, significant amount of hydrolysis would occur.

The modification of trichloropyrimidine dye with 4HBSA found to advantageous in terms of increasing the solubility of dyes, increasing the percent fixation and maintaining the high stability associated with pyrimidine group.

The performance properties were found to be excellent.

7.3 References

1. Patent GB1140998 (1969)
2. Patent GB1581019 (1980)
3. Patent DE2729497 (1979)
4. Lewis, D.M. and Wang, J.C. The use of fourier transform infrared (FT-IR) spectroscopy to study the state of heterobifunctional reactive dyes. *Dyes and Pigments*, 1998, **39**, pp.111-123.
5. Daimay, L.-V., Colthup, N.B., Fateley, W.G. and Grasselli, J.G. *The handbook of infrared and Raman characteristic frequencies of organic molecules*. London: Academic Press Ltd., 1991.

6. Matlok, F., Gremlich, H.U., Bruker Analytische Meotechnik and Merck eds. *Merck FT-IR atlas : a collection of FT-IR spectra*. Weinheim: Vch, 1988.
7. Keller, R.J. and Sigma-Aldrich Corporation. *The Sigma library of FT-IR spectra*. Missouri: Sigma Chemical Company, 1986.
8. Socrates, G. *Infrared and Raman characteristic group frequencies : tables and charts*. Chichester: Wiley, 2001.
9. Silverstein, R.M., Webster, F.X. and Kiemle, D.J. *Spectrometric Identification of Organic Compounds*. 7th ed. New York: John Wiley and Sons, 2005.
10. Clark, M., Yang, K. and Lewis, D.M. Modified 2,4-difluoro-5-chloropyrimidine dyes and their application in inkjet printing on wool fabrics. *Coloration Technology*, 2009, **125**, pp.184-190.
11. British Standards Institution. *Colour fastness to artificial light: Xenon arc fading lamp test*, ISO 105-B02:2013.
12. British Standards Institution. *Textiles - Tests for colour fastness - Part C06: Colour fastness to domestic and commercial laundering*, BS EN ISO 105-C06:2010.

8 Synthesis, Modification and Characterisation of Yellow Trichloropyrimidine Dyes for Inkjet Inks

This chapter details the synthesis, modification and characterisation of yellow dyes based on pyrimidine reactive group by the conventional heating method as well as microwave irradiation. The syntheses progression were monitored through MEKC and TLC and the structural changes were confirmed by FT-IR.

However, due to time limitation the inks were not evaluated to the full extent as other inks were evaluated.

8.1 Experimental

8.1.1 Materials

Yellow dye chromophore **d5_y** (100%), 2,4,5,6-tetrachloropyrimidine (97%), sodium 4-hydroxybenzenesulfonate dihydrate (98%), sodium metabisulfite, carboxymethyl cellulose, polysorbate 20 (Tween 20) and N-methylmorpholine N-oxide (NMO) were purchased from Sigma-Aldrich and used as received. Urea (MP Biomedicals), Alcopol O 60 (Acros organics), 2-pyrrolidone (Acros organics), 2-propanol (Fisher), Sandozin NIE (Clariant) were also purchased and used as received.

8.1.2 Synthesis of Yellow 7-[(2,5,6-Trichloro-4-pyrimidinyl)amino]-2-[(methylphenyl)azo]-1,3-Naphthalenedisulfonic Acid Dye (**d17_{yp}**)

8.1.2.1 Conventional Heating Method

Dye **d5_y** (4.65 g, 0.01 mol) was dissolved in water (50 cm³) which was adjusted to pH 7.0 by the addition of 2N sodium carbonate solution at 35 °C. A solution of tetrachloropyrimidine (2.38 g, 0.011 mol) in acetone (50 cm³) was added as thin stream to the dye **d5_y** solution. Once the addition of tetrachloropyrimidine was complete, the reaction mixture was stirred and the pH was maintained at 6.0 – 7.0 by the addition of 2N sodium carbonate solution. The reaction was stirred for further 6 hours (until the pH had stabilised) and was monitored with MEKC and analytical TLC. 2N sodium carbonate solution was added to raise the pH to 7.0 and

sodium chloride (8% w/v) was added to precipitate the dye. The reaction mixture was filtered and the crude dye was collected and was washed with brine ($2 \times 100 \text{ cm}^3$) and dried *in vacuo* (40 °C, 12 hours).

Purification of crude dye **d17_{yp}** using solvent-nonsolvent technique (1:2, DMF–acetone) afforded the pure dye **d17_{yp}** (3.86 g, 5.96 mmol, yield 59.7%) as yellow powder. The reaction is shown in Scheme 8.1.

8.1.2.2 Optimised Microwave-Irradiation Method

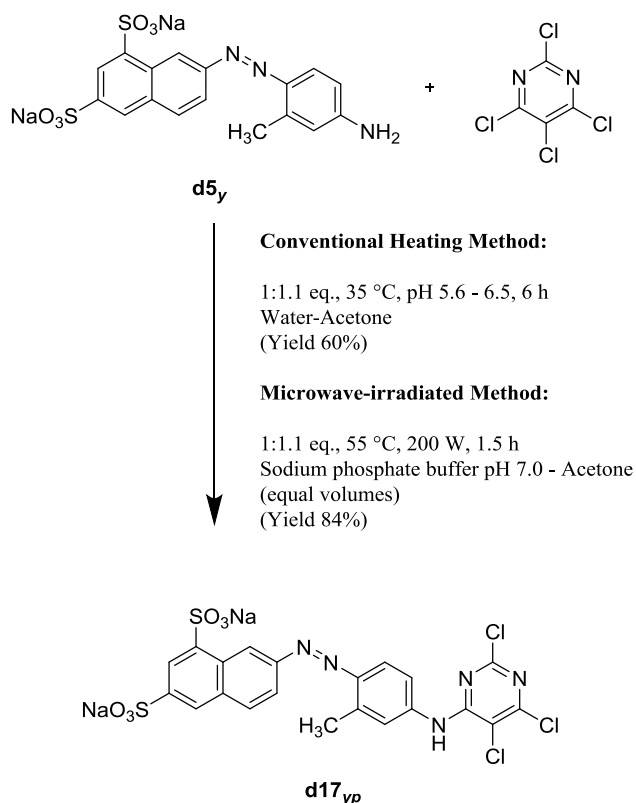
For the optimisation of microwave irradiated synthesis of **d17_{yp}**, initial investigations were undertaken using optimised conditions (discussed in section 6.2.6.2 and 7.1.6.2). However, at high temperatures (80 and 100 °C) decomposition and discoloration of the reaction mixture and the product was observed. Therefore, mild conditions, i.e. sodium phosphate buffer [Na_2HPO_4 (0.20 M, 2 ml) and NaH_2PO_4 (0.12 M, 8 ml), pH 7.0] at 55 °C, were used. Which resulted in high yield 84% in only 1.5 hours at 55 °C in contrast to 60% achieved from conventional heating in 6 hours.

8.1.2.2.1 Optimised Conditions for Synthesis of **d17_{yp}**

Yellow dye chromophore **d5_y** (0.465 g, 1 mmol, 1 eq.) and 2,4,5,6-tetrachloropyrimidine (0.238 g, 1.1 mmol, 1.1 eq.) were added to each of the ten 35 ml microwave reaction vials equipped with a magnetic stirring bars followed by addition of 10 ml of sodium phosphate buffer [Na_2HPO_4 (0.20 M, 2 ml) and NaH_2PO_4 (0.12 M, 8 ml), pH 7.0] and 10 ml of acetone.

The mixtures were capped, mixed and irradiated in the microwave oven (200 W) for 1.5 hours (90 minutes) at 55 °C. Then the reaction mixtures were transferred from the vials to beaker and sodium chloride (8% w/v) was added to precipitate the dye. The brine and dried *in vacuo* (40 °C, 12 hours).

Purification of crude dye **d17_{yp}** using solvent-nonsolvent technique (1:2, DMF– acetone) afforded the pure dye **d17_{yp}** (5.41 g, 8.36 mmol, yield 84%) as yellow powder. FT-IR analysis was conducted to confirm the presence of main functional groups in dye **d17_{yp}**. The reaction is shown in Scheme 8.1.



Scheme 8.1: Condensation of 2,4,5,6-tetrachloropyrimidine with yellow dye chromophore **d5_y to yield **d17_{yp}** by conventional and microwave irradiation method**

8.1.3 Comparative Study of Conventional and Microwave-Irradiated Synthesis of Dye **d17_{yp}**

It can be seen in Figure 8.1a and b, a reaction that takes 6 hours with conventional heating method, microwave irradiation of **d5_y** with 2,4,5,6-tetrachloropyrimidine in the presence of sodium phosphate buffer pH 7.0 gave **d17_{yp}** in 1.5 hours at 55 °C. In addition to the reduced reaction time, the yield of **d17_{yp}** was significantly better as well (conventional heating, 60% versus microwave heating, 84%).

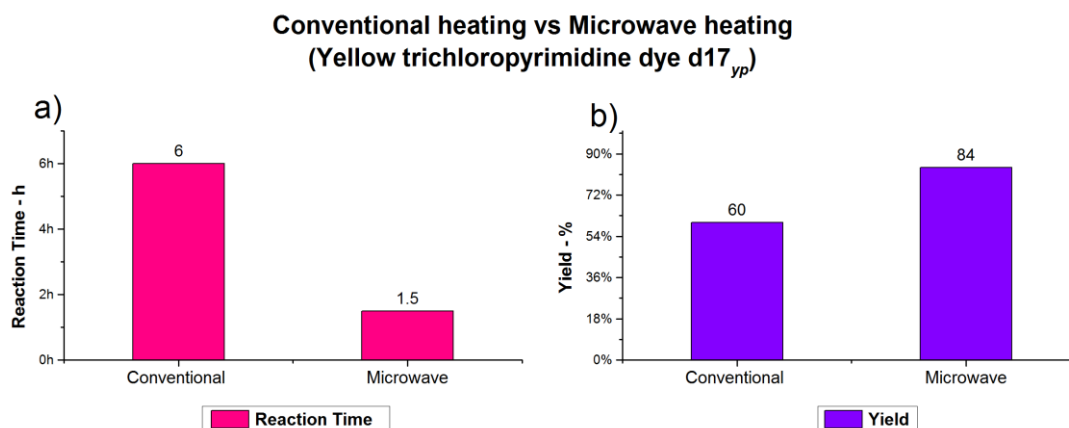


Figure 8.1: Comparison of reaction times and yields obtained by conventional heating and microwave heating

Therefore, it is concluded that the microwave irradiated method is an efficient, fast, simple method for the synthesis of yellow trichloropyrimidine dye $d17_{yp}$ which gave product of high purity in high yield.

8.1.4 Characterisation of Yellow 7-[(2,5,6-Trichloro-4-pyrimidinyl) amino]-2-[(methylphenyl)azo]-1,3-Naphthalenedisulfonic Acid Dye ($d17_{yp}$)

As shown in Figure 8.2b, water migrates quickly at the EOF velocity followed by $d5_y$ (5.2 min) and then $d17_{yp}$ (6.78 min), this is because dye $d17_{yp}$ has an increased molecular weight compared to dye $d5_y$ but no additional sulfonate groups that would increase the solubility of the dye $d17_{yp}$.

Moreover, the percent area of the $d17_{yp}$ shown in Figure 8.2c, was 100% which indicates that there was no hydrolysed dye in the final product.

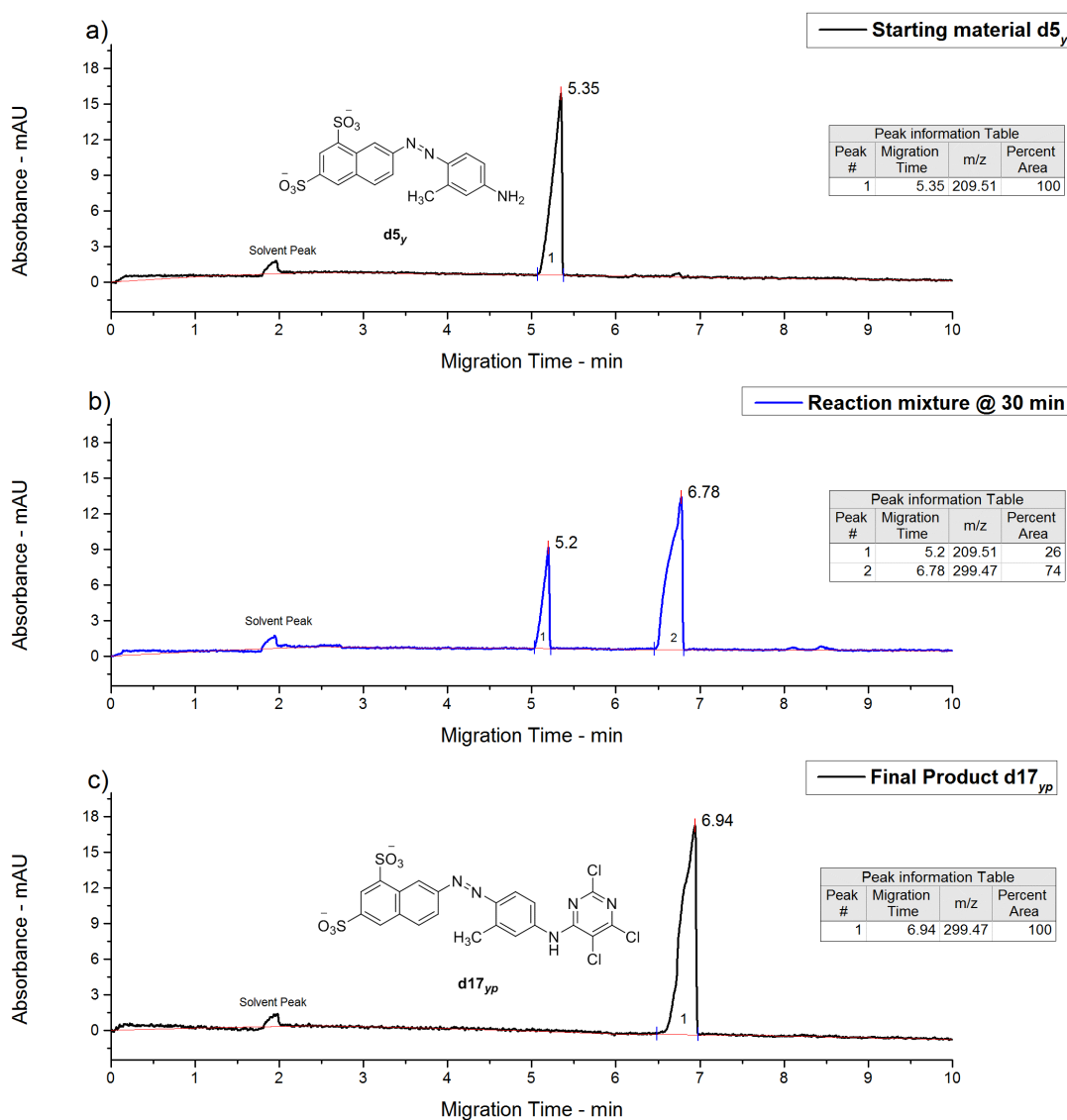


Figure 8.2: Electropherograms showing reaction progress of synthesis of $d17_{yp}$. (a) yellow dye chromophore $d5_y$; (b) $d5_y - d17_{yp}$ after 30 min reaction time; (c) final product $d17_{yp}$. MEKC conditions: running buffer, 20 mM sodium tetraborate, 50 mM sodium dodecyl sulphate (SDS), pH 9.3; pressure injection 0.5 psi for 10 s; voltage 25 kV; detection at 420 nm

The R_f values of starting material $d5_y$ and product $d17_{yp}$ were 0.63 and 0.66 respectively.

Analysis of FT-IR spectrum (Figure 8.3) of pure powder suggested that the compound has been $d17_{yp}$ since peaks due to the presence of primary amine in $d5_y$, Figure 4.2 (page 96) at 1588 cm^{-1} no longer present indicating that the primary amine had successfully reacted with 2,4,5,6-tetrachloropyrimidine. The appearance of new peaks at 1538 cm^{-1} and 1387 cm^{-1} reflect the presence of the C=N group in $d17_{yp}$. Moreover, in accordance with literature [1, 2], the appearance of the peaks at

the 1098 cm^{-1} and 849 cm^{-1} [3, 4] are attributed to the stretching vibrations of carbon chlorine bond on the diazine ring of the **d17_{yp}**.

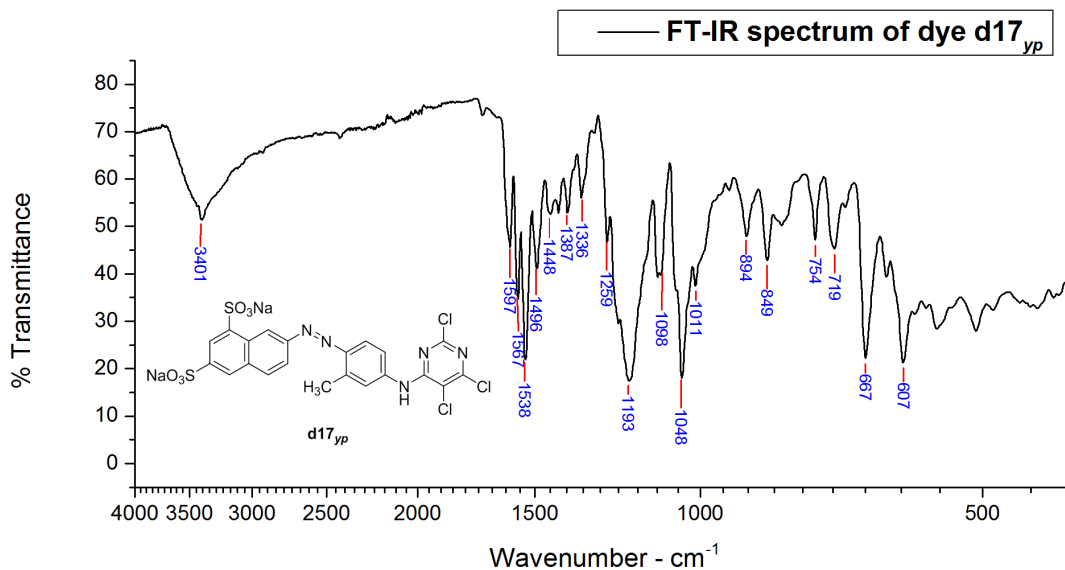


Figure 8.3: FT-IR spectrum of yellow trichloropyrimidine dye **d17_{yp}**

The detailed analysis of spectrum (Figure 8.3) is as follows [1, 2, 5, 6]; N–H stretch, 3401 cm^{-1} ; overtone or combinational bands, $2000\text{--}1667\text{ cm}^{-1}$; N–H bend, 1597 cm^{-1} ; C=C ring stretch, 1567 cm^{-1} , 1567 cm^{-1} , 1496 cm^{-1} ; azo group stretch, 1448 cm^{-1} ; C=N stretch, 1538 cm^{-1} , 1387 cm^{-1} ; C–N stretch, 1336 cm^{-1} ; sulfonate, 1193 cm^{-1} ; C–Cl stretch, 1098 cm^{-1} , 849 cm^{-1} ; in-plane C–H bend, 1048 cm^{-1} , 1011 cm^{-1} ; out of plane aromatic C–H bend, 754 cm^{-1} ; CH_3 rock 726 cm^{-1} .

8.1.5 Synthesis of Modified Yellow 7-[[2-(4-Sulfophenoxy)-5,6-dichloro-4-pyrimidinyl]amino]-2-[(methylphenyl)azo]-1,3-Naphthalenedisulfonic Acid Dye (**d18_{ypm}**)

8.1.5.1 Conventional Heating Method

Dye **d17_{yp}** (3.23 g, 0.005 mol, 1 eq.) was dissolved in water (50 cm^3) at $25\text{ }^\circ\text{C}$. A solution of sodium 4-hydroxybenzenesulfonate dihydrate (4HBSA) (2.32 g, 0.01 mol, 2 eq.) in water (50 cm^3) was added to the **d17_{yp}** solution; pH was maintained at 7.0 – 7.5 by the addition of saturated sodium carbonate solution. Once the addition of 4HBSA solution was complete, the reaction mixture was refluxed at $85\text{ }^\circ\text{C}$ and stirred until the pH had stabilised and was monitored with MEKC and TLC. The reaction is shown in Scheme 8.2.

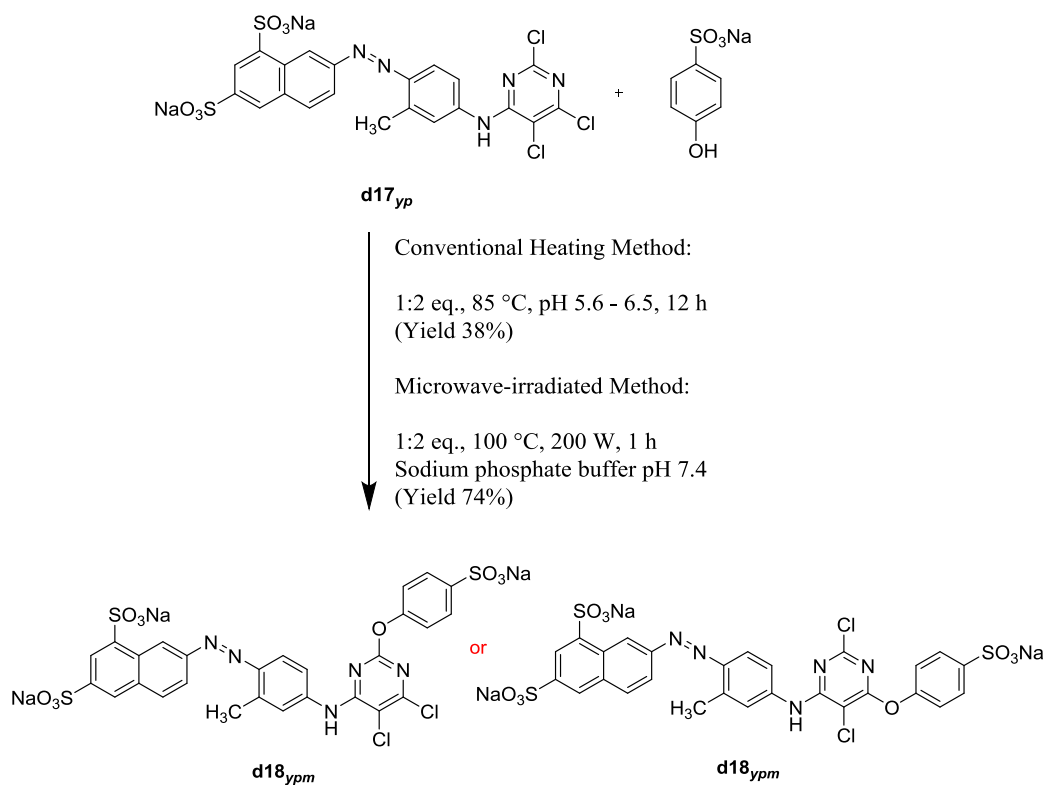
The conventional heating method resulted in longer reaction time (12 hours) and poor yield of 38%. Therefore, microwave irradiated synthesis was adopted for the modification of **d17_{yp}**.

8.1.5.2 Optimisation of Microwave-Irradiation Method

For the optimisation of microwave irradiated synthesis of **d18_{ypm}** several modifications and improvements have been sought. However, high yield (74%) was achieved by performing the reaction with sodium phosphate buffer pH 7.4 for 1 hour at 100 °C.

Yellow trichloropyrimidine dye **d17_{yp}** (0.646 g, 0.1 mmol, 1 eq.) and sodium 4-hydroxybenzenesulfonate dihydrate (4HBSA) (0.464 g, 0.2 mmol, 2 eq.) were added to each of the five 35 ml microwave reaction vials equipped with magnetic stirring bars followed by addition of 20 ml of sodium phosphate buffer [Na_2HPO_4 (0.20 M, 8 ml) and NaH_2PO_4 (0.12 M, 12 ml), pH 7.4].

The mixtures were capped and irradiated in the microwave oven (200 W) for 1 hours at 100 °C. The reaction mixtures were combined and purified through flash column chromatography to yield pure **d18_{ypm}** dye (2.96 g, 3.67 mmol, yield 74%) as yellow powder. The optimal conditions of reaction is shown in Scheme 8.2.



Scheme 8.2: Mono substitution of dye d17_{yp} with 4HBSA to yield dye d18_{ypm} by conventional and microwave irradiation

8.1.6 Comparative Results of Conventional and Microwave-Irradiated Synthesis of d18_{ypm}

A comparison between the results obtained under conventional heating and microwave-irradiated synthesis for the reaction times and yield are shown in Figure 8.4.

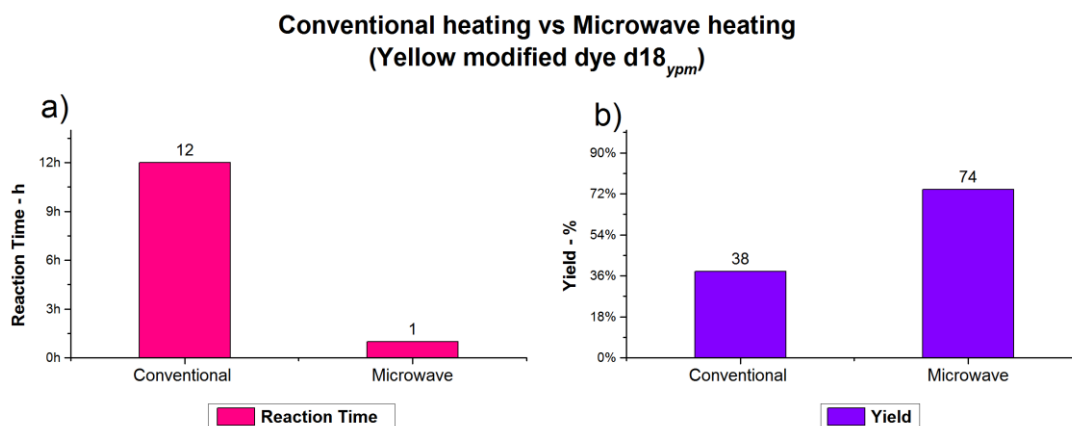


Figure 8.4: Comparison of reaction times and yields obtained by conventional heating and microwave irradiation (d18_{ypm})

As can be seen in Figure 8.4, microwave heating effectively reduced the reaction time from 12 hours to 1 hour. By using microwave radiation for heating, the modified mono-substituted dye **d18_{ypm}** was prepared in yield (74%) that was appreciably higher than the conventional method (38%).

In conclusion, efficient, clean, fast and high yielded synthesis of modified dye **d18_{ypm}** have been achieved by microwave irradiation.

8.1.7 Characterisation of Modified Yellow 7-[[2-(4-Sulfophenoxy)-5,6-dichloro-4-pyrimidinyl]amino]-2-[(methylphenyl)azo]-1,3-Naphthalenedisulfonic Acid Dye (d18_{ypm}**)**

The electropherograms from MEKC analysis are shown in Figure 8.5 which indicates the progression of the synthesis reaction from the starting dye **d17_{yp}** to the mono-substituted dye **d18_{ypm}** (peak 2 in Figure 8.5b).

As shown in Figure 8.5b, after reacting with 4HBSA the resultant dye **d18_{ypm}** migrates more quickly than the **d17_{yp}**. This occurs because the mono substitution of **d17_{yp}** with 4HBSA not only increases the molecular weight of modified dye **d18_{ypm}** but also increase a negative charge on it, therefore increasing the hydrophilicity of modified dye.

In addition, MEKC analysis also shows that starting material **d17_{yp}** was fully converted to modified dye **d18_{ypm}** in 1 hour.

Moreover, the percent area of the **d18_{ypm}** shown in Figure 8.5c, was 100% which indicates the purity of final product.

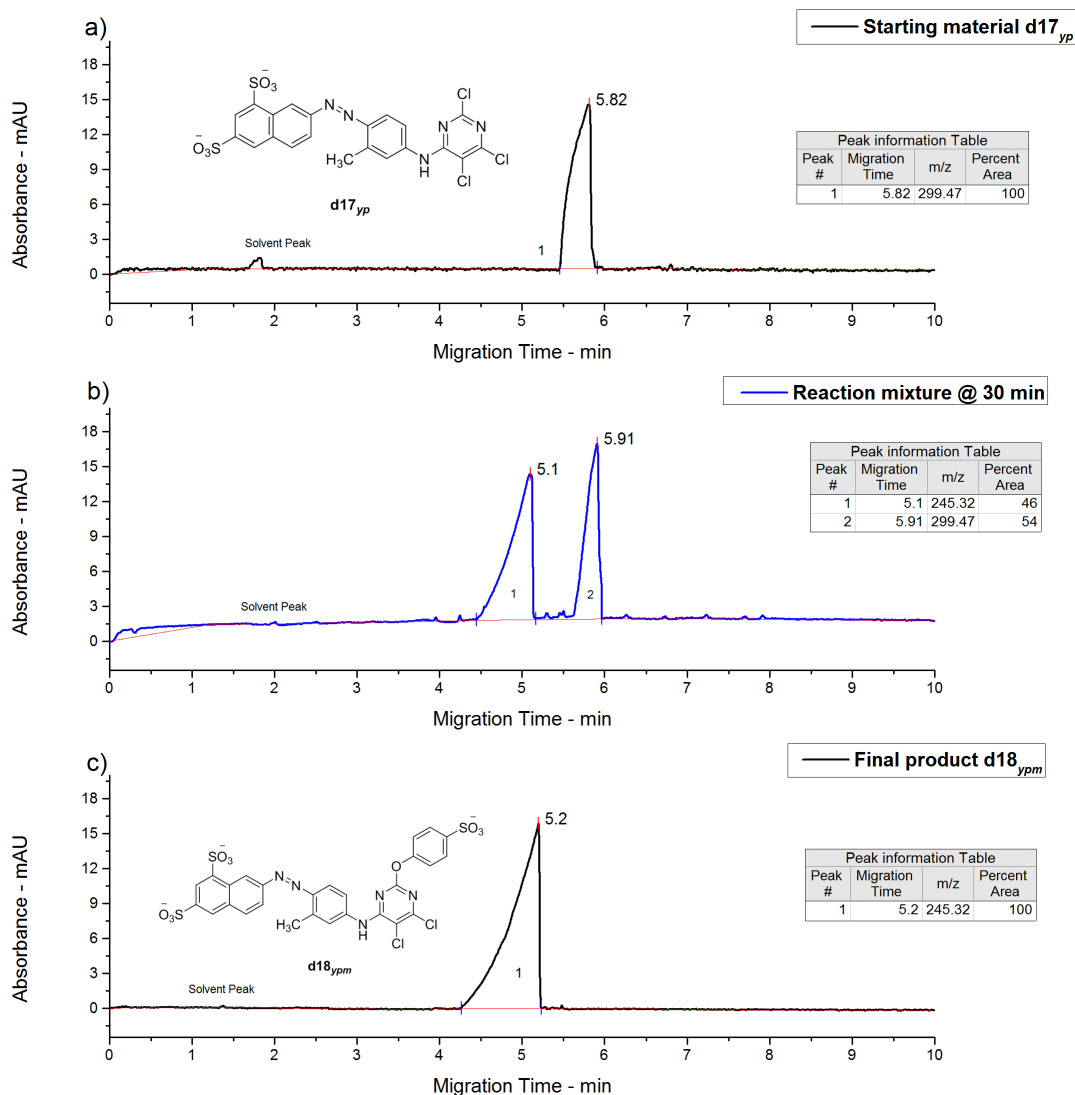


Figure 8.5: Electropherograms showing reaction progress of synthesis of $d18_{ypm}$. (a) yellow dye $d17_{yp}$; (b) $d17_{yp}$ – $d18_{ypm}$ after 30 min reaction time; (c) Final product $d18_{ypm}$. MEKC conditions: same as Figure 8.2

In FT-IR spectrum of the mono-substituted dye $d18_{ypm}$, Figure 8.6, the new peak at 1124 cm^{-1} is evident which can be attributed to the stretching vibration of C–O–C in its structure between the diazine and the 4HBSA. The peak at 827 cm^{-1} can be attributed to the presence of C–Cl after the mono substitution of dye $d17_{yp}$ with 4HBSA.

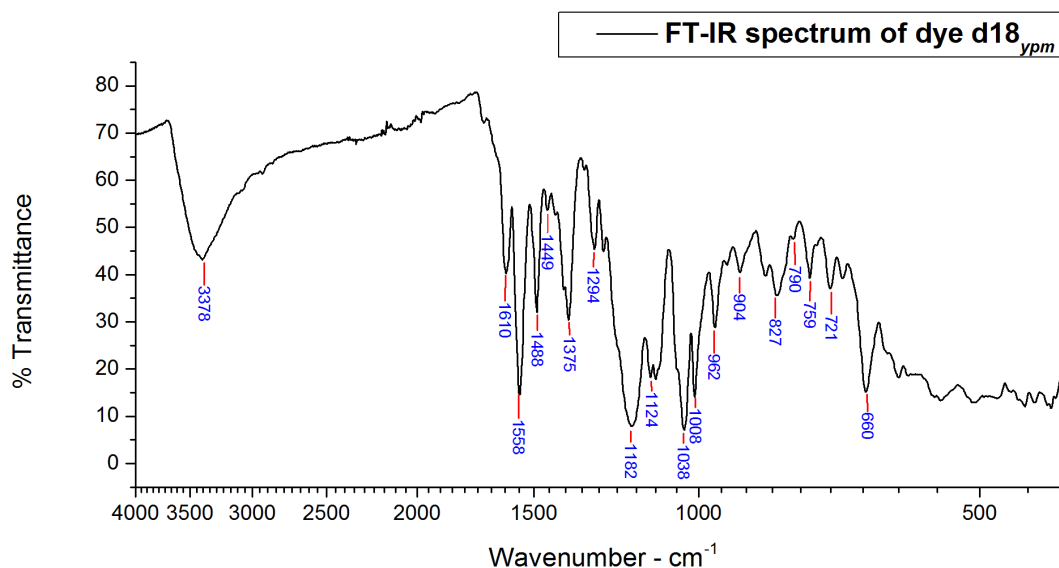


Figure 8.6: FT-IR spectrum of yellow mono-substituted dye **d18_{ypm}**

The detailed analysis of spectrum (Figure 8.6) is as follows ^[1, 2, 5, 6]; N–H stretch, 3378 cm⁻¹; overtone or combinational bands, 2000–1667 cm⁻¹; N–H bending, 1610 cm⁻¹; C=C ring stretch, 1488 cm⁻¹; azo group stretch, 1449 cm⁻¹; C=N stretch, 1558, 1375 cm⁻¹; C–N stretch (secondary amine), 1294 cm⁻¹; C–O–C stretch, 1124 cm⁻¹; sulfonate, 1182 cm⁻¹; C–Cl stretch, 827 cm⁻¹; in-plane C–H bend, 1038, 1008 cm⁻¹; out of plane aromatic C–H bend, 759 cm⁻¹.

8.2 Conclusions

With the help of microwave irradiation, the yellow trichloropyrimidine dye **d17_{yp}** and modified dye **d18_{ypm}** were prepared. By using the new method the reaction time was shortened and high yields of dyes in pure form were achieved in comparison with conventional synthesis at elevated temperatures.

By employing the microwave irradiation method dye **d17_{yp}** was successfully synthesised in adequate yield in 1.5 hours at 55 °C.

Moreover, the modification of **d17_{yp}** was successfully done by using microwave irradiation at 100 °C, quantitative conversion could be achieved with 1 hour.

8.3 References

1. Socrates, G. *Infrared and Raman characteristic group frequencies : tables and charts*. Chichester: Wiley, 2001.
2. Silverstein, R.M., Webster, F.X. and Kiemle, D.J. *Spectrometric Identification of Organic Compounds*. 7th ed. New York: John Wiley and Sons, 2005.
3. Lewis, D.M. and Wang, J.C. The use of fourier transform infrared (FT-IR) spectroscopy to study the state of heterobifunctional reactive dyes. *Dyes and Pigments*, 1998, **39**, pp.111-123.
4. Daimay, L.-V., Colthup, N.B., Fateley, W.G. and Grasselli, J.G. *The handbook of infrared and Raman characteristic frequencies of organic molecules*. London: Academic Press Ltd., 1991.
5. Keller, R.J. and Sigma-Aldrich Corporation. *The Sigma library of FT-IR spectra*. Missouri: Sigma Chemical Company, 1986.
6. Matlok, F., Gremlich, H.U., Bruker Analytische Meotechnik and Merck eds. *Merck FT-IR atlas : a collection of FT-IR spectra*. Weinheim: Vch, 1988.

9 Synthesis, Modification and Characterisation of Magenta Bis-Dichlorotriazine Dye for Inkjet Inks

In 1980, ICI patented dyes which contained differing combinations of chromophores and aliphatic or cycloaliphatic diamine linking groups ^[1]. The most notable of the dyes claimed, which relate to this study, were those in which a dye containing a dichlorotriazine reactive group was disubstituted with diamines such as ethylenediamine and then the terminal aliphatic amine groups further reacted with cyanuric chloride. These dyes were claimed to have exceptionally high levels of exhaustion and fixation when dyed on cellulosic fibres. The patent also claimed dyeings of excellent fastness properties which were highly resistant to staining. However, such claims were not substantiated by quantitative data.

More recently Morris *et al* ^[2], explored ethylenediamine as a bridging group for dyeings on cotton and concluded that when compared with the parent dichlorotriazine dye, the new dyes have high fixation efficiencies and the dye–fibre bond stability is very good.

Therefore, in this study, a multifunctional reactive dye containing bis-sulfophenoxy groups substituted to two dichlorotriazine groups linked through aliphatic amino groups through a third triazine system to the magenta amino chromophore residue has been prepared. The dye was synthesised stepwise from a specially synthesised dichlorotriazine dye **d2_{mt}** dye.

This chapter details the synthesis, modification and characterisation of bis-dichlorotriazine dye. The syntheses progression were monitored through CZE and the dye structural changes were confirmed through FT-IR.

However, when attempts were made to formulate these dyes into inks they produce unsatisfactory results due to their low solubility. Further work was carried out to improve the solubility of dyes in inks by the addition of 0.1% Tween 20 (surfactant). The addition of surfactant resolved the problem, however, due to time limitation the inks were not evaluated to the full extent as other inks were evaluated.

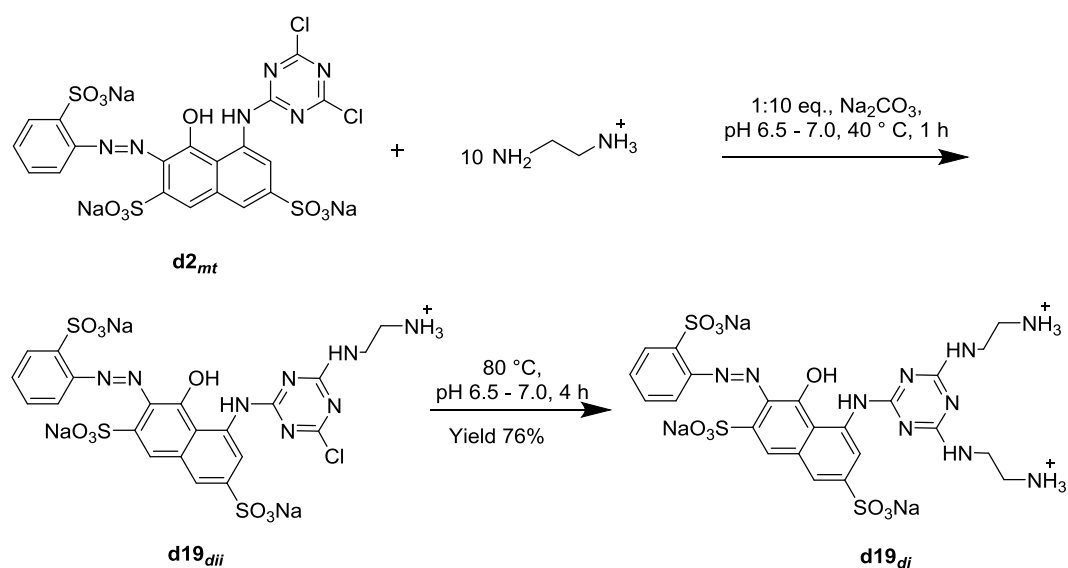
9.1 Experimental

9.1.1 Materials

Magenta dichlorotriazine dye **d2_{mt}** (100%), cyanuric chloride (99%), ethylenediamine, sodium 4-hydroxybenzenesulfonate dihydrate (98%), sodium bisulfite, carboxymethyl cellulose, Tween 20 and N-methylmorpholine N-oxide (NMMO) were purchased from Sigma-Aldrich and used as received. Urea (MP Biomedicals), alcopol O 60 (Acros organics), 2-pyrrolidone (Acros organics), 2-propanol (Fisher), sandozin NIE (Clariant) were also purchased and used as received.

9.1.2 Synthesis of Bis-Ethylenediamine Intermediate (**d19_{di}**)

In accordance with the method described in reference ^[2], ethylenediamine (0.2 mol, 12.01 g, 10 eq.) and sodium bicarbonate (1.5 eq.) were dissolved in water (100 cm³) which was adjusted to pH 7.0 by the addition of hydrochloric acid at 40 °C. A solution of **d2_{mt}** (0.02 mol, 14.34 g, 1 eq.) in water (50 cm³) was added dropwise to the ethylenediamine solution over 30 minutes. The reaction mixture was stirred and the pH was maintained at 6.5 to 7.0 by the addition of 2N sodium carbonate solution, while the temperature was kept at 40 °C. Once the addition of dye **d2_{mt}** solution was complete, the reaction was followed using CZE. The CZE analysis showed that the mono substitution reaction was complete after 1 hour, after which the temperature of the reaction mixture was raised to 80 °C to enable the di substitution to occur. After 4 hours, the CZE analysis showed that the second substitution was complete. The precipitated bis-ethylenediamine intermediate **d19_{di}** (11.62 g, 0.015 mol, 76%) was collected by filtration, washed with ethanol (to remove excess ethylenediamine) and dried *in vacuo*. FT-IR analysis was conducted to confirm the presence of main functional groups in dye intermediate **d19_{di}**. The reaction is shown in Scheme 9.1.



Scheme 9.1: Condensation reaction of **d2_{mt} with ethylenediamine**

9.1.2.1 Characterisation of Bis-Ethylenediamine Intermediate (**d19_{di}**)

CZE electropherograms showing the reaction progression between **d2_{mt}** and ethylenediamine in fused silica capillary at pH 9.0 are shown in Figure 9.1. The primary amino groups present on the intermediate might have decreased their effective negative charge thereby allowing them to elute faster. Under these conditions, **d2_{mt}** have -3 effective charge whereas **d19_{dii}** and **d19_{di}** has -2 and -1 respectively.

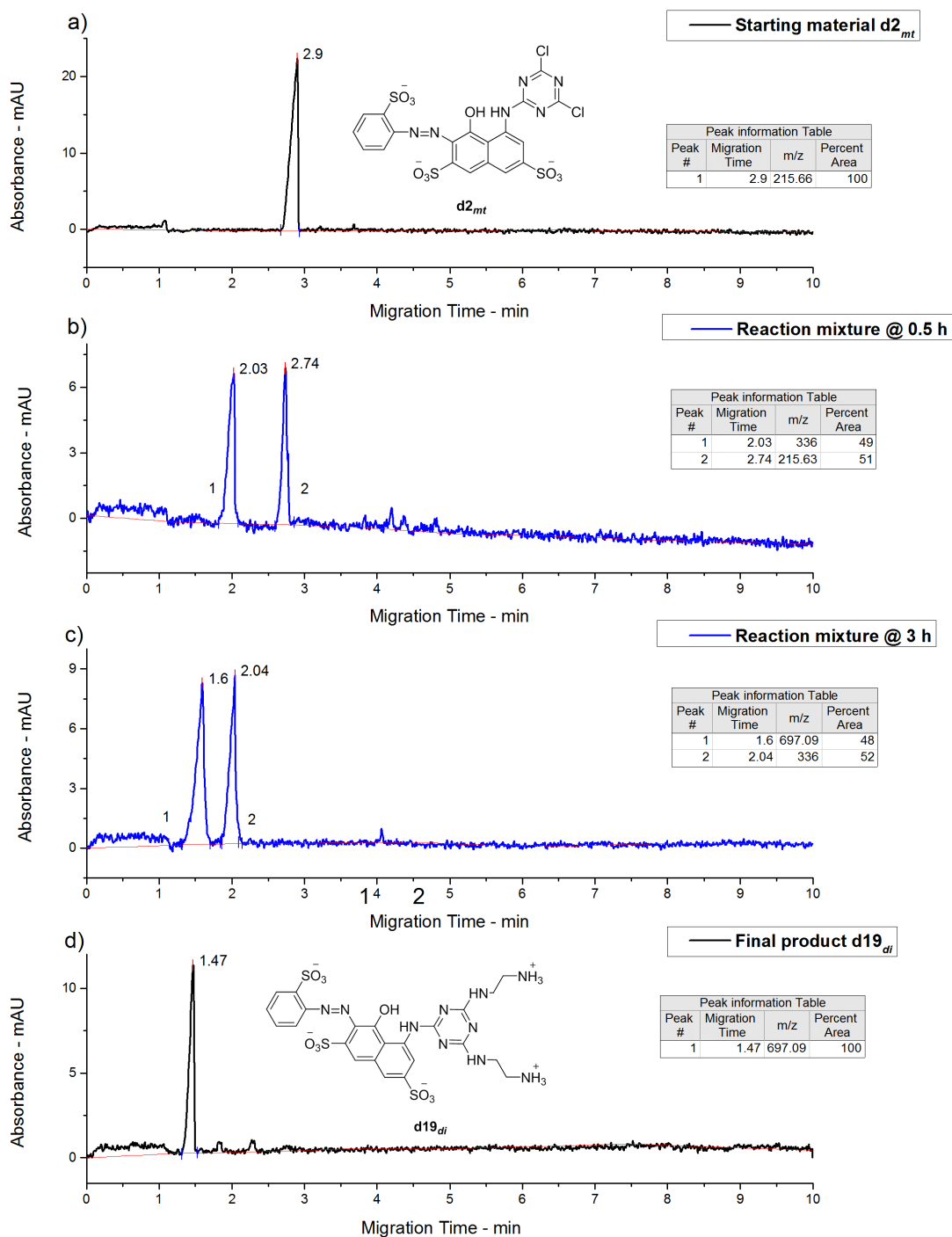


Figure 9.1: Electropherograms showing reaction progress of synthesis of $d19_{di}$. (a) Starting dye $d2_{mt}$; (b) $d2_{mt}$ – $d19_i$ after 0.5 hours reaction time; (c) $d19_i$ – $d19_{di}$ after 3 hours reaction time; (d) Final product $d19_{di}$. CZE conditions: running buffer, 6mM potassium dihydrogen phosphate and acetonitrile (10% v/v) pH 9.0; pressure injection 0.5 psi for 10 s; voltage 25 kV; detection at 542 nm.

It can be seen from the Figure 9.1c, that mono (2.04 min) and bis-substituted (1.6 min) intermediates migrate more quickly than $d2_{mt}$. Under the CZE conditions used $d19_{di}$ being highest mass to charge ratio elute first.

The FT-IR spectrum for the dichlorotriazine dye **d2_{mt}** (Figure 3.4, page 73) shows the presence of C–Cl bond at 1092 cm⁻¹ and 794 cm⁻¹; from the FT-IR spectrum for the bis- ethylenediamine intermediate **d19_{di}** (Figure 9.2) it can be seen that C–Cl bond are no longer present; instead, there is new peak which can be attributed to the methylene groups, now present, at 1439 cm⁻¹.

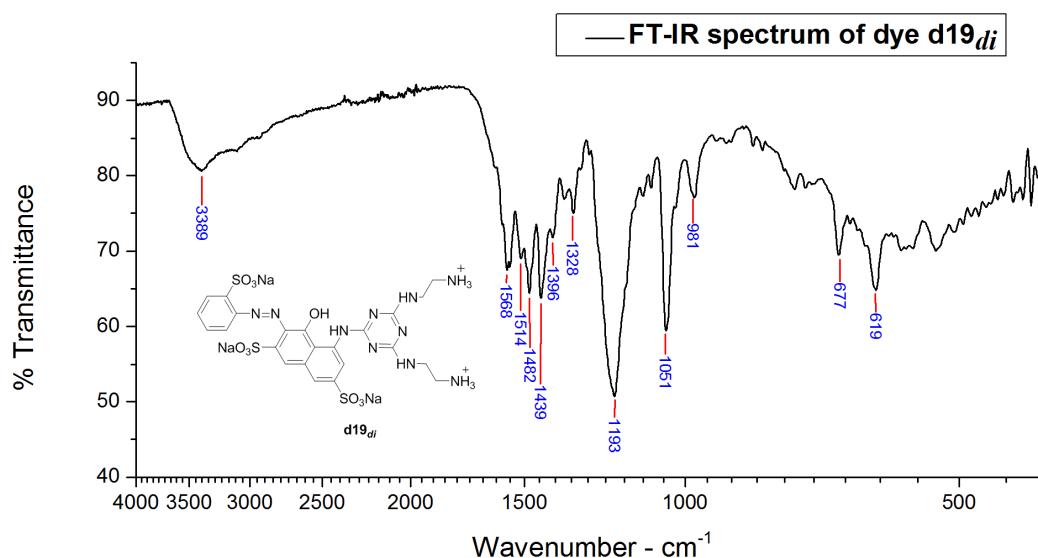


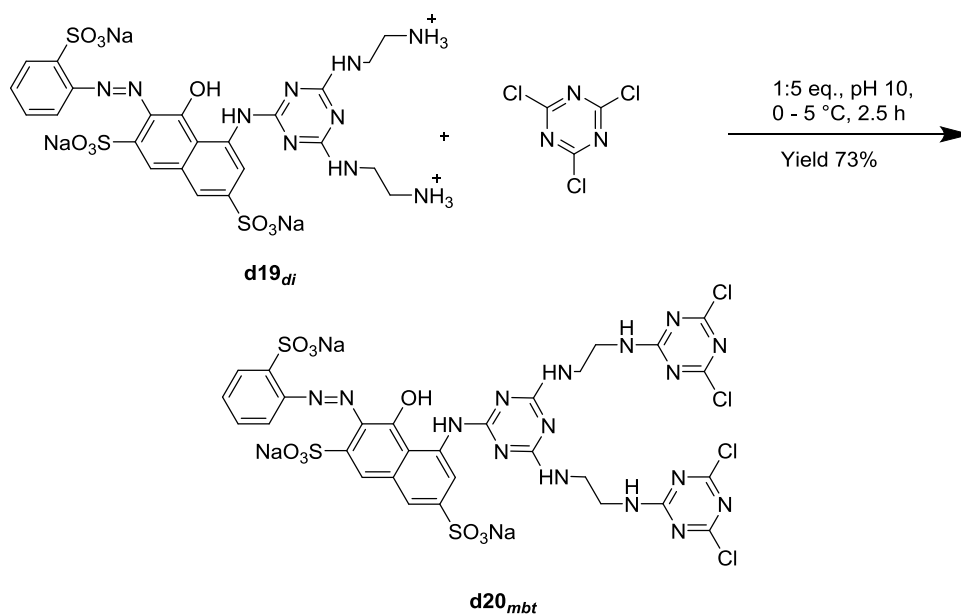
Figure 9.2: FT-IR spectrum of bis-ethylenediamine intermediate d19_{di}

The detailed analysis of spectrum (Figure 9.2) is as follows [3-6], N–H stretch, 3389 cm⁻¹; overtone or combinational bands, 2000-1667 cm⁻¹ ; C=C ring stretch, 1568, 1482, 1396 cm⁻¹; C=N stretch, 1514 cm⁻¹; C–N stretch, 1328 cm⁻¹; sulfonate, 1193 cm⁻¹; in-plane C–H bend, 1051, 981 cm⁻¹.

9.1.3 Synthesis of Bis-Dichlorotriazine Dye (d20_{mbt})

The bis-ethylenediamine dye **d19_{di}** (0.01 mol, 7.66 g, 1 eq.) was dissolved in a minimum amount of water at pH 13 (at this pH the amines are deprotonated maximising solubility), the pH of the solution adjusted to 10 by the addition of hydrochloric acid. The **d19_{di}** solution was added dropwise to an ice-cold solution of cyanuric chloride (0.05 M, 9.2 g, 5 eq.) in acetone (60 cm³) and stirred at 0 – 5 °C. Once the addition of **d19_{di}** was complete, the reaction was further stirred and maintained at pH 10 by the addition of 2N sodium hydroxide solution for 2.5 hours. The reaction was followed with CZE; once the pH had stabilised and the CZE showed a new single peak, the pH was lowered to 7 with hydrochloric acid and sodium phosphate buffer was added to buffer the pH to 6.4. The dye **d20_{mbt}** (7.75 g,

0.0073 mol, 73%) was precipitated by the addition of acetone, collected by filtration, washed with acetone (to remove any excess cyanuric chloride) and dried *in vacuo*. FT-IR analysis was conducted to confirm the presence of main functional groups in dye **d20_{mbt}**. The reaction is shown in Scheme 9.2.



Scheme 9.2: Condensation of cyanuric chloride with **d19_{di} (intermediate) to yield **d20_{mbt}****

9.1.3.1 Characterisation of Bis-Dichlorotriazine Dye (**d20_{mbt}**)

CZE electropherograms showing the progression of synthesis reaction of **d20_{mbt}** are shown in Figure 9.3.

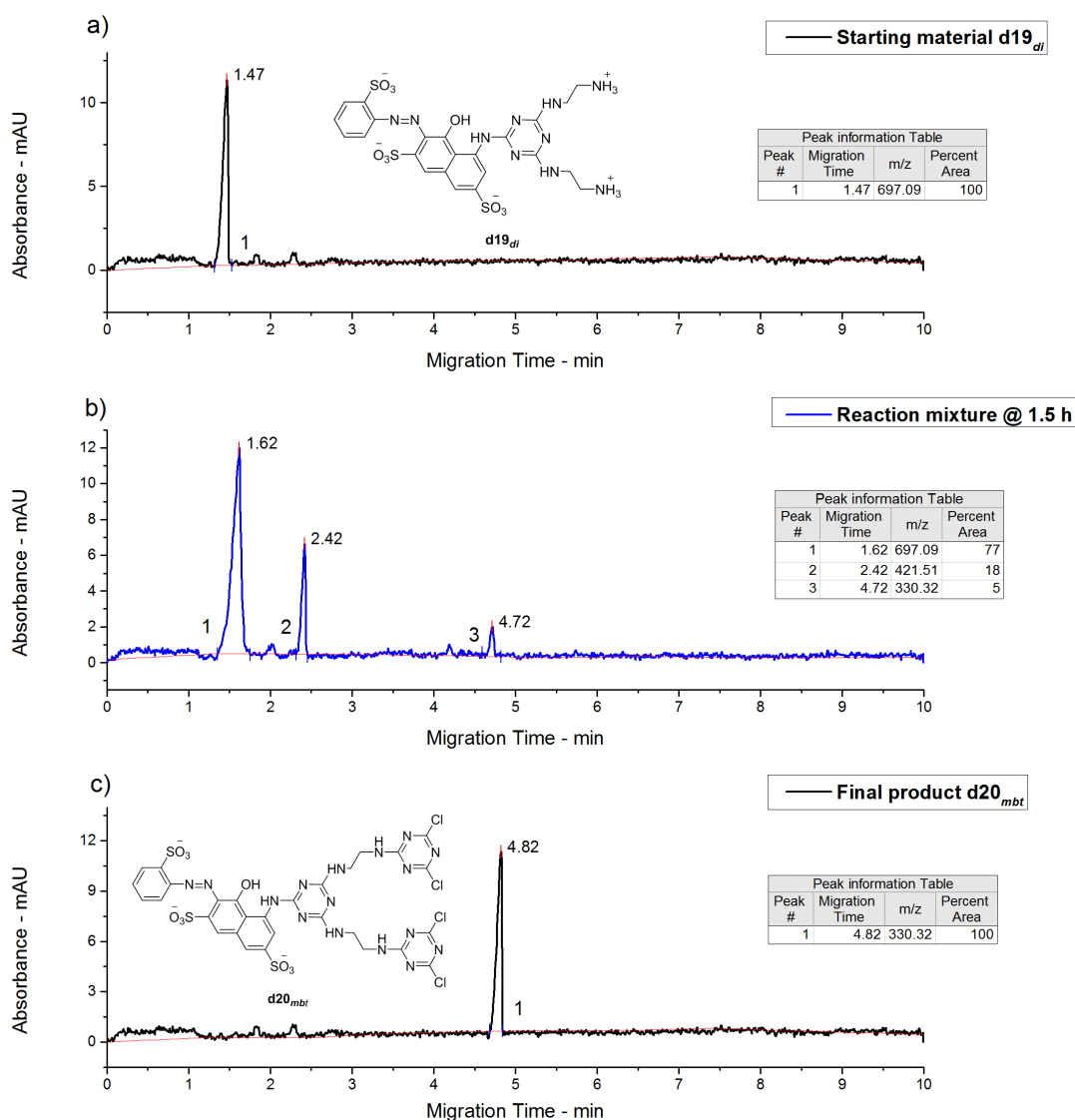


Figure 9.3: Electropherograms showing reaction progress of synthesis of $d20_{mbt}$. (a) Starting intermediate $d19_{di}$; (b) $d19_{di}$ – $d20_{mbt}$ after 1.5 hours reaction time; (c) Final product $d20_{mbt}$. CZE conditions: same as Figure 9.1

Most of the $d19_{di}$ was converted to the $d20_i$ (peak 2 in Figure 9.3b) after 1.5 hours of reaction although a small amount $d20_{mbt}$ (peak 3 in Figure 9.3b) was also formed. After the reaction between cyanuric chloride and the bis-ethylenediamine intermediate $d19_{di}$, the resultant bis-dichlorotriazine dye $d20_{mbt}$ elutes later. This is due to the smallest mass to charge ratio of $d20_{mbt}$.

In FT-IR spectrum of bis-dichlorotriazine dye $d20_{mbt}$ (Figure 9.4), the appearance of two new peaks at 1090 and 804 cm^{-1} signifies the presence of C–Cl bond in new dye. Along with methylene groups at 1438 cm^{-1} , appearance of peaks at 1546 cm^{-1} and 1393 cm^{-1} reflect the presence of the triazine group in $d20_{mbt}$. This

confirms that the amine groups present in **d19_{di}** was condensed successfully with cyanuric chloride.

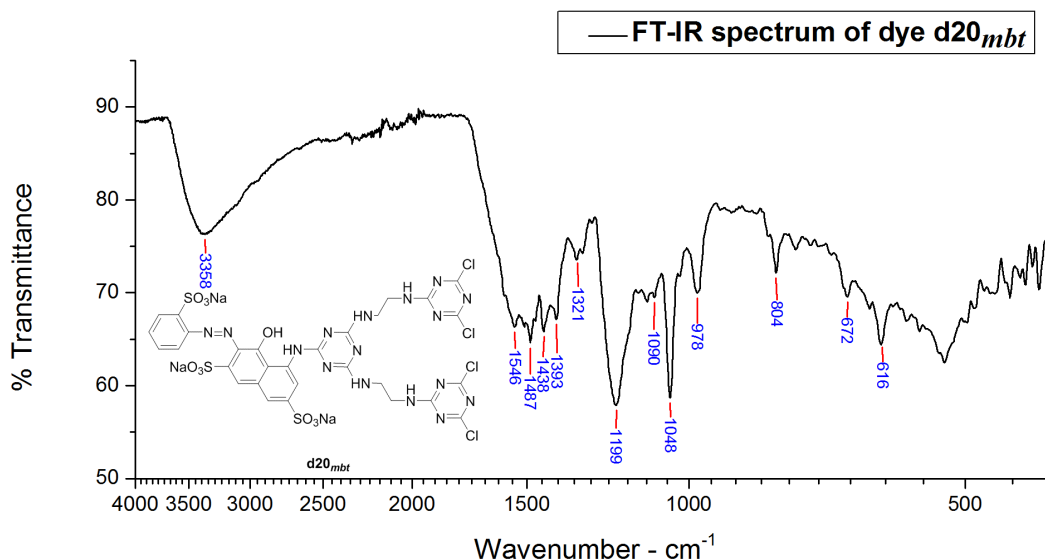


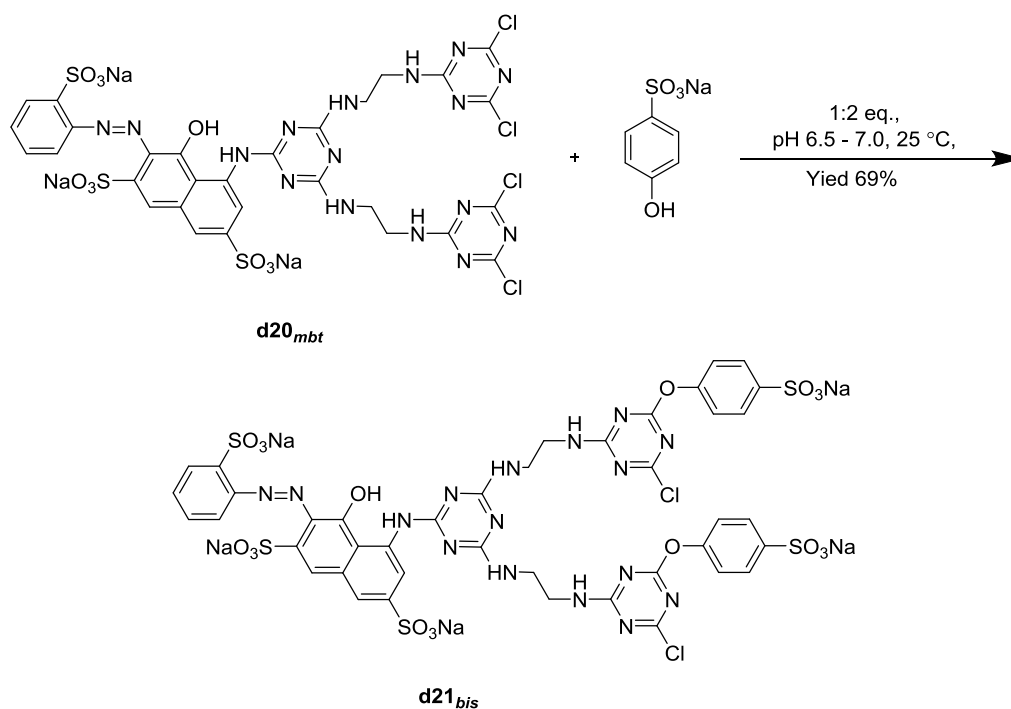
Figure 9.4: FT-IR spectrum of bis-dichlorotriazine dye **d20_{mbt}**

The detailed analysis of spectrum (Figure 9.2) is as follows ^[3-6]; N–H stretch, 3358 cm^{-1} ; overtone or combinational bands, 2000-1667 cm^{-1} ; C=C ring stretch, 1487; azo group stretch, 1438 cm^{-1} ; C=N stretch, 1546, 1393 cm^{-1} ; C–N stretch, 1321 cm^{-1} ; sulfonate, 1199 cm^{-1} ; in-plane C–H bend, 1048, 978 cm^{-1} .

9.1.4 Synthesis of Bis-(Monochlorotriazine/Sulfophenoxy) Dye (**d21_{bis}**)

Dye **d20_{mbt}** (0.005 mol, 5.30 g, 1 eq.) was dissolved in water (80 cm^3) and temperature was raised to 25 °C. A solution of 4HBSA (0.01 mol, 2.32 g, 2 eq.) in water (20 cm^3) was added dropwise over 10 minutes to the dye solution; the pH was maintained at 7.0 by the addition of saturated sodium carbonate. Once the addition of the 4HBSA solution was complete, the reaction was followed using CZE. When pH had stabilised, sodium chloride (10% w/v) was added to precipitate out the dye. The crude dye **d21_{bis}** was collected by filtration and dried *in vacuo*.

FT-IR analysis was conducted to confirm the presence of main functional groups in dye intermediate **d21_{bis}**. The reaction is shown in Scheme 9.3.



Scheme 9.3: Synthesis of bis-sulfophenoxy dye **d21_{bis}**

9.1.4.1 Characterisation of Bis-(Monochlorotriazine/Sulfophenoxy) Dye (**d21_{bis}**)

CZE electropherograms showing the reaction progression between **d20_{mbt}** and 4HBSA in fused silica capillary at pH 9.0 are shown in Figure 9.5. Under these conditions **d20_{mbt}** have -3 charge whereas **d21_{bis}** have -5.

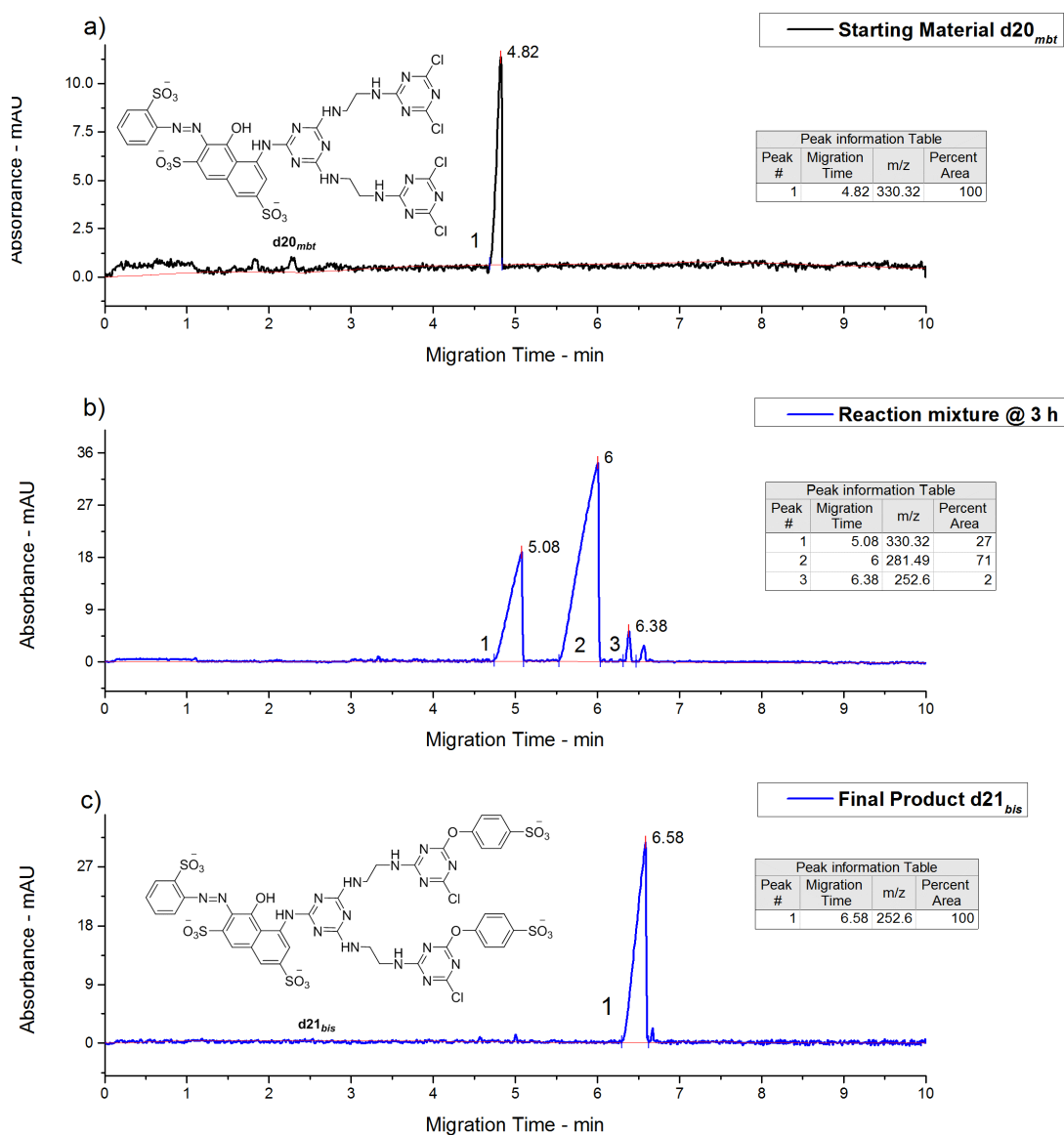


Figure 9.5: Electropherograms showing reaction progress of synthesis of **d21_{bis}. (a) Starting intermediate **d20_{mbt}**; (b) **d20_{mbt}** – **d21_{bis}** after 3 hours reaction time; (c) Final product **d21_{bis}**. CZE conditions: same as Figure 9.1**

After the modification, the mass to charge ratio of the **d21_{bis}** decreases compared to the bis-dichlorotriazine dye **d20_{mbt}**, therefore the migration time of the **d21_{bis}** increases. Since an increase in molecular size decreases electrophoretic mobility and increase in charge slows the migration towards the detector, therefore analytes with higher mass to charge ratio elute first and the analytes with lower mass to charge ratio elute last.

In FT-IR spectrum of the **d21_{bis}** (Figure 9.6), the new peak at 1125 cm^{-1} is evident which can be attributed to the stretching vibration of C–O–C in its structure

between the triazine and the 4HBSA. The peak at 800 cm^{-1} can be attributed to the presence of C–Cl after the modification of **d20_{mbt}** with HBSA.

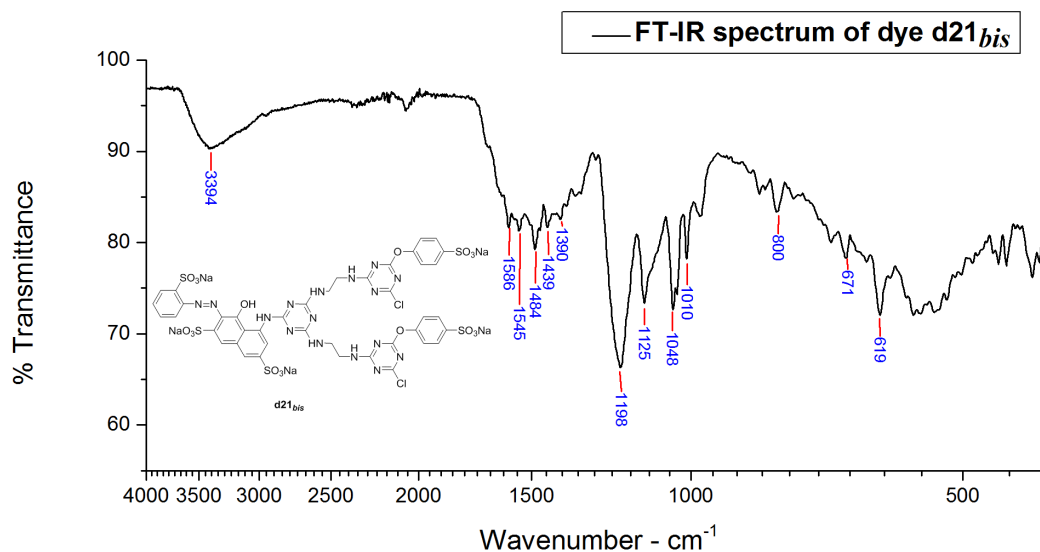


Figure 9.6: FT-IR spectrum of bis-sulfophenoxy dye (**d21_{bis}**)

9.2 Conclusions

The synthesis of the dyes based on replacing the bridging group involved a 2-step modification starting with the synthesis of dichlorotriazine reactive dye **d2_{mi}**; followed by bis-substitution of the triazine halogens with 10 equivalents of ethylenediamine to produce a bis-ethylenediamine intermediate **d19_{di}**. Intermediate **d19_{di}** was subsequently reacted with cyanuric chloride to produce a bis-dichlorotriazine **d20_{mbt}**.

Modification of dye **d20_{mbt}** with 4HBSA was done at $30\text{ }^\circ\text{C}$ (pH 7.0) to yield **d21_{bis}**. The structural changes of the **d20_{mbt}** were confirmed by FT-IR.

Furthermore, when these dyes (**d20_{mbt}** and **d21_{bis}**) were attempted to formulate into inks they produced unsatisfactory inks due to their low solubility. Further work was carried to improve the solubility of dyes in inks by the addition of 0.1% Tween 20 (surfactant). The addition of surfactant resolved the problem, however, due to time limitations the inks were not evaluated to the full extent as other inks were evaluated.

9.3 References

1. Patent GB2057479 (1980)
2. Morris, K.F., Lewis, D.M. and Broadbent, P.J. Design and application of a multifunctional reactive dye capable of high fixation efficiency on cellulose. *Coloration Technology*, 2008, **124**, pp.186-194.
3. Matlok, F., Gremlich, H.U., Bruker Analytische Meotechnik and Merck eds. *Merck FT-IR atlas : a collection of FT-IR spectra*. Weinheim: Vch, 1988.
4. Keller, R.J. and Sigma-Aldrich Corporation. *The Sigma library of FT-IR spectra*. Missouri: Sigma Chemical Company, 1986.
5. Socrates, G. *Infrared and Raman characteristic group frequencies : tables and charts*. Chichester: Wiley, 2001.
6. Silverstein, R.M., Webster, F.X. and Kiemle, D.J. *Spectrometric Identification of Organic Compounds*. 7th ed. New York: John Wiley and Sons, 2005.

10 Comparative Analysis of Synthesised Dyes-Based Inks and Commercial Jettex R Reactive Inks for Wool Fabric

10.1 Introduction

DyStar is a leading supplier of innovative inks for digital textile printing. They introduced Jettex R reactive inks for digital textile printing. The Jettex R range is based on standard reactive dyes used for textile printing, covering the entire colour space.

These inks are classed as outstanding inks for digital printing onto cellulose, silk and wool and are ideal for fashion fabrics for both women wear and menswear.

Particular advantages of Jettex R range of reactive inks are top colour fastness, brilliancy and easy wash-off.

Jettex R inks were applied onto wool fabric according to the procedure discussed in section 2.5.3 (page 52) and their performance in term of percent fixation and colour fastness (light and wash) were compared with reactive inks based on dyes that are synthesised in this study .

This chapter details the comparative analysis of synthesised parent and modified dyes (triazine and pyrimidine) based inks and commercially successful Jettex R reactive inks.

10.2 Materials

Inks based on triazine based modified dyes (magenta, **d3_{mtm}**, **d4_{mtd}**; yellow, **d7_{ytm}**, **d8_{ytd}**; blue, **d11_{btm}**, **d12_{btd}**) and pyrimidine based modified dyes (magenta, **d14_{mpm}**; blue, **d16_{bpm}**) were prepared. Samples of commercial Jettex R inks (magenta, yellow and blue) were provided by DyStar and used as received.

10.3 Results and Discussion

10.3.1 Characteristics of DyStar Inks

10.3.1.1 Surface Tension and Viscosity of Inks

It can be seen, from Table 10.1, that Jettex R inks (magenta, blue and yellow) had surface tension and viscosity within the operational range. However, all the modified dye based inks have lower viscosity as compared to Jettex R inks. This could be due to the use of different ink components; as choice of these components have a significant effect on both, *i.e.*, surface tension and viscosity.

Table 10.1: Comparative results of surface tension and viscosity of Inks

Ink formulation	Surface Tension (dynes.cm⁻¹)	Viscosity (cP)
Dystar Magenta	44.5	28.7
Dystar Yellow	41.0	30.0
Dystar Blue	43.1	23.3
Triazine based modified dyes		
Ink d3_{mtm}	44.0	10
Ink d4_{mtd}	45.0	8
Ink d7_{ytm}	44.5	6
Ink d8_{ytd}	45.5	8
Ink d11_{btm}	43.5	8
Ink d12_{btd}	43.0	8
Pyrimidine based modified dyes		
Ink d14_{mpm}	46.5	12
Ink d16_{bpm}	40.5	8

10.3.2 Comparative Study of Percent Fixation of Inks

Figure 10.1 (magenta), Figure 10.2 (blue), and Figure 10.3 (yellow) illustrate the superiority of the modified dye-based inks compared with the commercially successful Jettex R inks when digitally printed onto wool fabric.

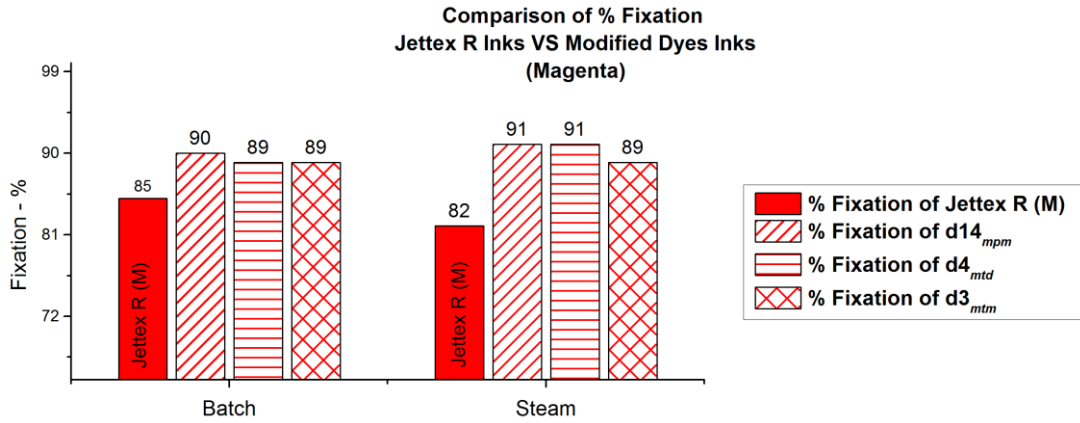


Figure 10.1: Comparison of percent fixation of magenta inks

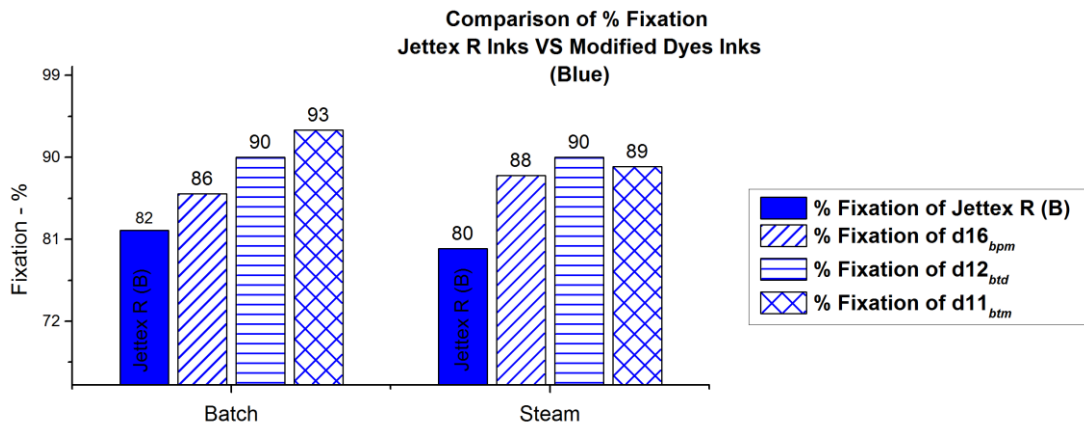


Figure 10.2: Comparison of percent fixation of blue inks

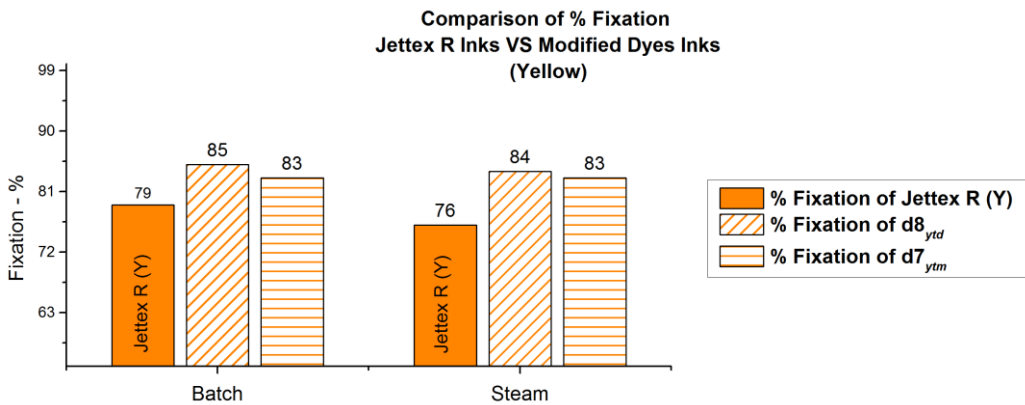


Figure 10.3: Comparison of percent fixation of yellow inks

This is clearly indicated in Figure 10.1, Figure 10.2 and Figure 10.3 that both the series, *i.e.* triazine and pyrimidine, of modified dyes in magenta, yellow and blue hue exhibit high level of dye fixation when compared to Jettex R inks. It is suggested that the enhanced dye fixation observed for these modified dyes are due to lower reactivity and high solubility of these dyes. Moreover, modified dyes based inks also showed higher stability in ink formulations.

10.3.3 Light Fastness

Light fastness testing was carried out according to the BS EN ISO 105-B02:2013 (Method 3) ^[1].

The samples printed with Jettex R inks (magenta, blue and yellow) were tested against blue wool reference 6 and the results are listed in Table 10.2.

All inks gave result 'equal to' *target wool reference 6*. Moreover, both the series of modified dyes based Inks showed better light fastness than commercial Jettex R Inks.

Therefore, modification of dichlorotriazine and trichloropyrimidine dyes in magenta yellow blue hue with sulfophenoxy groups(s) gave a better range of inks for digital printing of wool.

Table 10.2: Comparative results of light fastness of Inks

Dye/Ink	Target blue wool reference 6
Jettex R (M)	Equal to 6
Jettex R (B)	Equal to 6
Jettex R (Y)	Equal to 6
Triazine based modified dyes	
d3_{mtm}	Better than 6
d4_{mtd}	Better than 6
d7_{ym}	Better than 6
d8_{ytd}	Better than 6
d11_{btm}	Better than 6
d12_{btd}	Better than 6
Pyrimidine based modified dyes	
d14_{mpm}	Better than 6
d16_{bpm}	Better than 6

10.3.4 Wash Fastness

Wash fastness was carried out according to the BS ISO 105-C06:2010 [2] and the results are shown in Table 10.3. The Jettex R printed samples showed evidence of both colour loss and staining of multifibre adjacents specially on wool, acetate and cellulose acetate.

However, both the series of modified dye based inks exhibit outstanding wash fastness, indicating that modification adopted for dichlorotriazine and trichloropyrimidine dyes does not have detrimental effects on the wash fastness of dyes.

Table 10.3: Comparative results of wash fastness of Inks

Dye/Ink	Change in shade	Staining					
		CA	C	N	P	A	W
Jettex R (M)	4-5	3-4	5	5	5	4-5	3-4
Jettex R (B)	4-5	5	5	5	5	5	5
Jettex R (Y)	4-5	4-5	5	5	5	4-5	5
Triazine based modified dyes							
d3_{mtm}	5	5	5	5	5	5	5
d4_{mtd}	5	5	5	5	5	5	5
d7_{ytm}	5	5	5	5	5	5	5
d8_{ytd}	5	5	5	5	5	5	5
d11_{btm}	5	5	5	5	5	5	5
d12_{btd}	5	5	5	5	5	5	5
Pyrimidine based modified dyes							
d14_{mpm}	5	5	5	5	5	5	5
d16_{bpm}	5	5	5	5	5	5	5

CA: Cellulose Acetate; C: Cotton; N: Nylon; P: Polyester; A: Acrylic; W: Wool

See Appendix B for printed samples

10.4 Conclusions

The percent fixation of Jettex R inks (magenta, blue and yellow) along with colour fastness properties of printed inks were investigated. Percent fixation of 85%, 82% and 79% were achieved for magenta, blue and yellow, when samples were batched at elevated temperatures. However, percent fixation of 82%, 80% and 76% were achieved for magenta, blue and yellow, when samples were steamed at 102 °C. Therefore, batching proofs to be the choice of fixation method for Jettex R inks.

The comparative study of percent fixation, colour fastness to light and colour fastness to wash indicate the superiority of both triazine as well as pyrimidine based

modified inks. The better results of modified dyes based inks are due to lower reactivity and higher solubility.

10.5 References

1. British Standards Institution. *Colour fastness to artificial light: Xenon arc fading lamp test*, ISO 105-B02:2013.
2. British Standards Institution. *Textiles - Tests for colour fastness - Part C06: Colour fastness to domestic and commercial laundering*, BS EN ISO 105-C06:2010.

11 Conclusion and Future Work

11.1 Conclusion

In recent years inkjet printing has become increasingly popular as a result of: significant improvement in print speed of inkjet printers due to technical progress of image processing by means of a computer, and print head manufacturing; and high demands on market for digitalisation of print designs, as well as diversification and lot reduction in printing. Therefore, development of an ink set which is capable of providing printed fabrics having high quality and high fastness properties, and is also superior in stability has been demanded.

Thus, the aims of this study were to improve fixation properties, performance properties and the stability of existing reactive dyes when incorporated into inkjet inks. The approach taken in this study was to modify existing reactive dyes (dichlorotriazine and trichloropyrimidine) so that they can be utilised for the inkjet printing of wool.

Thus, two series of multifunctional reactive dyes in magenta, blue and yellow hue (which were suitable for application on wool) were synthesised from existing reactive dyes (dichlorotriazine and trichloropyrimidine). The synthesised dyes were formulated into a set of inks, applied onto wool fabrics through inkjet printing and fixed using different methods. The inks were then evaluated in terms of their stability, percent fixation and colour fastness and the results were compared with their parent analogues based inks and commercial Jettex R inks.

Series I

For the synthesis and modification of dichlorotriazine dyes in magenta, yellow and blue hue, the amino based chromophores were synthesised, followed by condensation with cyanuric chloride in 0 to 5 °C.

First modification of prepared dichlorotriazine dyes (magenta, **d2_{mt}**, yellow, **d6_{yt}** and blue, **d10_{bt}**) was done by substitution of the second chlorine atom by 4HBSA at a temperature range of 25 to 45 °C at a pH range of 3.0 to 7.0 to produce mono-substituted dyes (magenta, **d3_{mtm}**; yellow, **d7_{ytm}**; and blue, **d11_{btm}**) in pure form.

Second modification of dichlorotriazine dyes was done by substitution of the second chlorine atom by using two equivalent 4HBSA at 30 °C to complete mono substitution and then raising the temperature to 70 to 80 °C to produce di-substituted dyes (magenta, **d4_{mtd}**; yellow, **d8_{ytd}**; and blue, **d12_{btd}**) in pure form.

With respect to the formulation of synthesised parent and modified dyes into inks, the modified dyes were easily formulated into inks due to their increased solubility as compared to parent analogues. Moreover, the characteristic properties such as viscosity and surface tension of the ink set based on parent and modified dyes were found to be in operation range of 2 – 20 cP and 25 – 60 dynes.cm⁻¹.

The percent fixation (printing performance), under inkjet print–batch and inkjet print–steam methods, of the three mono-substituted dyes and three di-substituted dyes and their parent analogues were studied.

It has been shown in chapters 3, 4 and 5 that the mono-substituted dyes (magenta, **d3_{mtm}**; yellow, **d7_{ytm}**; and blue, **d11_{btm}**) and di-substituted dyes (magenta, **d4_{mtd}**; yellow, **d8_{ytd}**; and blue, **d12_{btd}**), synthesised from dichlorotriazine dyes (magenta, **d2_{mt}**, yellow, **d6_{yt}** and blue, **d10_{bt}**), showed significant improvement in percent fixation over their analogue parent dyes (see Appendix B). This was due to the incorporation of the sulfophenoxy reactive group, which reduced the reactivity of modified dyes. This was in contrast to the analogue parent dyes, which are highly reactive and are susceptible to hydrolysis during fixation, as well as storage.

Moreover, di-substituted dyes (magenta, **d4_{mtd}**; yellow, **d8_{ytd}**; and blue, **d12_{btd}**) have shown an increase in dye fixation compared to mono-substituted dyes (magenta, **d3_{mtm}**; yellow, **d7_{ytm}**; and blue, **d11_{btm}**). This is due to the incorporation of more than one sulfophenoxy reactive group, which leads to the development of the more stable reactive system compared to only one reactive group. Furthermore, the incorporation of the sulfophenoxy reactive group into the dyes is advantageous in two ways: (1) it increases dye solubility, and (2) it increases the stability of the reactive group against hydrolysis. Therefore, the increased solubility and low reactivity of chlorotriazine based modified dyes made them suitable for printing applications.

Furthermore, the modified dyes (magenta, **d3_{mtm}** and **d4_{mtd}**; yellow, **d7_{ytm}** and **d8_{ytd}**; and blue, **d11_{btm}** and **d12_{btd}**), can be suitably applied through inkjet print–batch as well as inkjet–steam.

With respect to the stability of modified dyes (magenta, **d3_{mtm}** and **d4_{mtd}**; yellow, **d7_{ytm}** and **d8_{ytd}**; and blue, **d11_{btm}** and **d12_{bid}**) in inks over a longer time, it was found that the modified dye based inks can be stored at room temperature for 3 to 12 months without deteriorating. This is due to the decreased reactivity of modified dyes, as compared to their parent analogues dichlorotriazine dyes.

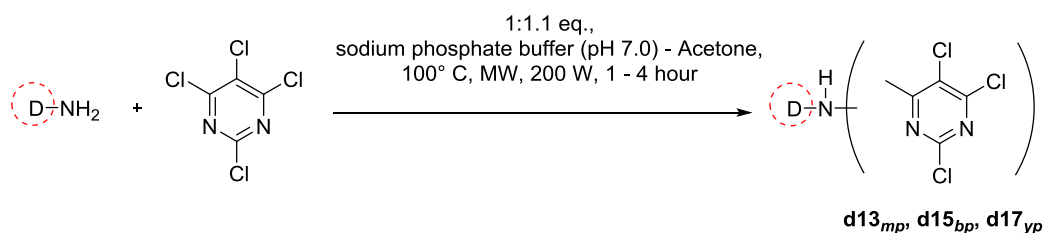
With respect to the fastness properties of the subsequent prints with modified dyes (magenta, **d3_{mtm}** and **d4_{mtd}**; yellow, **d7_{ytm}** and **d8_{ytd}**; and blue, **d11_{btm}** and **d12_{bid}**), light fastness was found to be increased by 0.5-1.0 grade on target blue wool reference 6, as well as improvements in their wash fastness when compared to their parent analogues. This improvement in fastness properties can be attributed to increased percent of fixation of reactive dyes that react covalently with the functional groups in the fibre structure of wool.

Series II

For the synthesis of trichloropyrimidine dyes (magenta, **d13_{mp}**; blue, **d15_{bp}**; and yellow, **b17_{yp}**), the most widely employed strategy which involves the condensation of 2,4,5,6-tetrachloropyrimidine with amino based dye chromophore (azo or anthraquinone) in the presence of sodium carbonate as acid binding agent at a temperature between 70 – 80 °C for several hours (15 – 50 hours) was employed. However, even after several hours at high temperature the reaction did not reach completion (discussed in chapters 5, 6, and 7) with a drawback of considerable formation of hydrolysed by-products.

It was observed that the reaction typically requires harsh conditions e.g., high temperatures and long reaction times, however, suffer from poor conversion and hence poor yields.

It has been shown in chapters 6, 7 and 8 that microwave irradiation could improve the condensation reactions by significantly enhancing the conversion to product, increasing product yield and accelerating the reaction. The present study thus discloses an improved method for the synthesis of trichloropyrimidine dyes **d13_{mp}**, **d15_{bp}** and **d17_{yp}**, wherein the method includes a microwave-irradiated condensation reaction according to Figure 11.1 wherein D is an amino based dye chromophore (azo or anthraquinone).



wherein,

D is amino based dye chromophore (azo or anthraquinone)

The -NH- group in the dye chromophore is directly linked to a carbon atom of the pyrimidine ring in 4-position

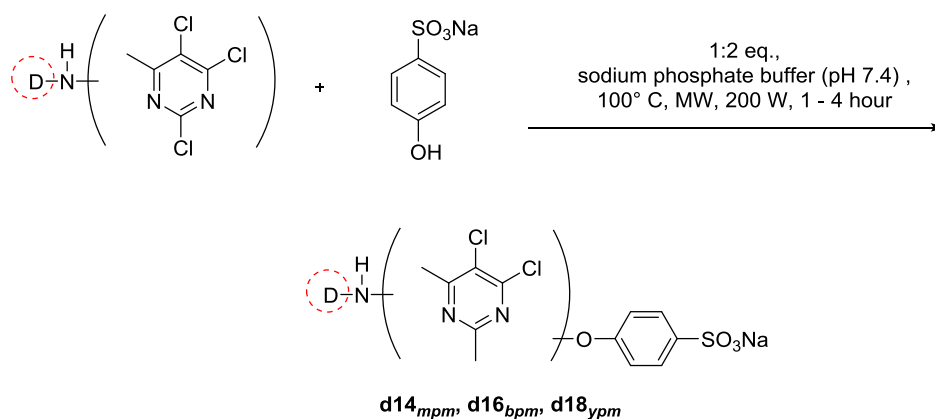
Figure 11.1: Optimal conditions for Microwave-irradiated synthesis of trichloropyrimidine dyes

According to the new method, the reaction mixtures were subjected to microwave irradiation, typically for only 1 – 4 hours at 100 °C applying 200 W. Instead of sodium carbonate (as acid binding agent), sodium phosphate buffer [Na₂HPO₄ (0.20 M) and NaH₂PO₄ (0.12 M), pH 7.0] was used.

The new method is characterised by dramatically increased yields (80 - 85% isolated) especially of dyes poorly accessible without microwaves in reaction duration of only about 1 – 4 hours.

The present study also discloses a method for the modification of trichloropyrimidine dyes, wherein the method comprises the mono substitution of trichloropyrimidine dye with 4HBSA in the presence of sodium phosphate buffer pH 7.4 at 100 °C.

According to the new method, the reaction mixtures were subjected to microwave irradiation, typically for only 1 - 4 hours at 100 °C applying 200 W in the presence of sodium phosphate buffer [Na₂HPO₄ (0.20 M) and NaH₂PO₄ (0.12 M), pH 7.4] shown in Figure 11.2. The mono-substituted dyes **d14_{mpm}**, **d16_{bpm}** and **d18_{ypm}** were formed almost exclusively, only small traces of by-products were detected through CE and TLC. The microwave-irradiation method resulted in dramatically increased yields (70 -75 % isolated).



in which

D means amino based dye chromophore (azo or anthraquinone)
and

The group -NH- in the dye chromophore is directly linked to a carbon
atom of the pyrimidine ring in 4-position

Figure 11.2: Optimal conditions for Microwave-irradiated synthesis of modified mono-substituted dyes

The percent fixation (printing performance), under inkjet print–batch and inkjet print–steam methods, of the two mono-substituted dyes and their parent analogues were studied.

As shown in chapter 6 the magenta parent trichloropyrimidine dye (**d13_{mp}**) and mono-substituted dye (**d14_{mpm}**), equally displayed higher levels of fixation, i.e. 94% and 90% respectively. This is thought to be due to the bifunctional behaviour of both dyes under the fixation conditions used.

As shown in chapter 7 the blue parent trichloropyrimidine dye (**d15_{bp}**), showed poorer fixation (72%) and unlevelled prints compared to mono-substituted dye (**d16_{bpm}**) which displayed higher levels of fixation (88%) under inkjet print-batch method. However, similar printing carried out under inkjet print-steam method showed better fixation as well as levelled prints. This is thought to be due to perfect steaming conditions used.

As has previously been discussed in chapter 6 that due to the low reactivity of trichloropyrimidine dyes, they are highly resistant to hydrolysis. Therefore, with respect to stability of modified dyes in inks, it was found that modification of trichloropyrimidine dye with 4HBSA does not have any unfavourable effect on the stability of dyes in inks when stored for prolonged time.

With respect to the fastness properties of the subsequent prints with parent analogues and modified dyes, all the dyes exhibit excellent colour fastness to light when tested against target blue wool reference 6, whereas, for wash fastness all the dyes exhibit excellent wash fastness properties except blue trichloropyrimidine dye **d15_{pp}**, which show a slight staining on adjacents and change in shade (4-5).

Thus it can be concluded from the above discussions that synthesis of parent trichloropyrimidine and modified dyes in high yields and shorter time through microwave-irradiation, which can easily be up-scaled may find industrial application for the preparation of dyes and will allow application of this highly promising and potential class of reactive group in inkjet printing of textiles.

Moreover, on comparative analysis of properties of modified dyes with commercially available Jettex R inks, it was found that the modified dyes based inks are superior in every aspect such as fixation properties, stability and colour fastness.

Therefore, the concept of modification of reactive dyes based on chlorotriazine and chloropyrimidine reactive groups by replacing the labile chlorine atom(s) by sulfophenoxy group(s) to increase percent fixation has been demonstrated to be viable and effective.

The superior application properties (fixation), enhanced stability (shelf life) and improved performance properties (colour fastness) of modified magenta, yellow and blue dyes, when compared with parent analogues and Jettex R inks were in agreement with the concept.

11.2 Future Work

Based on the results and conclusions presented in this thesis, the following aspects are suggested as being worthy of consideration for future work: (1) application and evaluation of yellow trichloropyrimidine dye along with modified dye; (2) application and evaluation of bis-dichlorotriazine dye along with bis-(monochlorotriazine/sulfophenoxy) dye; (3) application of synthesised dyes based inks onto other fibres and blends could be explored.

Appendix – A (List of Synthesised Dyes)




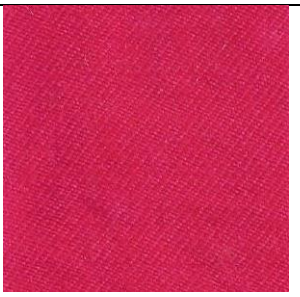





S. #	Dye	Code
Magenta Triazine based Dyes		
1	5-amino-4-hydroxy-3-[(2-sulfophenyl)azo]-2,7-naphthalenedisulfonic acid	d1_m
2	5-[(4,6-dichloro-1,3,5-triazin-2-yl)amino]-4-hydroxy-3-[(2-sulfophenyl)azo]-2,7-naphthalenedisulfonic Acid Dye	d2_{mt}
*3	5-[[4-chloro-6-(4-sulfophenoxy)-1,3,5-triazin-2-yl]amino]-4-hydroxy-3-[(2-sulfophenyl)azo]-2,7-naphthalenedisulfonic Acid Dye	d3_{mtm}
*4	5-[[4,6-(4-sulfophenoxy)-1,3,5-triazin-2-yl]amino]-4-hydroxy-3-[(2-sulfophenyl)azo]-2,7-naphthalenedisulfonic Acid Dye	d4_{mtd}
Yellow Triazine based Dyes		
5	7-[(4-amino-2-methylphenyl)azo]-1,3-naphthalenedisulfonic Acid Dye	d5_y
6	7-[(4,6-dichloro-1,3,5-triazin-2-yl)amino-2-methylphenyl]azo]-1,3-naphthalenedisulfonic Acid Dye	d6_{yt}
*7	7-[(4-chloro-6-(4-sulfophenoxy)-1,3,5-triazin-2-yl)amino-2-methylphenyl]azo]-1,3-naphthalenedisulfonic Acid Dye	d7_{ytm}
*8	7-[(4,6-(4-sulfophenoxy)-1,3,5-triazin-2-yl)amino -2-methylphenyl]azo]-1,3-naphthalenedisulfonic Acid Dye	d8_{ytd}
Blue Triazine based Dyes		
9	1-amino-4-[(3-amino-4-sulfophenyl)amino)]-anthraquinone-2-sulfonic Acid Dye	d9_b
10	1-amino-4-[[3-(4,6-dichloro)-1,3,5-triazin-2-yl]amino]-4-(sulfophenyl)amino)]-anthraquinone-2-sulfonic Acid Dye	d10_{bt}

S. #	Dye	Code
*11	1-amino-4-[3-(4-chloro-6-(4-sulfophenoxy)-1,3,5-triazin-2-yl)amino]-4-(sulfophenylamino)]-anthraquinone-2-sulfonic Acid Dye	d11_{mtm}
*12	1-amino-4-[3-(4,6-(4-sulfophenoxy)-1,3,5-triazin-2-yl)amino]-4-(sulfophenylamino)]-anthraquinone-2-sulfonic Acid Dye	d12_{btd}
Magenta Diazine (pyrimidine) based dyes		
13	5-[(2,5,6-trichloro-4-pyrimidinyl)amino]-4-hydroxy-3-[(2-sulfophenyl)azo]-2,7-naphthalenedisulfonic acid	d13_{mp}
*14	5-[(2-(4-sulfophenoxy)-5,6-dichloro-4-pyrimidinyl)amino]-4-hydroxy-3-[(2-sulfophenyl)azo]-2,7-naphthalenedisulfonic Acid Dye	d14_{mpm}
Blue Diazine (pyrimidine) based Dyes		
15	1-amino-4-[3-[(2,5,6-trichloro-4-pyrimidinyl)amino]-4-(sulfophenyl)amino]-anthraquinone-2-sulfonic Acid Dye	d15_{bp}
*16	1-amino-4-[3-[[2-(4-sulfophenoxy)-5,6-trichloro-4-pyrimidinyl]amino]-4-(sulfophenyl)amino]-anthraquinone-2-sulfonic Acid Dye	d16_{bpm}
Yellow Diazine (pyrimidine) based Dyes		
17	7-[(2,5,6-trichloro-4-pyrimidinyl)amino]-2-[(methylphenyl)azo]-1,3-naphthalenedisulfonic Acid Dye	d17_{yp}
*18	7-[[2-(4-sulfophenoxy)-5,6-dichloro-4-pyrimidinyl]amino]-2-[(methylphenyl)azo]-1,3-naphthalenedisulfonic Acid Dye	d18_{ypm}
Magenta Dyes based on ethylenediamine bridging group		
19	bis-ethylenediamine intermediate	d19_{di}
20	bis-dichlorotriazine dye	d20_{mbt}
*21	bis-(monochlorotriazine/sulfophenoxy) dye	d21_{bis}

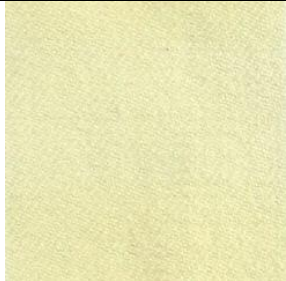
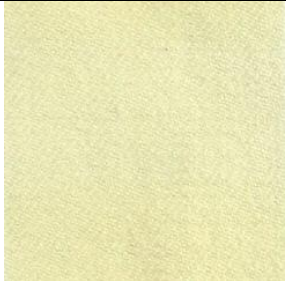
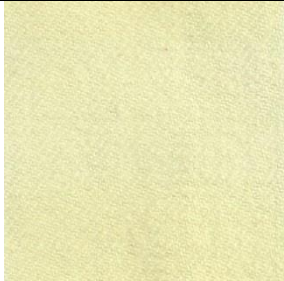






* : Modified Dyes

Appendix – B (Printed Samples)

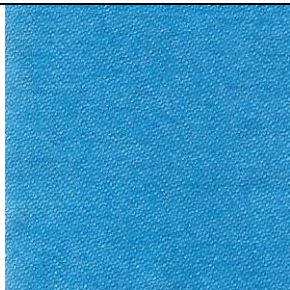








Printed Samples (Magenta triazine based Inks)

Batch @ 25 °C	Batch @ 65 °C	Steaming @ 102 °C
Ink d2_{mt}		
		
81% (4 hours)	83% (150 min)	83% (10 min)
Ink d4_{mtd}		
		
82% (4 hours)	89% (120 min)	89% (20 min)
Ink d3_{mtm}		
		
83% (4 hours)	89% (180 min)	91% (20 min)

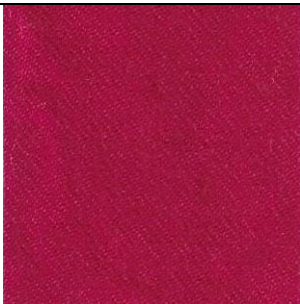
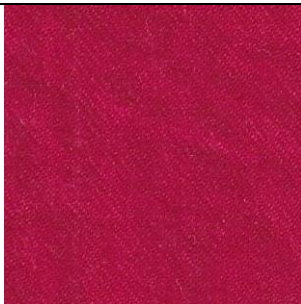


Printed Samples (Yellow triazine based Inks)

Batch @ 25 °C	Batch @ 65 °C	Steaming @ 102 °C
Ink d6_{yt}		
		
73% (4 hours)	65% (150 min)	76% (10 min)
Ink d7_{ym}		
		
79% (4 hours)	83% (180 min)	83% (20 min)
Ink d8_{yt}		
		
80% (4 hours)	85% (150 min)	84% (25 min)





Printed Samples (Blue triazine based Inks)

Batch @ 25 °C	Batch @ 65 °C	Steaming @ 102 °C
Ink d10_{bt}		
		
48% (4 hours)	59% (120 min)	61% (15 min)
Ink d11_{btm}		
		
68% (4 hours)	93% (60 min)	89% (20 min)
Ink d12_{btd}		
		
66% (4 hours)	90% (150 min)	90% (15 min)




Printed Samples (Magenta pyrimidine based Inks)

Batch @ 90 °C	Steaming @ 102 °C
Ink d13_{mp}	
	
94%	89%
Ink d14_{mpm}	
	
90%	91%

Printed Samples (Blue pyrimidine based Inks)

Batch @ 90 °C		Steaming @ 102 °C	
Ink d15_{bp}			
			
72%		84%	
Ink d16_{bpm}			
			
86%		88%	

Printed Samples (Jettex R Inks)

Jettex R (M)	Jettex R (Y)	Jettex R (C)
		
85%	79%	82%

Tri-colour prints using synthesised Inks (Sample 1)



Tri-colour prints using synthesised Inks (Sample 2)



Appendix – C (Elemental Analysis)

School of Chemistry
Elemental Analysis

Tel: 0113 34 36561



UNIVERSITY OF LEEDS

Request Form

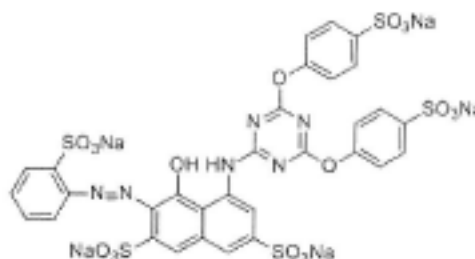
Name..... SAIRA FABAL	Account No..... 28010800
Sample ref..... SP/DTI	Supervisor..... PROF. LONG LIN
Department..... COLOUR SCIENCE	Signature.....
Room No..... 3.13 Tel..... 32810	Date..... 29-11-12
e-mail..... sra@leeds.ac.uk	(Please fill in fully & in BLOCK CAPITALS, failure could result in delay)

Properties & Hazards

	YES	NO	Unknown
Non Hazardous	<input type="checkbox"/>	<input type="checkbox"/>	<input checked="" type="checkbox"/>
Toxic	<input type="checkbox"/>	<input type="checkbox"/>	<input checked="" type="checkbox"/>
Carcinogenic	<input type="checkbox"/>	<input type="checkbox"/>	<input checked="" type="checkbox"/>
Explosive	<input type="checkbox"/>	<input checked="" type="checkbox"/>	<input type="checkbox"/>
Air Sensitive	<input type="checkbox"/>	<input checked="" type="checkbox"/>	<input type="checkbox"/>
Hygroscopic	<input type="checkbox"/>	<input checked="" type="checkbox"/>	<input type="checkbox"/>
Light Sensitive	<input type="checkbox"/>	<input checked="" type="checkbox"/>	<input type="checkbox"/>
Volatile	<input type="checkbox"/>	<input type="checkbox"/>	<input type="checkbox"/>
Electrostatic	<input type="checkbox"/>	<input type="checkbox"/>	<input checked="" type="checkbox"/>
Strong odour	<input type="checkbox"/>	<input checked="" type="checkbox"/>	<input type="checkbox"/>

Other.....
M/pt. / B/pt. NOT KNOWN..... °C
Solid [, Liquid [

Structure & Empirical Formula



C31H17N6Na5O18S5

Formula.....

Type of compound – PYRIMIDINE COMPOUND

Is there POSSIBILITY for the presence of FLUORINE? YES [] / NO [

Analysis Required	Theoretical (%)	Found (%)
Carbon [<input checked="" type="checkbox"/>	35.91	30.80
Hydrogen [<input checked="" type="checkbox"/>	1.65	3.06
Nitrogen [<input checked="" type="checkbox"/>	8.1	6.79
Sulphur [<input type="checkbox"/>
Halogen [<input type="checkbox"/>
Other #1 [<input type="checkbox"/>
Other #2 [<input type="checkbox"/>
Other #3 [<input type="checkbox"/>

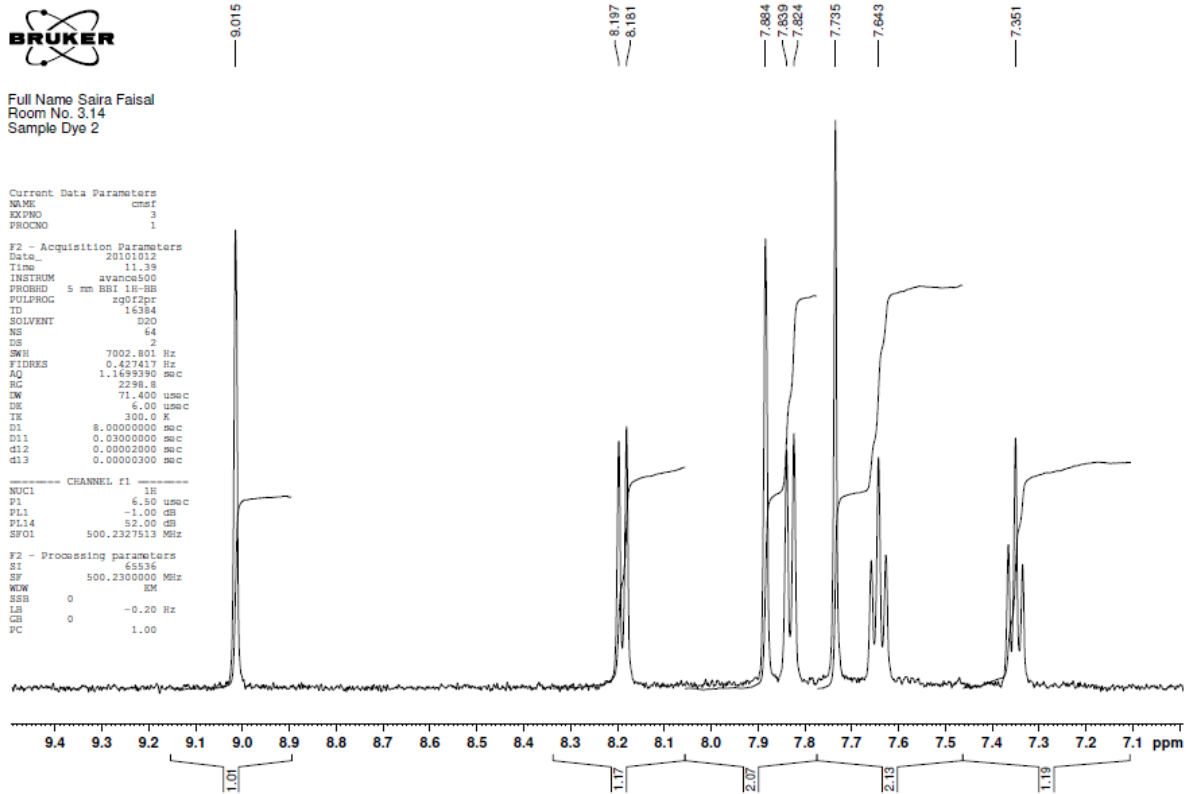
Micro ID:

; Signature:

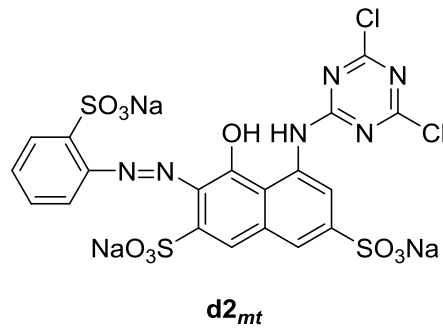
SB 18/12/12

(Office use only)

Appendix – D (¹H NMR)



¹H NMR of magenta dichlorotriazine dye (**d2_{mt}**)



¹H NMR (D₂O, 500 MHz) δ 7.35 (1H, J = 10 Hz, t), 7.64 (1H, J = 10, t), 7.73 (1H, s), 7.82 (1H, J = 10 Hz, d), 7.88 (1H, s), 8.18 (1H, J = 10, d), 9.02 (1H, s)



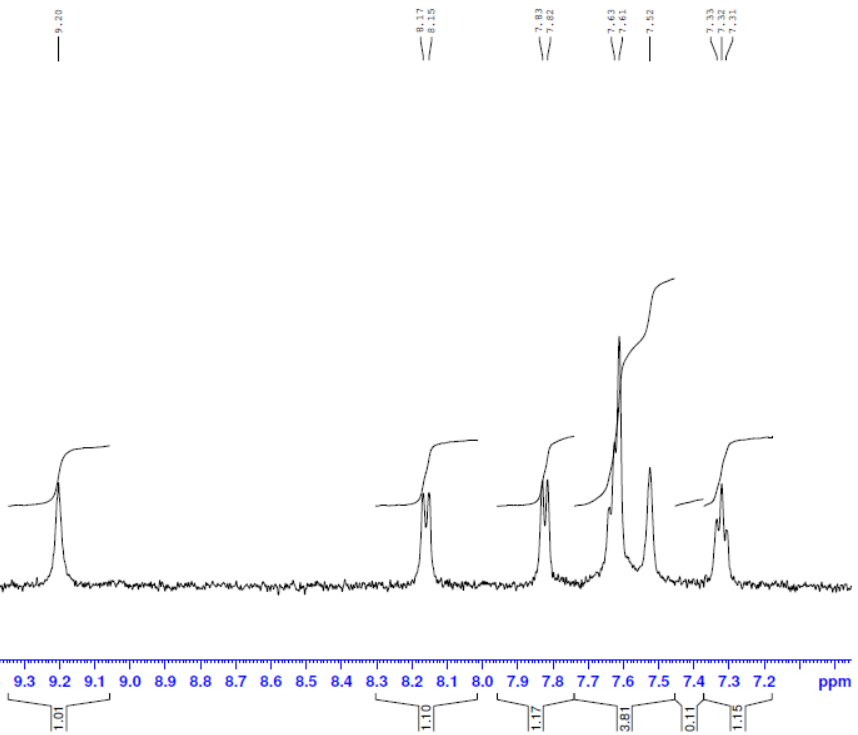
Full Name Saira Faisal
Room No. 3.14
Sample Dye 4

```
Current Data Parameters
NAME          sfd4
EXPNO        11
PROCNO       1

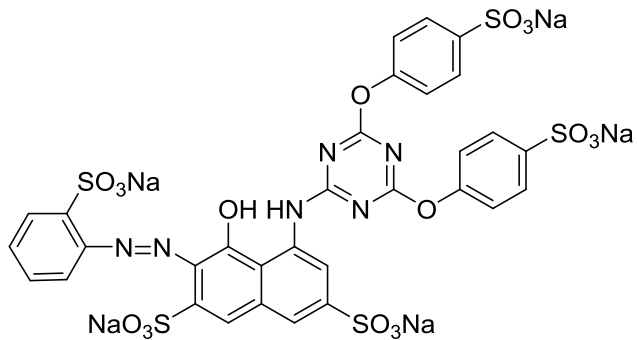
F2 - Acquisition Parameters
Date_        20101011
Time         14.50
INSTRUM      avance500
PROBHD       5 mm BBI 1H-BB
PULPROG      zgpg2pr
TD           16384
SOLVENT      D2O
NS           64
DS           2
SWH          7002.801 Hz
FIDRES       0.4274177 Hz
AQ           1.1699390 sec
RG           4597.6
DW           71.400 usec
DE           6.00 usec
TE           300.0 K
D1           8.0000000 sec
d11          0.0300000 sec
d12          0.0002000 sec
d13          0.0000300 sec

----- CHANNEL f1 -----
NUC1          1H
P1            6.50 usec
PL1          -1.00 dB
PL12         52.00 dB
SFO1          500.2327513 MHz

F2 - Processing parameters
SI            65536
SF           500.2300048 MHz
WDW          EM
SSB          0
LB           -0.20 Hz
GB           0
```



¹H NMR of Magenta Modified Dye



d4_{mtd}

¹H NMR (D₂O, 500 MHz) δ 7.32 (2H, J = 10 Hz, t), 7.52 (2H,s), 7.62 (6H, m), 7.82 (2H, J = 10 Hz, d), 8.15 (2H, J = 10 Hz, d), 9.20 (2H, s)



8.676
8.348
8.290
8.218
7.928
7.912
7.895
7.784
7.766
7.316
7.297
7.274
7.018
6.422
6.403
6.377

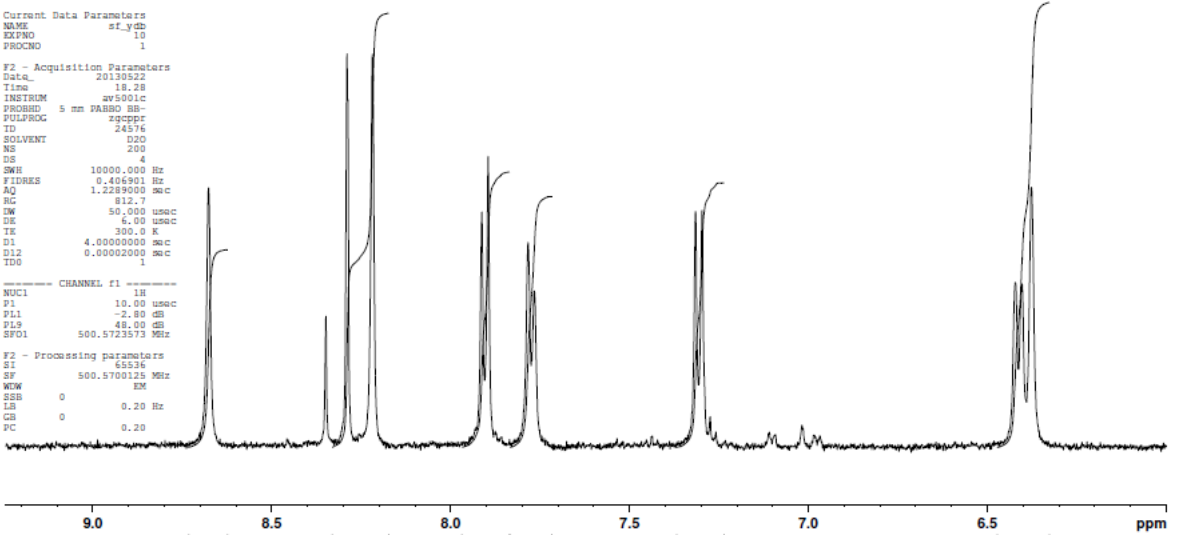
Name Saira Faisal
Room No 3.14
Sample YDBT

```
Current Data Parameters
NAME          sf_ydb
EXPNO        10
PROCNO       1

F2 - Acquisition Parameters
Date_        20130522
Time         18.28
INSTRUM      av5001c
PROBHD       5 mm PABBO BB-
PULPROG      zgpgpr
TD           24576
SOLVENT      D2O
NS           200
DS           4
SWH          10000.000 Hz
FIDRES       0.4063901 Hz
AQ           1.2283900 sec
RG           812.7
EW           50.000 usec
DE           4.00 usec
TE           300.0 K
D1           4.00000000 sec
D12          0.00002000 sec
TDO          1

----- CHANNEL f1 -----
NUC1         1H
P1           10.00 usec
PL1         -2.80 dB
PL2         40.00 dB
SFO1        500.5723573 MHz

F2 - Processing parameters
SI           65536
SF          500.5700125 MHz
WDW          EM
SSB          0
LB           0.20 Hz
GB           0
PC           0.20
```



9.0 8.5 8.0 7.5 7.0 6.5 ppm



8.676
8.348
8.290
8.218
7.928
7.912
7.895
7.784
7.766
7.316
7.297
7.274
7.018
6.422
6.403
6.377
4.102
4.083
4.064
2.276
2.249
2.216
2.201
2.156
2.144
2.114
2.120
1.966
1.539
1.536
1.500
1.516
1.511
1.504
1.500
1.494
1.480
1.283
1.277
1.269
1.256
1.245
1.239
1.230
1.225
1.224
1.212
1.201

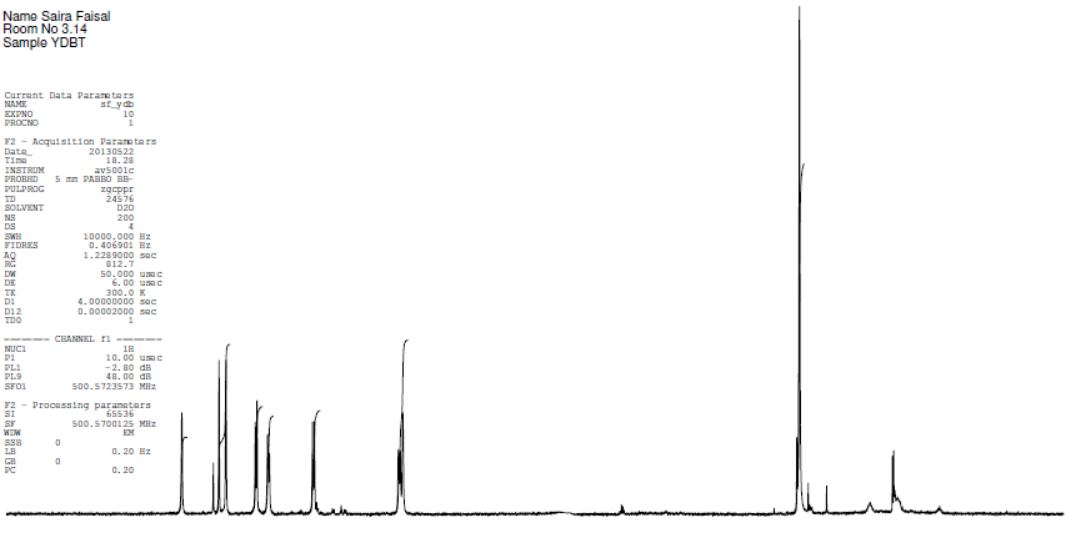
Name Saira Faisal
Room No 3.14
Sample YDBT

```
Current Data Parameters
NAME          sf_ydb
EXPNO        10
PROCNO       1

F2 - Acquisition Parameters
Date_        20130522
Time         18.28
INSTRUM      av5001c
PROBHD       5 mm PABBO BB-
PULPROG      zgpgpr
TD           24576
SOLVENT      D2O
NS           200
DS           4
SWH          10000.000 Hz
FIDRES       0.4063901 Hz
AQ           1.2283900 sec
RG           812.7
EW           50.000 usec
DE           4.00 usec
TE           300.0 K
D1           4.00000000 sec
D12          0.00002000 sec
TDO          1

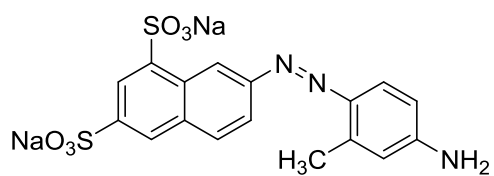
----- CHANNEL f1 -----
NUC1         1H
P1           10.00 usec
PL1         -2.80 dB
PL2         40.00 dB
SFO1        500.5723573 MHz

F2 - Processing parameters
SI           65536
SF          500.5700125 MHz
WDW          EM
SSB          0
LB           0.20 Hz
GB           0
PC           0.20
```



10.0 9.5 9.0 8.5 8.0 7.5 7.0 6.5 6.0 5.5 5.0 4.5 4.0 3.5 3.0 2.5 2.0 1.5 1.0 0.5 0.0 ppm

¹H NMR of yellow dye chromophore



d5_y

¹H NMR (D₂O, 500 MHz) δ 2.30 (3H, s), 6.38 (1H, s), 6.41 (1H, J = 10 Hz, d), 7.30 (1H, J = 10 Hz, d), 7.77 (1H, J = 10 Hz, d), 7.91 (1H, J = 10, d), 8.22 (1H, s), 8.29 (1H, s), 8.68 (1H, s)